MODELLING OCULAR MONOCHROMATIC ABERRATIONS USING SCHEMATIC EYES WITH HOMOGENEOUS OPTICAL MEDIA

ELAINE KATHRYN WHITE

Doctor of Philosophy

THE UNIVERSITY OF ASTON IN BIRMINGHAM

OCTOBER 1993

The University of Aston in Birmingham

MODELLING OCULAR MONOCHROMATIC ABERRATIONS USING SCHEMATIC EYES WITH HOMOGENEOUS OPTICAL MEDIA

Elaine Kathryn White

Ph.D. thesis
October 1993

SUMMARY

Previous research has indicated that schematic eyes incorporating aspheric surfaces but lacking gradient index are unable to model ocular spherical aberration and peripheral astigmatism simultaneously. This limits their use as wide-angle schematic eyes. This thesis challenges this assumption by investigating the flexibility of schematic eyes comprising aspheric optical surfaces and homogeneous optical media.

The full variation of ocular component dimensions found in human eyes was established from the literature. Schematic eye parameter variants were limited to these dimensions. The levels of spherical aberration and peripheral astigmatism modelled by these schematic eyes were compared to the range of measured levels. These were also established from the literature. To simplify comparison of modelled and measured data, single value parameters were introduced; the spherical aberration function (SAF), and peripheral astigmatism function (PAF). Some ocular components variations produced a wide range of aberrations without exceeding the limits of human ocular components. The effect of ocular component variations on coma was also investigated, but no comparison could be made as no empirical data exists.

It was demonstrated that by combined manipulation of a number of parameters in the schematic eyes it was possible to model all levels of ocular spherical aberration and peripheral astigmatism. However, the unique parameters of a human eye could not be obtained in this way, as a number of models could be used to produce the same spherical aberration and peripheral astigmatism, while giving very different coma levels. It was concluded that these schematic eyes are flexible enough to model the monochromatic aberrations tested, the absence of gradient index being compensated for by altering the asphericity of one or more surfaces.

KEY WORDS: Peripheral astigmatism, Spherical aberration, Coma, Conic surfaces.

For Paul and Mum and Dad

ACKNOWLEDGEMENTS

I would like to thank Mr. D.A. Barnes for his help and supervision.

I would also like to thank Dr. M.C.M Dunne for his sound advice and assistance.

LIST OF CONTENTS PAGE

CHAPTER 1
INTRODUCTION

CHAPTER 2
MEASUREMENT OF SPHERICAL ABERRATION IN HUMAN EYES

CHAPTER 3
MEASUREMENT OF PERIPHERAL ASTIGMATISM IN HUMAN EYES

CHAPTER 4
THE OPTICAL PARAMETERS OF THE HUMAN EYE

CHAPTER 5
WIDE- ANGLE SCHEMATIC EYES - A CRITICAL REVIEW

CHAPTER 6
THE EFFECTS OF INDIVIDUAL OCULAR PARAMETER CHANGES ON SPHERICAL ABERRATION.

CHAPTER 7
THE EFFECTS OF INDIVIDUAL OCULAR PARAMETER CHANGES ON PERIPHERAL ASTIGMATISM

CHAPTER 8
THE EFFECT OF INDIVIDUAL OCULAR PARAMETER CHANGES ON COMA

CHAPTER 9
SIMULTANEOUS MODELLING OF SPHERICAL ABERRATION AND PERIPHERAL ASTIGMATISM IN HUMAN SCHEMATIC EYE VARIANTS

LIST OF FIGURES PAGE

Fig. 9.24 - Plot of spherical aberration against pupil diameter for the human range (solid lines) and for a schematic eye giving the minimum SAF. 243

LIST OF TABLES PAGE

CHAPTER 1

INTRODUCTION

1.1 AIMS AND OBJECTIVES.

This study was designed to demonstrate the range of monochromatic aberrations, specifically spherical aberration, peripheral astigmatism and coma, which can be achieved within a schematic eye when the optical parameters are manipulated within the confines of known human ranges. The principal aim is to demonstrate that the full range of aberrations found in real eyes can be modelled by such schematic eyes without adding gradient index structures to the modelled crystalline lens. The gradient index properties of the crystalline lens are avoided for a number of reasons. Firstly, this makes schematic models much more complicated to work with. Secondly the gradient index is difficult to measure in real eyes so that very little empirical data exists. Smith et al. (1991), for instance, attempted to design a model of the human lens based on measured human values and concluded that more data would be necessary before an accurate model could be constructed. Thirdly (as will be will be shown later) a schematic eye incorporating aspheric surfaces and homogeneous optical media reproduces sufficiently representative aberrations of the eye.

The two main aberrations to be considered are spherical aberration and peripheral astigmatism as these are the most extensively measured aberrations of the human eye. Spherical aberration is considered to be the most important aberration on-axis and peripheral astigmatism the most important off-axis. Coma has not been measured directly, in real eyes, and there is some dispute as to its importance. Only monochromatic aberrations are considered in the present study. This is primarily for reasons of simplicity but also because the refringence of the optical media in the eye are not known.

Chapters two and three review previous investigations into ocular spherical aberration and peripheral astigmatism, respectively. A range of values is established for each, for comparison with values modelled in schematic eyes.

Chapter four reviews work on the measurement of optical parameters of human eyes. The axial separations, surface curvatures and asphericities will all be considered. A range will be established for each parameter.

Previous work on schematic eyes is reviewed in chapter five and attempts to model aberrations of the human eye are examined. The success or otherwise of these eyes is discussed with the aim of establishing the form of schematic eye to be used for this investigation.

Chapter six studies the effect on spherical aberration of altering each individual optical parameter within the established human ranges. The range of spherical aberration achieved by each parameter is compared to ranges found in real eyes as established in chapter two. Likewise chapter seven studies the effect on peripheral astigmatism and compares the results to the real values established in chapter three. The subject of chapter eight is the effect of parameter changes on comatic aberration, showing which parameter variations maximise or minimised coma.

In chapter nine examples are given, illustrating how the parameter values may be combined to give the full range of aberrations found in real eyes. By this means the flexibility of the optical system within human limits is investigated. Finally, chapter ten summarises the work and includes suggestions for future research.

The remainder of this chapter introduces the concept of image quality and discusses the methods used to assess it in optical systems. Optical aberrations, specifically spherical aberration and peripheral astigmatism and coma are defined and discussed. Wavefront aberrations, spread functions and modulation transfer functions are also defined. Measurement of aberrations and overall image quality in human eyes is discussed in order to establish the types of optical degradation found. The following discussions are drawn from published texts covering the theories of image degradation in optical systems (Fincham and Freeman, 1980; Smith, 1990).

1.2 THE PERFECT IMAGE

Before assessing the degradation in an optical image it is perhaps necessary to examine what constitutes a perfect image. Any object is made up of a large number of point light sources of different intensity. For a lens system to produce a perfect image it must produce a point image of every point source in the object. Further, the points must be arranged in the image in a geometrically similar way to that of the object, varying only in magnification. Even in a system free from any aberrations production of a perfect image is not possible; the finite aperture will cause diffraction, spreading each point object into a small disc like image. This image will then be further degraded by any aberrations inherent in the system. An image produced by a system free from aberrations is referred to as a diffraction limited image.

The amount of degradation exhibited by a system can be represented in a number of ways. It can be expressed as the final position of rays compared to the position of paraxial rays (section 1.3). From this the individual aberrations can be calculated and then be plotted

against height or incident angle of rays, to show the variation of aberration over the whole aperture of the system. The degradation can also be shown in the form of contour plots (section 1.4) where the contours join points of equal wavefront aberration, usually expressed in wavelengths. The way in which the light is spread by the system can be depicted as a point spread function or line spread function, or in two dimensions on the image surface as a spot diagram. The most comprehensive way of representing image quality is the optical transfer function (OTF) (section 1.5). This is a very complex function combining the modulation transfer function (MTF) and the phase transfer function (PTF). Not only does this give the amount of degradation caused by the aberrations of the system but can also include the effects of diffraction and scatter.

1.3 FIRST-ORDER OPTICS AND SEIDEL ABERRATIONS

We will firstly consider the monochromatic aberrations of a system as the deviation of ray position from the ideal paraxial image. As stated previously, a perfect image is formed if every ray from a point source on the object meets at a point on the image. The rays must therefore be bent or refracted by the system in such a way as to achieve this end. Refraction at a lens surface follows Snell's law:-

$$n \sin i = n' \sin i'$$

where n and n' are the refractive indices before and after refraction and i and i' are the incident and refracted angles of the ray.

The sine of an angle can be expressed as a series:-

$$\sin i = i - \frac{i^3}{3!} + \frac{i^5}{5!} - \frac{i^7}{7!} + \ldots + \frac{i^{2n-1}}{(2n-1)!}$$

when i is in radians.

Rays lying very close to the optical axis, with incident angles less than approximately 5° are called paraxial rays. The region through which these rays pass is the paraxial region. For such small angles the approximation sin i = i can be applied with little loss of accuracy and Snell's law reduces to ni=n'i'. The optical theories and equations applied to image formation in this region are sometimes called first-order or Gaussian optics. First-order optics predicts that all the rays leaving a point object will meet at a point image and that the magnification in any transverse plane is constant. Images formed in the paraxial region will only be distorted by diffraction and will therefore be 'diffraction limited'.

When higher order approximations of Snell's law are used the predictions of first-order optics will no longer be true. The behaviour of the rays will deviate from the ideal of paraxial optics. Such deviations are known as lens aberrations. Calculations including the second term in the sine series result in five aberrations called third-order or Seidel aberrations, after Von Seidel who first studied them in 1855. The aberrations are:-

S_I - Spherical aberration
S_{II} - Coma
S_{III} - Astigmatism
S_{IV} - Curvature of field
S_V - Distortion

The higher terms in the sine series give fifth- and seventh-order aberrations and so on. In some cases it may be sufficient to consider third-order aberrations only. Equations have been developed which allow these third-order aberrations to be calculated relatively easily (Welford, 1986). For high accuracy, however, it is necessary to calculate the paths of individual rays through the optical system by means of ray tracing (Smith 1990). The aberrations can then be deduced from the final positions of these rays relative to the position of paraxial rays. The present study uses such ray tracing procedures to calculate aberrations in schematic eyes and relates the values to those found in real eyes.

The two main aberrations considered in this study are spherical aberration and peripheral astigmatism. These are considered to be the most important aberrations in the human eye and are the only aberrations to be measured directly (see chapters two and three). Coma can be deduced indirectly from measures of wavefront aberration and spread functions. The remaining Seidel aberrations (curvature of field and distortion) are generally considered unimportant. Distortion is caused by a field angle dependant magnification change which is possibly compensated for by the higher visual centres (Ogle, 1950). Field curvature distortions may be eliminated by the curvature of the retina (Le Grand and El Hage, 1980).

1.3.1 SPHERICAL ABERRATION

Spherical aberration is the variation of focus position with ray height or aperture size. For a rotationally symmetrical centred system, spherical aberration is the only aberration present on-axis. Many investigators consider that the human eye is an approximately centred system and have therefore argued that spherical aberration is the cause of most of the degradation of on-axis images.

The human eye may be simply represented by a positive lens system which forms a real image on the retina, assuming it is emmetropic. Fig 1.1 shows a positive lens whose surfaces are spherical, and centred on an optical axis. Parallel rays of light which pass close to the optical axis will form an image at a point referred to as the paraxial focus. As the ray height increases the rays focus progressively closer to the lens. Rays passing through the very edge of the limiting aperture, referred to as marginal rays, will be focused closest to the lens.

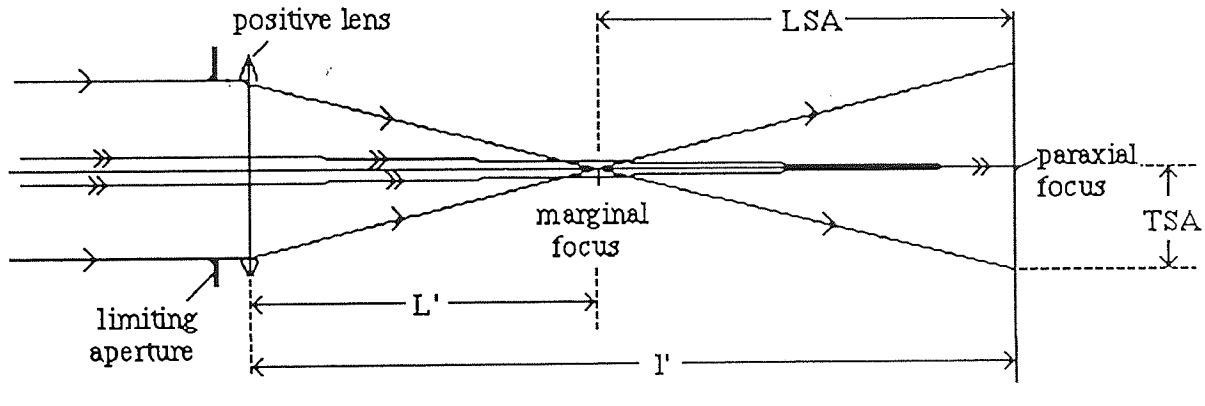

Fig. 1.1 Spherical aberration of a spherical surfaced positive lens.

The value of spherical aberration can be expressed as the distance along the axis between the paraxial focus and the focus at a specific ray height. This is called the longitudinal spherical aberration (LSA). In fig 1.1 the LSA for the marginal rays is calculated by measuring the marginal focal distance L' from a point on the axis and then subtracting from it the paraxial focal distance l' measured from the same axial point. This gives a negative value and such spherical aberration - produced by spherical, positive lenses - is termed negative or under-corrected spherical aberration. Spherical negative lenses form marginal foci beyond the paraxial focus. The LSA is then said to be positive or over-corrected. Spherical aberration can also be expressed in terms of the height at which rays hit the image plane; usually the plane coinciding with the paraxial focus. This is the transverse spherical aberration (TSA). Unlike LSA the Value of TSA will vary if the image plane is moved.

As spherical aberration varies with ray height or aperture radius it is often represented graphically by plotting the degree of spherical aberration as a function of ray height or

aperture radius. In classical optics the aberration is expressed in units of length, usually millimetres. Values in human eyes are more often expressed in dioptres, as values expressed in this way are more relevant to vision and are also more easily measured.

The human eye generally exhibits, reasonably well corrected, negative or under-corrected spherical aberration when relaxed. The low levels of spherical aberration are considered to be due mainly to the flattening of the anterior corneal surface in the periphery (Kiely et al, 1982; Guillon et al, 1986). As a refracting surface flattens its power will be reduced. Rays passing through the periphery of the cornea will not be refracted as much as they would be if the cornea were spherical. They will, therefore, focus closer to the paraxial focus and spherical aberration will be reduced.

The non-uniform refractive index structure of the crystalline lens is such that the refractive index reduces towards the periphery. This will also have the effect of reducing spherical aberration, but the degree to which it occurs is uncertain.

There is some dispute as to whether the cornea and lens of the eye have spherical aberration values which are of opposing sign, and therefore combine to reduce spherical aberration in the whole eye (El Hage and Berny, 1973), or if each single element is designed to minimise spherical aberration on its own with the contribution of the two adding to give the overall value (Millodot and Sivak, 1979).

The rationale behind using values of spherical aberration to compare on-axis image quality of real and schematic eyes in this study is as follows: Firstly, the schematic eyes used are rotationally symmetrical, centred systems and as such will only suffer from spherical aberration on-axis; Secondly, spherical aberration has been considered by many workers to be the most important aberration for axial images and so has been extensively studied providing a lot of empirical data (see chapter two).

1.3.2 PERIPHERAL ASTIGMATISM.

Peripheral astigmatism occurs when the object does not lie on the optical axis of the lens system i.e rays from that object strike the optical system obliquely. On-axis astigmatism will only occur if the system is not rotationally symmetrical.

Before describing peripheral astigmatism it is necessary to introduce the concept of sagittal and tangential rays. Consider fig. 1.2; rays travelling in the plane of oblique incidence (i.e

the unshaded fan of rays) are called meridional or tangential rays. The plane is known as the meridional or tangential plane.

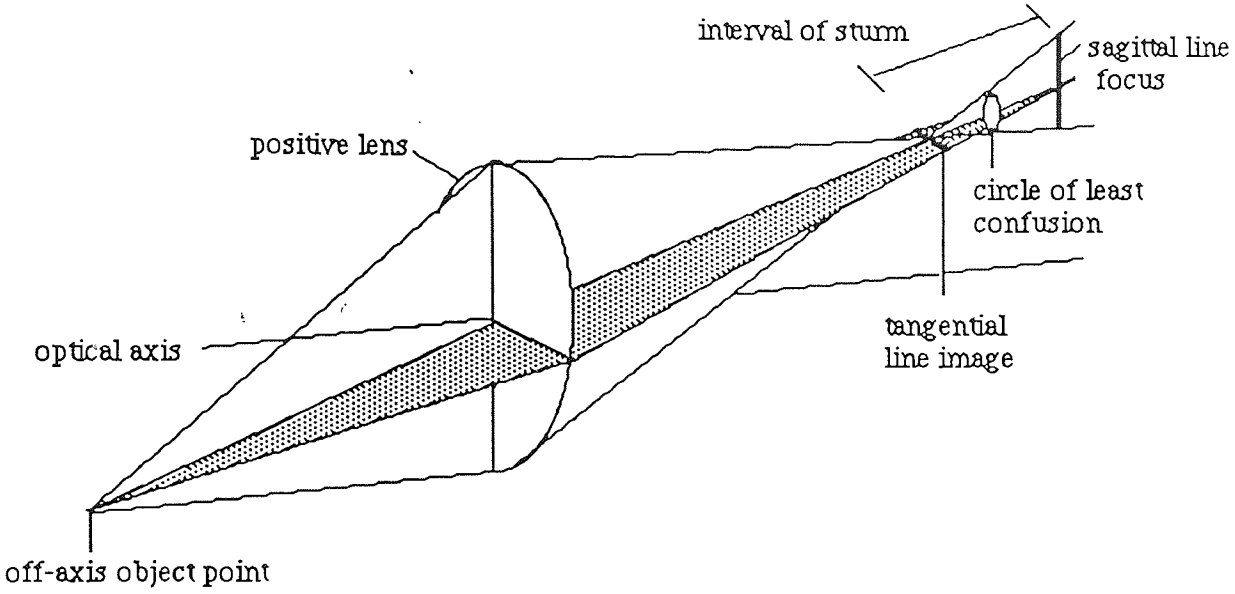

Fig. 1.2 Diagrammatic representation of the sagittal and tangential line foci, the circle of least confusion and the interval of Sturm.

The tangential ray passing through the centre of the pupil is known as the principal ray. Sagittal rays lie in the plane which is perpendicular to the tangential plane and which passes through the principal ray.

Fig. 1.2 shows a fan of tangential and sagittal rays passing through an optical system. The tangential rays form a line image which lies in the sagittal plane. The sagittal rays form a line image which lies in the tangential plane. In the presence of astigmatism these two lines do not coincide. The image of a point object will be two separate line images. The distance between these two images is called the interval of Sturm and gives the value of peripheral astigmatism. True peripheral astigmatism is expressed as distance between the sagittal and tangential foci of rays travelling very close to the principal ray.

The appearance of the astigmatic image will depend on the position of the image plane. If it is placed at either of the astigmatic foci the image will appear as a line, which may be spread into a rectangle by diffraction effects. As we move from one focus to the other the image firstly forms an ellipse with its major axes parallel to the nearest line focus. The

major axis of the ellipse reduces as we move away from the line focus and the minor axis increases until they become equal and a circular image is formed. This is called the circle of least confusion.

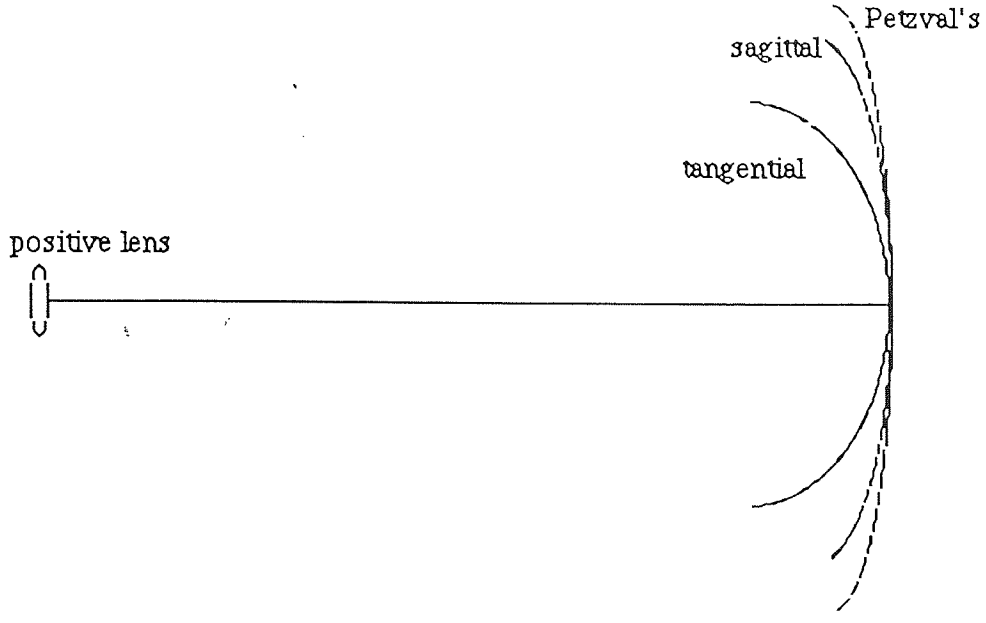

Fig. 1.3 The astigmatic image shells and Petzval surfaces produced by a positive lens.

The astigmatic line images rarely lie on a flat plane, instead they lie on curved surfaces (image shells) which are paraboloid for third-order astigmatism. If a system is free from peripheral astigmatism the two line images will coincide on a single curved surface known as the Petzval surface. The curvature of the Petzval surface is caused by the fourth Seidel aberration (field curvature). The relationship between these three image surfaces, caused by third-order astigmatism, is shown in fig. 1.3. The tangential image surface is three times as far from the Petzval surface as the sagittal image surface. The image plane for the circle of least confusion lies in the middle of the tangential and sagittal image surfaces. Inward curving surfaces are produced by a positive lens, a negative lens would produce outward curving surfaces. When the surfaces are inward curving the tangential surface is generally closer to the lens than the sagittal surface and the peripheral astigmatism is called under-corrected or negative. Conversely for outward curving surfaces the sagittal surface is closer to the lens and the peripheral astigmatism is over-corrected or positive. The human optical system generally exhibits under-corrected peripheral astigmatism.

The amount of astigmatism will usually increase as the object moves further off-axis, i.e. as the field angle increases. Peripheral astigmatism is also dependant on the shape of the lens and on the distance from the lens to the limiting aperture.

In human eyes measurements are made of the variation, with field angle, of the two line foci with respect to the retina. The retinal surface is usually found to fall between the two image shells formed by these line foci. If the distance from the retina to the line foci is plotted against field angle the result is a graph such as that depicted in fig. 1.4. The position of the retinal surface is represented by the horizontal axis. The vertical axis corresponds to the axis around which measurements are made, which for human eyes, is the visual axis. With increasing field angle the tangential image falls further and further in front of the retina, becoming more myopic and the sagittal focus falls further behind the retina, becoming more hyperopic. As a result the interval of Sturm increases with obliquity.

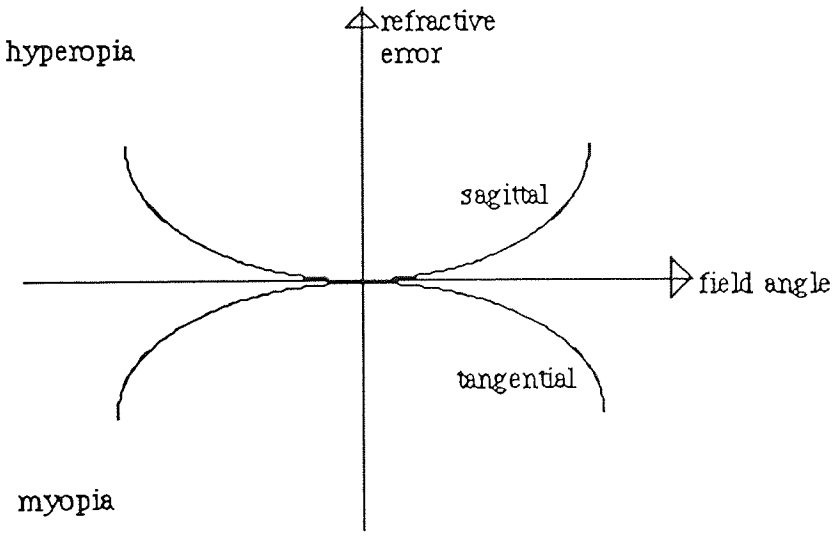

Fig. 1.4 A plot of refractive error against field angle for the sagittal and tangential foci. The horizontal axis, where the refractive error is zero, represents the retinal surface. The vertical axis, where field angle is zero, represents the visual axis.

In practice what is measured in the human eye is not true peripheral astigmatism. The two foci are determined from rays passing through the full extent of the limiting aperture and not by rays travelling very close to the principal ray. Measured values of peripheral astigmatism will therefore include effects due to other off-axis aberrations such as coma

and will be dependant on the size of the pupil. In this study modelled values of peripheral astigmatism are therefore calculated in schematic eyes for a finite pupil size. It is also usual to measure the interval of Sturm along the principal ray for each field angle, unlike optical engineers who measure the interval of Sturm along the optical axis.

The human eye suffers not only from peripheral or off-axis astigmatism but also from axial astigmatism. This is caused by toricity of the optical surfaces, particularly that of the anterior cornea, which results in the refractive power of the eye being greater in one meridian than the other. The cornea generally has a steeper curve (and hence greater refractive power) in, or close to, the vertical meridian. The type of astigmatism caused by this is called 'with the rule' astigmatism. Further causes of axial astigmatism are toricity of the lens surfaces, meridional variation in refractive index and any tilt of the lens relative to the cornea which will cause peripheral astigmatism 'on-axis'. Consider an optical system of an eye suffering from 'with the rule' axial astigmatism. If the tangential plane is the horizontal plane then, as the obliquity of rays entering this system increases, the tangential focus, which is initially behind the sagittal focus, will move closer to it. The 'with the rule' astigmatism will therefore be reduced. At some point in the periphery the tangential focus will fall at the same position as the sagittal focus and beyond this point it will fall in front of the sagittal focus. The point at which the two foci cross over, in relation to which of the optical surfaces produces the axial astigmatism, was explored by White et al. (1991). This investigation will be briefly covered in chapter three.

The rationale behind using peripheral astigmatism in this study to compare the off-axis image quality of real and schematic eyes is similar to that for using spherical aberration on-axis. There is a great deal of empirical data from which such comparison can be made (see chapter three) and peripheral astigmatism is the easiest off-axis aberration to calculate. No other off-axis aberration has been measured directly in the human eye.

1.3.3 Coma

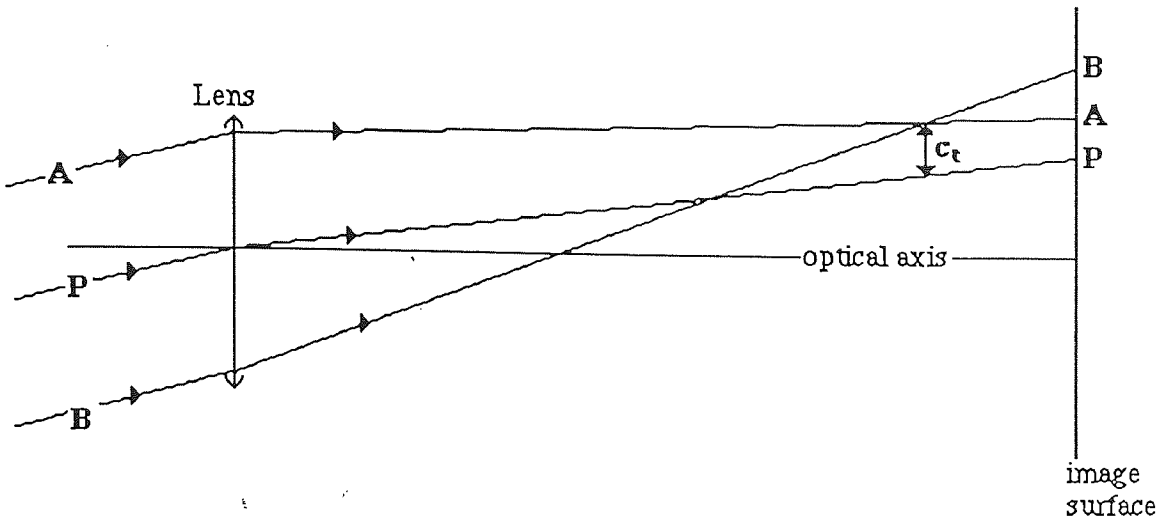

Fig. 1.5 C_t is tangential coma of the optical system measured from the principal ray (P) to the intercept of the two marginal rays (A and B). The three rays intercept the image surface at different heights.

Coma can be defined as the variation of magnification with aperture. It only occurs for off-axis objects. In fig. 1.5 oblique rays fall on a lens with coma. The marginal rays (A and B) passing through the edge of the lens intersect the image plane above the principal ray (P) passing through the centre of the lens. The distance, measured perpendicular to the optical axis, from the principal ray to the intercept of the two marginal rays is called the tangential coma. The tangential coma will decrease as both the ray height and the field angle decreases. Sagittal rays also intercept away from the principal ray, but sagittal coma is generally much smaller than tangential coma. Coma has the effect of spreading the light from a point object into a comet like flare.

Coma is affected by the shape of the optical surfaces, and by the aperture size and position. Smith (1990) shows that it varies linearly with surface curvature (provided the dioptric power of the lens remains constant) and with aperture position. Coma may be eliminated by chosing either the appropriate surface curvatures or aperture position. If we consider the coma shown in fig. 1.5 to be positive it follows that changing the lens shape or aperture position may produce negative coma. Hence the marginal ray intercept will be lower than the principal ray and the comatic flare will be in the opposite direction.

1.4 Wavefront aberration.

The second means of representing image degradation is in terms of wavefronts. Rays and wavefronts are closely related and are the two basic concepts of geometric optics. Rays are straight lines which represent the direction in which light is travelling. Wavefronts are perpendicular to these rays and join points on them which have travelled for an equal time. Rays diverging from a point source in a homogeneous medium will travel in straight lines. The wavefronts perpendicular to these rays will be spherical. If a perfect image is formed by the optical system all the rays will converge to meet at the paraxial image. The wavefront formed in the exit pupil of this system will, therefore, also be spherical, with its centre of curvature at the paraxial image point. The wavefront aberration is expressed in terms of the optical path difference (OPD), which is the distance between this perfect wavefront, or reference sphere, and the wavefront distorted by the aberrations of the system.The distance is usually very small and is often expressed in terms of wavelengths of light. The reference sphere may also be centred on some other image point giving the aberration for an image formed in a plane other than the paraxial plane. This enables us to study the effect of moving the image plane on the image formed by the system. The wavefront aberration can either be plotted against the height in the pupil plane or as a contour plot showing lines joining points of equal wavefront aberration. The individual aberrations have characteristic contour plots. Spherical aberration alone produces a series of concentric circular contours. If the interval of spherical aberration between each circle is constant a higher level of spherical aberration will result in smaller circles which are closer together. Peripheral astigmatism will cause elliptical distortion of the contours and coma produces asymmetry. The presence of the individual aberrations can, therefore, be deduced from the shape of the contour plots.

If we consider a simple positive lens on-axis the wavefront will be curved further in at the edges when compared to the reference sphere due to negative spherical aberration (fig 1.6). The OPD is measured along the radius of the reference sphere and is multiplied by the refractive index of the image medium.

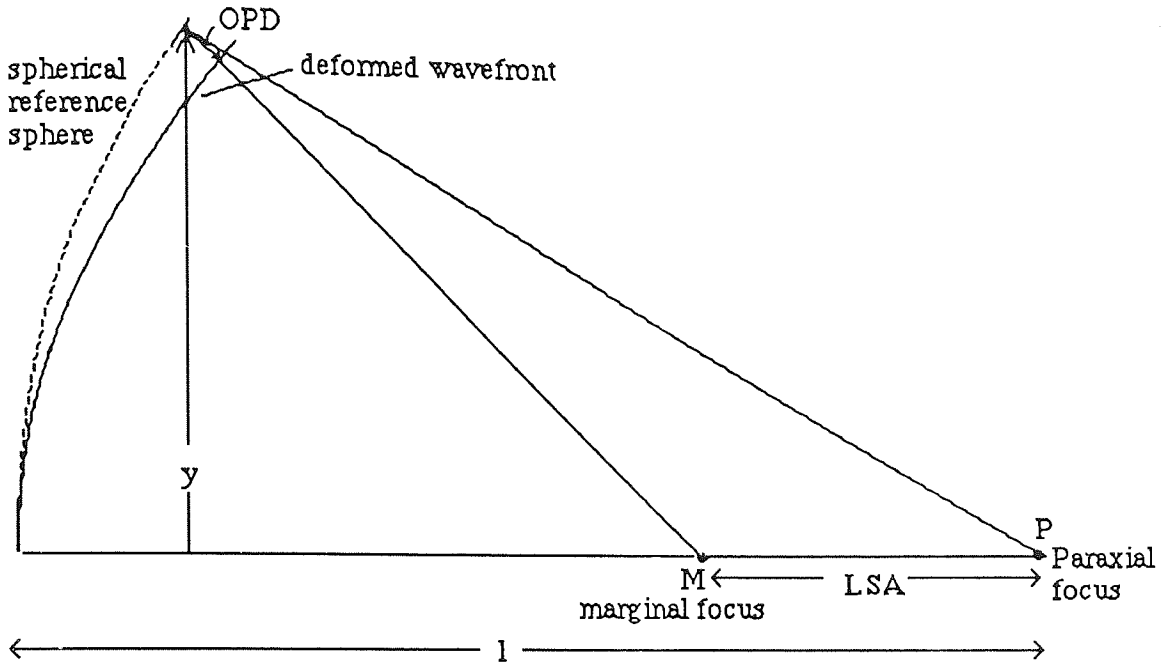

Fig. 1.6 Optical path difference (OPD), l is the radius of the reference sphere y is the ray height in the pupil plane.

Simple relationships exist between the optical path difference and the other aberrations. Smith (1990) showed the relationship between third-order spherical aberration and OPD to be:-

$$OPD = 1/2\ N \sin^2 u\ [1/2\ LSA_m\ (y/y_m)^2\ ]$$

where LSA_m is the longitudinal spherical aberration for marginal rays, y_m is the height of the marginal rays, y is the specific ray height at which the aberration is being considered, N is the refractive index in image space and u is the angle between the refracted paraxial ray and the optical axis.

As previously mentioned, wavefront aberration can be represented graphically as the OPD plotted as a function of ray height. Typical graphs for third-order spherical aberration are shown in fig. 1.7, (Smith, 1990). The effect of focus is shown by measuring the OPD for three different positions of the reference sphere.

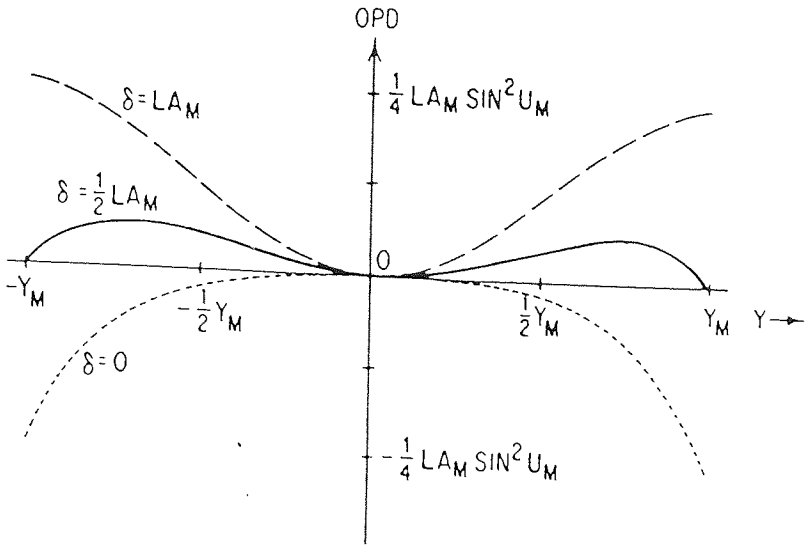

Fig. 1.7 The OPD of a system with third-order spherical aberration, plotted as a function of Y for three positions of the reference point. $\partial = 0$ when the reference point is at the paraxial focus. $\partial = 1/2\ LA_m$ when the reference point is half way between the paraxial and marginal foci. $\partial = LA_m$ when the reference point is at the marginal focus. (after Smith, 1990).

For an optical system with pure third-order peripheral astigmatism focussed at the sagittal image, the reference sphere will be centred at the centre of the sagittal line image. The optical path difference will depend on the meridional plane in which it is considered. It will be smallest in the sagittal plane and largest in the tangential plane. In the presence of peripheral astigmatism wave aberration contour plots are characteristically elliptical in shape.

1.4.1 MEASUREMENT IN HUMAN EYES

Measurement of wavefront aberration in human eyes has been reviewed by Charman (1983, 1991a). Measurement of axial wavefront aberration in real eyes shows a wide inter-individual variation (Smirnov, 1962; Howland and Howland, 1976, 1977; Walsh and Charman, 1985). Despite this variation the general results of these investigators tend to concur. Only a few eyes show the rotationally symmetrical plots expected from regular spherical aberration. Most plots are irregular in form and show evidence of axial astigmatism and coma. It is generally concluded that coma, and not spherical aberration is the dominant aberration for central vision. This is clearly an important result as past work has always assumed spherical aberration to be the most important axial aberration. Any axial coma within the eye is likely to be due to decentration or tilting of the refracting surfaces. Most axial astigmatism is caused by the toricity of the optical surfaces. Unfortunately, because of the difficulties involved in making off-axis measurements, no data exists for off-axis wavefront aberrations in human eyes.

1.5 SPREAD FUNCTIONS AND MTFS

Rays and wavefronts are purely geometrical representations of light. As such, image quality expressed by these means will not include the effects attributed to the wave nature of light (i.e diffraction and scattering). In order to study the effects of diffraction and light scatter, spread functions and modulation transfer functions (MTFs) must be used.

Spread functions describe the intensity distribution of light on the image surface and show the spread of light caused by optical degradation. Aberrations other than pure spherical aberration will cause asymmetries in the point spread function. As measurement of the point spread function is difficult in practice, the line spread function is usually preferred. This is the spread of the image of a very thin line and is equivalent to the integral of the point spread function in one linear direction. If the point spread function is asymmetrical in any plane the line spread function will vary according to its angular position in that plane (i.e. it will be orientation dependant). In other words a vertical line may have a different spread function to one positioned horizontally. The spread functions are also dependant on the position of the object. For example, generally the further off axis the object is the greater the amount of off-axis aberrations. Increased coma will cause an increase in the asymmetry of the spread. Increased peripheral astigmatism will result in a greater difference between the line spread for different angular orientation. Spread functions also vary according to the position of the imaging surface.

If a grating with a sinusoidal distribution is imaged by an optical system, the image distribution will also be sinusoidal and will differ only in modulation and phase. The modulation and phase difference are dependent on spatial frequency. The relationships between the phase difference and spatial frequency and the modulation transfer and spatial frequency are called the phase transfer and modulation transfer functions respectively. If the two transfer functions are combined they form the optical transfer function. The optical transfer function is related to the line spread function by the equation:-

$$OTF = \int_{-\infty}^{\infty} L(x)e^{-2\pi sx}\,dx$$ where s is the spatial frequency.

As image blur caused by spherical aberration alone can only be symmetrical it follows that the point spread function would also be symmetrical. The line spread function would then be the same for all angular orientations. The symmetrical nature of the image would also indicate that there is no phase change as light waves pass through the system, and so the

phase transfer function will be zero for all frequencies. The image quality would therefore be fully described by the modulation transfer function in such cases. For off-axis aberrations, such as astigmatism and coma, the point spread function is no longer symmetrical and the line spread function will therefore be orientation dependant. There will also be phase changes as light passes through the optical system and the full optical transfer function is needed to fully describe the image quality.

1.5.1 MEASUREMENT IN HUMAN EYES

Reviews on past work in this area can be found in Van Meeteren (1974) and Charman (1983,1991a). A number of investigators have attempted to measure the axial modulation transfer functions and spread functions of the human eye.

The two main measuring techniques use psychophysical methods and ophthalmoscopic methods. Psychophysical methods are subjective and were adopted by Arnulf and Dupuy (1960), Westheimer (1960), Campbell and Green (1965) and Bour (1980). The subject viewed a sinusoidal grating of frequency F and Modulation M. As the sinusoidal grating is imaged by the optical system of the eye the modulation is reduced. The modulation transfer function of the optical system is T(F) and the image produced on the retina has modulation $M \cdot T(F)$. If the modulation of the grating is reduced until it is just discernible to the subject's eye the threshold modulation of the external grating (M_t) is related to the threshold modulation at the retina (M_{rt}) by:-

$$M_t \, . \, T(F) = M_{rt}$$

The threshold modulation of the retina alone is found by producing an interference fringe which is imaged directly onto the retina therefore by-passing the optics of the eye. The frequency of the interference fringe is controlled by the separation of the two mutually coherent light sources producing it. The modulation is determined by their relative intensities or by use of a masking field. Once the external and retinal threshold modulations are known the transfer function can be calculated. If M_{it} is the threshold modulation of the interference fringe on the retina and M_t is the modulation of the external grating at threshold then:-

$$M_{it}(F) = M_t\,(F) \cdot T(F) \quad \text{or}$$

$$T(F) = M_{it}(F) \,/ M_t\,(F)$$

Results generally show that the modulation transfer function is very close to that of the diffraction limited eye for pupil sizes up to around 1mm. The optimum MTF was found for pupil sizes of around 2 to 3 mm. For smaller pupils the MTF is reduced by diffraction and for larger pupils it is reduced by aberrations.

The principal criticism of this subjective technique is that it does not account for the modulation reduction of the interference fringes by light scatter. If light scatter does degrade the interference fringes then their modulation, produced on the retinal surface, would be reduced. This would lead to an erroneously high value for the threshold modulation (M_{it}) and an over-estimation of the MTF.

Objective, ophthalmoscopic techniques have been adopted by Westheimer and Campbell (1962), Campbell and Gubisch (1966), Jennings and Charman (1978, 1981), Gorrand (1979) Santamaria et al. (1987) and Navarro et al. (1993) . The object is either a line or a spot of light which is imaged on to the retina. The reflection of light from the object by the retina is then measured by a photomultiplier and the spread function is calculated from the results. The MTF can then be calculated from the spread function. The reflected image is degraded while passing through the optics into the eye, and while passing back out after reflection. The calculation is based on the fact that, provided the reflection at the retina is diffuse, the single pass MTF is the square root of the double pass MTF.

Spread functions measured in human eyes using this method are found to be very symmetrical, even far into the periphery. This would suggest that the eye is well corrected for off-axis coma, which would cause asymmetries in the light spread. This is contrary to the findings from wavefront aberration measurements which show large amounts of coma are present on-axis. Jennings and Charman (1981) surmised that the absence of coma could be due to the eye being very nearly a homocentric system (Guidarelli,1972). In chapter eight it will be shown that this is not so, and that any asymmetry in the spread at the retinal surface may be obscured by the second traverse of the optical system.

1.6 SUMMARY

This chapter has introduced the concept of image quality and the ways in which it can be represented. These have then been discussed with reference to the human optical system to illustrate the type of aberrations found.

The main goal of this study is to determine whether monochromatic aberrations, measured in human eyes, can be reproduced in schematic eyes with known human ranges of surface

positions, radii and asphericities.The aberrations to be used for comparison are spherical aberration (on-axis) and peripheral astigmatism (off-axis). Both have been extensively studied and are relatively easy to model.

Evidence from measured values of wavefront aberrations indicates that coma and not spherical aberration may be the major aberration on-axis. This is likely to be due to the relative tilts and/or translations of the ocular surfaces. However, there has been no direct measurement of coma with which comparisons can be made. Consequently axial coma will be neglected at this stage. It may be considered by further refinement of the schematic eyes in future studies.

CHAPTER 2
MEASUREMENT OF SPHERICAL ABERRATION IN HUMAN EYES

2.1 INTRODUCTION

The reasons for comparing modelled and measured spherical aberration as an indicator of on-axis performance have been developed in chapter one. This chapter serves to review previous investigations into the spherical aberration of human eyes. The data is collated to derive the range of values of spherical aberration expected in human eyes, in preparation for comparison with modelled values in a later chapter. The present review is based on a number of articles by Koomen et al. (1949), Jenkins (1963a), Rosenblum and Christensen (1976) and Charman (1983,1991a).

2.2 METHODS OF MEASUREMENT

Two methods have principally been used for measuring the spherical aberration of human eyes. The first, used by the majority of investigators, was developed by Thomas Young as early as 1801, and is an adaption of his optometer method. The second uses annular rings of differing sizes and was developed by Koomen et al. in 1949.

2.2.1 YOUNG'S OPTOMETER

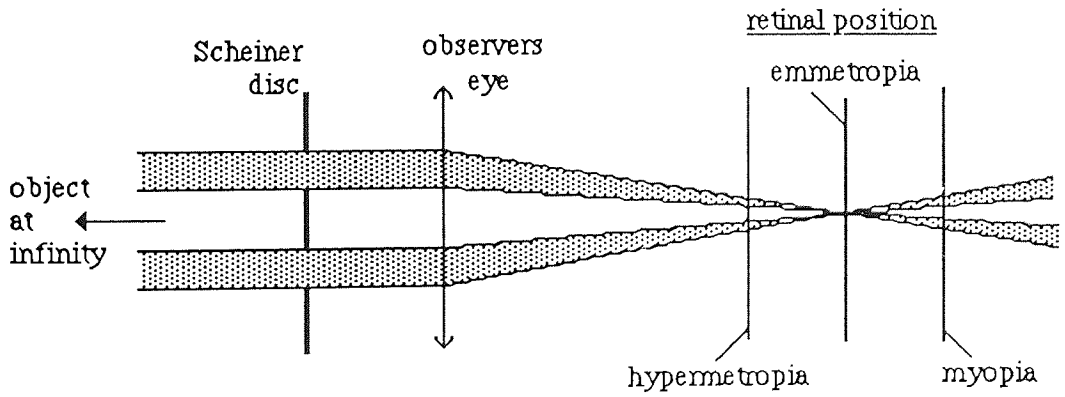

Fig. 2.1 The Scheiner disc principle for measuring refractive error.

Young's optometer uses the principle of the Scheiner disc, which is often used in ophthalmic instruments. An opaque disc is pierced with two small holes, their centres about 2 to 4 mm apart (fig. 2.1). A distant object viewed through these two holes will appear double unless the images of the two apertures coincide on the retina (i.e. the eye is emmetropic). By the addition of the appropriate lens in front of the disc any doubling can be eliminated and the refractive error of the eye can be deduced. To distinguish between myopia and hyperopia one of the apertures is occluded. For a hyperopic eye the two images

produced on the retina are uncrossed, i.e. the image produced by the upper most aperture falls uppermost on the retina. However, on projection into visual space the images become crossed and, if the upper aperture is occluded, the lower image will seem to disappear. The reverse will be true for a myopic eye.

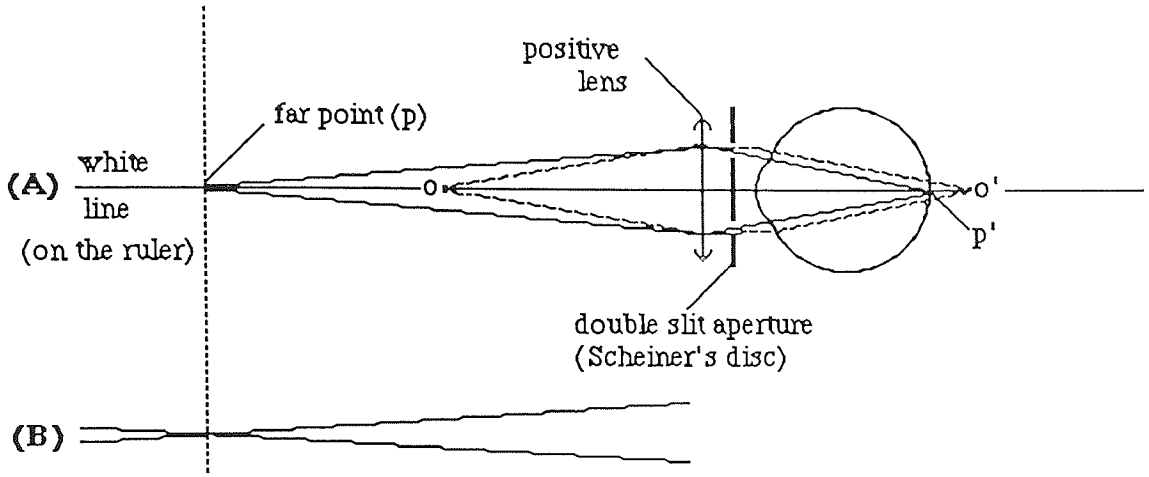

Fig. 2.2 (A) Young's optometer.
(B) the image seen by the observer.

Young's Optometer (fig.2.2a) consists of a short black ruler with a fine white line drawn along its length. At the end of the ruler is a positive lens which makes the observer artificially myopic. An aperture with two vertical slits is placed between the lens and the eye. Rays travelling from the artificial far point, p, of the observers eye and passing through the two slits will be focused at a point p' on the retina. The point on the line will then appear single. Any other point along the line, for example o (fig. 2.2A) the rays passing through the two slits will intercept at a point o' some distance from the retina. These points will therefore appear double and the line will be perceived as two lines which cross at the far point (fig. 2.2b). A cursor is used to indicate where the two apparent lines cross and this gives a measure of the subjects refractive error. If the far point is at the focal point of the lens then the eye is emmetropic.

Young adapted this method to measure spherical aberration, using an aperture with four slits; an inner pair and an outer pair. He observed the images of the line produced by the two sets of slits and found that while his eye was relaxed all four lines appeared to cross at the same point. However, when his eye was accommodated the images through the outer slits seemed to cross at a point beyond those seen through the inner slits. This would

indicate that his eye was well corrected for spherical aberration while relaxed but exhibited over-corrected spherical aberration when accommodated.

Other investigators who have used methods based on Young's optometer are Ames and Proctor (1921) Von Bahr (1945) Jenkins (1963a) Millodot and Sivak (1979) and Pomerantzeff et al. (1984).

2.2.2 ANNULAR RINGS

Asymmetries in the optical system of the human eye cause irregularities in the spherical aberration. In other words at a particular height above the axis the spherical aberration will not be equal in all meridians. In order to obtain a reasonable mean value for the spherical aberration at each height measurements must be made in a number of meridians and an average taken.

Koomen et al. (1949) overcame this by using a number of annular ring apertures of varying diameter. These isolated a particular zone of the pupil with light passing through the aperture at the same height from the reference axis in all meridians at the same time. The observers were required to judge when an object, viewed through the annular rings, was in focus. The focus was varied using spectacle lenses. The dioptric power of the spectacle lens chosen for each annular ring was then compared to that chosen for a small central pupil to give the spherical aberration. Other investigators who used this method were Otero and Duran (1942) - cited by Koomen et al (1949), and Charman et al. (1978).

Methods used by previous investigators to measure the spherical aberration were all based on one of the above methods. There were, however, a number of variations which could have affected the values found. These are discussed individually below.

2.2.3 THE CHOICE OF REFERENCE AXIS

Measurements of spherical aberration must be made with reference to a particular axis. The choice of this reference axis varies from study to study. Both Ivanoff (1956) and Millodot and Sivak(1979) used the achromatic axis, defined by a ray passing through the fovea and entering the eye at a point which causes no chromatic dispersion. Koomen et al. (1949) used the axis around which the greatest symmetry of spherical aberration occurred. However, as pointed out by Koomen et al. (1956), on average the achromatic axis coincides with the axis of greatest symmetry.

Jenkins (1963a) used the visual axis as his reference axis. If the optical system of the eye is approximately centred along the optical axis then the axis of greatest symmetry will be close to it. The visual axis is considered to be, on average, 5° from the optical axis (Tscherning, 1924). Hence aberrations measured relative to the visual axis could be expected to be more asymmetrical. However if average values are taken from all four quadrants measured by Jenkins the asymmetries will be partially compensated for. Averaging will also tend to eliminate any differences between Jenkins' values and those found by other workers using alternative reference axes.

2.2.4 RAY HEIGHT MEASUREMENT

In order to compare data from the different studies it is necessary to be able to compare values for the same height from the axis. The planes at which these heights are measured vary from study to study. Koomen et al. (1949) took the height as the mean radius of the annular rings placed close to the eye, Jenkins (1963a) determined the height 2cm in front of the eye. In the study by Millodot and Sivak (1979) the height was determined by apertures in a disc held just in front of the eye. Pomerantzeff et al. (1984) measured the height in the entrance pupil which is generally very close to the anterior corneal surface. These differences in reference plane for the ray height could obviously cause difficulties in comparing values especially as its position in some studies is not known accurately. For the unaccommodated eye, however, the object can be considered to be at optical infinity for emmetropia. As an illustration of the errors which may occur consider the method of Jenkins (1963a). The position of the object, eye and plane at which the image height is measured is shown in fig. 2.3. This is not drawn to scale for the sake of clarity.

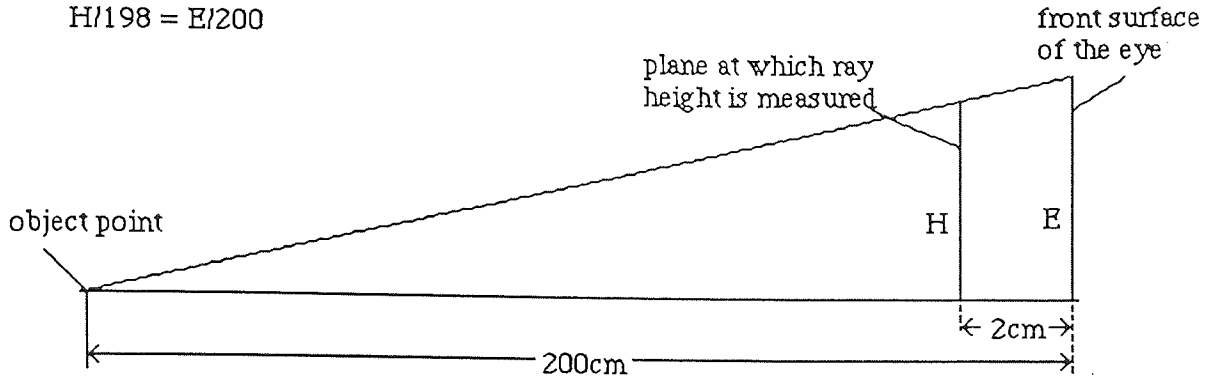

Fig. 2.3 Demonstration of the difference in height at the plane at the eye compared to that the plane at which the ray height is measured. The dimensions used are those of Jenkins' (1963) subjective method.

Using similar triangles it can be seen that the ray height in the plane at the apex of the cornea will be 200/198 times greater than at the reference plane. This will result in a ray height of 0.4 mm being increased to 0.404 mm giving only a 1 per cent error in spherical aberration of about 2 D. An eye with 3 D of myopia corrective lenses will bring the object to a position 33·33 metres in front of the eye. The ray height at the corneal plane will now be 33.33/31.33 times greater than at the reference plane. This results in a ray height of 0.426 mm from an initial height of 0.4 mm and approximately a 6 per cent error for spherical aberration values of approximately 2 D.

2.2.5 SPHERICAL ABERRATION OF LENSES USED DURING MEASUREMENT

Another possible cause of error in spherical aberration measurements is in neglecting the spherical aberration of lenses used in the experimental set up. Jenkins (1963a) and Millodot and Sivak (1979) considered this problem and either took measures to minimise it or considered it to be negligible in all lenses used. Others appear to have overlooked it.

2.3 REVIEW OF INVESTIGATIONS INTO THE SPHERICAL ABERRATION OF HUMAN EYES.

All previous investigations have been in general agreement as to the type of spherical aberration found in human eyes. They all found it to be positive for adult eyes with relaxed accommodation.

2.3.1 INTER-INDIVIDUAL VARIATIONS

Wide inter-individual variation in spherical aberration has been noted by all previous investigators. For example Koomen et al. (1949), who only made measurements on three eyes, found values ranging from 0.75 D to 2 D in the outer most pupil zones for unaccommodated eyes. The wide range of values found imply that mean values, for small samples, do not give reliable representations of the spherical aberrations of human eyes. If a mean value is to be considered representative, it must be taken from a very large sample. Most sample sizes in the previous studies do not meet this requirement. The only large sample size is that of Pomerantzeff et al. (1984) who measured spherical aberration in 100 eyes. Unfortunately, the results of this study were presented in millimetres, not dioptres and, as such, are not comparable with results found from other studies or those calculated in the present study. Van Meeteren (1974) took the mean values from four previous studies and made his own estimate of the mean spherical aberration of human eyes. His values will be used as the mean in the present study as they are already widely accepted.

2.3.2 MERIDIONAL VARIATIONS.

A number of workers measured spherical aberration in more than one meridian (Ames and Proctor, 1921; Von Bahr, 1945; Ivanoff, 1956; Jenkins, 1963a; Pomerantzeff et al., 1984). They found that the spherical aberration varied across meridians in most cases. Jenkins found the maximum variation to be as high as 5 D. Variation is caused by the asymmetry of the optical system. This is due to asymmetrical surface shapes and relative tilts, and/or translations of the optical surfaces.

2.3.3 VARIATION WITH ACCOMMODATION

Koomen et al.(1949), Ivanoff (1947) and Jenkins (1963a) all measured spherical aberration for various states of accommodation. Generally the aberration was found to be positive for the unaccommodated eye and reduced with increasing accommodation, sometimes becoming negative at high levels of accommodation.

2.3.4 VARIATION WITH AGE

An extensive study into the variations of spherical aberration with age was carried out by Jenkins (1963a). He used a retinoscope to measure refraction for a central area of 3 mm diameter and a peripheral zone at the edge of the observer's dilated pupil. Results were taken from 164 eyes of 133 subjects, their age ranging from two to sixty years. The type of

aberration was discussed in relation to age. In general it was found that under the age of six small amounts of negative spherical aberration were exhibited. At the age of six the aberration changed from small negative values to small positive values which increased over the next few years. Jenkins considered this to be due to the growth of the lens. The aberration then seemed to remain constant until around the age of 35 when there was a considerable increase. This was thought to be due to the central zone of the eye becoming hypermetropic while the periphery remained constant. The relative myopia in the periphery would then lead to an increase in positive spherical aberration.

2.3.5 CONTRIBUTION OF THE CRYSTALLINE LENS AND THE CORNEA

Investigators who have studied the spherical aberration of the crystalline lens and the cornea include El Hage and Berny (1973), Millodot and Sivak (1979), Sivak and Kreuzer (1983) and Tomlinson et al. (1993). Two alternative ideas, as to how these two optical elements contribute to the overall spherical aberration of the eye, have arisen . Millodot and Sivak (1979) found that generally the mean spherical aberration values for the whole eye the lens and the cornea were all positive and low. They concluded that spherical aberration was well corrected for each of the optical components of the eye, their contributions being added to give the total aberration. El Hage and Berny (1973) and Tomlinson et al. (1993) both found that for most eyes the cornea had positive spherical aberration higher than that of the whole eye. They concluded that the crystalline lens must therefore have negative spherical aberration, in order to cancel out some of the positive spherical aberration of the cornea. Sivak and Kreuzer (1983) found lenses with both positive and negative spherical aberration.

2.4 MEAN AND RANGE OF SPHERICAL ABERRATION VALUES

The plots of mean spherical aberration against pupil radius for four previous studies are shown in fig. 2.4. The broken line is the curve proposed by Van Meeteren (1974) who based his estimations on the work of Koomen et al. (1949), Francon (1951), Ivanoff (1956) and Schober et al. (1968). The continuous line is the mean, derived for this study, from the four individual studies. The difference in these two estimated mean values can be attributed to the large inter-individual differences in the values found in human eyes.

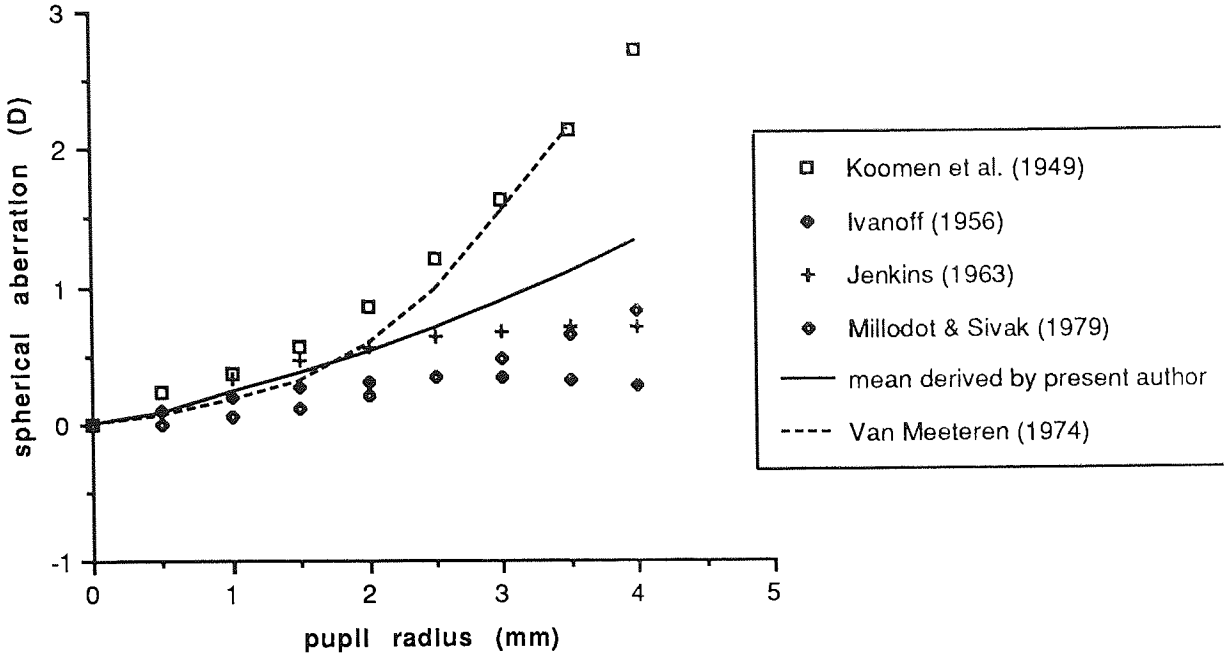

Fig. 2.4 Plot of the mean values of spherical aberration found in previous studies. Also shown are the mean values derived from these studies by the present author and the values given by Van Meeteren (1974).

The data from previous studies has been collated to give a range of values. Not all investigations gave spherical aberration values for individual eyes so in order to obtain a range of values only three of the studies were used, Koomen et al. (1949), Ivanoff (1956) and Jenkins (1963a). Minimum and maximum values are taken from Jenkins' study. Ivanoff's results are considered to be less reliable as they are taken only in two meridians compared to the four taken by Jenkins. This will make the average value for each ray height less accurate. The range is shown in fig. 2.5 along with Van Meeteren's curve and the mean derived by the present author. The range and mean values will be used to compare the on-axis performance of schematic eyes modelled in chapter six with that of human eyes.

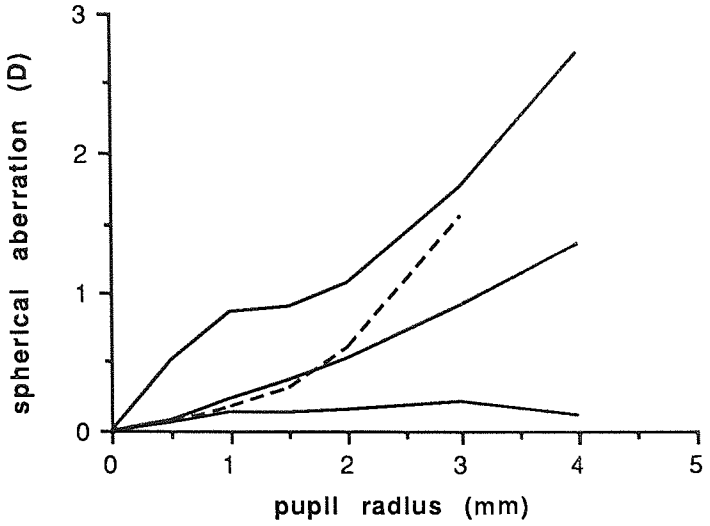

Fig 2.5 The range and mean values of spherical aberration. The solid lines show the maximum and minimum values and the mean derived by the present author. The broken line shows the curve proposed by Van Meeteren (1974).

2.4.1 SPHERICAL ABERRATION FUNCTIONS (SAFS)

A plot of spherical aberration against image height, or aperture radius, is closely fitted by a second order polynomial in most cases. Integration of the equation for the polynomial between 0 and 6 mm aperture radius will give a value for the area under the curve between these limits. This value will be known as the spherical aberration function or SAF. There are two main reasons for calculating SAFs. Firstly, they give a simple numerical value for comparison of overall spherical aberration between eyes. Secondly, they eliminate any irregularities in spherical aberration due to tilts, decentrations and other asymmetries in real eyes. This makes comparison with modelled values easier. The SAF values found for the mean of some of the studies mentioned above are given in table 2.1.

study	N	method	mean SAF
Koomen et al. (1949)	3	annuli	4.0
Ivanoff (1956)	10	Young's	1.4
Jenkins (1963a)	12	Young's	2.6
Charman et al. (1978)	2	annuli	2.4
Millodot and Sivak (1979)	20	Young's	1.1

Table 2.1 Summary of spherical aberration found in previous studies. N is the sample size. The method is either using annular rings or is based on Young's method. The mean SAFs are calculated from the mean plots of spherical aberration against pupil size for each of the studies.

The SAF values for the maximum and minimum eyes from Jenkins' (1963a) study and for the curve proposed by Van Meeteren (1974) are given in table 2.2

	SAF
minimum	5.2
mean	0.8
maximum	2.9

Table 2.2 The range and mean of SAFs found in human eyes

The mean and range of SAFs will be used in this study for comparison with the values given by schematic eyes.

2.5 SUMMARY

The two principal methods of measuring the spherical aberration of human eyes have been explained. Variations between the methods used by individual investigators, and their effect on the results, have been discussed.

The results of previous studies have been briefly reviewed. Generally, the findings were in agreement. They all found positive spherical aberration for unaccommodated eyes with large inter-individual variations. Spherical aberration was found to decrease with accommodation becoming negative in some cases.

Spherical aberration was also found to vary with age; changing from small negative values to small positive values at about six years of age. It then remains fairly constant until the age of 35, after which there is a considerable increase.

The individual contributions of the crystalline lens and the cornea to the total spherical aberration is in dispute. Some workers claim that both have small amounts of spherical aberration which are added together. Other believe that the contribution of the crystalline lens cancels out some of that of the cornea.

The data from previous studies has been collated in order to give a range of values. A quick and easy method for comparing spherical aberration in different eyes has been proposed (the spherical aberration function, SAF). SAF values for the maximum, minimum and mean spherical aberration and for individual studies were calculated. This information can now be used for comparison with modelled data (chapter six).

CHAPTER 3
MEASUREMENT OF PERIPHERAL ASTIGMATISM IN HUMAN EYES

3.1 INTRODUCTION

The rationale behind comparing modelled and measured peripheral astigmatism as an indicator of off-axis performance has been developed in chapter one. This chapter serves to review previous investigations into the peripheral astigmatism of human eyes. The data is collated to derive the range of values for the purpose of comparison with modelled values in a later chapter. The present review is based on work by Charman (1983, 1991a).

3.2 METHODS OF MEASUREMENT

There are three techniques used to measure peripheral astigmatism, retinoscopy, refractometry and subjective methods.

3.2.1 RETINOSCOPY

A standard streak retinoscope is used to measure the refractive error for sagittal and tangential images in the periphery. The investigator firstly takes readings on-axis with the observer looking straight ahead. The observer is then required to fixate a series of targets positioned at predetermined field angles. This method was used by Rempt et al. (1971) and Millodot and Lamont (1974).

3.2.2 REFRACTOMETRY

Measurement of the refractive error in the periphery of the eye using the refractometer is achieved in two ways. Either the refractometer is modified so that it can rotate around the observer's stationary eye (Dunne, 1987; Ferree et al. 1931) or the subjects are required to fixate on peripheral targets (Millodot, 1981; Dunne, 1987). The refractive error can then be measured for varying field angle. To measure refraction for sagittal and tangential images the instrument can be rotated through 180°.

3.2.3 SUBJECTIVE

Jenkins (1963b) measured peripheral astigmatism using horizontal and vertical line targets. These were presented to the eye of the observer at varying field angles. The refractive error was deduced by moving the targets to the position of best focus. Millodot and Lamont (1974) used Landholt Cs as their targets. They determined maximum clarity using correction lenses placed before the observers eye.

Millodot and Lamont (1974) compared the astigmatism of three subjects using the three different methods. The refractive error measures differed by as much as 1 D at 50° field angle; however, the astigmatism values showed closer agreement. The mean of the three subjects at 50° gave a value of about 3 D for refractometry and retinoscopy, and about 3.5 D for the subjective method. At 60° the refractometry method gave a peripheral astigmatism value of approximately 5.7 D, two dioptres higher than for the subjective method at this angle. Measurements using the retinoscope were considered to be unreliable for a 60° field angle.

3.2.4 ERRORS

The errors in the measurement of peripheral astigmatism have two main causes; inaccuracy in measuring the refractive error and inaccuracy in measuring the field angle. Any lens introduced into the system may itself contribute to the peripheral astigmatism and will also alter the angle of the rays entering the eye. Inaccuracies in the field angle occur if rotation is not around the nodal point of the eye. Careful positioning and stability of the subject's head is, therefore, important . No mention is made as to the accuracy of head position or field angle measures in any of the studies. Dunne (1987) took three repeat readings for each measurement of the refractive error to estimate the precision of the refractometers he used. For the Hartinger optometer at 40° he found an average standard deviation of between 0.25 D and 0.43 D. For the Canon Autorefractometer R-1 at 30° he found values of between 0.11 D and 0.37 D. Ferree et al. (1931) found an error of 0.25 D in the centre and mid periphery and 0.37 D to 0.5 D in the far periphery. For retinoscopy Rempt et al. (1971) considered the precision of measurements, taken by different examiners, to be 1 to 1.5 D for a 60° field angle.

A further error, in objective methods, is due to the image being reflected from the fundus and not from the layer of the percipient elements. Ferree et al. (1931) suggest that, for this reason, subjective methods would give more accurate results. Unfortunately, subjective assessment of the position of peripheral focus is difficult and requires a lot of practice.

3.3 REVIEW OF INVESTIGATIONS INTO THE PERIPHERAL ASTIGMATISM OF HUMAN EYES

3.3.1 INTER-INDIVIDUAL VARIATIONS

As for spherical aberration, large inter-individual variations of peripheral astigmatism have been found within the population. Most eyes were found to have significantly increasing peripheral astigmatism with increasing field angle (the type A eyes of Ferree et al., 1931). The tangential image shell becomes progressively myopic increasing field angle whilst the sagittal image shell becomes more hyperopic. Ferree et al (1931) found that 57 per cent of eyes were of this form, Rempt et al. (1971) found it in 51per cent of eyes and Millodot (1981) in 91 per cent of eyes. A few eyes showed almost constant values of peripheral astigmatism with increasing field angle. In these cases both the tangential and sagittal images tends to become more hypermetropic with increasing field angle. Ferree et al. referred to these as type B eyes and found them in 29 per cent of the sample measured. Rempt et al. found 24 per cent of eyes to be type B and Millodot in only 8 per cent. The third type, type C eyes of Ferree et al. (1931) is discussed in section 3.3.2. Rempt et al. (1971) added two more groups to the three of Ferree et al., making a total of five. Their groups are classified according to the general shape of their image shells (fig 3.1)

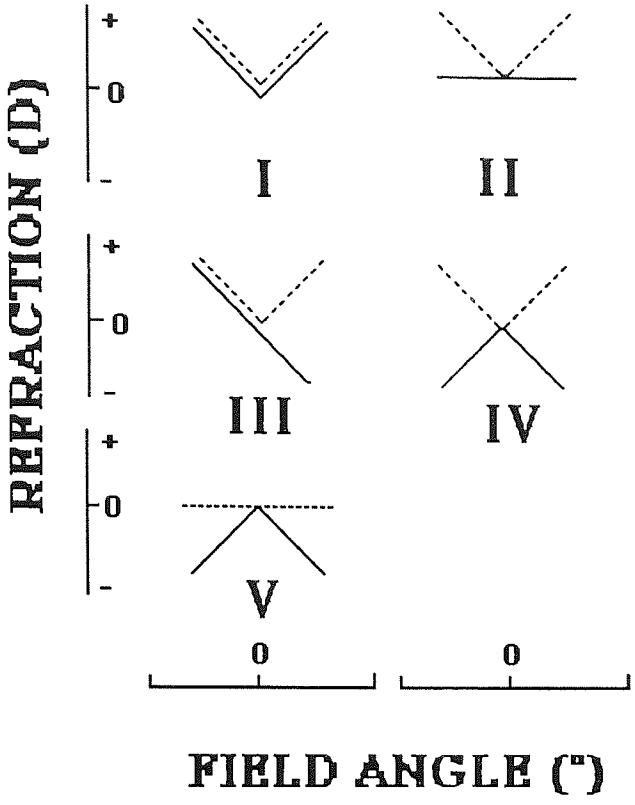

Fig 3.1 The five types of oblique astigmatic image shells of Rempt et al. (1971). The broken lines represent the sagittal image shells and the solid lines the tangential image shells plotted over the horizontal plane. The zero degree field angle coincides with the visual axis and the temporal retina is to right of each diagram.

Type I eyes are the same as the type B eyes of Ferree et al. and are found most frequently amongst myopic subjects. Type IV matches the type A eyes of Ferree et al. (1931) and the majority of eyes exhibit this type of astigmatism, especially among emmetropic and hyperopic eyes. The asymmetrical Type III peripheral astigmatism was only found in near emmetropic eyes and was considered to be due to asymmetry of the optical system. This agrees with the theories of Ferree and Rand (1933). Types II and V are caused by retinal shape variations. The retina lies close to the tangential astigmatic foci in type II eyes and close to the sagittal image foci in type V eyes.

3.3.2 ASYMMETRY

Astigmatic image shells generally show some asymmetry, giving higher values of astigmatism in the temporal half of the retina. This is considered to be due to angle alpha; the angle between the visual and optical axis (Ferree et al., 1931; Rempt et al.,1971;

Millodot, 1981; Barnes et al., 1987, Dunne et al., 1993b). Higher amounts of asymmetry may be attributed to asymmetries in the shape of the eyeball and/or in the optical system due to the relative tilt or translation of optical surfaces. Extreme amounts of asymmetry are probably due the corneal shape (Barnes et al., 1987). Ferree et al. (1931) classified eyes with large amounts of asymmetry as type C eyes. They found 14% of eyes to be of this type, as did Millodot (1981). Rempt et al. found only 3% of eyes with this type of astigmatism.

Ferree et al. (1931) found three eyes with highly asymmetric astigmatic image shells. These were discussed in detail in later papers (Ferree et al., 1932; Ferree and Rand, 1933). They concluded that the shape of the sagittal curve was determined primarily by the shape of the retina and its distance from the nodal point of the optical system. An asymmetrical sagittal curve will be the result of an asymmetrical retina. The shape of the tangential curve was further affected by the refracting system. Hence, the tangential curve and its relation to the sagittal curve gives information as to the symmetry of the refracting surfaces. Asymmetry may be due to tilting or translation of the lens surfaces in relation to the cornea. Consequently asymmetrical astigmatic curves can be caused either by an asymmetrical retina or by asymmetries in the refractive system or by a combination of the two.

Rempt et al. (1971) also measured peripheral astigmatism in the vertical meridian for seven eyes with asymmetric image shells. Four of the subjects exhibited similar vertical asymmetry, but less occurred in the remaining three. The smaller amount of asymmetry in the vertical meridian may indicate that the asymmetry is due to the tilt and/or decentration of the crystalline lens with respect to the cornea. This tends to be greater around the vertical axis (Tscherning 1924) and so would cause greater asymmetries in the horizontal meridian.

3.3.3 VARIATION WITH REFRACTIVE ERROR

An investigation into the effect of ametropia on the peripheral refraction was carried out by Millodot (1981). He used a refractometer to measure the refractive error for angles of 0 to 60° in 32 subjects (62 eyes). He divided the subjects into three groups in accordance with their ametropia. These groups consisted of 30 myopic eyes (-1 D to -7.87 D), 13 near emmetropes (-0.99 D to +0.74 D) and 19 hypermetropes (+0.75 D to 4.5 D).

On average emmetropic eyes exhibit mixed astigmatism in the periphery. Myopic eyes exhibit compound myopic astigmatism and hyperopic eyes exhibit compound hyperopic

astigmatism with mixed astigmatism in the far periphery. The amount of astigmatism, however, was found to be independent of ametropia.

The rate of change in the sagittal refractive error is greatest for myopes and lowest for hypermetropes the reverse is true for the tangential refractive error. Charman and Jennings (1982) considered that, as the interval of Sturm is independent of ametropia, this difference in the rate of increase can be attributed to differences in the length of the eye. They concluded that the principal cause of ametropia to be the axial length; predicting that for high peripheral angles, near to the equator of the eye, all eyes would have similar refractive errors. This is nearly the case for Millodot's three groups at 60° field angles. This was subsequently modelled in schematic eyes by Dunne et al. (1987)

3.3.4 VARIATION WITH ACCOMMODATION

The variation of astigmatism with accommodation was examined by Millodot and Thibault in 1985. Astigmatism was measured in 122 eyes, using an autorefractometer. Accommodation was controlled by changing the viewing distance. They found that, on average, the change in astigmatism with accommodation is clinically insignificant.

3.3.5 VARIATION WITH AGE

Millodot (1984) found that young and old aphakic eyes have approximately the same amount of peripheral astigmatism and so concluded corneal astigmatism does not change with age. In phakic eyes peripheral astigmatism does increase with age, this increase is attributed to the change in curvature of the lens, as the refractive index is found to be constant. Millodot believed that the lens became flatter near the axis and more curved in the periphery.

3.3.6 CONTRIBUTION OF THE CRYSTALLINE LENS AND CORNEA

The peripheral astigmatism in human eyes is lower than that found in spherical surfaced schematic eyes (Le Grand 1967). Millodot and Lamont (1974) attempted to ascertain if the asphericity of the corneal surface is responsible for the reduction in peripheral astigmatism. They added a spherical contact lens to one of their subject's eyes and remeasured the peripheral astigmatism. No appreciable difference was found and they concluded that the lens surface shape and gradient index is responsible for reduction in peripheral astigmatism. Reaching this conclusion on the evidence given by only one eye does seem a little hasty, considering the wide range of shapes of corneas found in the human

population. The shape of the cornea to which the contact lens was added was not noted and may have already been spherical.

Millodot (1984) also carried out a further study, to ascertain whether astigmatism is due principally to the cornea, the lens or to both equally. He measured peripheral refraction with a refractometer in 16 aphakic eyes and 10 phakic eyes. Millodot found that in aphakic eyes the peripheral astigmatism was 1/2 to 1/3 that of phakic eyes, suggesting that the lens generally contributes more astigmatism than the cornea. However the age of the subjects ranged from 62 to 84 and as peripheral astigmatism of the lens increases with age the same conclusion cannot be drawn for younger eyes.

3.4 MEAN AND RANGE OF PERIPHERAL ASTIGMATISM VALUES

The mean value for the investigation of Rempt et al. (1971) was taken from Lotmar and Lotmar (1974) . They read the values from the diagrams of Rempt et al. to the nearest dioptre, excluding all subjects with greater than 1 D ametropia or central astigmatism; by this means 363 cases remained. The mean values showed a high degree of similarity for left and right eyes. Asymmetry occurred between temporal and nasal values of peripheral astigmatism. As noted in section 3.3 the higher values of astigmatism in the temporal half of the retina were considered to be due to angle alpha. They showed that a high degree of symmetry is achieved about the optical axis when angle alpha was taken to be 4°. Sturm's interval (Δ) could then be approximated by:-

$$\Delta = a^{1.5} \times 10^{-2}$$

where a is the visual angle in degrees.

The results from a number of studies are shown graphically in fig 3.2.

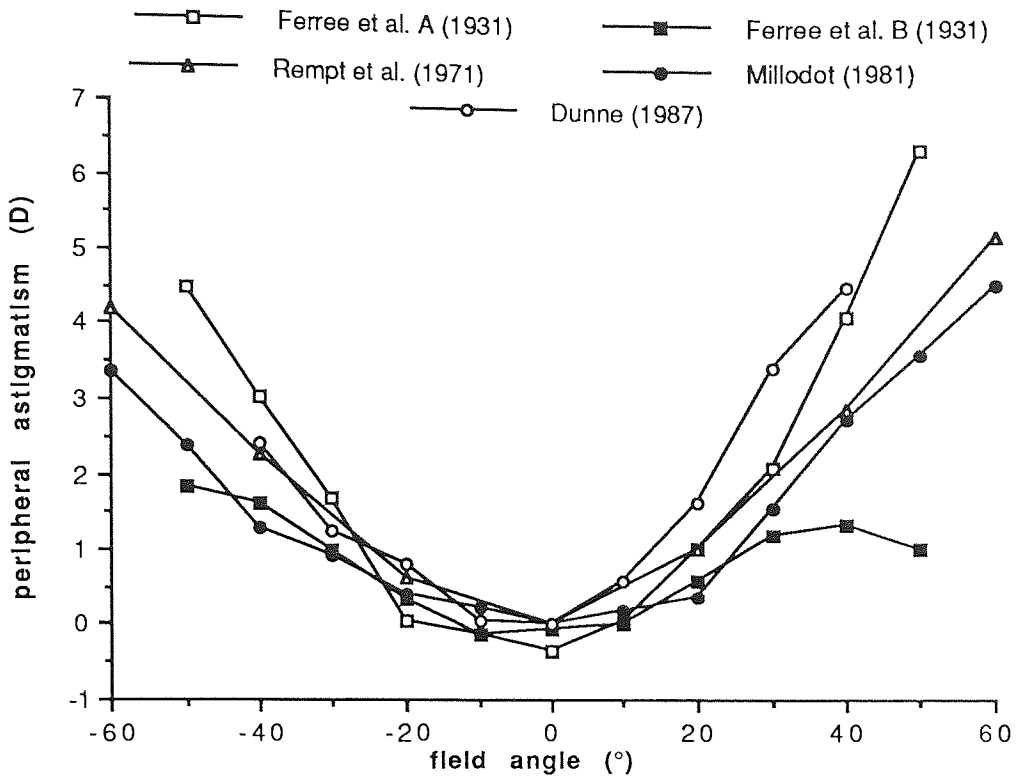

Fig. 3.2 Comparison of measures of peripheral astigmatism in human eyes from previous studies.

In order to obtain a range of values for peripheral astigmatism, for comparative purposes, individual values are needed. These are only given by Ferree et al. (1931), Jenkins (1963b) and Dunne (1987). The maximum and minimum values used in this study were found in the work of Ferree et al. (1931). The mean value is that of Lotmar and Lotmar (1974), taken from the data of Rempt et al. (1971). This study had by far the greatest sample size and is considered to be the most representative mean. The plot of astigmatism against field angle for the range and mean is shown in fig. 3.3.

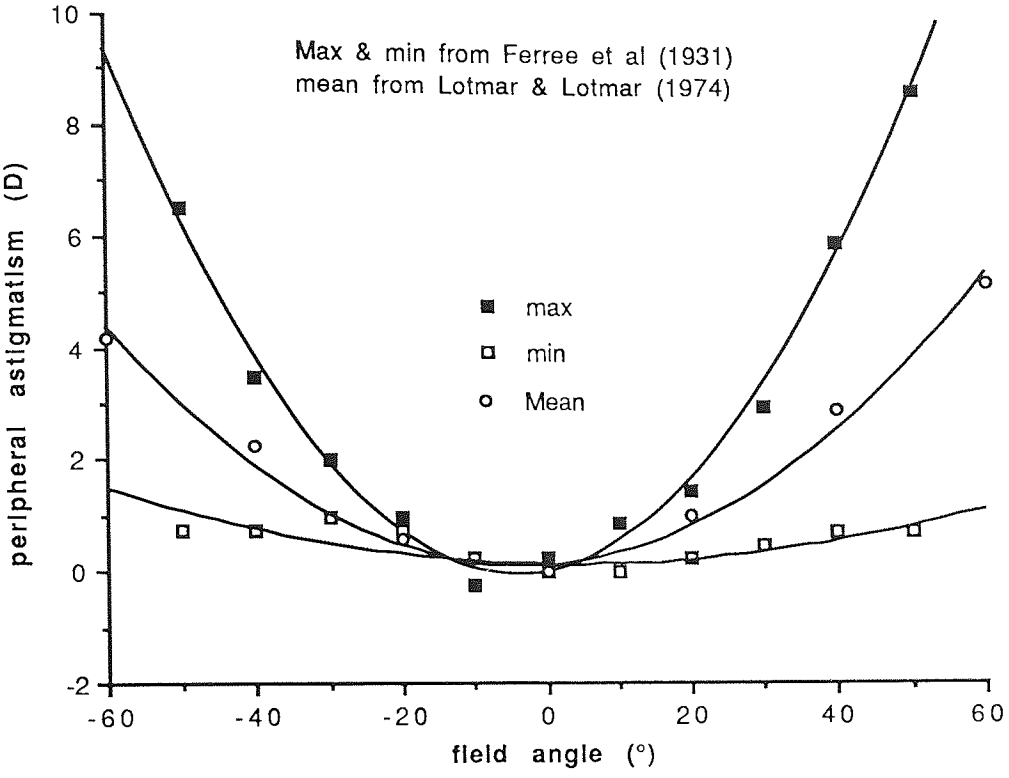

Fig. 3.3 The maximum, minimum and mean values of peripheral astigmatism as a function of field angle. The maximum and minimum values are taken from the study of Ferree et al. (1931). The mean values are taken from Lotmar and Lotmar (1974) who calculated the mean from the data of Rempt et al. (1971).

3.4.1 PERIPHERAL ASTIGMATISM FUNCTIONS (PAFs)

As for spherical aberration in chapter two, peripheral astigmatism can be expressed in terms of a single value called the peripheral astigmatism function (PAF). Second-order polynomials are fitted to the plots of peripheral astigmatism against field angle. The area under these curves from 40° nasally to 40° temporally is calculated by integration, this gives the PAF. The PAF of the mean values given in the studies shown in fig. 3.2 are shown in table 3.1.

study	N	method	mean PAF
Ferree et al. (1931) - type A	6	refractometry	100.2
- type B	5	refractometry	34.4
Rempt et al. (1971)	363	retinoscopy	66.0
Millodot (1981)	62	refractometry	53.4
Dunne (1987)	34	refractometry	103.5

Table 3.1 Summary of the mean peripheral astigmatism results found in previous studies. N is the sample size. The mean PAFs in dioptres x degrees were calculated from the mean plots of peripheral astigmatism versus field angle for each study. The mean PAFs for Ferree et al (1931) type A and type B eyes are give (see Section 3.3.1)

The mean PAF values for the individual studies clearly vary greatly (table 3.1). This may be for a number of reasons. The large variation of astigmatism from individual to individual is well documented in the studies mentioned above. The methods used have also been shown to give differing values and so could explain some of the variation in mean values from study to study.

The PAF values for the mean, maximum and minimum values are shown in table 3.2.

	PAF (D°)
minimum	24.7
mean	66.0
maximum	128.8

Table 3.2 The range and mean of PAFs found in human eyes.

The mean and range values will be used in this study for comparison with the values given by schematic eyes.

3.5 SUMMARY

The three methods for measuring peripheral astigmatism have been explained. The problems and errors of each have been discussed.

The results of previous investigations have been briefly reviewed. As for spherical aberration, the findings were generally in agreement. In the majority of eyes the interval of Sturm was found to increase with obliquity. However, in some eyes it was found to be

almost constant as obliquity increased. A small amount of asymmetry, attributed to angle alpha, was found in most eyes. Some eyes showed much larger amounts of asymmetry, the probable causes for this have been discussed.

The variation with refractive error was shown to be mainly due to the difference in axial length. No significant variation with accommodation was found, but peripheral astigmatism has been found to increase with age.

Comparison of measurements from aphakic and phakic eyes have suggested that the lens contributes more towards the total peripheral astigmatism of the eye than the cornea. It was also suggested that the flattening of the cornea in the periphery does not reduce peripheral astigmatism. The evidence, however, is thought to be inconclusive.

The data from previous studies has been collated in order to give a range of values. A new method for comparison of peripheral astigmatism has been proposed using a single value called the PAF, similar to the SAF introduced in chapter two. The PAF values for maximum, minimum and mean peripheral astigmatism and for individual studies were calculated. This information can now be used to compare with the modelled data of chapter seven.

CHAPTER 4
THE OPTICAL PARAMETERS OF THE HUMAN EYE

4.1 INTRODUCTION

The purpose of this chapter is to establish a range of values for each of the optical parameters of the human eye. In later chapters they will be incorporated into schematic eyes in order to show the range of aberrations attainable by altering each individual parameter within measured ranges. An overview of the methods used to measure each of the optical parameters is included, with a brief account of the general ocular anatomy. Studies measuring each of the optical parameters are reviewed to determine mean, maximum and minimum values.

A number of reviews of biometric measurement techniques have been written (Bennett and Rabbetts, 1984; Dunne, 1987; Royston, 1990; Charman, 1991b; Henson, 1991). The anatomy of the eye is described in many text books. Bennett and Rabbetts (1984) provide a short description. A more detailed treatment is found in Charman (1983, 1991a). The general structure of the eye is shown in schematic horizontal section in fig. 4.1. Each of the optical parameters are discussed separately below.

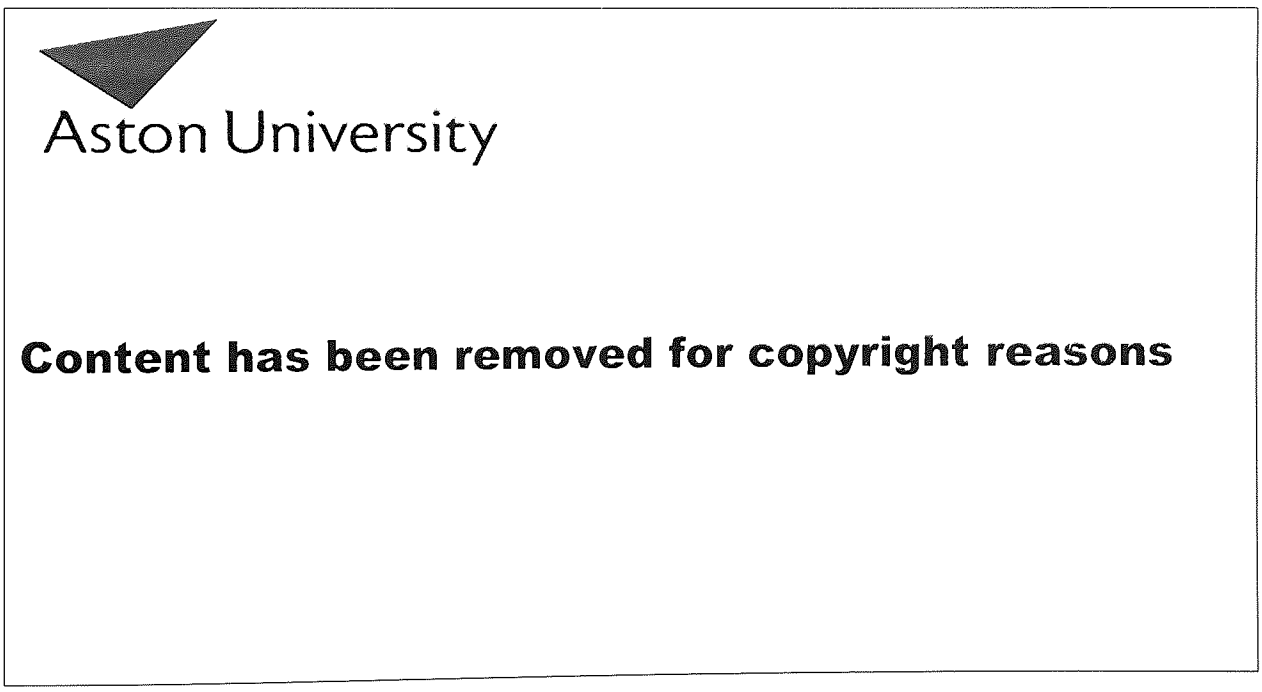

Fig. 4.1 A schematic horizontal section of the human eye - from Smith, 1990

4.2 THE CORNEA

The cornea has a complex structure made up of a number of layers; the anterior epithelium, Bowman's membrane, the stroma, Descemet's membrane and the posterior endothelium. Refractive indices of these layers vary slightly from each other, causing scattering of light

which allows the cornea to be viewed with a slit-lamp microscope. The average refractive index is about 1.3371. The stroma makes up about 90 per cent of the overall thickness of the cornea and as such its structure is of most interest. Constituent collagen fibres are seemingly of uniform size and are arranged in a regular pattern which results in transparency of the cornea. The surface of the cornea is covered by a thin tear film between 7-9 μm thick (Ehlers, 1965; Maurice, 1967). Refractive effects of this thin layer are often ignored, but Charman (1991a) considers that irregularities in its thickness must have some effect on the quality of the retinal image. Central thickness of the cornea is about 0.5 mm thickening to 0.7 mm in the periphery (Hirji and Larke, 1978; Azen et al. 1979).

The cornea has an average horizontal diameter of about 11 mm and an average vertical diameter of about 12 mm. Its anterior surface radius is approximately 7.8 mm and its posterior surface radius approximately 6.5 mm (Le Grand and El Hage, 1980). Stenstrom (1946, 1948) collated the results of measurements of optical parameters, including corneal radii, from a number of studies resulting in a sample size of one thousand eyes.

The contour of the anterior corneal surface has been studied extensively since the advent of contact lenses. It is of particular interest as the anterior cornea makes the greatest contribution to the overall refractive power of the eye (approximately 49 D of the total 60 D). The cornea generally has its steepest curvature at the anterior pole and then flattens out towards the periphery. There are wide variations in the topography however and in some instances the cornea curvature may even steepen towards the periphery (e.g. Keily et al., 1982). Assuming rotational symmetry, sources have described its shape with a variety of mathematical expressions (e.g.Bonnet and Cochet, 1962; Keily et al., 1982; Kooijman, 1983, Guillon, 1986). Kiely et al. (1982) used a conicoid equation:

$$x^2 + y^2 + (1 + Q)z^2 = 2zr_o$$

where z is measured along the axis of rotational symmetry and x and y are cartesian coordinates perpendicular to this axis, r_o is the radius of curvature at the corneal apex and Q is the asphericity parameter which specifies the form of the conicoid. Kooijman (1983) and Guillon et al.(1986) use the conic constant, p which is related to the asphericity parameter, Q by the equation:

$$p = 1 + Q$$

The forms of the conicoids specified by these two parameters are:

$Q > 0$ $(p > 1)$	An ellipsoid (major axis in x/y plane)
$Q = 0$ $(p = 1)$	A sphere
$-1 < Q < 0$ $(0 < p < 1)$	An ellipsoid (major axis along z-axis)
$Q < -1$ $(p < 0)$	A hyperboloid

For a surface which is rotationally symmetrical about the z-axis, the term $(x^2 + y^2)$ in the conicoid equation can be replaced by a single term y^2, where y is the distance perpendicular to the z-axis. Keily et al. (1982) found the average value of Q to be -0.26 (p = 0.74) with a standard deviation of 0.18, the results of Guillon et al. (1986) were similar with an average conic constant, p of about 0.8 and standard deviation of 0.15. Kooijman (1983) uses a p value of 0.75 in his average schematic eye.

In reality the corneal surface is not rotationally symmetrical. Peripheral flattening usually occurs more rapidly on the nasal than the temporal side and usually more superiorly than inferiorly (Gullstrand 1924). In addition it is also decentred horizontally from the line of sight by as much as 0.5 mm although there is some disagreement as to the directional trend; some workers found it to be predominantly temporal (Gullstrand, 1924; Bonnet and Cochet, 1962) while others found no trend (Mandell and St Helen, 1971).

The corneal surface also tends to be toric in shape with generally greater curvature in, or close to, the vertical meridian rather than in the horizontal meridian. This results in vertical rays, travelling parallel to the optical axis, focussing in front of horizontal rays which are at the same distance from the axis. This is referred to as with-the-rule astigmatism (see Bennett and Rabbetts, 1984).

The posterior corneal surface has been given very little attention. This is partly because of the difficulty in measuring it ,due to it being inaccessible, but also because its contribution to the overall dioptric power of the eye is small (~-6 D) compared to that of the anterior surface (~48 D). However, studies of the variation of the corneal thickness suggests that its shape closely follows that of the anterior cornea (Tomlinson, 1972). Although Lowe and Clark (1973) considered that the cornea becomes thicker in the periphery not only because the posterior cornea has a smaller radii of curvature but also because it does not flatten out as rapidly.

4.2.1 CORNEAL THICKNESS MEASUREMENTS

a) PACHOMETRY

This is a method used to measure the thickness of the cornea and the anterior chamber depth using slit lamp techniques. It was first described by Blix (1880) who focussed the slit lamp firstly on the anterior and then on the posterior surface of the cornea. He used the distance moved between successive foci to measure the apparent thickness. The true distance could then be calculated knowing the refractive index of the cornea and the power of its anterior surface. Unfortunately this method suffers from errors introduced by eye movements. Von Bahr (1948) modified this method to overcome these problems. He used two glass plates which could be rotated to make the images from the anterior and posterior surfaces coincide. The angular rotation of the glass plates required to achieve this can be related to the true thickness of the cornea using trigonometry. The standard deviation found for measurements of the corneal thickness was ±0.013 mm. A number of other sources have made slight changes to this method in an attempt to improve its accuracy (Maurice and Giardini, 1951; Donaldson, 1966; Mandell and Polse, 1969; Hirji and Larke, 1978).

Lowe (1966) uses a Haag Streit 900 slit lamp and it is now the most widely used pachometer technique. The random errors for this method were assessed by Alsbirk (1974) who found errors in triple readings of ±0.007 mm and in successive readings over several weeks of ±0.013 mm. Royston (1990) took 3 readings for each measurement and found an estimated precision of between 0 and 0.023 mm, with a mean of 0.018 mm. Edmund and La Cour (1986) also studied the precision of pachometry measurements and found that Diurnal variations were ±0.006 mm, slit lamp adjustment caused variations of ±0.005 mm and pachometer adjustment variations of ±0.013 mm.

One criticism which may be levelled at the Haag Streit 900 slit lamp technique is that the depth measurements are made with respect to the line of sight. This may induce errors as the line of sight does not pass through the geometric centre of the cornea. Alsbrick (1974), however, found no systematic difference in the measurements taken for right and left eyes which would result if the misalignment caused significant errors.

b) ULTRASONOGRAPHY

Direct measurement of axial separations is only possible at present by using ultrasonic techniques. X-ray techniques were used in the past to measure the total axial length, but this method is no longer used because of the danger of damage to the eyes.

Ultrasonic techniques measure the time taken for an ultrasonic wave to travel to and from the ocular surfaces. Distances can then be deduced from the velocity of the waves in each of the media through which it has travelled. Ultrasonic waves are produced by a probe which is placed in contact with the anterior corneal surface. The reflected echoes produce an electric voltage which can be recorded as peaks on an oscilloscope. The axial distances correspond to the products of the time for the echoes to return and the velocity of the ultrasonic waves in the corresponding media. Accurate calculation of axial lengths from the measured time delays rely heavily on the accuracy of the assumed velocities of the ultrasonic waves through the ocular media.

To achieve a precision of around ±0.1 mm an ultrasound frequency of 20 MHz would be needed (see Charman, 1991b). Lower frequencies give poorer resolution but better penetration. In ophthalmology typical frequencies are between 6 and 20 MHz. Zadnik et al. (1992) found the 95 per cent limits of agreement for ultrasonic measurement of the axial separations. For the anterior chamber depth they found the variability to be ±0.29 mm. This was considered to be partially due to the applanation of the corneal surface caused by the contact probe. Lens thickness measurements were found to be the most reliable having a repeatability of ±0.20 mm. For the vitreous chamber the repeatability was found to be ±0.37 mm.

Comparison of axial length from measurement by ultrasonography and calculation from optical measurements revealed that ultrasound gave a shorter length of approximately 0.1 mm (Zadnik et al., 1992). This statistically significant difference arises from the fact that ultrasonic measurements are taken from the outermost surface of the retina whereas optical methods are referenced to the photoreceptor layer behind. When comparing their values of ultrasonic and optical measurements Sorsby et al. (1957, 1961) added an arbitary 0.5 mm to their ultrasound result. They also found their 95 per cent limits of agreement of the two methods to be as high as ±0.64 mm (Sorsby et al., 1963).

c) IN-VITRO MEASUREMENTS

Most early investigators carried out biometric measurements on sections of dead eyes. This resulted in inaccurate measurements because of the anatomical changes which take place once the eye is dead. The intra-ocular pressure is no longer maintained causing the eye to collapse and the shape of surfaces and their separations alter. Also the pumping system which keeps the cornea at a constant level of hydration stops and the cornea hydrates and thickens. Early measurements of corneal thicknesses were double those found with the more modern optical techniques (see Scammon and Wilmer, 1950).

The mean and range of corneal thickness values were taken from later studies. These were:- Von Bahr (1948), Maurice & Giardini (1951), Donaldson (1966), Giglio et al. (1968), Martola & Baum (1968), Lowe (1969b), Mandell & Polse (1969), Kruse-Hansen (1971), Leighton & Tomlinson (1972), Hirji & Larke (1978), Azen et al. (1979), Olsen & Ehlers (1984), Royston (1990).

4.2.2 ANTERIOR CORNEAL RADIUS MEASUREMENTS - KERATOMETRY

Keratometers are designed to measure the curvature of the anterior corneal surface. The principle of the method is to image an object of known size by reflection from the anterior corneal surface and then measure the size of this image (Purkinje image I). The resulting magnification can be used to calculate the radius of curvature. First order optical equations are used which lead to inaccuracies in the results. To overcome this keratometers are calibrated to spheres of known curvature.

There are a variety of keratometers presently in use, only the basic principles will be described here. The object consists of two mires, representing the ends of an extended object, which are separated by a small distance. The radius of curvature of the corneal surface is directly proportional to the separation of the two images formed by these two mires . In practice it is difficult to measure the separation of the image against a scale because of involuntary eyes movements. To overcome this a doubling technique is employed whereby the image size is measured by the lateral displacement needed to make a double image coincide. For toric corneal surfaces, keratometers are designed so that location of principal meridians can be readily found.

Since the cornea usually flattens in the periphery the separation of the mires will affect the accuracy of the readings. Separation is usually about 3 mm and never smaller than 2 mm. Bennett and Rabbetts (1984) consider than the error in the measurement of the radius

would probably not exceed 0.05 mm in normal eyes. Attempts to increase accuracy by having the mires closer together was shown to reduce the precision of the measurement (Charman, 1972) . Focussing errors, caused by aberrations of the examiner's eye, may affect the focus of the instrument. Also, local distortion of the subject's cornea can distort the mires making them difficult to focus and position. Stone (1962) showed that errors due to incorrect focussing of the mires and eyepiece and accommodation of the observer's eye could be as large as 0.4 mm for radius measurements.

Charman (1972) estimated the effects of diffraction on the accuracy of keratoscopes and concluded that it would limit the precision of readings to about ±0.04 mm (±0.2 D). Clark (1973) gave an average standard deviation of ±0.015 mm for the reproducibility of a number of readings. This concurs with the conclusion of Charman if it is considered that 95 per cent of the range of a normal population will fall within the limits of two times the standard deviation. Zadnik et al. (1992) took repeat readings on two occasions and found a much higher value for the 95 per cent limits of agreement of ±0.93 D. This is equal to 0.15 mm if the refractive index of the cornea is assumed to be 1.3771.

Measurement of the anterior corneal radius has been carried out by the following:- Tscherning (1898), Stenstrom (1948), Sorsby et al.(1957), Sorsby et al. (1962), Lowe (1969a), Leighton & Tomlinson (1972), Clark (1974), Francois & Goes (1977), Kiely et al. (1982), Guillon et al. (1986), Dunne et al. (1992)

4.2.3 POSTERIOR CORNEAL RADIUS MEASUREMENTS

Lowe and Clark (1973) used pachometry to estimate the radius of the posterior cornea. Dunne et al. (1992) adopted a method which involved measuring the Purkinje image heights (I and II), from photographs, in three fixed meridians. From knowledge of the anterior corneal radius, the corneal thickness and the ratio of the two Purkinje image heights the posterior corneal radius could be calculated. Good repeatability was achieved, the correlation between repeat values being as high as 0.96.

4.2.4 ANTERIOR CORNEAL ASPHERICITY MEASUREMENTS

a) TOPOGRAPHIC KERATOMETRY

The asphericity of the cornea can be measured by taking a number of measures of radii of curvature in the periphery. The accuracy of this method is proportional to the separation of the mires (Mandell and Polse, 1969). Investigators have attempted to increase accuracy by

reducing the separation of the mires (e.g. Bonnet and Cochet, 1962) but this results in a reduction in precision. Charman (1972) found the lowest limit of precision to be 0.1 mm.

b) KERATOSCOPY AND PHOTOKERATOSCOPY

Keratoscopes are used to examine the corneal contour over a large area. They use the reflection from the anterior corneal surface, as does the keratometer, only the objects are a number of concentric bright rings which are reflected from the corneal surface. The shape of the reflected images of these rings give an indication of the shape of the cornea. Elliptically shaped reflections are an indication of astigmatism, while distorted or asymmetrical reflections are caused by surface irregularities.

In order to make quantitative measures of the corneal contour photokeratoscopy is used. This involves photographing the reflected images of the bright rings and then analysing the photograph. Because the images of the rings suffer from field curvature a hemispherical or elliptical object surface is used that is concentric with the cornea. This allows all the rings to be in focus at one time on the flat image surface. Obviously the shape of the object surface will not give accurately focussed images for all corneas because of the inter-individual variation of radii and asphericity.

During analysis each of the rings is treated as a separate object and the results are then combined to give a value for the corneal profile. Conic curve equations can be fitted to the results (see section 4.3.1). Most of the problems experienced in photokeratoscopy are involved with the film on which the photograph is taken. Instabilities in film - such as shrinkage - can lead to inaccuracies as can unclear images which make it difficult to locate the edges of the ring images.

Zadnik et al. (1992) found keratoscope values to be less repeatable than keratometer values. Keratoscopes gave 95 per cent limits of agreement of ±2.02 D. This equals 0.31 mm if the corneal refractive index is assumed to be 1.3771. This contradicted previous findings that showed repeatability was improved using a keratoscope, as oppose to a keratometer. The large variability was found to be due to the video/computer analysis of the cornealscope photographs for two of the subjects. Zadnik et al. considered that poor repeatability limits the usefulness of keratoscopes. Other investigators have found cornea modelling can be achieved with acceptable repeatability, over large corneal areas using such computer assisted corneal topographic modelling systems (Hannush et al., 1990).

Measurements of the anterior corneal asphericity have been taken by:- Knoll (1961), Pretchtel & Wesley (1970), Mandell & St Helen (1971), Fujii et al. (1972), Clark (1974), Kiely et al. (1982), Edmund & Sjontoft (1985), Guillon et al (1986), Dingeldein & Klyce (1989)

4.3 THE ANTERIOR CHAMBER

The anterior chamber is filled by a colourless, transparent liquid called the aqueous humour. It is an excellent optical medium causing very little scattering of light unless contaminated with debris. The depth of the anterior chamber is usually measured from the anterior corneal surface to the anterior lens surface, and so includes the thickness of the cornea. Average values of about 3.6 mm have been found by most sources. This reduces with increasing age because of the corresponding increase in the thickness of the lens (e.g. Weale, 1963). The anterior chamber also decreases with accommodation. Table 4.1 reviews previous investigations measuring the anterior chamber depth.

4.3.1 MEASUREMENT OF ANTERIOR CHAMBER DEPTH - SLIT LAMP TECHNIQUES

The anterior chamber depth can be measured by using ultrasound, pachometry or other slit lamp techniques.

Slit lamps can be used to measure the axial separations and surface curvature of ocular surfaces. They consist of a light source, which produces a slit beam of light at the eye and a microscope and sometimes a camera attachment. The slit beam produces an optical section of the eye. This is viewed by the microscope for clinical examination or photographed for biometric measurement. The optical section is produced by the scatter of light at each of the optical surfaces.

The central problem in using photographs of these sections to measure the parameters of the eye is that the images from the optical surfaces do not focus at the same distance from the camera objective. The small depth of focus of most slit lamps ensures that not all of the section will be in focus at one time. A solution to this problem was formulated by Brown (1973). He adapted the techniques, used by Scheimpflug, an architect, to photograph large buildings. This entailed either the objective plane or the film plane being tilted so that all the section will be in focus at one time.

The measurements made from slit lamp sections only give apparent axial separations, from which real separations must be calculated. The calculations require an estimate for the corneal radii and lenticular equivalent mirror surface radii, the central refractive error and refractive indices. Paraxial equations are then used which rely on a number of assumptions. The accuracy of the final measures of the ocular parameters are therefore dependant on the accuracy of all the other measures.

Previous measurements of anterior chamber depth has been carried out by the following investigators:- Raeder (1922), Stenstrom (1948a), Sorsby et al. (1957), Calmettes (1958) - Translation (1966), Sorsby et al. (1962a), Gernet & Fraceschetti (1967), Giglio et al.(1968), Leighton & Tomlinson (1972), Francois & Goes (1977)

4.4 THE PUPIL

The pupil is a circular opening in the iris and is situated approximately tangentially to the anterior lens surface. It is an essential part of the optical system. It controls the amount of light reaching the retina and also affects the image quality because of its effects on diffraction, aberration and depth of focus.

The size of the pupil is controlled mainly by ambient lighting. A number of other factors, accommodation, emotion and drugs have also been identified (see Charman, 1983, 1991a). The diameter of the pupil normally varies between 2 and 5 mm (Zinn, 1972). On average it is decentred temporally with respect to the line of sight (Gullstrand, 1924; Jennings and Charman, 1978). The finite thickness of the pupil means that its size is effectively reduced for off-axis imaging.

4.5 THE CRYSTALLINE LENS

The crystalline lens is a transparent, bi-convex structure. It is built up of layers of hexagonal fibres which stretch from the anterior to the posterior pole. The elasticity of its structure allows it to deform and vary its thickness to focus objects at varying distances onto the retina.

Layers are added to the lens throughout life, increasing its size with age (e.g Weale, 1963). The onion like layers have progressively decreasing refractive indices towards the cortex.The highest refractive index at the nucleus is about 1.41 and the lowest at the cortex about 1.38 (Nakao et al., 1969). For an homogeneous lens to be of equivalent power it would need a refractive index of 1.42 (Gullstrand, 1924).

The average thickness of the lens is about 3.6 mm and ranges from about 2.9 to 4.5 mm (Stenstrom, 1946). Accommodation of the lens not only increases its thickness and alters the surface curvature and shape, but also alters the gradient index structure. The aberrations of the eye will, therefore, change with accommodation. Previous measures of lens thickness are reviewed in table 4.6. The average curvature of the lens surfaces are about 10 mm for the anterior surface and -6 mm for the posterior surface (Le Grand And El Hage, 1980).

Measurement of the surface shapes of the crystalline lens is far more difficult than for the anterior corneal surface, and little data exists. The most recent work has been reviewed by Smith et al. (1991). On average both surfaces appear to flatten peripherally . Kooijman revised his 1983 average values of p (taken from the work of Howcroft and Parker, 1977) to give values of p = -5.05 (Q = -6.05) for the anterior surface and p = -0.19 (Q = -1.19) for the posterior surface (see Smith et al. 1991). As for other ocular parameters, the range of values is vast. Smith et al. (1991) noted the unpublished data of Parker which gave standard deviations of ± 9.41 for the anterior surface and ± 1.74 for the posterior surface. Hence, some lenses may steepen in the periphery for both surfaces. Aspheric flattening of the lens will reduce spherical aberration. Reviews of previous investigations into the asphericity of the anterior and posterior lenticular surfaces are given in tables 4.9 and 4.10 respectively.

Brown (1973) found that the central radius of the anterior lens surface decreases considerably with accommodation. In all but very young eyes the peripheral radius was found to increase with accommodation, making the surface more conicoid. He also discovered that the posterior surface central radius reduces with accommodation but to a lesser extent than the anterior. The peripheral posterior radius showed little change in any of the subjects. The conicoid shape of the posterior cornea will therefore be less marked than for the anterior surface. This increased flattening of the lens surfaces in the periphery, with accommodation, would explain the reduction in spherical aberration observed by a number of investigators - (e.g.Koomen et al., 1949; Ivanoff, 1956) - see section 2.3.3.

There is some controversy over the age related changes of the crystalline lens radii. The most general view seems to be that the central radius of the lens increases with age, explaining the tendency toward hypermetropia in older eyes (Bennett and Rabbetts, 1984). The thickness of the lens increases by about 1mm between the ages of 20 and 65. During this time the lens also moves forward, decreasing the anterior chamber depth by about 0.6 mm. However Brown (Brown, 1974) found that the central and peripheral radii of the

anterior and posterior surfaces decrease with age, the posterior surface changes being at a slower rate.

4.5.1 MEASUREMENT OF THE THICKNESS OF THE CRYSTALLINE LENS

The crystalline lens thickness can be measured using either in-vitro methods, ultrasound or slit lamp techniques. Previous investigators are:- Stenstrom (1948), Gernet & Franschetti (1967), Giglio et al. (1968), Leighton & Tomlinson (1972), Francois & Goes (1977), Howcroft & Parker (1977), Dunne (1987), Pierscionek (1989) - cited Smith et al. (1991).

4.5.2 MEASUREMENT OF CRYSTALLINE LENS RADII

a) PHAKOMETRY

Phakometry is the term used to describe the method of measuring the curvature of the anterior and posterior surfaces of the crystalline lens. It uses Purkinje images III and IV to calculate the equivalent mirror radii for the anterior and posterior lens surfaces. The equivalent mirror radius for each lens surface is given by the ratio of its Purkinje image size to the Purkinje image size for the anterior cornea, multiplied by the actual corneal radius. The cornea is treated as a single surface lens and its radius is measured using a keratometer. In order to calculate the actual radii it is necessary to assume either the anterior chamber depth and the refractive index of the aqueous or the vitreous depth and the refractive index of the vitreous. The equivalent mirror theorem, used to calculate the actual radii, is explained by Bennett and Rabbetts (1984) and Dunne (1992).

The principal techniques for measuring the equivalent mirror radii are comparison phakometry and Tscherning's method. For comparison phakometry two circular light sources, in the same vertical plane, are positioned so as to produce two Purkinje images from the lens surface and the cornea. The images are photographed and the heights of the Purkinje images measured between the centres of the two circular images. The ratio of the two images, and hence the equivalent mirror radius of the lens, can then be calculated. Tscherning's method uses his ophthalmophakometer. Two fixed bright lamps give the Purkinje images from the lens surface. The positions of two dimmer lamps are adjusted so that the separation of Purkinje image I from the anterior cornea is equal to the separation of the Purkinje images from the lens surface. The ratio of the separation of the lamps producing Purkinje image I to the separation of the lamps producing Purkinje image III or IV is used to give the equivalent mirror radius.

Dunne (1992) proposed a method for calculating the radii of curvature of the lens surfaces in a four-surfaced eye. It involved measuring Purkinje Images I, II and IV from photographs. Purkinje image III could not be photographed at the same time as it was found that the separation of the light sources required to give Purkinje image II caused Purkinje image III to be obscured by the pupil. This was remedied by using an arbitary value for the anterior lens surface power in the initial calculation. From this an initial value for the radius and power of the posterior lens can be derived. Applying the equivalent mirror theorem then gives an estimate for the height of Purkinje image IV. This is then compared to the actual Purkinje image height for the posterior lens surface. The difference indicates that the choice of the power of the anterior lens surface was incorrect. The anterior lens power is subsequently altered until good agreement is reached between the estimated and actual height of Purkinje image IV. The final chosen anterior lens power and calculated posterior lens power give the true values for the lens.

The accuracy of phakometry is limited for a number of reasons. The image reflected from the anterior lens surface is of poor quality which makes it difficult to measure its size. Also the two images III and IV cannot be in focus at the same time. Consequently measurements must either be taken with one or both of the images out of focus, or from two separate images. Added to this are the errors introduced because of inaccurate measures of the anterior corneal radius, axial separations and refractive indices. Ludlam et al. (1965) calculated an error in the lenticular power measurements of 0.27 D. Zadnik et al. (1992) used a video system which they claimed had improved repeatability because of computer analysis of multiple frames. The 95% limit of agreement was found to be ±0.88 D.

Dunne and Barnes (1993) compared the errors arising from three different methods of phakometric computation by making measurements on two different occasions. They compared methods using Purkinje images I, II and IV; methods using I and III only; and methods using I and IV only. The precision was taken as 95 per cent of the distribution of repeat readings. The precision of anterior lens power measurements for the first two methods was found to be the same (±0.57 D) whereas the precision of the third method was much worse, ±2 D. For posterior lens power measurements the first and third methods had almost equal precision of ±1.12 D and 1.16 D respectively. The precision for the second method was found to be ±2.41 D. Dunne and Barnes (1993) also estimated the precision in measuring the three Purkinje images by taking 9 repeat readings of each. They found that measurements of Purkinje image III is subject to almost twice as much error as for images I and IV. The 95 per cent level of agreement for III was found to be ±0.18 mm and for I and IV it was ±0.10 mm.

b) SLIT LAMP TECHNIQUES

Photographs of the slit lamp sections can also be used to make measurements of the lenticular radii. This is done by using a plane mirror to draw a set of normals to the lenticular surfaces. The surface curvature is estimated by noting where these normals intersect each other (Brown, 1973).

c) IN-VITRO METHODS

Howcroft and Parker (1977) measured the aspheric curvatures of photographs of dissected human lenses some of which were fresh (mean time after enucleation = 2.7 days) and some frozen. From their average thickness measurements they concluded that any artifacts due to the use of cadaver material were small. It seems unlikely, however, that there would not be some changes due to the change in intra-ocular pressure and the relaxing of the zonules which attach the lens and control accommodation. The time period between the eyes being removed and frozen is not given but even in a very short space of time many changes may occur. In-vitro measurements were also carried out by Pierscionek (1989) - cited by Smith et al. (1991).

Measurements of crystalline lens curvatures are given by:- Tron (1929) - cited by Michaels (1980), Sorsby et al. (1962a), Ellerbrook (1963) - from Borish (1970), Brown (1974), Charles & Brown (1975) - from Smith et al. (1991), Howcroft & Parker (1977), Pierscionek (1989) - from Smith et al. (1991).

4.5.3 MEASUREMENT OF CRYSTALLINE LENS ASPHERICITY

The asphericity of the crystalline lens surfaces have only been measured by in-vitro techniques. Measurements have been made by:- Howcroft & Parker (1977), Pierscionek (1989) and Parker (1985). Pierscionek (1989) and Parker (1985) are cited by Smith et al (1991). Kooijman (1983) used the results of Howcroft and Parker (1977) to calculate the mean p values for the lens surfaces of his schematic eye.

4.5.4 MEASUREMENT OF THE GRADIENT INDEX PROFILE OF THE CRYSTALLINE LENS

Measurements of the gradient index profile of the crystalline lens have all been taken on enucleated lenses. Earlier methods used sections of frozen crystalline lenses from animal eyes (e.g. Nakao et al., 1969). Campbell (1984) suggested that freezing may affect the

refractive index distribution. She proposed a method of measuring the refractive index in an intact crystalline lens. This involved tracing the paths of two parallel laser beams, one passing through the centre of the lens and the other at a known distance from it. The emergent angles, along with the corresponding separation of the two parallel beams, were used to derive the refractive index distribution at various radial distances from the centre of the lens. Campbell's method, which was used for measurements on rat lenses was adapted by Pierscionek and Chan (1989) to make measurements on human lenses.

The change in refractive index profiles post mortem was investigated by Munger et al. (1992). They found a region of partial opacification developed in the lens after several hours. This was a result of a discontinuity in the refractive index profile, which was not found in fresh crystalline lenses. It highlights the need to take measurements on the lenses as soon as possible after enucleation.

4.6 THE VITREOUS

The vitreous body is a transparent gel which is almost homogeneous in early life. In adulthood it tends to liquify. The consistency then increases from the lens toward the retina and from the centre out to the periphery. In young eyes the vitreous forms a good optical medium. In older eyes the inhomogeneous medium may lead to irregularities in its refractive power (Weale, 1963). The average depth of the vitreous is about 16 mm in adults (Francois and Goes, 1977; Hosaka, 1988). The refractive index is about 1.336 (Le Grand and El Hage, 1980).

The vitreous depth does not affect the aberrations of the system and so holds little interest to the present study. It does, however, affect the central refractive error and it may be pertinent to calculate the range of refractive error which result from the range of its depth in each of the schematic eyes modelled in later chapters. Most investigators give values for the total axial length (which is the combined length of the anterior chamber depth, the lens thickness and the vitreous depth) rather than the separate vitreous length.

4.6.1 MEASUREMENT OF AXIAL LENGTH

The axial length can be measured by ultrasonic or slit lamp techniques. Measurements have been made by:- Tron (1929) - cited Michaels (1980), Stenstrom (1948), Scammon & Wilmer (1950), Sorsby et al. (1957), Sorsby et al. (1961), Sorsby et al. (1962a), Mohindra (1962) - from Borish (1970), Francois & Goes (1977).

4.7 THE RETINA

The retina is the photosensitive surface which receives the image formed by the optical system of the eye. Clearly, for a sharp image to be formed, the retina must be positioned correctly. If it is too far behind the optical system the image will be focussed in front and myopia occurs. Conversely a retina too close to the optical system will result in hypermetropia. Also the shape of the retina should ideally follow the curvature of the image surface if the optimum image quality is to be achieved in the periphery. Fortunately this would seem to be the case in the human eye, the retina approximately falling half way between the tangential and sagittal foci (Ames and Proctor, 1921).

The retina approximates to a spherical surface with an average radius of 12 mm. Kooijman (1983) used previous empirical data to work out the p value for the shape of the retina. He found the value to be 1.346. This gives it an elliptical shape with the curvature steepening in the periphery. The retina rarely has perfect rotational symmetry. As shown by Ferree et al. (1932), this can lead to asymmetries in the astigmatic image planes. Although the retina has no influence on the aberrations of the image, it may contribute to its degradation as the light sensitive receptors are positioned to the rear. This means the light has to pass through the inner layers before it is detected and may be scattered in the process.

4.8 MEAN AND RANGE OF BIOMETRIC MEASUREMENTS

From the data collected from previous publications a range of values can be established for each of the optical parameters. The earlier data is ignored as later studies are considered to be more reliable. The earliest study from which data is used is that of Stenstrom (1948a). The values from this study of 1000 eyes was used by Bennett and Rabbetts (1984) to give a mean, maximum and minimum powered cornea and crystalline lens. These were then combined in every permutation to give 9 schematic eyes of different dioptric power.

The mean values are taken from Kooijman's (1983) schematic eye. This is chosen as the parameters used are based on average empirical data and on the whole agrees with the mean values given by the data reviewed in this study. A possible objection is that the value for the thickness of the cornea is a little large. This, however, is kept the same for comparison with previous studies (Barnes et al., 1987; Dunne and Barnes, 1987,1990).

Generally the parameters are based on the most recent studies. In cases where there is a lot of disagreement in the literature the largest studies are used. For the anterior and posterior

lens radii of curvature the extensive study of Stenstrom (1948) is used. For the anterior and posterior lens asphericity the values of Parker (1985 - cited by Smith et al. 1991) were used. This was the largest study, based on 59 lenses, and is also the only large study to give standard deviations. In order to obtain a range of values it is assumed that the asphericity values of human lenses follow a normal distribution, as is true for other ocular parameters. The range is then based on the 95 per cent confidence limits as for a normal distribution 95 per cent of the population fall within ±1.96 times the standard deviation. This is clearly not an ideal way of calculating the range but in the absence of other data it is the only method available.

There is no data for the asphericity of the posterior cornea but, as mentioned in section 5.2.1 the shape of the posterior cornea was found by many to follow the shape of the anterior cornea. Kooijman (1983) treated the posterior cornea in his schematic eye in such a way, giving it the same asphericity as the anterior cornea. It will be treated similarly for the purpose of this study.

Parameter	Mean	Min	Max	Source
anterior corneal radius	7.8	7.0	8.9	Guillon et al. (1986)
anterior corneal asphericity	0.75	0.10	1.50	Kiely et al. (1982) & Guillon et al. (1986)
corneal thickness	0.55	0.40	0.60	Lowe (1969b)
posterior corneal radius	6.5	5.8	7.4	Dunne et al. (1992)
posterior corneal asphericity	0.75	0.10	1.50	no data - based on anterior cornea
anterior chamber depth	3.6	2.5	4.6	Stenstrom (1948) & Sorsby et al. (1967)
anterior lens radius	10.2	7.7	13.8	Stenstrom (1948)
anterior lens asphericity	-5.05	-23.5	13.4	Parker (1985) - cited Smith et al. (1991)
lens thickness	4.0	2.9	5.0	Stenstrom (1948) & Francois and Goes (1977)
posterior lens radius	-6.0	-4.6	-8.3	as anterior lens radius
posterior lens asphericity	-0.19	-3.59	3.21	as anterior lens asphericity

Table 4.1 Showing the mean, maximum and minimum values of the ocular parameters of human eyes collated from previous data. The asphericity is given as p values, all the other parameters are given in millimetres.

As mentioned previously the the vitreous length does not affect the aberrations of the eye but will determine its refractive state. The range of axial lengths found in human eyes is

therefore of some interest. Sorsby et al. (1957) found the axial length in emmetropic eyes ranged from 21 to 26 mm. Sorsby et al. (1962a) found a full range of values of 19.2 to 36. From the sample of 1000 eyes Stenstrom (1948a) found the range to be 20 to 29.5.

4.9 SUMMARY

These parameters can be used in the following chapters to construct a range of schematic eyes. Starting with the schematic eye of Kooijman (1983), which incorporates the mean parameter values given in the table, each parameter will be altered individually. In this way the aberrations for the maximum and minimum values of each parameter can be found by ray tracing through each schematic eye.

CHAPTER 5
WIDE- ANGLE SCHEMATIC EYES - A CRITICAL REVIEW

5.1 INTRODUCTION

This chapter gives an overview of the types of schematic eyes used in previous studies. A number of schematic eyes are compared and their success in modelling the aberrations of real eyes, their similarity to the true optical system and their complexity are considered. Reviews of schematic eyes can be found in Le Grand and El Hage (1980), Bennett and Rabbetts (1984) and Charman (1983, 1991a).

5.2 PARAXIAL SCHEMATIC EYES

The earliest schematic eyes were simply used to calculate image size and position on-axis. Their structure therefore only needed to be precise enough to calculate the paths of paraxial rays passing through very small pupils. Paraxial or first-order optical equations were used, hence the term paraxial schematic eyes. They all had spherical surfaces, the dimensions being taken from average data of real eyes (e.g. Gullstrand, 1924; Le Grand and El Hage, 1980; Fincham and Freeman, 1980). These eyes varied in complexity. Gullstrand (1924) developed two schematic eyes, one incorporating a two surfaced cornea and four surfaced lens, the other with a one surfaced cornea and two surfaced lens. Schematic eyes with one corneal surface and two lens surfaces are referred to as simplified eyes. The systems were sometimes further simplified so that the whole refractive power of the eye is included in a single refracting surface. These types of schematic eyes are known as reduced eyes (see Le Grand and El Hage, 1980). The schematic eye of Le Grand And El Hage (1980) is shown in figure 5.1. It has four refracting surfaces; two corneal and two lenticular. The pupil, which is not shown in the diagram, is coincident with the vertex of the anterior lens surface, as in real eyes. This type of schematic eye has since been the basis of more complex systems some of which will be discussed later.

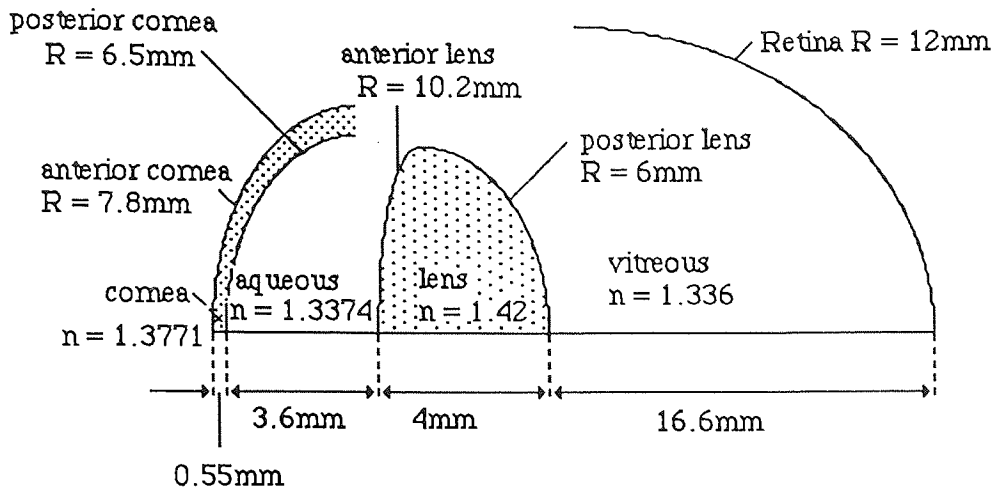

Fig. 5.1 The unaccommodated eye with four refracting surfaces of Le Grand and El Hage (1980).

5.3 WIDE-ANGLE SCHEMATIC EYES

For calculations involving larger pupils or off-axis objects these simple schematic eyes are no longer appropriate. Models of greater complexity which more closely represent the structure of real eyes must be used. These may include aspheric surfaces and/or a crystalline lens with a gradient index optical structure. These more complex models are often referred to as finite pupil or wide-angle schematic eyes. Finite pupil because the pupil size is not limited to being very small and wide-angle because they can be used for ray tracing from off-axis objects.

Optical systems which approximate the imaging properties of the real eyes can be produced given a knowledge of mean ocular dimensions. A number of basic assumptions are made, however, which affect the image forming properties of the system. The misalignment of the optical surfaces, in relation to the effects it has on peripheral astigmatism was discussed in section 3.3.2. Schematic eyes generally assume all surfaces to be centred on a common optical axis. Surface toricity and the inhomogeneous nature of the optical media of the cornea and lens were discussed in chapter four. The optical surfaces of schematic eyes are assumed to be rotationally symmetrical and many models have a single value for the refractive indices of the cornea and lens. However some investigators have incorporated a gradient index structure in the crystalline lens of their models.

5.3.1 MODELS INCLUDING ASPHERIC SURFACES

Investigators who included aspheric surfaces in their schematic eyes are, Lotmar (1971), Drasdo and Fowler (1974), Kooijman (1983), Navarro et al. (1985), Clement et al. (1987), Barnes et al. (1987), Dunne and Barnes (1987, 1990).

Lotmar (1971) used the parameters of Le Grand and El Hage (1980) as a basis for his schematic eye. The model included anterior cornea and posterior lens surfaces which were rotationally symmetric aspherics. A polynomial was used for the cornea, based on the values measured by Bonnet and Cochet (1960, 1964). A second order parabola was used for the posterior surface of the lens, designed to compensate for the lack of the gradient index structure of the crystalline lens. The lens was assumed to be homogeneous because of lack of information of the layer structure. The retina was a spherical surface positioned for paraxial emmetropia.

Drasdo and Fowler (1974) developed a model to calculate the retinal projection in the periphery. They used a three surfaced model incorporating two spherical lenticular surfaces and a corneal surface with an eccentricity value of 0.5. The retinal surface was an ellipsoid. They calculated the internal angle of rays traced at varying field angles and found good agreement with the more complex model of Lotmar (1971). They also found that the retinal area subtended by a constant solid angle of light decreased rapidly in the periphery. This naturally results in an increase in retinal irradiance.

A schematic eye based on that of Le Grand was proposed by Kooijman (1983). All four surfaces were aspherical and described by conic constants (see section 4.2), the values of which are deduced from empirical data. The model was initially designed to study the light distribution on the retina. He found similar results to Drasdo and Fowler (1974) for the internal angles and change in retinal area per unit angle of light for varying field angle. He also measured the reduction in apparent pupil size with eccentricity. This results in reduction of the amount of light entering the eye . He found that if this reduction in light was combined with the reduction of retinal area in the periphery the relative retinal illuminance remained fairly constant. Similar results were found in real eyes (Kooijman and Witmer, 1986).

At the same time as Kooijman was developing his model, Navarro et al. (1985) developed a very similar model. In addition they included varying refractive indices of the ocular media for varying wavelengths of light. These were chosen to fit experimentally determined chromatic aberration and were therefore not anatomically correct.

Clement et al. (1987) developed a method for ray tracing through a wide-angle schematic eye. They used the schematic eye of Kooijman (1983) and traced skew rays through it using a linear algebraic method. The method was initially used to calculate the positions of the Purkinje images and has subsequently been adapted for studying the aberrations of wide-angle schematic eyes. Studies using the ray-tracing programme of Clement et al. will be discussed in sections 5.3.3 and 5.4.

5.3.2 MODELS INCLUDING GRADIENT INDEX OPTICS

Models which included Gradient index optics were designed by Pomerantzeff et al. (1971), Watkins (1972), Blaker (1980), Fitzke (1981), Wang et al. (1983), Pomerantzeff et al. (1984), Raasch and Lakshminarayanan (1989), Smith et al. (1991)

Blaker (1980) and Raasch and Lakshminarayanan (1989) limited their studies to the axial behaviour of an accommodating lens with a gradient index structure. Blaker adapted the Gullstrand no.1 eye (Gullstrand, 1924) using a polynomial to describe the gradient index structure, starting with Gullstrand's refractive indices for the anterior pole of 1.387 and central core 1.406. The cardinal points were found to be in reasonable agreement with known values. Raasch and Lakshminarayanan proposed the use of optical matrices to simplify calculations of cardinal point position and hence retinal image size.

Fitzke (1981) based his model on empirically determined data found in literature and included aspheric surfaces as well as a layer structure for the crystalline lens. He used this model to estimate the contribution of optical factors to psychophysical measurements. His results were very similar to those of Drasdo and Fowler (1974) and Kooijman (1983) giving constant relative retinal irradiance as a function of field angle if relative reduction in pupil size is considered.

Watkins (1972) developed a model, based on empirical data, which had elliptical corneal surfaces and lens surfaces described by expansion polynomials with coefficients of sixth-order, or higher. The gradient index structure of the lens was described by a fourth power function with one independent variable. The surface asphericities and gradient index power function were designed so that both the cornea and lens were corrected for spherical aberration. Clearly this does not represent the image forming properties of real human eyes, which suffer from small amounts of positive spherical aberration. Watkins then used his model to determine the retinal image quality on-axis. He found that the model conformed to paraxial predictions.

Pomerantzeff et al. (1971, 1984) also based their schematic eye on empirical values. All the surfaces were aspherical and were described by standard aspherical surface equations (see section 4.2). The lens was made up of 200 layers. The distribution of axial curvatures, thicknesses and refractive indices of these layers were determined by polynomial equations.

The parameters of the layer structure of the lens and the shape of the corneal surface were adjusted so that the values of spherical aberration given by the model matched the mean values found in 100 living eyes. Their aim was not to reproduce the physical shape and structure of the lens or cornea, only to reproduce their optical performance. They found, however, that the resultant corneal surface was indistinguishable from the mean values measured by Bonnet and Cochet (1960, 1964) and used by Lotmar (1971). When the values of spherical aberration for the two corneal surfaces were compared, however, it was noted that Bonnet and Cochet's cornea had over-corrected spherical aberration centrally becoming under-corrected in the periphery. The modelled cornea of Pomerantzeff et al. (1984) produced under-corrected spherical aberration throughout. This illustrated that minutely small changes in the shape of optical surfaces can have a significant effect on optical performance.

Smith et al. (1991) used all the empirical data available on surface shape and gradient index in order to model the human lens. They discussed the variability and limitations of the available data for the surface asphericities and refractive index distributions of crystalline lenses. To test the optical performance of the lens models, equivalent power and spherical aberration were calculated for each. Smith et al. used two very different but reasonable sets of data to construct two models of the lens. Both gave reasonable values for the equivalent power of about 20 D. However, they gave very different spherical aberration values; the first giving negative spherical aberration and the second positive. Measurements of the spherical aberration of crystalline lenses in real eyes have led to seemingly contradictory results. Some studies have found positive spherical aberration, others negative and others a mixture of the two (see section 2.3.5). Smith et al. concluded that these results were either inconclusive or reflected the variations in aberration within the population. The variation in the form of the refractive index profile was found to have a strong influence on both the power and the aberrations of the lens. They concluded from their results that more information on surface asphericity and the index profile in the sagittal plane was required to allow more accurate modelling.

5.3.3 ASYMMETRIC MODELS - MODELLING ANGLE ALPHA

Tscherning (1924) made the first measurements of angle alpha using his ophthalmophakometer. He located the axis along which the Purkinje images from the anterior corneal surface (I), the anterior lenticular surface (III) and the posterior lenticular surface (IV) appear to be aligned. Tscherning considered this to be the closest approximation to an optical axis. He took its angular separation from the visual axis, which joins the visual fixation point to the fovea, to be angle alpha. He found angle alpha to be approximately 5° with the optical axis lying temporal to the visual axis in object space.

Clement et al. (1987) showed that both a 5° rotation of the whole eye and a 5° tilt of the lens both misalign the Purkinje images in the manner described by Tscherning (1924). However it must be noted that if the lens were indeed tilted with respect to the cornea then there would be no optical axis and Tscherning would not have been able to align the Purkinje images.

In the presence of angle alpha the optical axis will intercept the retina nasally to the fovea. Peripheral astigmatism is measured relative to the visual axis. The levels of peripheral astigmatism will therefore be asymmetrical about the visual axis with higher values being found temporally. The field angle around which peripheral astigmatism is found to be symmetrical will be angle alpha, if the asymmetry is due purely to rotation of the whole eye.

Stimson (1957) found that angle alpha disappeared in aphakic eyes. This led Barnes et al. (1987) to conclude that eye rotation may not be the predominant cause of angle alpha. To test this conclusion they used the method of Clement et al. (1987) to investigate the effects of translation and rotation of ocular components on off-axis aberrations. They ray traced sagittal and tangential rays through the margins of a circular pupil. Because of the effects of coma the two marginal rays did not intersect the principal ray at the same point. Barnes et al. therefore considered three foci; two where each of the marginal rays intercepted the principal ray and the third where they intercepted each other. The first two were considered to be the outer limits of the comatic image. In this way the effects of translations and rotations of the ocular components on comatic aberration and peripheral astigmatism were observed.

A 5° rotation of the lens such that the nasal side moves towards the front of the eye and a 1 mm translation nasally produced similar results. The interval of Sturm increases temporally

and decreases nasally which is consistent with the results of measurement in real eyes by Ferree et al. (1931) and Rempt et al. (1971) - see section 3.3.1. This evidence, along with the previous evidence that a 5° rotation of the lens produces misalignment of Purkinje images consistent with that observed in real eyes, suggested that rotation of the lens may be responsible for angle alpha.

Nasal rotation and translation of the cornea were also found to increase the interval of Sturm temporally and decreased it nasally, but to a greater extent than for the lens. Barnes et al. considered that such corneal rotation or translation may therefore be responsible for the small number of eyes which have large levels of peripheral astigmatic asymmetry (see section 3.3.2).

Dunne and Barnes (1989) presented more evidence to argue that angle alpha is is due to rotation of the whole eye. They reasoned that eye rotation not only explains angle alpha but other experimental findings as well. These include decentration of the pupil and anterior corneal surface with respect to the visual axis, residual astigmatism and asymmetries observed in optical degradation of the retinal image and peripheral refraction.

A recent study (Dunne et al., 1993b) has provided further evidence of the origin of angle alpha. Peripheral astigmatism and angle alpha has been measured in the same 34 eyes (described by Dunne and Barnes, 1990). Angle alpha was measured by alignment of Purkinje images I and IV using the canon R-1 autorefractometer. Peripheral astigmatism measurements were made from 40° nasally to 40° temporally in 10° steps with the Hartinger refractometer and to 30° nasally and temporally with the Cannon autorefractometer. The peripheral astigmatism was plotted against field angle for each eye and a second-order polynomial was fitted to the datum points. The point of astigmatic symmetry, taken to be the minimum of the curve, was calculated by differentiation. The resulting field angle gave the angular separation of the point of symmetry from the visual axis (0° field angle).

In a sample of 34 eyes Dunne et al. (1993a) compared the measured levels of eye rotation with the point of peripheral astigmatic symmetry. On average, 5° eye rotation was found whereas peripheral astigmatism was symmetrical at a point 9° on the nasal retina. The simplest and most optimistic interpretation of this is that the eye is indeed rotated by 5° which accounts for that amount of shift of the peripheral astigmatic point of symmetry towards the nasal retina. The remaining 4° is then the result of additional asymmetry in the curvatures of one, or a combination, of the surfaces either side of the visual axis. The most pessimistic interpretation involves the assumption that the corneal and crystalline lens surfaces are all aligned. This assumption is necessary in order to determine eye rotation

using alignment of Purkinje images I and IV. If this assumption is not so then the measures are a function of surface misalignment and not eye rotation at all. Tscherning (1924) has provided evidence for and against the assumption. He found 5° eye rotation by aligning Purkinje images I, III and IV but he also found that the images were not alignable in some eyes.

5.4 ABERRATIONS OF SCHEMATIC EYES

The spherical aberration of the schematic eye of Lotmar (1971) was found to be slightly under-corrected as found in real eyes. As the spherical aberration of the polynomial anterior cornea was almost fully corrected, the balance of under-corrected spherical aberration was due to the lens. Lotmar also calculated the spherical aberration for a hypothetical 7 layer model lens and found that it reduced the under-corrected spherical aberration. However because of lack of data as to the structure of the human lens and the increased complexity this would introduce to the model no further calculations were attempted.

In order to assess the level of peripheral astigmatism produced by Lotmar's eye model rays were traced up to a 90° field angle in steps of 10°. The astigmatism was found to be similar to that of the type A eye of Ferree et al. (1931) or the type IV eye of Rempt et al. (1971) - see section 3.3.1.

In 1974, Lotmar and Lotmar carried out a statistical analysis of the measurements of peripheral astigmatism of Rempt et al. (1971) to compare the results with those found in their schematic eye. Close agreement was found for angles up to 30°. Beyond this the values given for the schematic eye were larger becoming almost twice as high for a 60° field angle. Lotmar and Lotmar pointed out, however, that the values found from their model did not fall outside the range of experimental findings and 10% of cases would fit quite close to their predicted values.

The interval of Sturm at 50° was found to be 6.25 D which was considered to be in good agreement with the value of 5.5 D measured in real eyes. The value for Le Grand's paraxial schematic eye with spherical surfaces (Le Grand and El Hage, 1980) is as high as 15.1 D, Lotmar and Lotmar concluded that the flattening of the cornea has a strong influence on peripheral astigmatism. They went on to suggest that further flattening of the anterior corneal surface could produce astigmatism values similar to those found in type B eyes of Ferree and Rand (1931). Lotmar and Lotmar considered that further improvements could be made to the mean values either by further flattening of the corneal surface or by introduction of a gradient index into the lens.

The peripheral astigmatism of the more complex model eye of Pomerantzeff et al. (1971, 1984), which was designed to give mean values of spherical aberration found in 100 eyes, was investigated by Wang et al. (1983). They calculated peripheral astigmatism for field angles of 10° to 70° in steps of 10°. The astigmatism at 50° was found to be 8.8 D. This is much higher than the average value of 6.41 D found by Ferree et al. (1931) and higher, even, than their maximum value of 8.75 D. Other investigators found even lower mean values in real eyes. Rempt et al. (1971) found about 3.4 D of peripheral astigmatism at 50°; Millodot and Lamont (1974) found a value of 3.75 D. Considering these studies the values given by the model of Pomerantzeff et al. are much higher than empirical values.

The aberrations of Kooijman's schematic eye (Kooijman, 1983) have been investigated by Dunne and Barnes (1987). They found that the values of spherical aberration were close to the average values given by Van Meeteren (1974) (see section 2.4). However peripheral astigmatism values were found to be much higher than the average values given by Rempt et al. (1971) (see section 3.4). Dunne and Barnes suggested that the average gradient index structure of the crystalline lens has the effect of further decreasing the peripheral astigmatism.

The spherical aberration of the model of Navarro et al. (1985) agrees well with the values of Van Meeteren (1974). The individual spherical aberration values for the cornea and lens were found to be of opposite signs. The smaller, negative contribution of the lens compensates for some of the positive spherical aberration of the cornea. This is in agreement with the empirical findings of El Hage and Berny (1973) - see section 2.3.5. On inspection of their graph, however, it was noted that the total spherical aberration of their model eye is shown to be larger than that of the cornea alone. If the negative spherical aberration of the lens does indeed compensate for some of the positive spherical aberration of the cornea the the total spherical aberration should be less than that of the cornea. As for Lotmar (1971), Navarro et al. (1985) concluded that since spherical aberration values are accurately modelled by aspheric surfaces alone, it is controlled by the asphericities of the eye. However, gradient index is needed in order to model the off-axis aberrations.

Bennett and Rabbetts (1984 - chapter 15) showed how peripherally flattening the cornea of a schematic eye from spherical to paraboloid affected peripheral astigmatism. The eye with the spherical surfaced cornea had peripheral astigmatism which conformed to the pattern of the type A eye of Ferree et al. (1931) - section 3.3.1. Bennett and Rabbetts found that peripherally flattening the cornea caused both the sagittal and tangential foci to move in the direction of hypermetropia. The tangential focus moved approximately twice as much,

therefore reducing the interval of Sturm and resulting in peripheral astigmatism resembling that of the type B eyes of Ferree et al. (1931).

Dunne and Barnes (1987) attempted to model the average peripheral astigmatism values of type A and type B eyes of Ferree et al. (1931) described in section 3.3.1 They used the schematic eye of Kooijman (1983) and progressively flattening the anterior lens surface, with more negative conic constant values, until the required levels of peripheral astigmatism were achieved. They found that flattening the anterior lens surface decreased peripheral astigmatism but also greatly increased central hypermetropia. This could not be compensated for by manipulating the posterior lens surface as any change in its conic constant value produced an increase in peripheral astigmatism. However Dunne and Barnes found that increasing the lenticular refractive index reduced peripheral astigmatism at the same time as increasing the central dioptric power, therefore reducing central hypermetropia. By a combination of lenticular refractive index increase and anterior lens surface flattening they were able to model type A and Type B eyes; although the conic constant values needed to achieve this were way beyond the limits of values measured in any human eyes. These large amounts of peripheral flattening also resulted in large amounts of over-corrected spherical aberration unlike the under-corrected values normally found in human eyes (see section 2.4). This unsuccessful attempt was limited to manipulation of only two of the optical parameters of the eye. By investigating the effects of the other optical parameters and manipulating a number of them simultaneously it may be possible to obtain reasonable levels of peripheral astigmatism and spherical aberration with realistic parameter values. This will be studied in the following chapters.

A number of previous schematic eyes have successfully modelled average levels of spherical aberration found in human eyes (Lotmar, 1971; Kooijman, 1983; Pomerantzeff et al.,1971,1984). An attempt has also been made to model average levels of peripheral astigmatism (Dunne and Barnes, 1987). No Schematic eye has yet managed to model the two aberrations simultaneously.

The peripheral astigmatism values of three schematic eyes are compared to the average empirical values of Lotmar and Lotmar (1974) in figure 5.2. The spherical surfaced schematic eye of Le Grand and El Hage (1980) has peripheral astigmatism levels far above the average human values. The peripheral astigmatism for the model of Lotmar (1971), which includes aspheric surfaces, is almost identical to empirical values up to 30° in the periphery. For higher field angles it gives values which become increasingly higher than the empirical values. The more complex model of Pomerantzeff et al. (1971), which

incorporates both aspheric surfaces and a gradient index crystalline lens, can be seen to give peripheral astigmatism values which are much higher than empirical values.

The models of both Pomerantzeff et al. (1971) and Lotmar (1971) were initially designed to model the spherical aberration of real eyes. Smith et al. (1991) asserted that if only the spherical aberration is used to determine the parameters of a simple lens then the solution is not unique. The more variables there are, the more solutions there will be. For the very complex model of Pomerantzeff et al. (1971) the variables include the central curvatures and asphericities of the optical surfaces, and the lens refractive index distribution. This could lead to a great many solutions to the problem of modelling average spherical aberration. It is feasible that one of these solutions could also give the correct levels of peripheral astigmatism. The same applies to the model of Lotmar (1971). Although, as there are fewer variables within the schematic eye, there will be fewer solutions. The relatively simple approach of Lotmar (1971) was initially more successful in simultaneously modelling the average spherical aberration and peripheral astigmatism of human eyes. It therefore seems unnecessary to add the further complication of refractive index variations to the lens, as this appears to be reasonably successfully compensated for by aspheric surfaces.

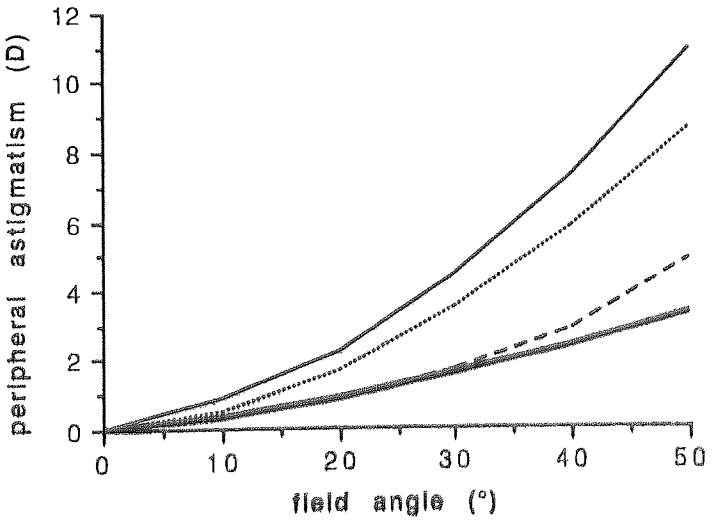

Fig. 5.2 A plot of peripheral astigmatism against field angle for the spherical surfaced model of Le Grand and El Hage (1980) - the thin continuous line, the schematic eye of Pomerantzeff et al.(1971) which includes aspherical surfaces and a gradient index lens - the dotted line, the aspheric surfaced model of Lotmar (1971) - the dashed line and measured mean values of real eyes calculated by Lotmar and Lotmar (1974) from the data of Rempt et al (1971) - the thick continuous line.

Dunne and Barnes (1987) showed that the peripheral astigmatism values of Kooijman's schematic eye were close to empirical values for field angles of up to 30°. This schematic eye was also thought to have spherical aberration close to human values. As the parameters of the eye were based on mean empirical parameter values it was considered a good starting point for the investigations of the present study. Also, the surface shapes are given in terms of conic constants which is convenient for incorporation in to the computer models used in this research.

A brief comparison of the levels of peripheral astigmatism in schematic and real eyes can be made by using the single value parameter called the PAF which was discussed in chapter three.

Lotmar and Lotmar (1974)	measured values	66.0
Lotmar (1971)	aspheric surfaces	81.3
Kooijman (1983)	aspheric surfaces	100
Pomerantzeff et al. (1971)	aspheric surfaces + gradient index	154.88
Le Grand and El Hage (1980)	spherical surfaces	198.1

These values clearly show that the astigmatism for the Lotmar and Kooijman schematic eyes gives values which are much closer to human mean values than for the Pomerantzeff eye. They also demonstrate the large difference in values given by spherical surfaced models and aspheric surfaced models; the PAF value being more than halved by the introduction of aspherical surfaces in the Lotmar model.

As Kooijman's schematic eye has been chosen as the basic model for this study it is necessary to examine it in greater detail.The values for the parameters of the schematic eye are given in table 5.1. The initial conic constants for the lenticular surfaces were later revised as Kooijman discovered an error in his calculations (see Smith et al., 1991). These revised values are used in the present study and are given in brackets in table 5.1. The difference in the spherical aberration and peripheral astigmatism values which result from the alteration in conic constant values can be demonstrated by comparing the SAF and PAF values for the two schematic eyes. The original Kooijman values give a SAF of 3.3 and a PAF of 102.3. The revised Kooijman values give a SAF of 2.2 and a PAF of 100. Clearly the change in asphericity of the lens surfaces has serious implications if we consider the spherical aberration. The revised values give a SAF value which is two thirds that given by the original values. However the peripheral astigmatism changes very little; the PAF reducing very slightly when the revised conic constants are used.

	refractive index	Apical Radius (mm)	conic constant, p	Distance from Corneal Vertex (mm)
Cornea	1.3771	7.8 (anterior)	0.75	0
		6.5 (posterior)	0.75	0.55
Aqueous	1.3374	-	-	-
Lens		10.2 (anterior)	-2.06 (-5.05)	3.6
		-6 (posterior)	0 (-0.19)	7.6
Vitreous	1.336	-	-	-
Retina	-	-14.1	1.346	24.2

Table 5.1 The parameters of the theoretical eye of Kooijman (1983). Revised values for the conic constants of the lens surfaces (see Smith et al, 1991) are given in brackets.

The spherical aberration values, in comparison to the range found in human eyes, and the mean values of Van Meeteren (1974) are shown in fig 5.3. The peripheral astigmatism of Kooijman's schematic eye in comparison to the human range and the mean values given by Lotmar and Lotmar (1974) are shown in fig 5.4. The spherical aberration values for Kooijman's schematic eye follow closely the values given by Van Meeteren (1974) as being representative of the mean of human eyes. The astigmatism values are very close to the mean values of Lotmar and Lotmar up to about 30° on the temporal side of the retina, but close to maximum values on the nasal side. If the nasal and temporal measured values were averaged the peripheral astigmatism of Kooijman's schematic eye would fall between the mean and maximum values (Dunne and Barnes, 1987).

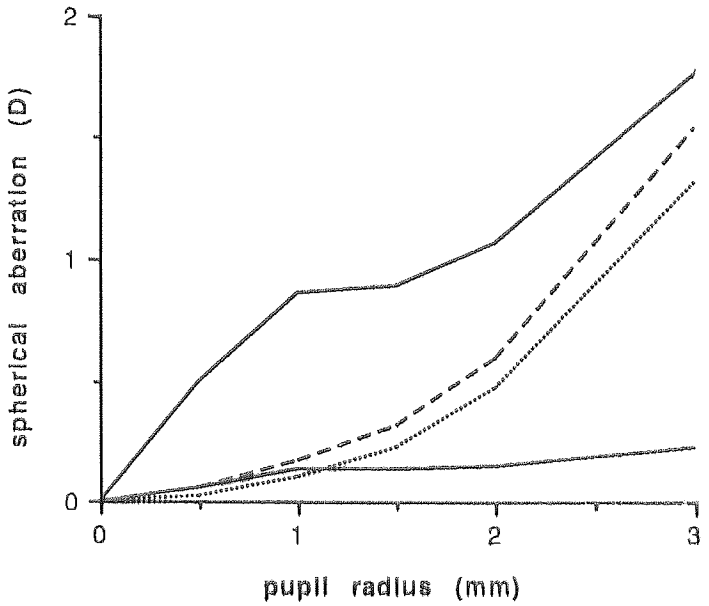

Fig. 5.3 A plot of spherical aberration against pupil radius for maximum and minimum measured values of real eyes - the continuous lines, the mean measured values modelled by Van Meeteren (1974) - the dashed line and values calculated from the Kooijman schematic eye (Kooijman,1983) - the dotted line.

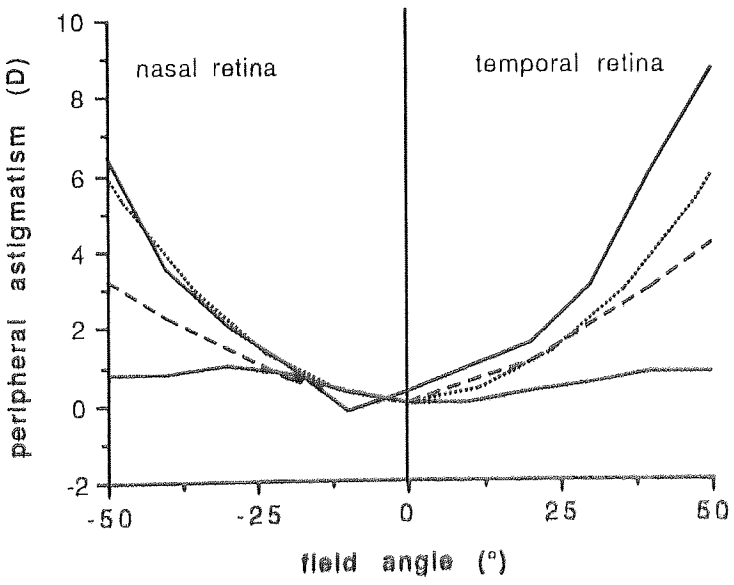

Fig. 5.4 A plot of peripheral astigmatism versus field angle for the maximum and minimum measured values of real eyes - the continuous lines, the mean measured values of Lotmar and Lotmar (1974) - the dashed line and the values calculated from Kooijman's schematic eye (Kooijman, 1983) - The dotted line.

5.5 MODELS OF INDIVIDUAL EYES WITH KNOWN PERIPHERAL ASTIGMATISM AND BIOMETRIC DATA

a) PAST RESEARCH

Dunne and Barnes (1990) measured the peripheral astigmatism up to 40° field angles in 34 eyes for which they had also measured the optical dimensions. From the average values of this biometric data they then constructed three three surfaced schematic eyes: one comprising only spherical surfaces; one with an aspheric cornea (p = 0.76) and the third also including average aspheric values for the two lens surfaces. The lens asphericity values were taken from Kooijman (1983) and are the uncorrected values given in table 5.1 as the revised values were unavailable at the time. The calculated peripheral astigmatism values from this model were compared to the average values from the 34 eyes.

All models gave peripheral astigmatism values which were higher than the empirical values for high field angles. The second model with an aspheric cornea gave values which were close to empirical values up to 30°. Making the lens surfaces aspheric caused the peripheral astigmatism for small field angles to fall below empirical values. Results showed that even the spherical surfaced model gave peripheral astigmatism values which fell within the limits measured in the real eyes. The aspheric cornea reduced values of peripheral astigmatism and aspherical lens surfaces reduced them further. The implication of this is that in some individuals, measured levels of peripheral astigmatism may even exceed values modelled in spherical schematic eyes. This raises the question of whether aspheric surface flattening and gradient index optics are mechanisms to reduce peripheral astigmatism or merely components which lead to inter-individual variation.

b) PRESENT RESEARCH

Dunne et al. (1993a) have re-analysed the data from the study of Dunne and Barnes (1990) in order to investigate the effect of inter-individual variations of ocular component dimensions upon peripheral astigmatism. Schematic eyes were constructed from each subjects individual biometric data. Only two models were constructed for the original study, as individual data for the asphericity of the lenticular surfaces was not available. However, the present author has constructed a third model for each individual eye which includes mean asphericity values for the lens surfaces. These are the corrected values of Kooijman (see table 5.1). In all three models the optical media are homogeneous, the gradient index structure of the lens being ignored as it could not be measured in-vivo. For

all three models of each eye the peripheral astigmatism was calculated using the computer scheme of Clement et al. (1987). These values were then expressed as PAF values (see section 3.4.1) to facilitate easy comparison.

Table 5.2 demonstrates that the mean peripheral astigmatism values of the first two models exceeds that of measured values. However, the mean values for model 3 are found to be lower than measured values. The difference between mean and measured values for the spherical surfaced model 1 is statistically significant (one sample t-test, $P<0.01$). For model 2, with the measured asphericity values of the cornea added, the difference is greatly reduced and no longer reaches statistical significance. Making the corneal surfaces aspheric actually reduces the difference between the mean modelled and measured values by 69 per cent. This suggests that the asphericity of the cornea plays the major role in minimising peripheral astigmatism. Adding average values for the asphericity of the lens surfaces reduces mean peripheral astigmatism to values below the mean measured values. This would seem to indicate that in some cases the lens asphericity and Gradient index structure serves to increase peripheral astigmatism.

If we compare the mean PAF of the measured values to the mean PAF (66.0) given by Lotmar and Lotmar (1974) - See section 3.4.1 - it is clearly much higher. It is possible that the experimental method results in artificially high values of peripheral astigmatism. The difference in the mean values, however, may also be due to the large inter-individual variation of peripheral astigmatism found in the population. If we compare this high mean PAF value to the PAF given by Kooijman's schematic eye (PAF = 100) they are clearly very close. It would therefore be feasible to consider the Kooijman to give both spherical aberration and peripheral astigmatism values which are close to human mean values. Unfortunately this mean PAF value is unusually high when compared to the values given by other studies (see section 3.4.1). Only the average of the type A eyes of Ferree et al (1931) giving as high a value. Also, because of the small sample size, the mean is unlikely to be as representative as that of Lotmar and Lotmar (1974).

	PERIPHERAL ASTIGMATISM FUNCTION (PAF)			
N = 34	measured	model 1	model 2	model 3
mean	103.33	123.61	109.55	93.75
standard deviation	±30.20	±12.32	±16.70	±15.43
minimum	41.54	98.13	72.54	64.40
maximum	157.87	153.60	153.60	136.97
range	116.33	55.47	81.06	72.57

Table 5.2 Peripheral astigmatism functions derived from measured data, from data calculated using schematic eyes with spherical surfaces (model 1), schematic eyes incorporating aspheric corneal surfaces (model 2) and schematic eyes incorporating aspheric corneal surfaces and aspheric lens surfaces (model 3).

The distribution of empirical PAF values and the PAF values for the first two models representing the measured biometric data of the individual eyes is shown in figs. 5.5 to 5.7. The empirical PAFs are clearly not normally distributed (fig. 5.5). The highest frequency of individual values are towards the higher end of the range, the peak frequency being for PAFs of between 108 and 125. The mean value falls slightly lower than this. The PAFs for the spherical surfaced (fig. 5.6) and aspheric surfaced (fig. 5.7) schematic eyes are also not normally distributed. For the spherical schematic eyes the highest frequency of PAF values are found between 114 and 122, which is slightly towards the lower half of the range. The mean is slightly higher at 123.61. For the aspherical schematic eyes the distribution is also skewed slightly towards the lower values, with the highest frequency of PAF values falling between 95 and 119. The mean of 109.55 is near the middle of this range.

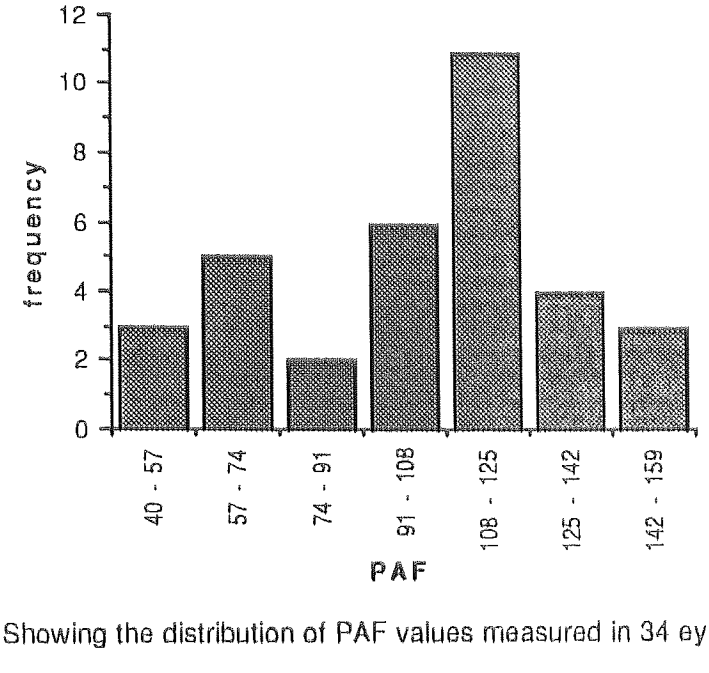

Fig. 5.5 Showing the distribution of PAF values measured in 34 eyes.

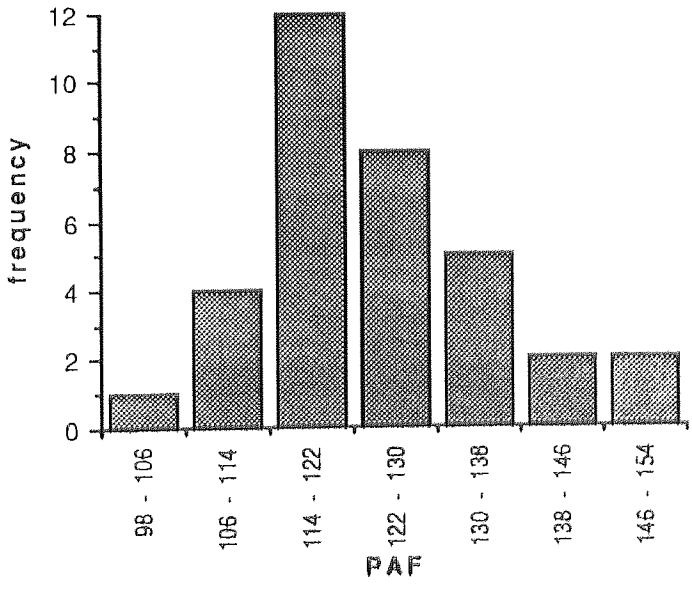

Fig. 5.6 Showing the distribution of PAF values given by 34 spherical surfaced schematic eyes modelled from measured individual biometric data.

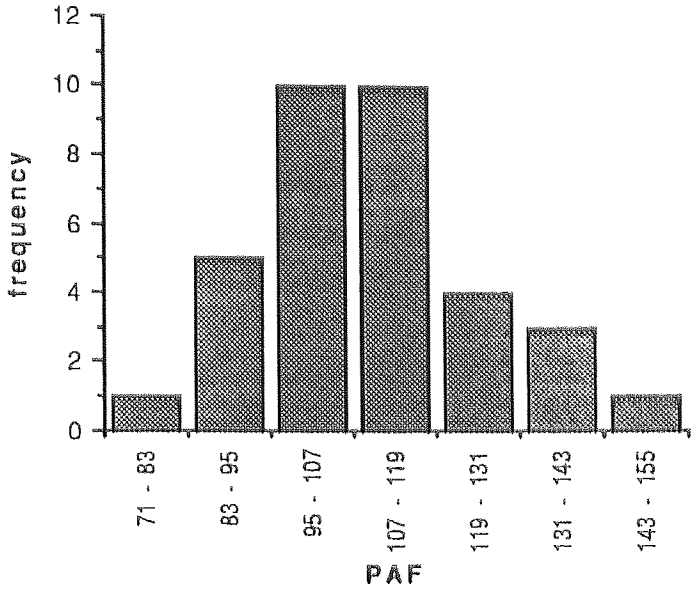

Fig. 5.7 Showing the distribution of PAF values given by 34 aspherical surfaced schematic eyes modelled from measured individual biometric data.

No statistically significant correlation was found between the measured PAF values and those given by models 1 and 2 (correlation coefficient = 0.11 and 0.20 respectively). Therefore, measured variations in central surface radii, axial distance or corneal surface asphericity were unable to account for individual variations in peripheral astigmatism. This leads to the conclusion that inter-individual variation is mainly accounted for by fluctuations in the crystalline lens surface asphericity and gradient index optical nature. Whether these fluctuations mainly increase or decrease peripheral astigmatism can be deduced from observation of the individual results.

	MEASURED PAF - MODELLED PAF		
N = 34	model 1	model 2	model 3
mean	21.27	6.20	-8.59
standard deviation	±31.35	±31.49	±30.82
minimum	-38.74	-51.82	-71.15
maximum	80.75	67.95	55.25
range	119.49	119.77	126.40

Table 5.3 The range of differences found between peripheral astigmatism functions (PAF) derived from measured and modelled data. Model 1 represents schematic eyes with spherical surfaces, model 2 schematic eyes with aspheric corneal surfaces and model 3 schematic eyes with aspheric corneal surfaces and aspheric lens surfaces.

Table 5.3 indicates the range of differences between measured and modelled PAF values found in individual eyes. It can be seen that even in spherical surfaced eye models in some cases (26.5 per cent) the modelled PAFs are lower than the measured PAFs. When corneal asphericity is accounted for, more (47.1 per cent) of the individual eyes have lower modelled PAFs. Addition of average asphericity values for the lens surfaces increases this percentage to 58.8 per cent. Since nearly half the modelled eyes with aspheric corneas have values below measured values it would appear that, rather than serving to decrease peripheral astigmatism, as the average values of lens asphericity do, the asphericity and gradient index of the crystalline lens actually increase it in almost 50 per cent of cases.

This study has shown that comparing average values for measured and modelled values of peripheral astigmatism may be too simplistic. It seems to indicate that both the asphericity of the cornea and the asphericity and gradient index of the lens serve to decrease peripheral astigmatism in human eyes; asphericity of the cornea being the major factor. A more detailed look at the individual results reveals that in 26.5 per cent of cases the combination of aspherical surfaces of the cornea and lens and the gradient index of the lens actually increases the peripheral astigmatism. In this study the addition of aspheric corneal surfaces to the the models decreased peripheral astigmatism for every eye, although if experimental error is taken into account it may be increased in a few eyes. The percentage of model two eyes with peripheral astigmatism below the measured values rose to 47.1 per cent. It would seem that the unmeasured sources of variation, i.e. crystalline lens asphericity and gradient index optical properties, increase peripheral astigmatism as often as they decrease it in individual eyes.

5.6 SUMMARY

As a result of the large degree of inter-individual differences in both the optical parameters and the aberrations of human eyes average model eyes are likely to represent very few individual human eyes; either in their parameter values or the amount of aberration they exhibit. Investigators modelling average eyes using average spherical aberration values have found the peripheral astigmatism values are higher than mean values. For the study of Dunne and Barnes (1987), where mean values of peripheral astigmatism have been achieved, the spherical aberration is vastly over-corrected. The parameters values in their schematic eyes also bear no resemblance to values measured in real eyes. No investigator has yet been able to model both the mean ocular spherical aberration and the peripheral astigmatism simultaneously. The aspheric surfaced schematic eye of Lotmar (1971) has

come nearest to achieving this goal with spherical aberration levels close to mean values and peripheral astigmatism values which are close to mean values for field angles up to to 30°. The gradient index model of Pomerantzeff et al. (1971) gave peripheral astigmatism values which were much higher than human mean values. It is the aim of this study to discover if schematic eyes, such as that of Lotmar, without the added complication of gradient index, can model the levels of spherical aberration and peripheral astigmatism found in human eyes.

Kooijman's schematic eye (Kooijman, 1983), which is based on average empirical values gives levels of spherical aberration which are close to accepted human mean values. Unfortunately the peripheral astigmatism values are high. They do, however, fall within the human range. As this schematic eye uses mean values for its parameters it is considered a good starting point from which to study the effects of parameter changes on aberrations. As such it will be taken as the mean eye for this study.

Asymmetries in the optical aberrations found in eyes have been thought to be due to angle alpha. Before this can be modelled in schematic eyes it is necessary to know the origin of angle alpha. Several studies have offered evidence of it being caused by eye rotation or rotation of the crystalline lens. A recent study has shown that poor agreement exists between angle alpha and the point around which peripheral astigmatism levels are symmetrical in the same eyes. This poor agreement is thought to be due either to asymmetry of the optical surfaces in the periphery or to relative non-alignment of the optical surfaces. If caused by the latter the concept of an approximate optical axis and, therefore, angle alpha are meaningless.

A present research project has shown that in almost half the studied human eyes the asphericity and gradient index structure of the lens actually serve to increase peripheral astigmatism. In following chapters it will be shown whether parameter values within human ranges do in fact serve to increase or decrease the optical aberrations.

This study aims to model the complete range of aberrations found in human eyes using the full range of measured parameter values. The parameter ranges have been established, from the literature, in chapter four. The range of spherical aberration, peripheral astigmatism and coma obtained by incorporating these parameter ranges in schematic eyes will be calculated in the following chapters. The range of the first two aberrations will then be compared to those found in human eyes, which have been established in chapters two and three

CHAPTER 6
THE EFFECTS OF INDIVIDUAL OCULAR PARAMETER CHANGES ON SPHERICAL ABERRATION.

6.1 INTRODUCTION

The purpose of this chapter is to determine the influence of each optical parameter upon spherical aberration. Ocular parameter variations are limited to ranges previously found in real eyes (chapter four). The aberration is initially presented in a conventional manner, as a plot of spherical aberration for varying pupil sizes. Comparison of the plots resulting from variation of each ocular parameter gives a clear representation of the effects they have on the spherical aberration. The data is then presented as plots of SAF versus parameter value. This allows easy comparison of the size of the effect of each parameter. The modelled SAFs are also compared to the measured range established in chapter two.

When comparing the effect of changes in the individual parameter values on spherical aberration, or on peripheral astigmatism and coma, it must be pointed out that comparisons are not being made of the effect of unit change. What is being compared is the variation in spherical aberration which can be achieved by the full range of each parameter found in human eyes. For example, unit change in the asphericity value, p , for the anterior corneal surface will cause the greatest change in spherical aberration. This is by virtue of its high dioptric power, compared to that of the other three surfaces. From empirical data, however, (see chapter four), the range of p values for the anterior cornea was found to be far smaller than for the lens surfaces. The lens surfaces are, therefore, capable of producing a larger spread in spherical aberration values.

6.2 OCULAR PARAMETER VARIATIONS AND SPHERICAL ABERRATION

6.2.1 COMPUTERISED RAY TRACING

The spherical aberration of schematic eyes was determined by exact ray tracing. A linear algebraic ray tracing program was used, which traces skew rays through second order aspheric surfaces (Clement et al., 1987, Barnes et al. 1987)). A detailed description of the operating procedures of the program was given by Dunne (1987).

In order to calculate the spherical aberration two marginal rays - lying in a single plane perpendicular to the optical axis - were traced, initially, through a very small pupil (0.1 mm). The ray tracing program calculates the refractive error, i.e. the dioptric difference between the position of the retina and the intersection of the two rays. For the 0.1 mm pupil the result was considered to be the refractive error for paraxial rays. The pupil diameter was then increased, in steps of 0.5 mm, from 0.5 to 6 mm. The refractive error for each pupil

diameter was subtracted from that of the 'paraxial pupil' to give the spherical aberration in dioptres. The spherical aberration values were then plotted against pupil diameter and a polynomial curve was fitted to the datum points.

Calculations were initially carried out on Kooijman's schematic eye (Kooijman, 1983) incorporating the corrected lens surface asphericity values. The parameters of this schematic eye were given in section 5.4. The parameters of Kooijman's schematic eye represent "average" human values.

In the ray tracing program surface shape is determined in three dimensions by entering three radii of curvature values along three mutually perpendicular axes, X, Y and Z. The Z axis follows the optical axis. Surface location is represented by distances along the three axes. The apex of the anterior lenticular surface is taken to be the system centre. The centre of the pupil is also located here. All radii of curvature are measured from this centre. To position the apex of each surface correctly its location along the Z axis must be calculated. This is determined by the radius of curvature of the surface in the Z direction and the required distance of the surface apex from the system centre. Calculation of surface radii and location parameters is described in detail in Dunne (1987).

6.2.2 ALTERATION OF OCULAR PARAMETERS

The thickness of the cornea was varied by altering the location of the posterior corneal surface. This was done in order to avoid simultaneously varying the anterior chamber depth, measured from the anterior corneal surface to the anterior lenticular surface. For the same reason, lens thickness was altered by moving the posterior lenticular surface. Anterior chamber depth was altered by moving both the corneal surfaces.

Each of the eleven parameters were assigned four values, in addition to the mean value given in Kooijman's schematic eye (table 6.1). These were the maximum and minimum values found in human eyes (see table 4.1) and two other intermediate values. This resulted in 45 different schematic eyes, Kooijman's schematic eye and four models incorporating the four other values for each of the 11 variable parameters . The intermediate values were necessary to establish a relationship between the SAF and the parameter value by curve fitting.

Parameter	1.min.	2.	3.mean	4.	5.max.
anterior corneal radius	7.0	7.4	7.8	8.4	8.9
anterior corneal asphericity	0.1	0.425	0.75	1.125	1.5
corneal thickness	0.4	0.47	0.55	0.57	0.6
posterior corneal radius	5.8	6.2	6.5	7.0	7.4
posterior corneal asphericity	0.1	0.425	0.75	1.125	1.5
anterior chamber depth	2.5	3.05	3.6	4.1	4.6
anterior lenticular radius	7.7	9.0	10.2	12.0	13.8
anterior lenticular asphericity	-23.45	-18.4	-5.05	9.2	13.35
lens thickness	2.9	3.5	4.0	4.5	5.0
posterior lenticular radius	-4.6	-5.3	-6	-7.2	-8.3
posterior lenticular asphericity	-3.59	-1.8	0.19	1.6	3.21

Table 6.1 Showing the five values used for each of the eleven optical parameters. The table shows the maximum, mean and minimum values determined in chapter 2 and two intermediate values. Radii and thickness values are given in millimetres.

6.2.3 RESULTS

The variation in spherical aberration against pupil diameter for each of the eleven parameters is plotted in figures 6.1 to 6.11. The axes of each graph are drawn to the same scale to allow the relative effect of each of the parameters to be easily seen.

i) SURFACE ASPHERICITY

Modification in corneal and lenticular asphericity (figs 6.2, 6.5, 6.8 and 6.11) is clearly the most effective means of adjusting the spherical aberration. In the optical system of the eye the posterior corneal surface has negative dioptric power whilst the other three surfaces are positive. Increasing the conic constant of the positive surfaces, thereby steepening the surface curvature in the periphery, leads to increased levels of under-corrected spherical aberration. Alternatively, reducing the conic constant reduces under-corrected spherical aberration and, for extreme values, leads to slightly over-corrected spherical aberration. Reduction of spherical aberration is best achieved by peripheral flattening of the anterior corneal surface (fig. 6.2). The most effective increase is achieved by steepening the lenticular surfaces (figs. 6.8 and 6.11), particularly the anterior surface.

Adjusting the asphericity of the negative posterior corneal surface affects the spherical aberration in an opposite manner to the other three surfaces. Peripheral flattening increases

spherical aberration and peripheral steepening decreases it. Comparing fig. 6.5 to figs. 6.2, 6.8 and 6.11 it is clear that varying the asphericity of the posterior cornea within the human limits does not produce as wide range of spherical aberration values compared to those for the other three surfaces.

ii) SURFACE RADIUS

Variation in surface radius (figs. 6.1, 6.4, 6.7 and 6.10) does not influence spherical aberration to the same extent as variation in asphericity. For the anterior corneal (fig. 6.1) and posterior lenticular surfaces (fig. 6.10), decreasing the central radius of curvature increases spherical aberration. The reverse is true for the posterior corneal (fig. 6.4) and anterior lenticular (fig. 6.7) surfaces. Posterior corneal radius variations can be seen to cause very little variation in spherical aberration.

iii) SURFACE POSITION

Axial separation variations (figs. 6.3, 6.6 and 6.9) have the smallest effect on spherical aberration. Corneal thickness variation gives negligible difference. The effects of anterior chamber depth changes are negligible, giving a very slight increase with increasing depth. The effects of lens thickness variation are slightly more noticeable, with spherical aberration decreasing with decreasing thickness.

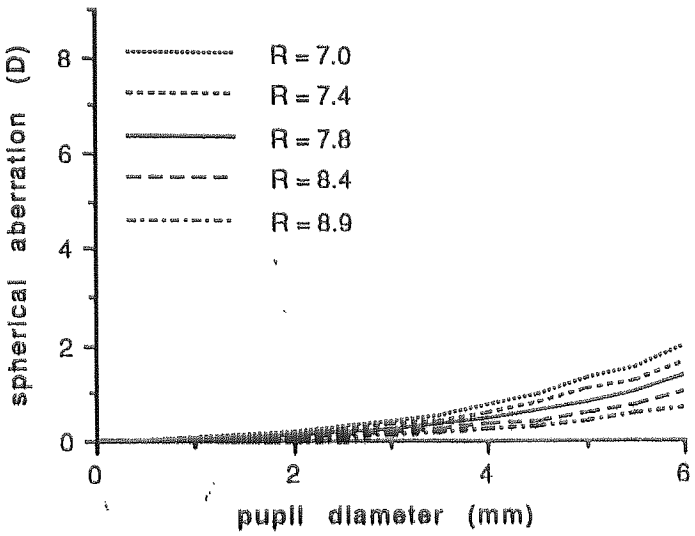

Fig. 6.1 Plots of spherical aberration versus pupil diameter for the full range of anterior corneal radii, R, (mm) reported in human eyes.

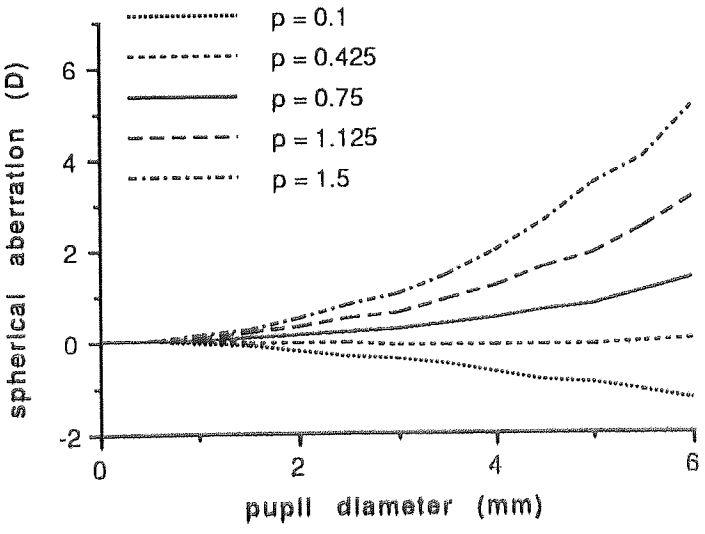

Fig. 6.2 Plots of spherical aberration versus pupil diameter for the full range of anterior corneal asphericities, p, reported in human eyes.

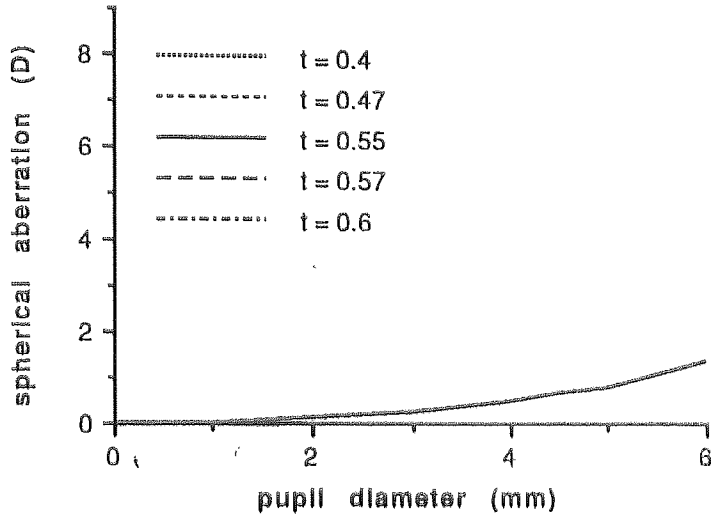

Fig. 6.3 Plots of spherical aberration versus pupil diameter for the full range of corneal thicknesses, t, (mm) reported in human eyes.

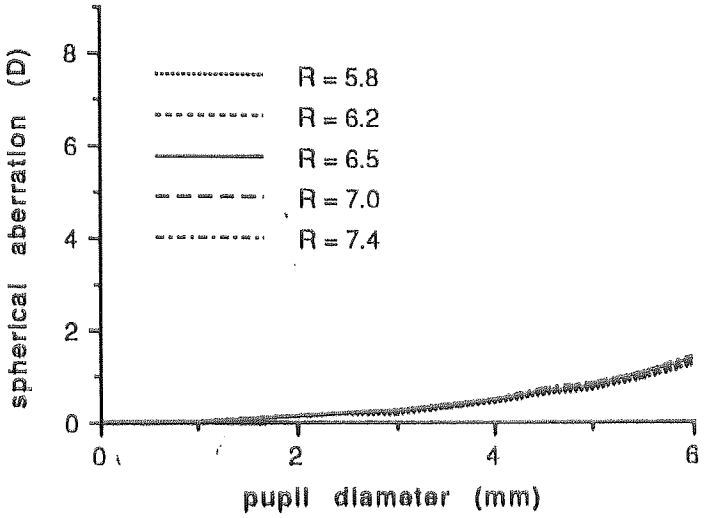

Fig. 6.4 Plots of spherical aberration versus pupil diameter for the full range of posterior corneal radii, R, (mm) reported in human eyes.

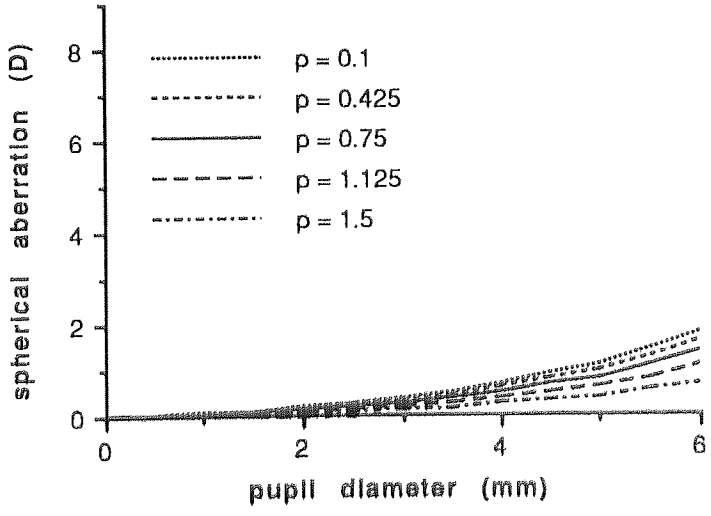

Fig. 6.5 Plots of spherical aberration versus pupil diameter for the full range of posterior corneal asphericities, p, reported in human eyes.

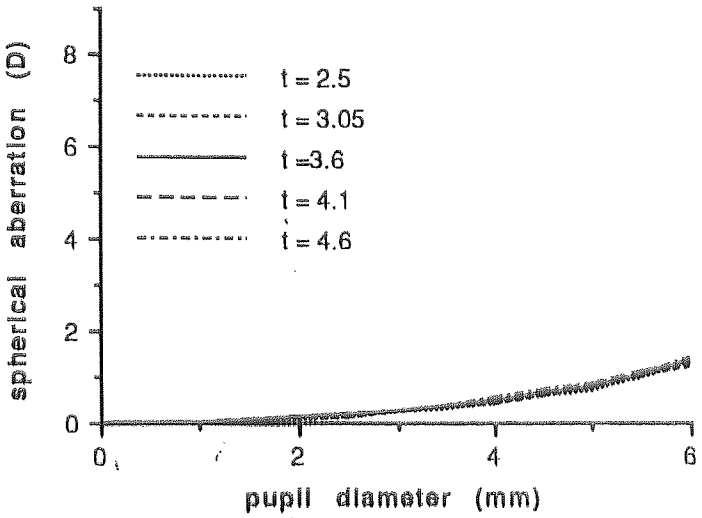

Fig. 6.6 Plots of spherical aberration versus pupil diameter for the full range of anterior chamber depths, t, (mm) reported in human eyes.

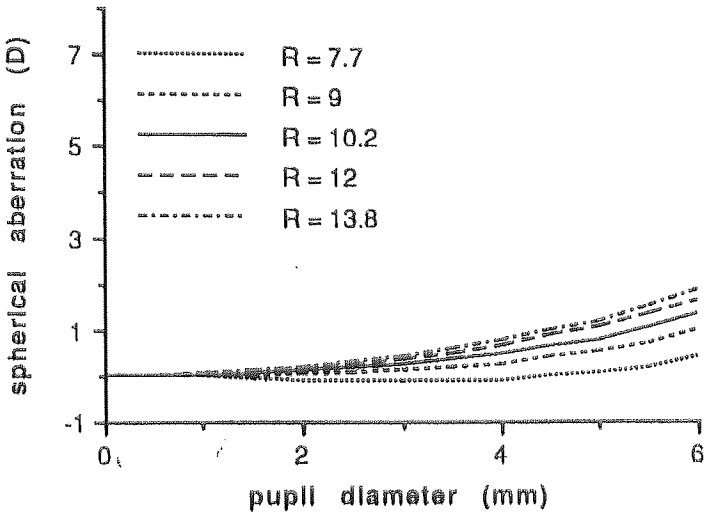

Fig. 6.7 Plots of spherical aberration versus pupil diameter for the full range of anterior lenticular radii, R, (mm) reported in human eyes.

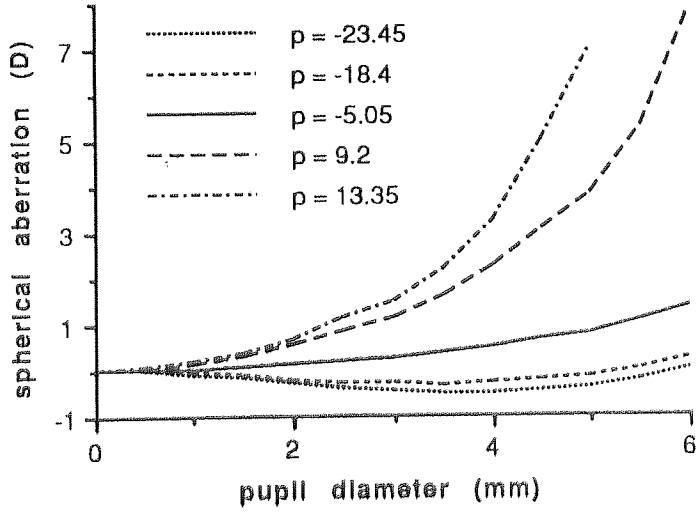

Fig. 6.8 Plots of spherical aberration versus pupil diameter for the full range of anterior lenticular asphericities, p, reported in human eyes.

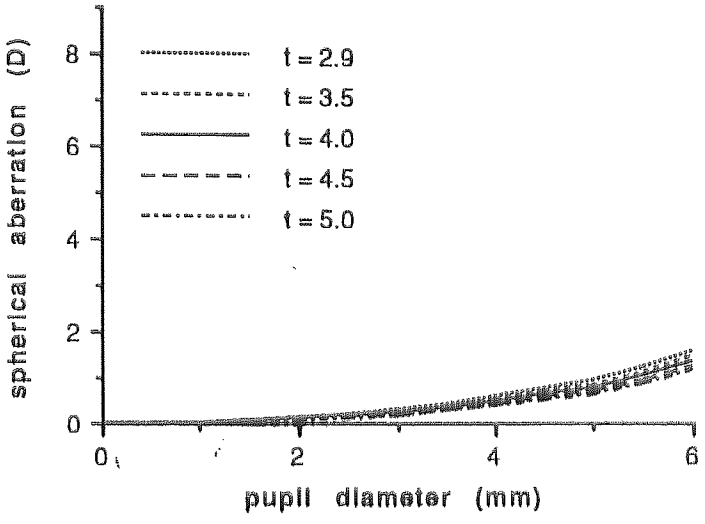

Fig. 6.9 Plots of spherical aberration versus pupil diameter for full range of lens thicknesses, t, (mm) reported in human eyes.

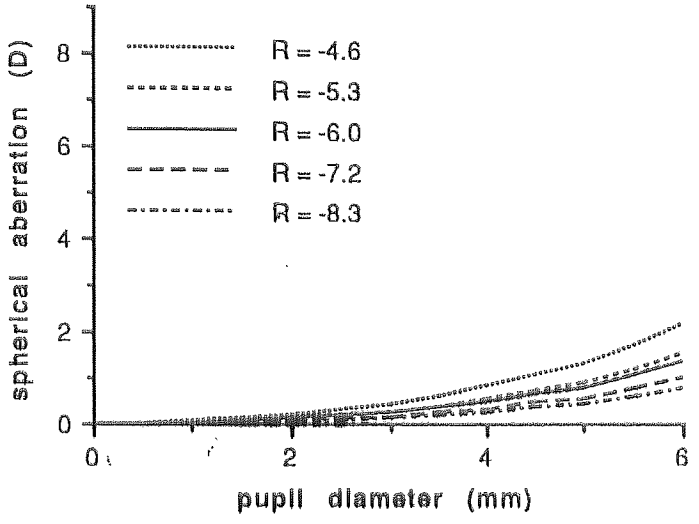

Fig. 6.10 Plots of spherical aberration versus pupil diameter for the full range of posterior lenticular radii, R, (mm) reported in human eyes.

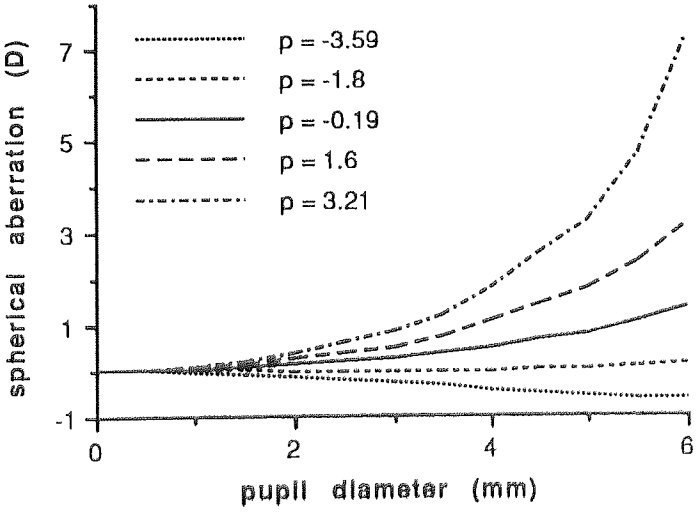

Fig. 6.11 Plots of spherical aberration versus pupil diameter for the full range of posterior lenticular asphericities, p, reported in human eyes.

6.3 OCULAR PARAMETER VARIATIONS AND SAF

6.3.1 CONVERSION FROM REAL TO ENTRANCE PUPIL DIAMETER

An observer looking at the front of an eye sees a magnified image of the real pupil formed by refraction at the cornea. This so called entrance pupil is situated just in front of the anterior corneal surface. Spherical aberration measured in real eyes is given in relation to the entrance pupil size and not the real pupil. The spherical aberration, calculated for schematic eyes in section 6.2 is plotted against real pupils. This is acceptable, as only the relative effects, on spherical aberration, of each of the parameters within the schematic eyes has been considered. To compare the values from the schematic eyes with those of real eyes, however, it is necessary to relate the calculated spherical aberration values to entrance pupil sizes. The entrance pupil diameter can easily be obtained from the ray tracing program used to calculate spherical aberration.

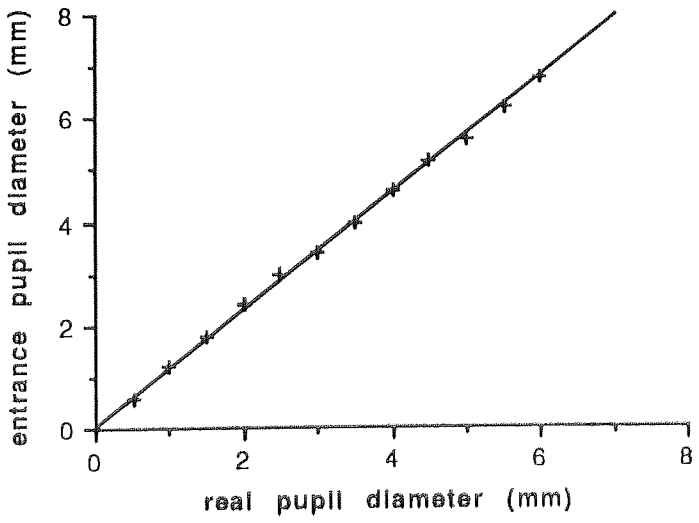

Fig. 6.12 Plot of entrance pupil diameter against real pupil diameter for Kooijman's Schematic eye (Kooijman, 1983).

The relationship between real pupil and entrance pupil for Kooijman's schematic eye (Kooijman, 1983) is plotted in fig. 6.12. A straight line is fitted to the datum points, the equation of which is:-

Entrance pupil diameter = 0.021 + 1.136 x real pupil diameter

In reality a real pupil of zero size would give an entrance pupil of zero size. The constant in the equation is,therefore, due to round off errors in the ray tracing program. The entrance pupil should be directionally proportional to the real pupil, the constant of proportionality being the magnification due to the cornea.

A plot of spherical aberration versus entrance pupil diameter for Kooijman's schematic eye results in a SAF of 1.6. This is clearly less than the value of 2.2 calculated from the plot of spherical aberration versus real pupil diameter. It is also a great deal lower than the SAF (2.9) given by the mean empirical values of Van Meeteren (1974). Hence, Kooijman's schematic eye does not model the mean spherical aberration of real eyes.

As mentioned in section 5.4.1., Dunne and Barnes (1987) considered that the spherical aberration exhibited by Kooijman's schematic eye was close to the values derived by Van Meeteren (1974). Unfortunately, they erred in plotting spherical aberration against the diameter of the real pupil and not the entrance pupil; thereby giving artificially high values. In fig 6.13 the spherical aberration values of Van Meeteren are compared to those of Kooijman's schematic eye, plotted against real pupil diameters and entrance pupil diameters. Values plotted against real pupil diameters closely follow those of Van Meeteren's curve, whereas values plotted against entrance pupil diameters are much smaller. Further, Dunne and Barnes used the original, uncorrected lenticular surface asphericity values for Kooijman's schematic eye (see section 5.4). The SAF values in this case are 3.3 for a real pupil and 2.5 for an entrance pupil. The SAF for real pupils is only slightly higher than the SAF given by Van Meeteren's spherical aberration plot. It is, therefore, understandable that Dunne and Barnes should consider that there was a close match between the spherical aberration of this schematic eye and the values of Van Meeteren. The SAF given by entrance pupils is also close to Van Meeteren's; being only slightly lower. From this evidence it would seem that Kooijman's original schematic eye modelled human spherical aberration better than the later, corrected version.

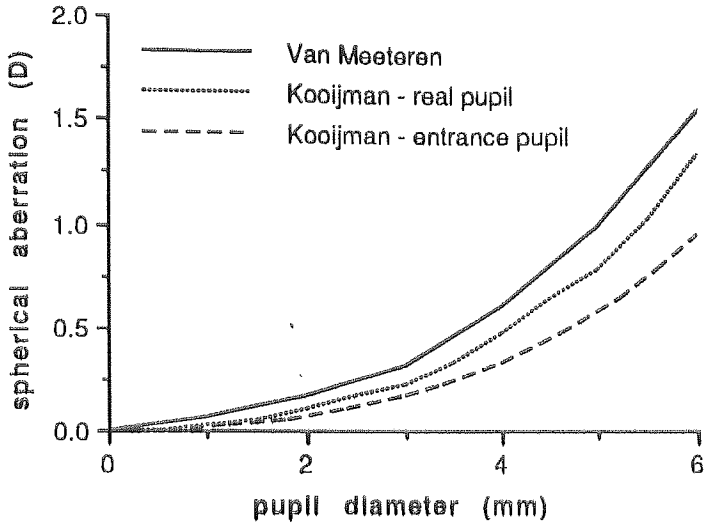

Fig. 6.13 Plot of spherical aberration versus pupil diameter. The mean values given by Van Meeteren (1974) are plotted against entrance pupil diameter. For comparison the results given by Kooijman's schematic eye (Kooijman, 1983) are shown plotted against the real pupil diameter and the entrance pupil diameter.

6.3.2 CALCULATION OF SAF

For each of the 45 schematic eyes described in section 6.2.2 a polynomial was fitted to the plot of spherical aberration versus entrance pupil diameter. In the majority of cases a second order polynomial gave a sufficiently close fit to the datum points. This suggests that the spherical aberration of these schematic eyes is almost purely third order, as third order spherical aberration is directly proportional to the square of the pupil size. However, the polynomial equations all include small constant and first order terms. This indicates that the relationship between spherical aberration and and the square of the pupil is not directly proportional. This may be due to round off errors or to the presence of small amounts of higher order aberrations. Some of the spherical aberration plots have shapes which are clearly not second order. In these cases higher order spherical aberration must contribute a larger proportion to the total. For example fifth order spherical aberration is directly proportional to the fourth power of the pupil size. Hence it is expected that the plots for schematic systems with significant amounts of higher order spherical aberration will be closely fitted by fourth order polynomials or higher. Third order polynomials were sufficient for many of these plots. From this it may be infered that higher order spherical aberration is still quite small in these systems.

Higher order aberrations normally become more significant in well corrected optical systems (Smith, 1990). Low levels of spherical aberration plotted against pupil diameter

would therefore be fitted by higher order polynomials. The results from the 45 schematic eyes show this to be the case. For example the SAF for an anterior corneal asphericity of 0.425 was found to be -0.4, showing very low levels of spherical aberration. The plot of spherical aberration versus pupil diameter for this schematic eye needed a third-order polynomial to give a close fit. This also applied to the schematic eye with a posterior lenticular asphericity of -1.8 (SAF = -0.1), and that with an anterior lenticular radius of 9 mm (SAF = 0.9).

Integration, between 0 and 6 mm pupil diameter, of the polynomial equations for each plot of spherical aberration verus entrance pupil gives the SAF values. SAF values were calculated for the five values given to each parameter and were then plotted against parameter value. Another polynomial was fitted to each of these plots. Knowing the relationship between the SAF and single parameter values, it is possible to predict the SAF level for any value of that parameter, provided the rest of the optical system remains unchanged. It is also possible to calculate the parameter value required to give a specified SAF by solving the polynomial equation.

6.3.3 RESULTS

SAFs for variations in each of the eleven parameters shown in table 6.1 are plotted in figures 6.14 to 6.24. The vertical axes (SAF) for each graph have been given the same scale to aid comparison. For all but one of the plots second order polynomials were fitted to the data. The plot of SAF against anterior lenticular asphericity required a third order polynomial for a close fit. It is important to stress that the relationships between SAF and parameter value will only hold if all other parameters retain their mean value. Multiple parameter variation would violate this condition.

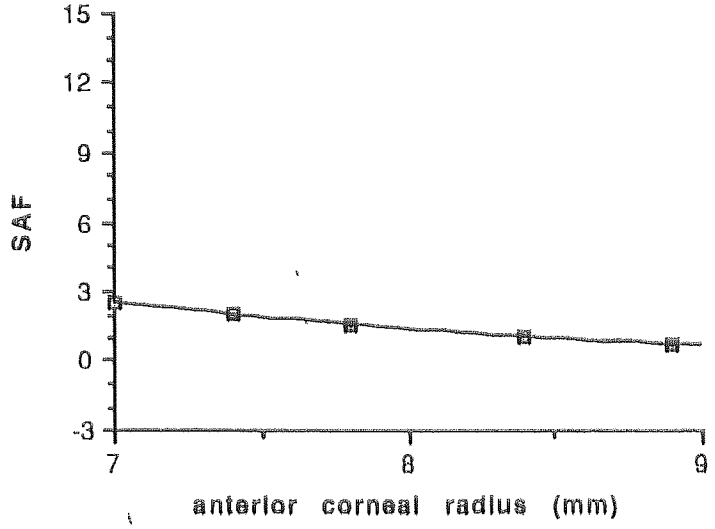

Fig. 6.14 Plot of the variation in the SAF for varying anterior corneal radius (mm). The equation of the curve is: SAF = 20.201 - 3.807R + 0.1824R^2 - where R is the anterior corneal radius.

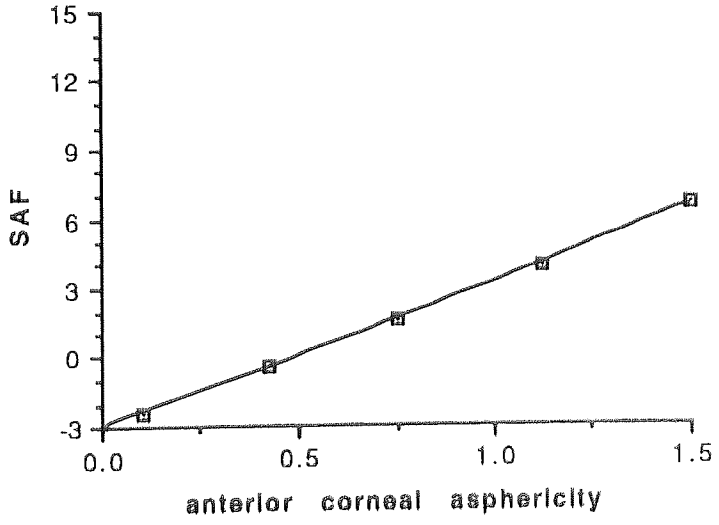

Fig. 6.15 Plot of the variation in the SAF for varying anterior corneal asphericity. The equation of the curve is: SAF = -2.950 + 5.655p + 0.487p^2 - Where p is the anterior corneal asphericity value or conic constant.

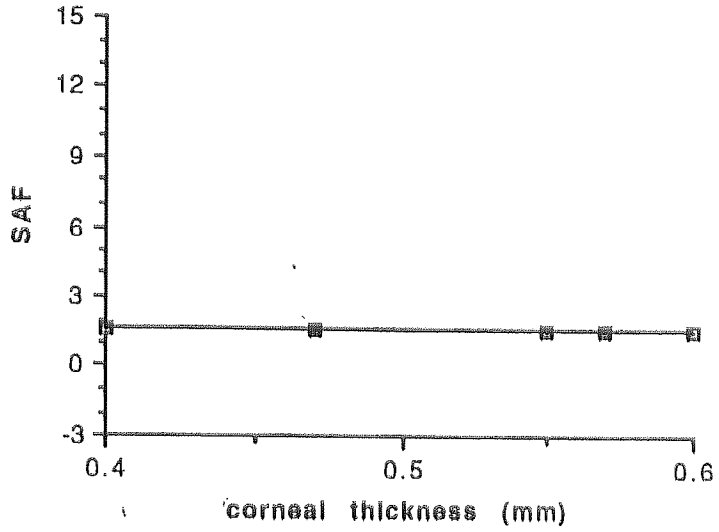

Fig. 6.16 Plot of the variation in the SAF for varying corneal thickness (mm). The equation of the curve is: SAF = 1.556 + 0.106t - 0.042 t^2 - Where t is the corneal thickness.

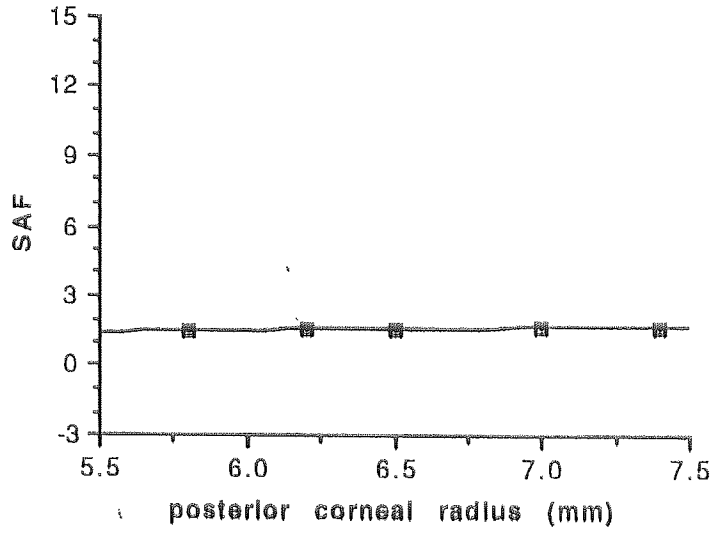

Fig. 6.17 Plot of the variation in the SAF for varying posterior corneal radius (mm). The equation of the curve is: SAF = -2.629 + 1.150R - 0.077R^2 - where R is the posterior corneal radius.

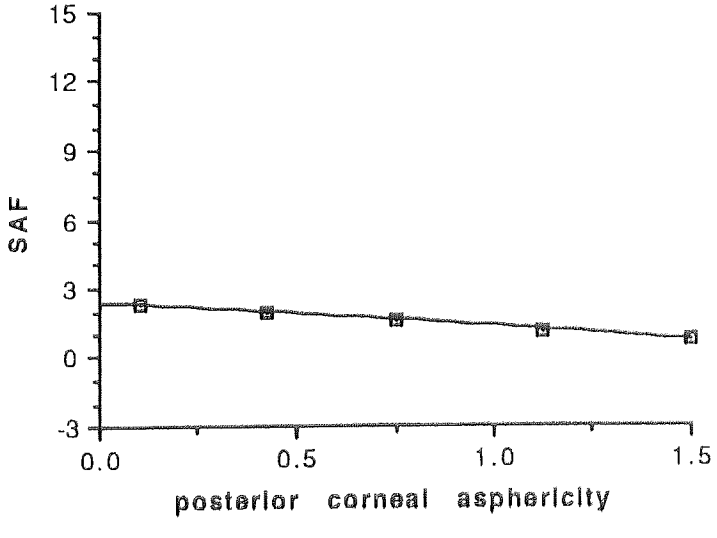

Fig. 6.18 Plot of the variation in the SAF for varying posterior corneal asphericity. The equation of the curve is: SAF = 2.338 - 0.877p - 0.138p^2 - where p is the posterior corneal asphericity or conic constant.

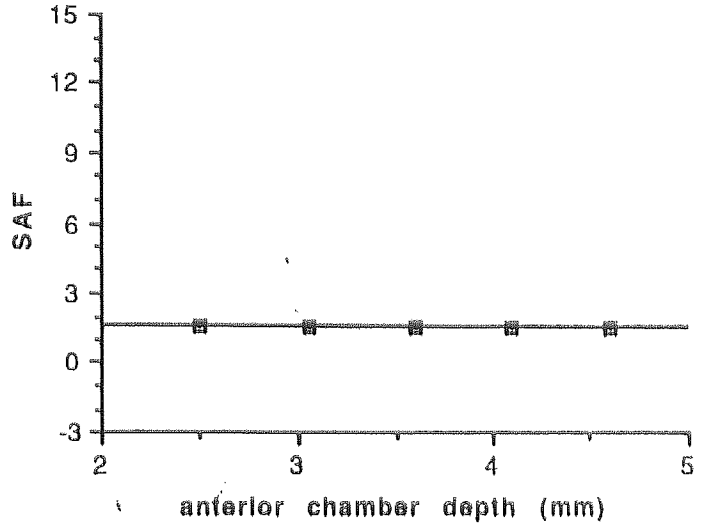

Fig. 6.19 Plot of the variation in the SAF for varying anterior chamber depth (mm). The equation of the curve is: SAF = 1.633 - 0.003t - 0.002 t^2 - where t is the anterior chamber depth.

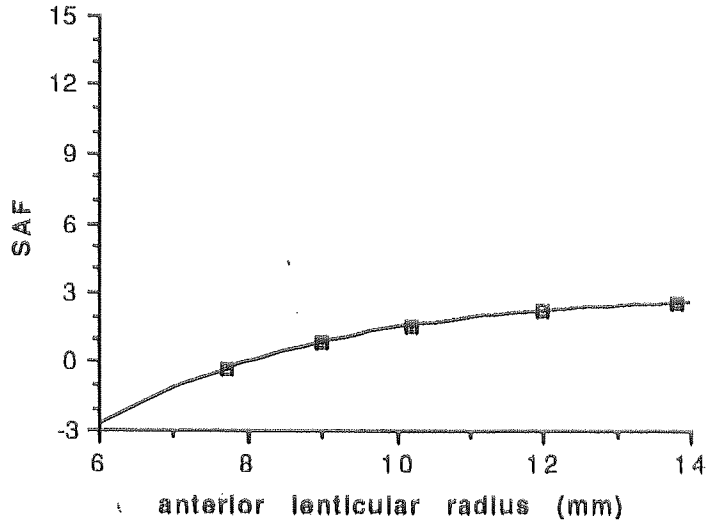

Fig. 6.20 Plot of the variation in the SAF for varying anterior lenticular radius (mm). The equation of the curve is: SAF = -12.084 + 2.124R - 0.077R^2 - where R is the anterior lenticular radius.

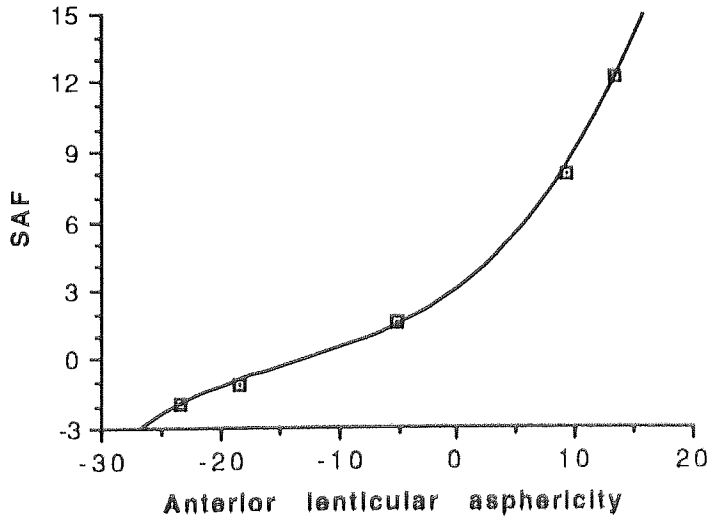

Fig. 6.21 Plot of the variation in the SAF for varying anterior lenticular asphericity. The equation of the curve is: SAF = 2.963 + 0.386p + 0.017p^2 + 0.0004p^3 - where p is the anterior lenticular asphericity or conic constant.

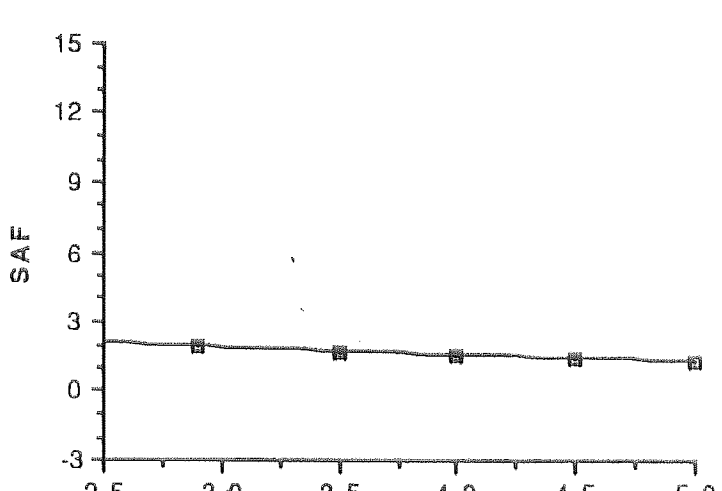

Fig. 6.22 Plot of the variation in the SAF for varying lens thickness (mm). The equation of the curve is: SAF = 2.924 - 0.394t + 0.016 t^2 - where t is the lens thickness.

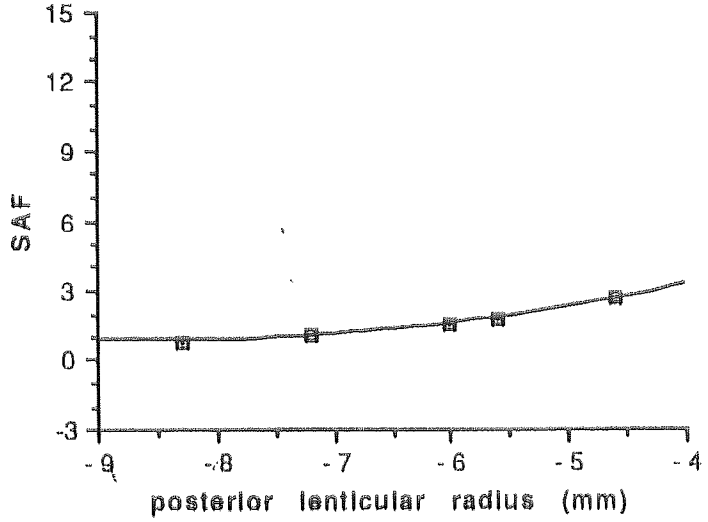

Fig. 6.23 Plot of the variation in the SAF for varying posterior lenticular radius (mm). The equation of the curve is: SAF = 9.548 + 2.035R + 0.119R^2 - where R is the posterior lenticular radius.

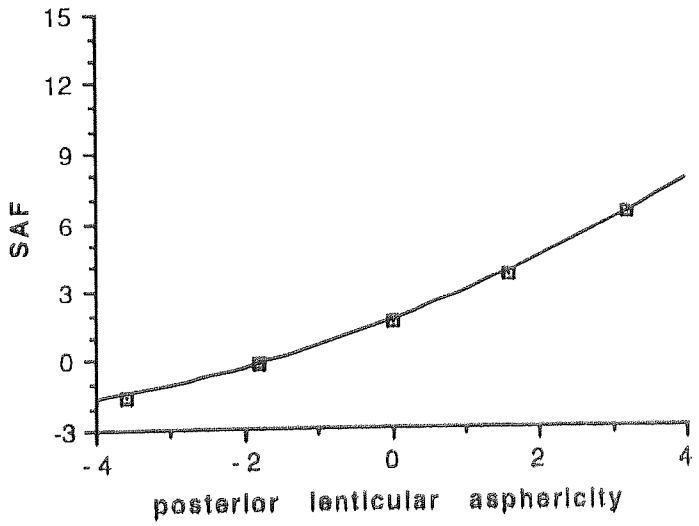

Fig. 6.24 Plot of the variation in the SAF for varying posterior lenticular asphericity. The equation of the curve is: SAF = 1.595 + 1.175p + 0.088p^2 - where p is the posterior lenticular asphericity or conic constant.

Table 6.2 summarises the results shown in figures 6.14 to 6.24. The table shows the effect on the spherical aberration of increasing each parameter. Increasing the asphericity of a surface means it becomes steeper in the periphery. An increase in the surface radius results in a flatter surface. SAF range is the range obtained by varying the parameter between the maximum and minimum measured human values. It gives an indication of which parameter variations have the greatest effect on spherical aberration.

Increasing parameter	effect on SAF	SAF range
anterior corneal radius	decrease	1.7
anterior corneal asphericity	increase	9.1
corneal thickness	increase	0.0
posterior corneal radius	increase	0.2
posterior corneal asphericity	decrease	1.5
anterior chamber depth	decrease	0.0
anterior lenticular radius	increase	3.0
anterior lenticular asphericity	increase	14.2
lens thickness	decrease	0.6
posterior lenticular radius	decrease	1.9
posterior lenticular asphericity	increase	7.9

Table 6.2 Summary of the results showing the effect of increasing parameter values. In the final column the range of SAF values, achieved by altering the parameters within the measured human range, is given. An increase in asphericity results in peripheral steepening of the ocular surface.

6.3.4 ERRORS

As the paraxial focus is calculated using a very small, but finite pupil this will induce a small error. Further errors will occur if the polynomial curve fitted to the datum point is not of a high enough order. This was found to lead to errors in the SAF as high as 8 per cent in some cases. The errors are negligible, however, when compared to measurements made in real eyes (section 2.2).

6.4 COMPARISON BETWEEN MODELLED AND EMPIRICALLY DERIVED SAFS

In section 2.4.1 of this thesis the maximum and minimum SAF values for real eyes were found. These are shown, along with the maximum and minimum values produced by variation of the individual parameters within human limits, in table 6.3.

Parameter	Maximum	Minimum
real eyes	5.2	0.8
anterior corneal radius	2.5	0.8
anterior corneal asphericity	6.7	-2.4
corneal thickness	1.6	1.6
posterior corneal radius	1.7	1.5
posterior corneal asphericity	2.2	0.7
anterior chamber depth	1.6	1.6
anterior lens radius	2.6	-0.3
anterior lens asphericity	12.3	-1.9
lens thickness	1.9	1.4
posterior lens radius	2.7	0.8
posterior lens asphericity	6.3	-1.5

Table 6.3 The maximum and minimum SAF values given by real eyes and by each parameter when its value is varied within measured human limits.

The maximum and minimum SAFs, given by each parameter, were compared with the maximum and minimum SAF given by real eyes. The range of asphericity values for the anterior cornea and the anterior and posterior lenticular surfaces were capable of encompassing the whole range of human SAF values. Indeed these three parameters produce SAFs which extended beyond the human range. By altering the radii of the anterior cornea and the anterior lens it is possible to reduce the SAF to the minimum empirical value, but not to increase it to the maximum. The maximum value can only be reached by altering the three asphericity values mentioned above. The large amounts of positive spherical aberration found in some eyes are, therefore, possibly the result of peripheral steepening in the anterior cornea and/or lens surfaces. Low levels of spherical aberration in eyes may be caused by any of the following: a large anterior corneal radius; a small anterior lens radius; anterior corneal and lenticular surfaces which flatten markedly in the periphery; or a posterior cornea which steepens in the periphery. These conclusions evidently ignore any effect due to the gradient index nature of the crystalline lens. The spread of spherical aberration due to this parameter would clearly be of interest.

6.5 DISCUSSION

The results show a pronounced lack of variation of spherical aberration with variation in the three axial separation parameters. It was noted that, when plotted against entrance pupil diameter, spherical aberration decreased with increasing anterior chamber depth. When plotted against real pupil diameters, however, spherical aberration increased with increasing anterior chamber depth. Parallel rays traced from the edge of the entrance pupil, into the eye, will be refracted by the cornea and converge as they travel through the anterior chamber. If the depth of the anterior chamber is increased the rays will travel further before reaching the pupil plane and will cross this plane closer to the optical axis. Spherical aberration will, therefore, be reduced. Consider the same rays traced back out of the eye along the same path. Increasing the anterior chamber will cause an increase in the entrance pupil size. This increases the spherical aberration due to the cornea and hence the overall spherical aberration is increased. The same reasoning could be applied to any change in the thickness of the cornea. However, the small range of variation in the corneal thickness used has negligible effect on spherical aberration.

Crystalline lens thickness is increased by moving the posterior lens surface backwards, towards the retina. Consequently, the converging rays passing through the lens will have further to travel and will intersect the posterior lenticular surface closer to the optical axis. This will have the effect of reducing the spherical aberration. The opposite will be true when the crystalline lens thickness is reduced. Variation in lens thickness over the full range has a slightly larger effect than found for corneal thickness and anterior chamber depth, but the effect is still small.

Altering the radius of curvature of the posterior corneal surface also causes little difference in spherical aberration. This is not surprising when we consider that the posterior cornea has low dioptric power due to the small difference between the refractive indices of the cornea and the aqueous (1.3771 and 1.3374 respectively). Any change in the curvature of the posterior corneal surface will result in very little change in its dioptric power and hence its spherical aberration.

Decreasing any surface radius will increase its dioptric power, causing the foci of rays at all heights to move closer to the lens surface if the surface is positive. The effect is greater for marginal rays than it is for rays close to the optical axis. Therefore, as the dioptric power of a positive lens is increased, its positive spherical aberration will also be increased. An increase in the dioptric power of a negative lens will increase its negative spherical aberration. If we perceive each surface of the eye as a separate lens element, the posterior

corneal surface is negative and the other three surfaces positive. It may be expected that increasing the radii of curvature of the three positive surfaces will increase the positive spherical aberration. Similarly, decreasing the radius of curvature of the negative posterior cornea should decrease the positive spherical aberration. The results are as predicted for the corneal surfaces and the posterior lens surface. In the case of the anterior lens surface, however, the results follow the opposite trend to what would be expected. Evidently we can not consider each individual surface in isolation but must also consider its interaction with the other optical surfaces in the system.

Altering the asphericity of a surface adjusts the vergence of marginal rays while paraxial ray vergence remains unaffected. This has clear advantages when designing optical systems as spherical aberration can be varied without altering the paraxial dioptric power of the optical system. It also explains why asphericity changes have a greater effect than surface radii changes. The distance between the paraxial and marginal foci, is more effectively reduced if the power in the periphery is decreased whilst the paraxial power remains constant.

The full range of asphericity values for the anterior corneal, the anterior lenticular and the posterior lenticular surfaces result in SAF values which encompass the full range found in human eyes. The minimum anterior lens asphericity value (-23.45) gives the largest overall SAF value of 12.3. This is more than double the maximum found in human eyes. If anterior lens surfaces do exist with such a low asphericity value, and the spherical aberration is to remain within the limits so far measured in human eyes, other parameters must compensate for its effect.

The minimum empirical SAF value of 0.8 reflects the fact that negative spherical aberration is not found in relaxed adult eyes. The extreme values of some parameters do result in negative spherical aberration. It is, therefore, likely that the effects on spherical aberration caused by such extreme parameter values are counteracted by other parameters which increases spherical aberration to more realistic levels.

Variations in the parameters of the lens have added interest in relation to the changes which take place during accommodation and the ageing of the lens (see section 4.5). The variation in spherical aberration caused by accommodation and aging was discussed in sections 2.3.3 and 2.3.4. The variation in peripheral astigmatism with accommodation and age was discussed in sections 3.3.4 and 3.3.5. The ways in which the results of this study relate to these findings will be investigated in chapter nine. The effect of lens parameter variations on spherical aberration and peripheral astigmatism will then be discussed simultaneously.

6.6 SUMMARY

A study of the variation in spherical aberration with variation in parameter values has revealed that:-

i) Variation in asphericity of either the anterior cornea, the anterior lens or the posterior lens, within human limits, can produce all levels of spherical aberration which have been found in human eyes.

ii) Variation in the posterior corneal asphericity will give minimum but not maximum values of human spherical aberration.

iii) Minimum spherical aberration can also be achieved by extreme values of the anterior corneal radius and the anterior lens radius. Variation in these two parameters will not produce maximum spherical aberration. Variation in the posterior lens radius gives nearly minimum values.

iv) Variations in corneal thickness, anterior chamber depth, lens thickness and posterior corneal radius have little effect on the spherical aberration.

The results from this chapter will be used in conjunction with results from the next chapter to model eyes which exhibit varying levels of spherical aberration and peripheral astigmatism.

CHAPTER 7
THE EFFECTS OF INDIVIDUAL OCULAR PARAMETER CHANGES ON PERIPHERAL ASTIGMATISM

7.1 INTRODUCTION

The purpose of this chapter is to determine the influence of each ocular parameter upon peripheral astigmatism. Ocular parameter variations were limited to ranges previously found in real eyes (chapter 4). As for spherical aberration in chapter 6, peripheral astigmatism is initially represented in the conventional manner, giving its value for varying field angle. The PAF is then calculated to show the rate of the variation of peripheral astigmatism with parameter value and to allow easy comparison with empirical values.

7.2 THE EFFECT OF CENTRAL ASTIGMATISM UPON PERIPHERAL ASTIGMATISM

When considering the astigmatism of an optical system it is important to differentiate between peripheral, or off-axis astigmatism, and central, or on-axis astigmatism. Peripheral astigmatism is caused by the obliquity of rays entering the system from off-axis points. Central astigmatism may occur for a variety of reasons. An optical system with rotationally symmetrical refracting surfaces, which are all centred on a common optical axis, will have no central astigmatism. Indeed, as discussed in section 1.3.1, the only aberration it will suffer from on-axis is spherical aberration. In the human eye central astigmatism is caused by the toricity of the refracting surfaces. There is also some evidence that the whole eye, or some of its constituent surfaces, are decentred with respect to the visual axis (see Barnes et al., 1987; Clement et al., 1987 and Dunne and Barnes, 1989). Decentration of individual surfaces means that there is no true optical axis and, therefore, no axial rays. In the case of rotation of the whole eye, rays travelling parallel to the visual axis will be oblique to the optical axis. In both situations astigmatism on the visual axis will arise due to the obliquity of rays to the axes of one or more of the optical surfaces. Whatever the cause, the amount of central astigmatism will influence the amount of peripheral astigmatism found in the eye.

7.2.1 THE EFFECTS OF EYE ROTATION ON CENTRAL ASTIGMATISM.

Previous research has shown that total eye rotation or ocular surface decentration produce only small amounts of central astigmatism. The effect on peripheral astigmatism can also be expected to be small. This previous research will firstly be discussed in relation to total eye rotation.

Total eye rotation does not influence the overall level of peripheral astigmatism. It does, however, alter the symmetry of the curve which describes the peripheral astigmatism as a function of field angle. For example, consider that in image space the eye is rotated 5°

temporally to the visual axis in the horizontal meridian. Tscherning considered this to be the average rotation of the human eye (Tscherning, 1924). The curve of peripheral astigmatism versus field angle would be symmetrical about the point 5° to the nasal side of the retina. There would then be peripheral astigmatism along the visual axis but this would amount to less that 0.25 D.

Dunne et al. (1993b) have measured the degree of eye rotation using the alignment of Purkinje images I and IV (see section 5.3.3). In 34 eyes they determined the amount of rotation from the visual axis required to line up the two images and also measured the Peripheral astigmatism. On average, 5° eye rotation was found whereas peripheral astigmatism was symmetrical at a point 9° on the nasal retina.

Other investigators, who have attempted to account for peripheral astigmatic asymmetry about the visual axis, have concluded that it is consistent with eye rotation of between 4° and 5° (Lotmar and Lotmar, 1974; Le Grand, 1967). The results of Dunne et al. are at variance with these findings but this may be due to the combined effects of measurement inaccuracies and a small sample of eyes.

7.2.2 THE EFFECTS OF OCULAR SUFACE MISALIGNMENT ON CENTRAL ASTIGMATISM

The author has constructed table 7.1 from the work of Barnes et al. (1987), who investigated the effects of rotation and translation of the cornea and crystalline lens on astigmatism. Ray traces were carried out through Kooijman's schematic eye (Kooijman, 1983) with a 2.5 mm pupil. The sagittal and tangential foci were determined for 5° rotation and 1mm translation of the cornea and lens in both nasal and inferior directions. The results are summarised in table 7.1 showing the amount of astigmatism induced on-axis, an estimation of the point around which the astigmatic image shells are symmetrical and the angular distance between the two points of axis change. The terms 'against-the-rule' and 'with-the-rule' will be explained in the next section.

parameter manipulated	nature of manipulation	estimated central astigmatism	estimated point of symmetry	estimated region of overlap of image shells
cornea	5° N rot. 1 mm N trans. 5° I rot. 1mm I trans.	~ 0.4 D A.T.R ~ 0 D ~0.3 D W.T.R ~ 0 D	~ 12° N ~15° N ~ 0° ~ 0°	0 ~ 0° - 30° N ~ 10° N - 10° T 0
crystalline lens	5° N rot. 1 mm N trans. 5° I rot. 1mm I trans.	~ 0 D ~0 D ~0 D ~0 D	~ 0° ~ 7° T ~ 0° ~ 0°	0 ~ 0° - 14° T 0 0

Table 7.1 Summary of the results of Barnes et al. (1987) showing the effects of rotation (rot.) and Translation (trans.) of the cornea and crystalline lens on astigmatism. The results show the point on the retina about which the sagittal and tangential astigmatic image shells are symmetrical. The final column shows the estimated points where these two image shells overlap. The abbreviations are N - nasal, I - inferior, T - temporal, A.T.R - against-the- rule, W.T.R - with-the-rule.

It is clear from the previous research discussed above that eye rotation and ocular surface misalignment produces very small amounts of central astigmatism. The major cause of central astigmatism in human eyes is therefore likely to be the toricity of the ocular surfaces. This will now be studied in the next section.

7.2.3 THE EFFECT OF SURFACE TORICITY ON CENTRAL AND PERIPHERAL ASTIGMATISM

i) BACKGROUND

If the surface toricity is such that the dioptric power of the eye is stronger vertically than horizontally the central astigmatism is said to be 'with-the-rule' (fig 7.1a). If the dioptric power of the eye is strongest horizontally then the central astigmatism is termed 'against-the-rule' (fig 7.1b). In a system with 'with-the-rule' astigmatism, central rays in the vertical plane will focus in front of central rays travelling in the horizontal plane, passing at the same height from the optical axis. In this study the plane of obliquity (the tangential plane) is considered to be the horizontal plane. Hence, for 'with-the-rule' astigmatism, centrally, the sagittal rays focus in front of the tangential rays. As the field angle of the rays increase,

the two foci move closer together and the interval of Sturm is decreased. At some point in the periphery the two foci meet and then cross over, so that the tangential focus lies in front of the sagittal focus. This cross over of the two foci has been described by Millodot (1981) as an axis change.

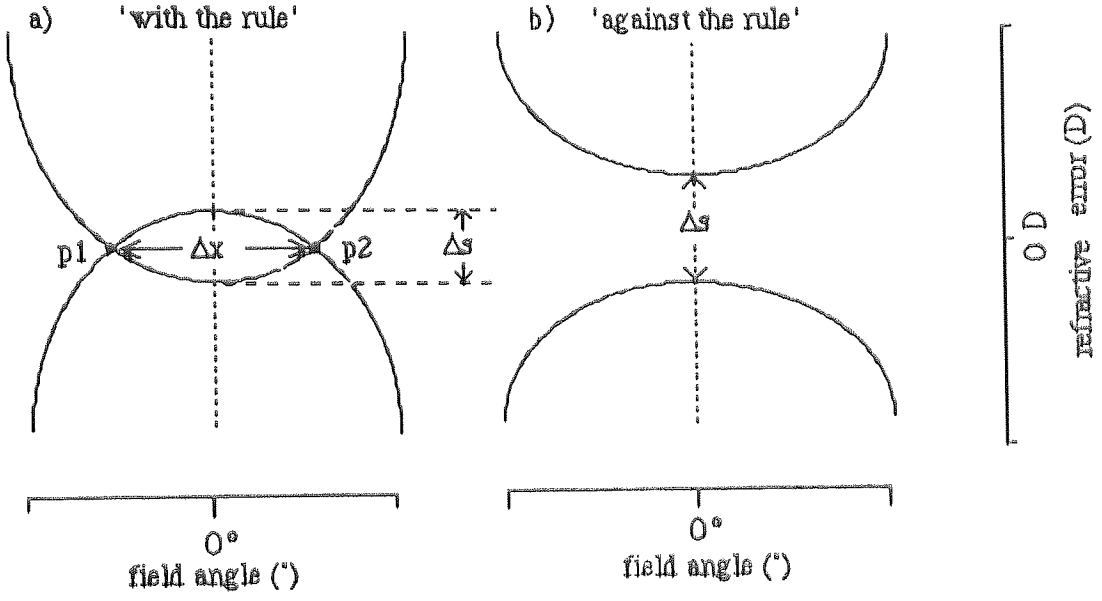

Fig. 7.1 a) Diagram showing 'with-the-rule' astigmatism. p1 and p2 are the points at which the axis changes take place. Δs is the central astigmatism. Δx is the angular distance between the two points of axis change. b) Diagram showing 'against-the-rule' astigmatism.

ii) COMPUTERISED RAY TRACING

This investigation was undertaken to find the effect corneal and lenticular toricity has upon peripheral astigmatism. An additional line of interest was whether toricity of different surfaces affected central and peripheral astigmatism in the same way (White et al.1991). Rays were traced using the techniques of Clement et al. (1987) and Barnes et al. (1987). The schematic eye used was the spherical surfaced model of LeGrand and El Hage (1980) with a 4 mm real pupil. The central radii, axial separations and refractive indices for this model are:

anterior corneal radius	= 7.8 mm
posterior corneal radius	= 6.5 mm
anterior lenticular radius	= 10 mm
posterior lenticular radius	= -6 mm
retinal radius	= 12 mm

cornea thickness	= 0.55 mm
anterior chamber depth	= 3.6 mm
lens thickness	= 4 mm
vitreous depth	= 16.6 mm
corneal refractive index	= 1.3771
aqueous refractive index	= 1.3374
lenticular refractive index	= 1.42
vitreous refractive index	= 1.336

The effect on astigmatism of the toricity of each surface was studied in turn. The horizontal radius was altered to give a rotationally asymmetric surface which produced 'with-the-rule' astigmatism. The horizontal radii of the anterior cornea and the two lens surfaces were increased. The horizontal raduis of the negative posterior corneal surface was decreased. Four ray traces were carried out for each surface. For the first trace the horizontal radius of the surface was altered by 0.1 mm from the radius of the original spherical surface. For the subsequent ray traces a further 0.1 mm was added or subtracted from the radius value. Rays were traced with internal angles (i.e. the angle at the physical pupil) from 50° nasally to 50° temporally in intervals of 10°. The resulting field angles varied according to the horizontal dioptric power of the system. The sagittal and tangential refractive errors, in dioptres, were noted for for each angle. The amount of central astigmatism induced depends on the power of the refracting surface. Changing the horizontal radius of the anterior corneal surface therefore produces the greatest amount of central astigmatism. The radii of curvature and central astigmatism values for each surface are given in table 7.2

surface	vertical radius	horizontal radius	central astigmatism
anterior cornea	7.8 mm	7.9 mm	-1.1 D
	7.8 mm	8.0 mm	-2.1 D
	7.8 mm	8.1 mm	-3.0 D
	7.8 mm	8.2 mm	-4.0 D
posterior cornea	6.5 mm	6.4 mm	-0.2 D
	6.5 mm	6.3 mm	-0.3 D
	6.5 mm	6.2 mm	-0.5 D
	6.5 mm	6.1 mm	-0.7 D
Anterior lens	10 mm	10.1 mm	-0.1 D
	10 mm	10.2 mm	-0.2 D
	10 mm	10.3 mm	-0.3 D
	10 mm	10.4 mm	-0.4 D
posterior lens	-6 mm	-6.1 mm	-0.3 D
	-6 mm	-6.2 mm	-0.5 D
	-6 mm	-6.3 mm	-0.7 D
	-6 mm	-6.4 mm	-1.0 D

Table 7.2 showing the central astigmatism induced by the toricity of the four ocular surfaces.

A graph of refractive error versus field angle for the sagittal and tangential foci was plotted for each trace. Second order polynomials were then fitted to the image shells. These could subsequently be used to calculate the distance between the two points of axis change.

Second order polynomials have the general form:-

$$y = Ax^2 + Bx + C$$

where A, B and C are constants.
for the purpose of this study y is the refractive error and x is the field angle.
For the tangential and sagittal curves we can write:-

$$y_T = ax_T^2 + bx_T + c$$
$$y_S = dx_S^2 + ex_S + f$$

At the two points of axis change the interval of Sturm is zero and so:

$$y_T = y_S = y \quad \text{and} \quad x_T = x_S = x$$

and $ax^2 + bx + c = dx^2 + ex + f$

rearranging gives:-

$$(d-a)x^2 + (e-b)x + (f-c) = 0$$

This can be solved for x using the quadratic formula:-

$$x = \frac{-B \pm \sqrt{(B^2 - 4AC)}}{2A}$$

Where A=(d-a), B=(e-b) and C=(f-c).

This will give two values for the field angle (p1 and p2 - see fig 7.1) which will be equal, but of opposite sign, due to the symmetry of the astigmatic curves about zero field angle. The distance between the two points of axis change (Δx) is given by p2 - p1.

Example of calculation of the points of axis change:

The values are taken from the curves fitted to the image shells for the model with a horizontal anterior corneal radius of 7.9 mm. This induces 1.1 D of central astigmatism.

Tangential curve:	a = -0.0022,	b = -3.313×10^{-6},	c = 0.5478
Sagittal curve:	d = 9.058×10^{-4}	e = -3.290×10^{-6},	f = -0.5587

$A = (d-a) = 3.11\times10^{-3}$

$B = (e-b) = 2.3\times10^{-8}$

$C = (f-c) = -1.1065$

using the quadratic formula

$$\Delta x = \left(-2.3\times10^{-8} \pm \sqrt{\left[(2.3\times10^{-8})^2 - 4 \times 3.11\times10^{-3} \times (-1.1065) \right]}\right) \div 2 \times 3.11\times10^{-3}$$

p1 = -18.875° and p2 = 18.875°

$\Delta x = p2 - p1 = 37.75°$

But the central astigmatism - $\Delta S = (f-c)$
and (e-b) is negligible and so the equation can be reduced to:-

$\Delta x = \sqrt{(-4\Delta S /(d-a))}$

The second-order term of the polynomials fitted to the image shells remained fairly constant and (d-a) was found to be approximately equal to 0.003 for each set of astigmatic curves. Therefore, Δx can be said to be approximately proportional to $\sqrt{\Delta S}$:-

$$\Delta x \approx \sqrt{\frac{4000}{3}\Delta S}$$

With this equation we can calculate approximately how far into the periphery the image shell cross over points will be for any amount of central astigmatism. For example, for a system with 2 D of central astigmatism $\Delta x = 51.6°$. The cross over points will thus be found at approximately 25.8° on the nasal and temporal retina.

In the second part of the study, 1.0 D of central astigmatism was induced by altering the horizontal radii of the anterior corneal and posterior lenticular surfaces by the appropriate amounts. The values were 7.8946 mm for the anterior corneal horizontal radius and - 6.4120 mm for the posterior lenticular horizontal radius.

iii) RESULTS

The image shells resulting from toric anterior corneal surfaces are shown in fig 7.2. As previously noted, the value of the x^2 terms in the equations fitted to each of the curves was almost constant. The curvature of the image shells was, therefore, expected to be similar. In fig. 7.2 the variation in curvature of the image shells only becomes distinguishable for field angles of greater than approximately 40°. For increasing toricity, the increase in peripheral astigmatism caused by the increase in curvature of the tangential image shell is partially compensated for by the decrease in curvature of the sagittal image shell. Indeed, it was found that if the central astigmatism was added to the peripheral astigmatism at each field angle the values were very close to the peripheral astigmatism given by a system with no toricity. For example, taking the system with 3.0 D of central astigmatism, induced by a toric anterior cornea, adding 3.0 D to the peripheral astigmatism at 60° gave a value of

11.7 D. The peripheral astigmatism for the schematic eye without toric surfaces was 10.9 D at 60°, a difference of only 0.8 D. For a 40° field angle the difference was only 0.2 D. The overall result of introducing toric surfaces into a system may consequently be considered as a shift in the tangential image shell by the amount of central astigmatism induced.

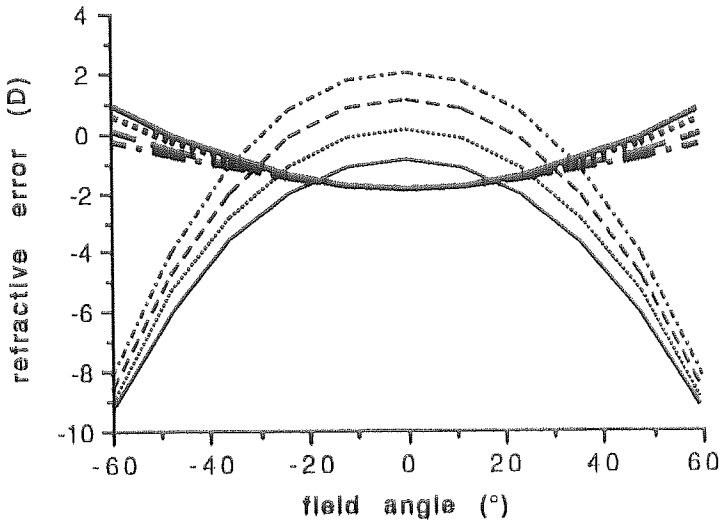

Fig 7.2 The tangential (fine lines) and Sagittal (bold lines) image shells for toric anterior corneal surfaces. The values for the vertical radius is constant at 7.8 mm the values for the horizontal radii are 7.9 (continuous line), 8.0 (dotted line), 8.1 (dashed line) and 8.2 (Dashed and dotted line)

The second part of the study investigated the effects of inducing the same amounts of central astigmatism with two different ocular surfaces. The results are shown in fig 7.3.

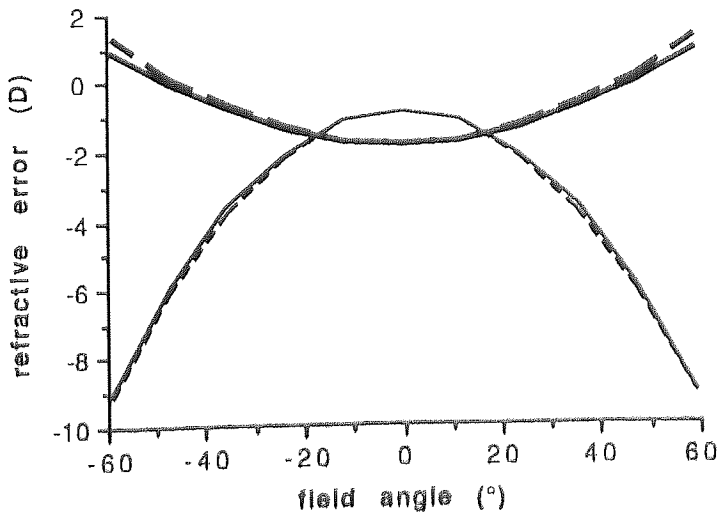

Fig 7.3 Sagittal (bold lines) and Tangential (fine lines) image shells when 1.0 D of central astigmatism is induced by the anterior cornea (continuous line) and the posterior lens (dashed line).

The tangential image shells for the schematic eyes with 1 D of central astigmatism induced by the anterior cornea and the posterior lens were seen to be closely superimposed on one another (fig 7.3). Surprisingly the sagittal image shells are less accurately superimposed. The points at which the image shell crossed, calculated using the method described above, were the same regardless of which surface caused the central astigmatism.

iv) CONCLUSIONS

The principal effect of toricity of optical surfaces was found to be a shift in the tangential image shell by the amount of induced central astigmatism. The image shells produced by two different ocular surfaces with the same amount of central astigmatism were almost indistinguishable.

The angular distance between the two points of axis change (Δx), either side of the optical axis was found to be approximately proportional to the central astigmatism (ΔS). Furthermore, the relationship between Δx and ΔS was approximately the same for all four of the ocular surfaces. It was concluded that it was not possible to identify which surface was responsible for the central astigmatism by examining the position of the points of axis change. What did emerge, however, is that surface toricity has the effect of reducing peripheral astigmatism. This could account for the low levels found in some eyes. For example a horizontal corneal radius of 8 mm induces central astigmatism of 2.1 D. At a field angle of 40° the peripheral astigmatism is 3 D. For the schematic eye with no central astigmatism the peripheral astigmatism 40° into the periphery is 4 D.

The schematic eyes used in this study have rotationally symmetrical ocular surfaces and, therefore, no central astigmatism. The studies from which the empirical data was taken all took measures of peripheral astigmatism in eyes with little or no central astigmatism. It is, therefore, feasible to compare the modelled values of peripheral astigmatism found in this study with this empirical data. However, if peripheral astigmatism is to be modelled accurately for individual eyes, account must be taken of any central astigmatism.

7.3 OCULAR PARAMETER VARIATION AND PERIPHERAL ASTIGMATISM

7.3.1 COMPUTERISED RAY TRACING

Using the linear algebraic ray tracing program of Clement et al. (1987) adapted by Barnes et al. (1987) peripheral astigmatism was calculated for the same 45 schematic eyes used in chapter 6. Principal rays were traced out of the eye starting at the physical pupil centre.

This is coincident with the vertex of the anterior lenticular surface. Rays were traced from 0° to 50° either side of the optical axis in 10° steps. For the purpose of this study negative angles are taken to represent the nasal retina and positive angles the temporal retina.The angles the principal rays made with the optical axis on emerging from the eye were taken to be the field angles. Each principal ray was then tracked back down its path, accompanied by four parallel marginal rays either side in the vertical and horizontal planes. For a pupil of 4 mm diameter, the position of the marginal rays was determined by increasing their distance from the principal ray incrementally from 0 in 0.1 mm steps until they hit the physical pupil edge. The five rays were then traced through the remainder of the schematic eyes optical system and the two foci were determined. The intersection of the vertical rays is the sagittal focus and the intersection of the horizontal rays the tangential focus. The horizontal plane was chosen as the plane of obliquity (the tangential plane), as peripheral astigmatism has been most often studied in the horizontal plane of real eyes (see chapter 3). The program converts the distance along the principal ray, from each focus to the retina, into dioptres using the formula of Lotmar and Lotmar (1974). The foci are then expressed as the refractive error in dioptres from the retinal surface. The computer program calculates peripheral astigmatism as the refractive error of sagittal marginal rays minus the refractive error of tangential marginal rays. This method mirrors the way in which peripheral astigmatism is measured in real eyes.

As discussed previously (section 5.3.3), comatic distortion in the system results in three foci in each meridian. Two foci at the point where each marginal ray crosses the principal ray and the third where the marginal rays cross each other. The latter was used to calculate peripheral astigmatism, and the two former foci represent the outermost limits of the comatically distorted image.

7.3.2 RESULTS

Figures 7.4 to 7.14 are plots of peripheral astigmatism versus field angle for the eleven parameters under consideration. Each figure shows the five plots resulting from the five values assigned to the parameter (see section 6.2.2). The axes of each graph are identical in order for the relative effect of varying the value of each parameter within human limits to be easily compared. The results are plotted on only one side of the optical axis (field angle 0°) as peripheral astigmatism is symmetrical about this axis for centred systems.

The peripheral astigmatism of Kooijman's schematic eye lies between maximum and mean values found in real eyes (section 5.4). Only a minimal increase from this value is required

to reach the maximum peripheral astigmatism found in real eyes. A much larger decrease in peripheral astigmatism is required to reach minimum human values.

i) SURFACE ASPHERICITY

In general asphericity changes (figs. 7.5, 7.8, 7.11, 7.14) produce a greater variation in peripheral astigmatism compared with the variation caused by changes made to the central radius (figs. 7.4, 7.7, 7.10, 7.13). Anterior corneal asphericity (fig. 7.5) gives the second largest reduction for the minimum p value of 0.1. Altering the posterior corneal asphericity (fig. 7.8), however, has very little affect on peripheral astigmatism. Peripheral steepening of the anterior and posterior lenticular surfaces causes large increases in peripheral astigmatism. Flattening the surfaces peripherally to their minimum p values give levels of peripheral astigmatism which are only very slightly smaller than levels given by their mean values. For the maximum posterior lenticular asphericity ($p = 3.21$) no values of peripheral astigmatism could be obtained for field angles of greater than approximately 30° due to marginal rays missing the surface.

ii) SURFACE RADIUS

Changes in the posterior corneal radius (fig. 7.7) have negligible effect on peripheral astigmatism. For the other three surfaces the effect appears to be very similar (figs 7.4, 7.10, 7.13). However, the anterior lenticular surface has the opposite directional effect to the other two surfaces. Increasing the anterior lenticular radius decreases peripheral astigmatism; whereas increasing the anterior corneal and posterior lenticular surface radii increases it.

iii) SURFACE POSITION

Anterior chamber depth variation (fig. 7.9) would appear to have the greatest influence on peripheral astigmatism, achieving the lowest values given by any of the parameters when the depth is increased to its maximum value of 4.6 mm. Adjustment in corneal thickness (fig. 7.8) has negligible effect and adjustment of lens thickness (7.12) only a small effect on the peripheral astigmatism.

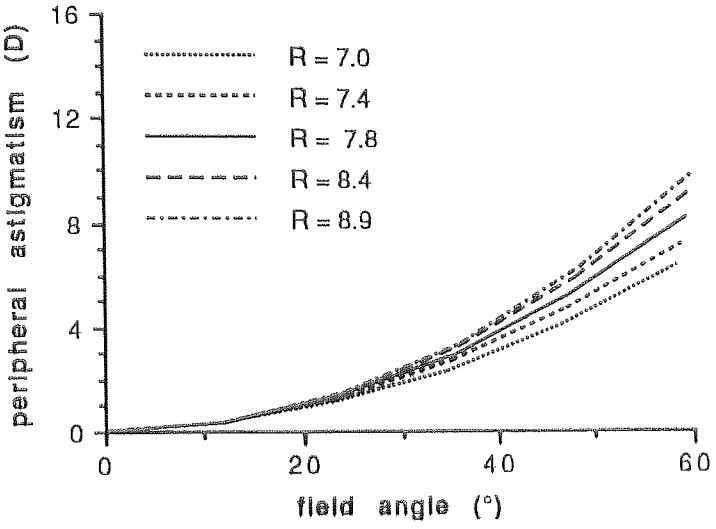

Fig. 7.4 Plots of peripheral astigmatism versus field angle for the full range of anterior corneal radii , R, (mm) reported in human eyes.

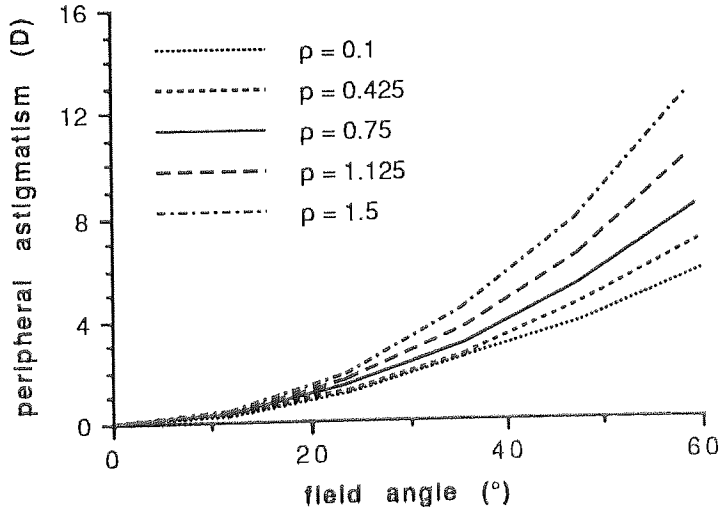

Fig. 7.5 Plots of peripheral astigmatism versus field angle for the full range of anterior corneal asphericities, p, reported in human eyes.

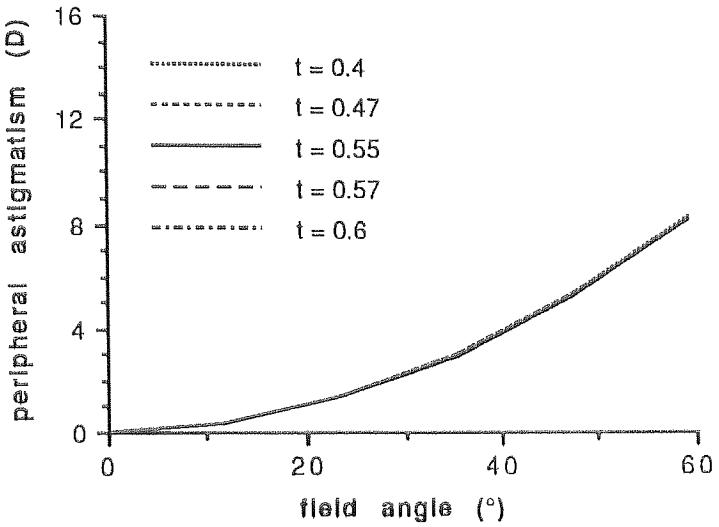

Fig. 7.6 Plots of peripheral astigmatism versus field for the full range of corneal thicknesses, t, (mm) reported in human eyes.

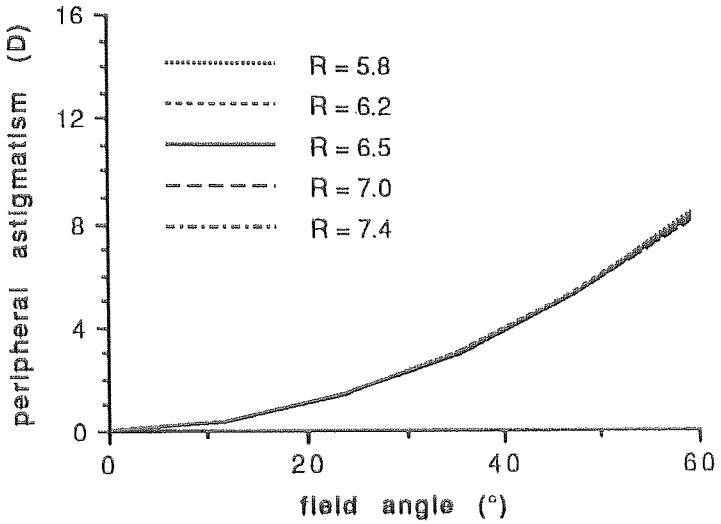

Fig. 7.7 Plots of peripheral astigmatism versus field angle for the full range of posterior corneal radii , R, (mm) reported in human eyes.

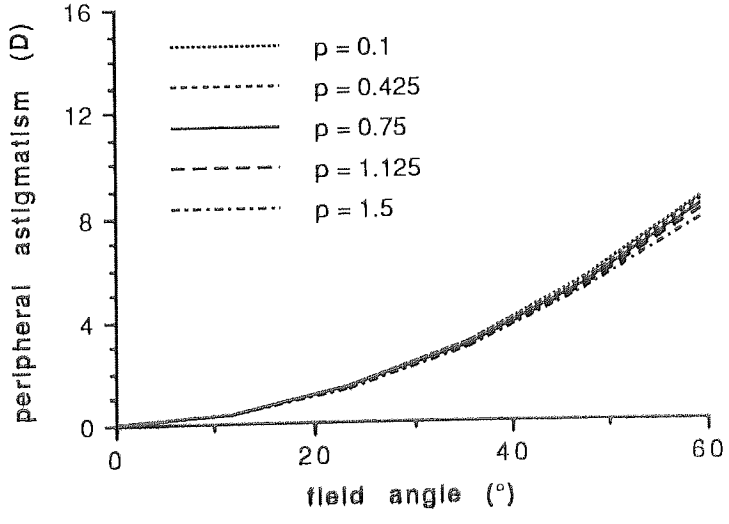

Fig. 7.8 Plots of peripheral astigmatism versus field angle for the full range of posterior corneal asphericities, p, reported in human eyes.

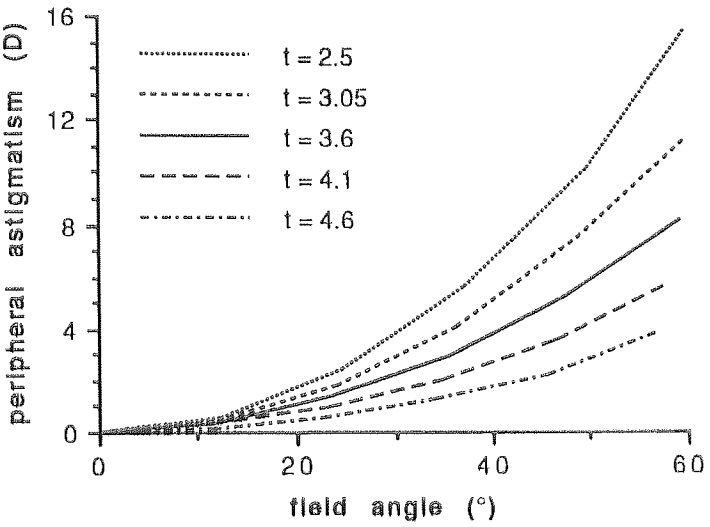

Fig. 7.9 Plots of peripheral astigmatism versus field angle for full range of of anterior chamber depths, t, (mm) reported in human eyes.

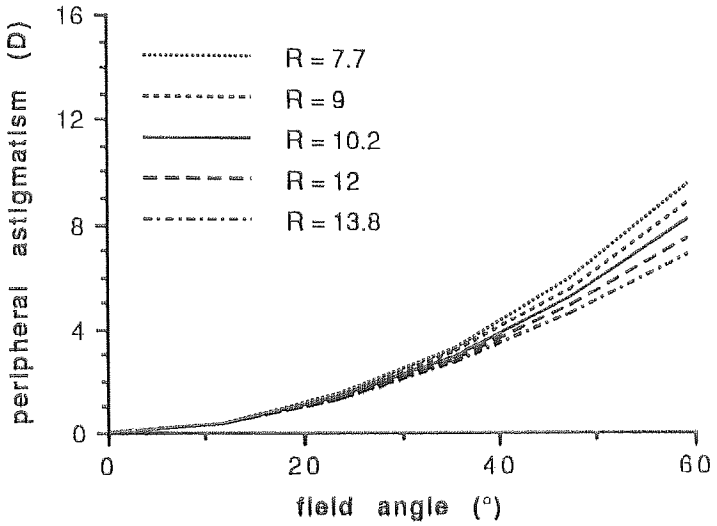

Fig. 7.10 Plots of peripheral astigmatism versus field angle for the full range of anterior lenticular radii , R, (mm) reported in human eyes.

Fig. 7.11 Plots of peripheral astigmatism versus field angle for the full range of anterior lenticular asphericities, p, reported in human eyes.

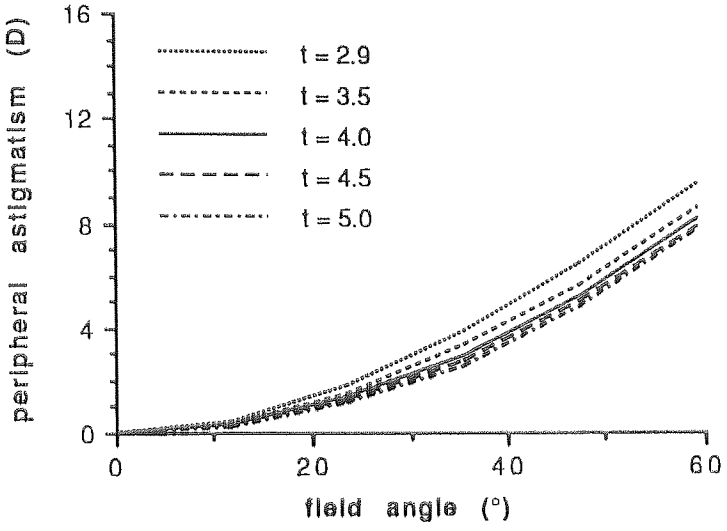

Fig. 7.12 Plots of peripheral astigmatism versus field angle for the full range of lens thicknesses, t, (mm) reported in human eyes.

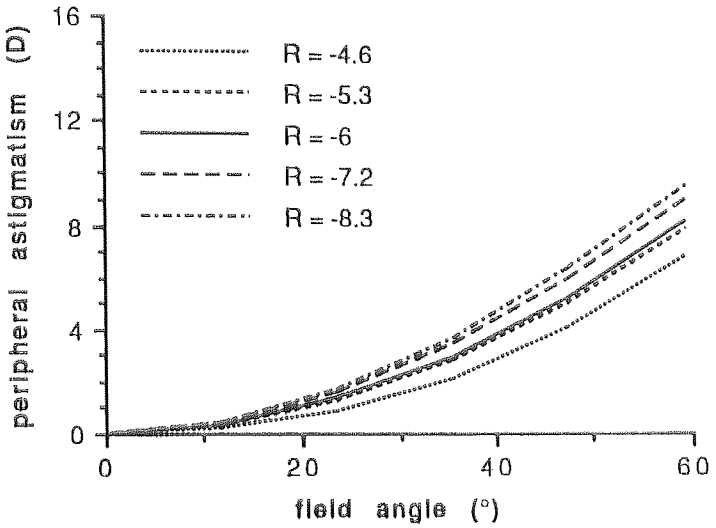

Fig. 7.13 Plots of peripheral astigmatism versus field angle for the full range of posterior lenticular radii , R, (mm) reported in human eyes.

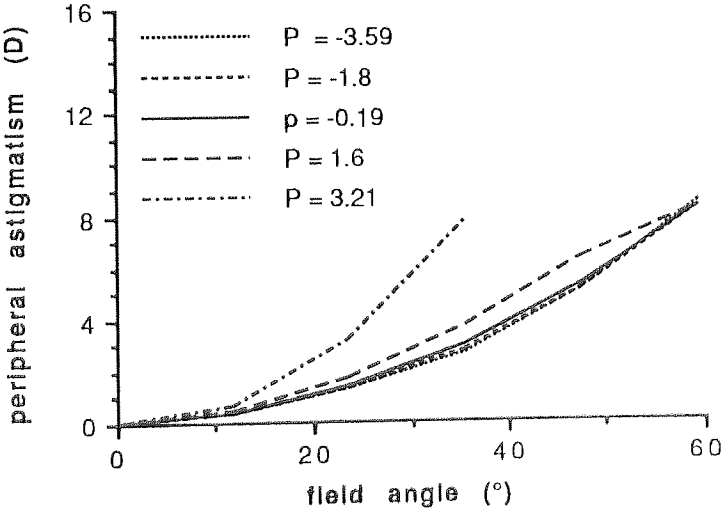

Fig. 7.14 Plots of peripheral astigmatism versus field angle for the full range of posterior lenticular asphericities, p, reported in human eyes.

7.4 OCULAR PARAMETER VARIATIONS AND PAF

7.4.1 CALCULATION OF PAF

For each of the 45 schematic eyes polynomial curves are fitted to the plots of peripheral astigmatism versus field angle. In almost all cases a second-order polynomial gave a sufficiently close fit to the datum points. However, for some of the plots a fourth-order polynomial was required. Given that third-order peripheral astigmatism is proportional to the square of the field angle it would appear that few of the schematic eyes suffer from significant amounts of higher-order peripheral astigmatism. Fourth-order polynomials are generally required if the peripheral astigmatism values are low or very high. For example, for the maximum anterior chamber depth of 4.6 mm, The PAF given by a fourth-order polynomial is 43.5 and for a second-order polynomial it is 46.8. This gives a seven per cent error in the PAF value when a second-order polynomial is fitted to the datum points. The largest errors occur if second-order polynomials are fitted to the plots given by the maximum values of asphericity for the anterior and posterior lenticular surfaces, which give high PAF values. For the maximum anterior lens asphericity (p = 13.35) a second-order polynomial gives a PAF of 175.3 and a forth-order polynomial gives a PAF of 135.5. The difference in these two values represents a 29.4 per cent error in the PAF if a second-order polynomial is fitted to the plot of peripheral astigmatism against field angle. For low levels of peripheral astigmatism, the need to fit a forth-order polynomial can be explained by the higher significance of higher-order aberration (see section 6.3.2).

Integration of the polynomials between -40° and 40° gives the PAF values. For each parameter five PAF values were calculated and plotted against parameter values.

7.4.2 RESULTS

The relationship between PAF and parameter value for each of the eleven parameters is plotted in figs. 7.15 to 7.25. The vertical axis, representing the PAF values, is standardised to allow easy comparison of the results. A polynomial is fitted to the datum points which, in most cases, are well fitted by second-order equations. However, in the case of anterior and posterior lenticular asphericity third- and fourth-order equations, respectively, are needed to give a reasonable fit. These higher-order relationships were confirmed by calculating two further PAFs. In both cases the two extra datum points fell on the fitted curves. A third-order polynomial was also found to give a better fit to the relationship between PAF and corneal thickness. However, since the variation in PAF is so small, any

inconsistency between the datum points and a second-order polynomial may be due to errors.

The PAF plots clearly show the small amount of variation in peripheral astigmatism for changes in corneal thickness (fig. 7.17), posterior corneal radius (fig. 7.18) and posterior corneal asphericity (fig. 7.19). They also show the relatively large variations with anterior corneal asphericity (fig. 7.16), anterior chamber depth (fig. 7.20), anterior lenticular asphericity (fig. 7.22) and posterior lenticular asphericity (fig. 7.25). The curves fitted to the plots for the anterior and posterior lenticular asphericities become almost horizontal for lower asphericity values, clearly showing how the PAF is little affected by reducing asphericity below the mean value.

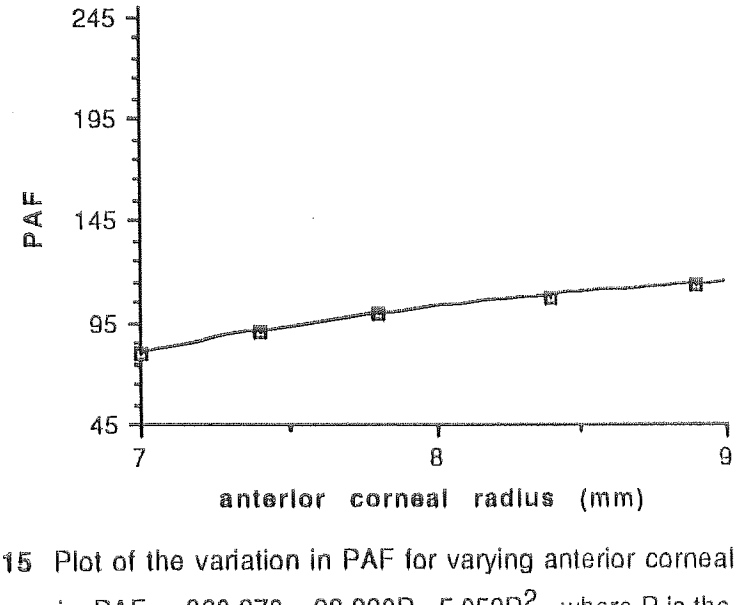

Fig. 7.15 Plot of the variation in PAF for varying anterior corneal radius. The equation of the fitted curve is: $PAF = -360.270 + 98.330R - 5.052R^2$ - where R is the anterior corneal radius.

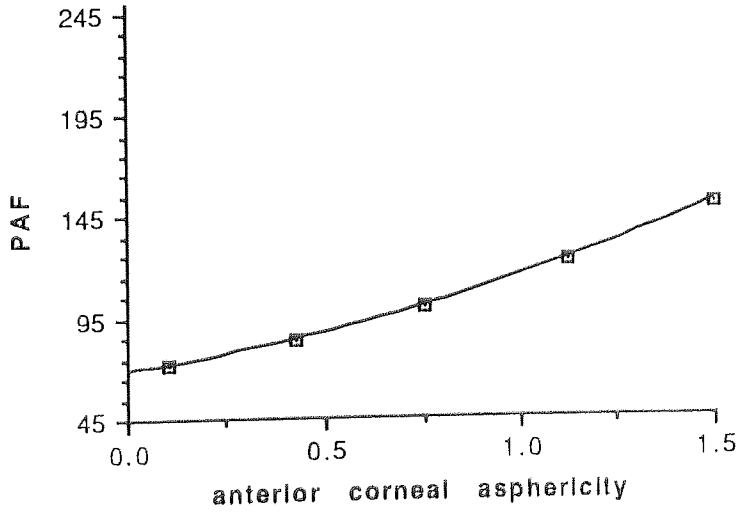

Fig. 7.16 Plot of the variation in PAF for varying anterior corneal asphericity. The equation of the fitted curve is: $PAF = 69.074 + 27.550p + 18.234p^2$ - where p is the anterior corneal asphericity.

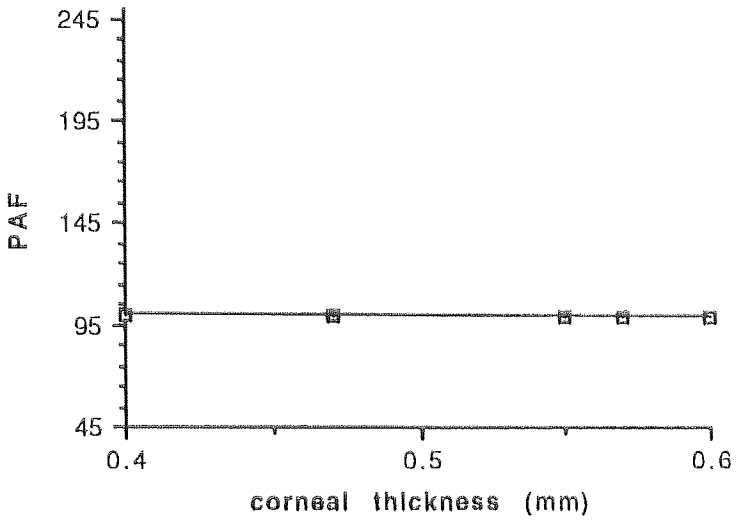

Fig. 7.17 Plot of the variation in the PAF for varying corneal thickness. The equation of the fitted curve is: $PAF = 58.201 + 252.150t - 496.410t^2 + 320.030t^3$ - where t is the corneal thickness.

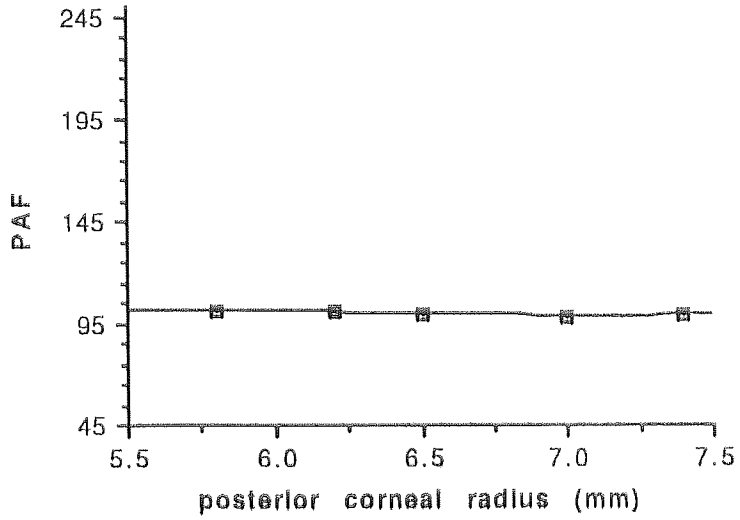

Fig. 7.18 Plot of the variation in PAF for varying posterior corneal radius. The equation of the fitted curve is: PAF = 156.760 - 15.836R + 1.091R^2 - where R is the posterior corneal radius.

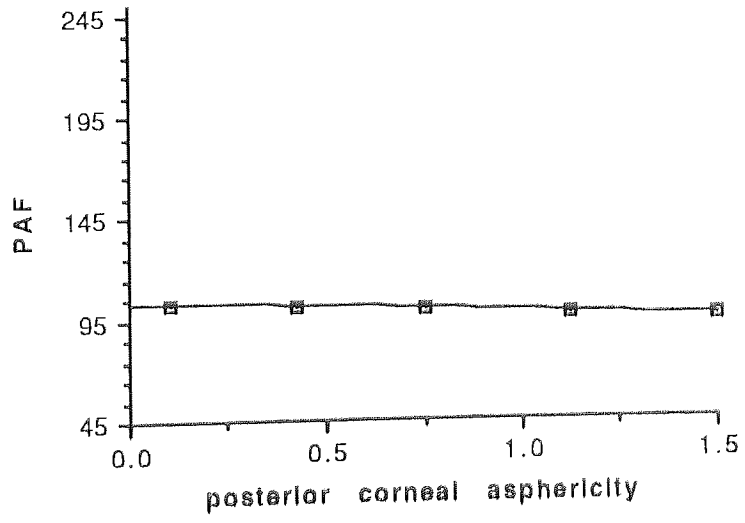

Fig. 7.19 Plot of variation in PAF for varying posterior corneal asphericity. The equation of the fitted curve is: PAF = 102.810 - 2.936p - 1.237p^2 - where p is the posterior corneal asphericity.

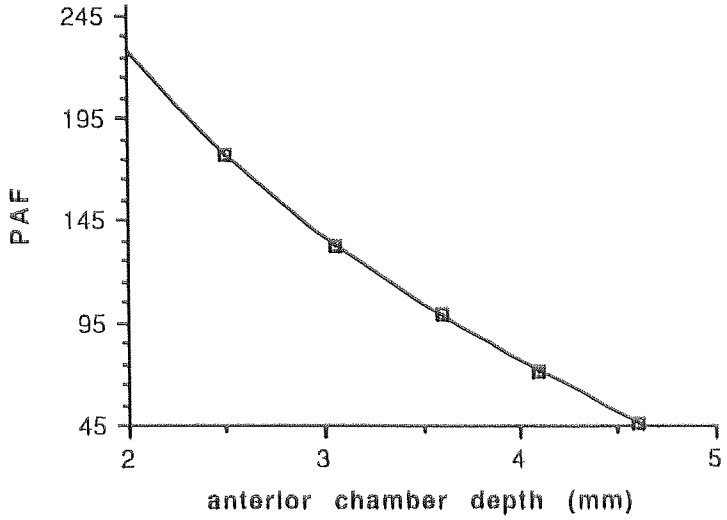

Fig. 7.20 Plot of variation in PAF for varying anterior chamber depth. The equation of the fitted curve is: $PAF = 436.430 - 126.360t + 9.079t^2$ - where t is the anterior chamber depth.

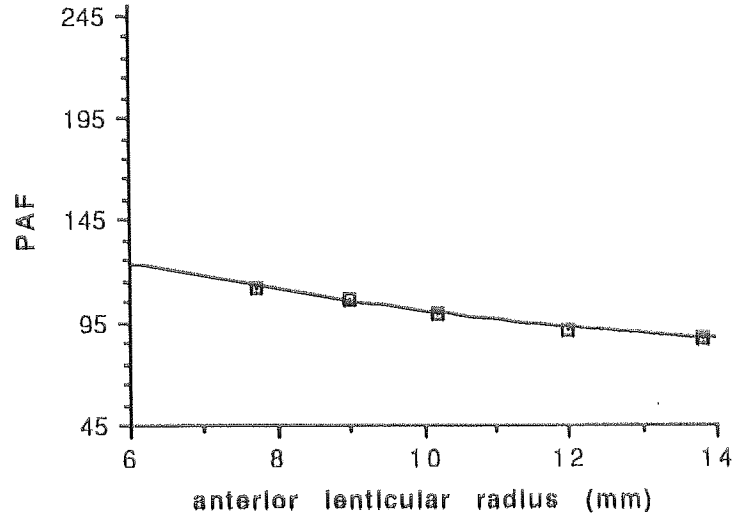

Fig. 7.21 Plot of variation in the PAF for varying anterior lenticular radius. The equation of the fitted curve is: PAF = 173.430 - 10.000R + 0.275R^2 - where R is the anterior lenticular radius.

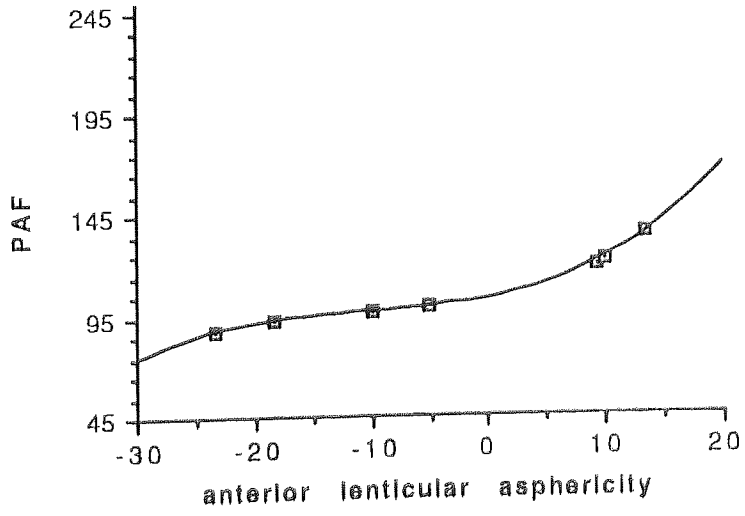

Fig. 7.22 Plot of variation in the PAF for varying anterior lenticular asphericity. The equation of the fitted curve is: PAF = 103.340 + 1.077p + 0.068 p^2 + 0.002 p^3 - where p is the anterior lenticular asphericity.

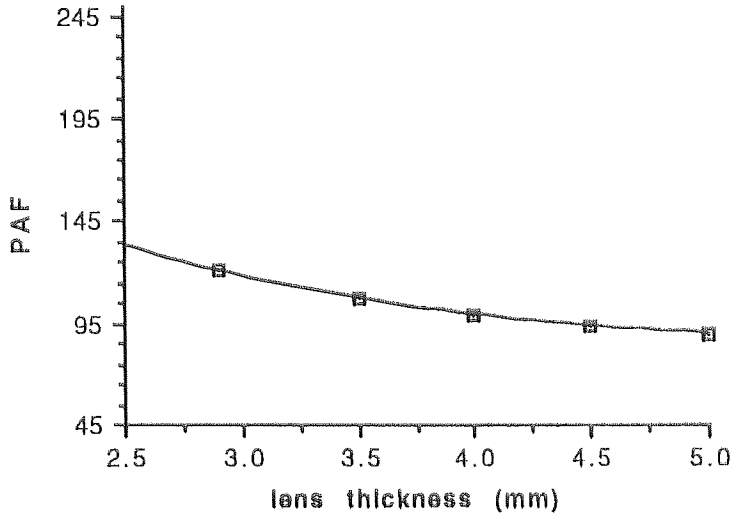

Fig 7.23 Plot of the variation in the PAF for varying lens thickness. The equation of the fitted curve is: PAF = 233.720 - 53.329t + 4.968t ^{2} - where t is the lens thickness.

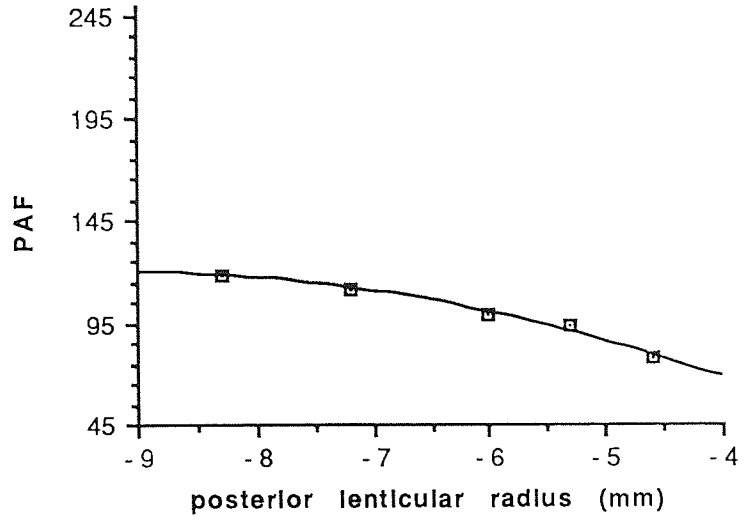

Fig. 7.24 Plot of the variation in PAF for varying posterior lenticular radius. The equation of the fitted curve is: PAF = -44.692 - 36.340R - 2.008R^2 - where R is the posterior lenticular radius.

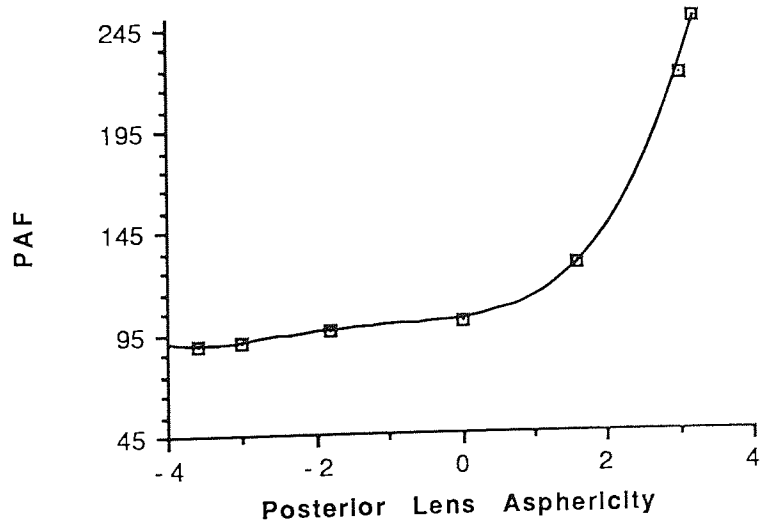

Fig. 7.25 Plot of the variation in the PAF for varying posterior lenticular asphericity.The equation of the fitted curve is: PAF = 100.670 + 4.466p + 3.816p^2 + 1.985p^3 + 0.272 p^4 - where p is the posterior lenticular asphericity.

The results from figs. 7.15 to 7.25 are summarised in table 7.3. The table shows the effect of increasing each of the parameters has on the peripheral astigmatism. The PAF range is the range of values achieved by varying the parameters within the limits found in human eyes. It indicates which parameters have the greatest effect on peripheral astigmatism. Corneal thickness has such a small effect that it neither effectively increases or decreases the PAF.

increased parameter	effect on PAF	PAF range
anterior corneal radius	increase	34.6
anterior corneal asphericity	increase	79.4
corneal thickness	-	0
posterior corneal radius	decrease	2.4
posterior corneal asphericity	decrease	6.5
anterior chamber depth	decrease	131.2
anterior lenticular radius	decrease	24.5
anterior lenticular asphericity	increase	87.4
lens thickness	decrease	30.0
posterior lenticular radius	increase	41.0
posterior lenticular asphericity	increase	159.1

Table 7.3 Summary of the results showing the effect of increasing parameter value. The PAF range is the range of values achieved by altering parameters within the limits found in human eyes. An increase in the asphericity results in peripheral steepening of the ocular surface peripherally.

7.5 COMPARISON BETWEEN MODELLED AND EMPIRICALLY DERIVED PAFS

The PAF for the mean values found in human eyes given by Lotmar and Lotmar (1974) was found to be 66.0 (see section 3.4.1). As anticipated, this is much lower than the PAF value of 100 for Kooijman's 'mean' schematic eye (Kooijman, 1983). The maximum and minimum values for the PAF found in human eyes are shown in table 7.4. They are compared to the maximum and minimum values obtained by varying each of the eleven parameters in the schematic eyes.

Parameter	Maximum	Minimum
real eyes	**128.8**	**24.7**
anterior corneal radius	115.0	80.4
anterior corneal asphericity	151.4	72.0
corneal thickness	100	100
posterior corneal radius	101.5	99.1
posterior corneal asphericity	102.3	95.8
anterior chamber depth	178.0	46.8
anterior lenticular radius	112.4	87.9
anterior lenticular asphericity	175.3	87.9
lens thickness	121.0	91.1
posterior lenticular radius	119.3	78.3
posterior lenticular asphericity	255.9	97.1

Table 7.4 The maximum and minimum PAF values given by real eyes and by each parameter when its value is varied within measured human limits.

From table 7.4 it is evident that, for a single parameter variation within the limits of human values, the mean human value can only be achieved by an increase of the anterior chamber depth. Even for the deepest anterior chamber, the PAF is still higher than the minimum human value. To achieve the minimum peripheral astigmatism levels it is clear that a number of 'PAF reducing' parameter values will have to be combined in one schematic eye. The maximum human PAF can be easily achieved by variation of either the anterior corneal asphericity, the anterior chamber depth, the anterior lenticular asphericity or the posterior lenticular asphericity. The maximum PAF values given by variation of these four parameters are higher than found in any human eyes. If levels of astigmatism are to be kept within the range so far measured the high levels of peripheral astigmatism produced by these parameter values must be compensated for by other parameters within the system.

7.6 DISCUSSION

The most striking finding from the study of the variation in peripheral astigmatism with parameter value is the large variation given by anterior chamber depth changes. This is of still more interest if we consider the simultaneously small effect changes in this parameter have on spherical aberration. This makes it possible to reduce peripheral astigmatism quite drastically while keeping spherical aberration at a constant level. Of further interest would to see if eyes with low peripheral astigmatism do have large anterior chamber depths. From inspection of the data taken on 34 subjects in a previous study (see section 5.5) it would

seem that it is not the general rule that eyes with large anterior depths have low peripheral astigmatism. However, the three eyes with the largest anterior chamber depths all had measured PAF values below the mean value given by all 34 eyes. The mean PAF was 103.3. Subject number 4 had an anterior chamber depth of 4.14 mm and a PAF of 41.5. Subject number 14 had an anterior chamber depth of 4.27 mm and a PAF of 82.9. Subject number 26 had an anterior chamber depth of 4.27 mm and a PAF of 91.4. Also subject number 4 with the lowest PAF value had the third largest anterior chamber depth of all 34 eyes.

Corneal thickness and posterior corneal surface changes vary the peripheral astigmatism very little. The reasons for the small effects of these parameters were discussed in chapter six. As these parameters have negligible effect on both the peripheral astigmatism and spherical aberration, their manipulation will not be used to obtain the required levels of aberration in the schematic eyes. Alteration in the lens thickness seems to have slightly more effect on peripheral astigmatism than on spherical aberration, but still has limited use.

Altering the asphericity of the optical surfaces has a similar effect on the peripheral astigmatism as it does on the spherical aberration. Firstly, the effect is greater than that caused by altering the central curvature. Secondly, peripheral flattening of all three positive surfaces decreases both aberrations. Peripheral flattening of the negative posterior corneal surface asphericity value causes an increase in both aberrations.

Apical radius changes have the opposite effect on peripheral astigmatism as on spherical aberration. For the anterior corneal and posterior lenticular surfaces an increase in apical radius increases peripheral astigmatism, but decreases spherical aberration. An increase in apical radius of the anterior lens decreases peripheral astigmatism and increases spherical aberration. So, if it is desirable to increase one aberration while decreasing the other the central radii of the optical surfaces should be altered. Alternatively, if both aberrations need to be increased or decreased simultaneously the surface asphericities should be manipulated.

Peripheral steepening of the posterior lenticular surface appears to produce the greatest increase in peripheral astigmatism. However, for the highest values of p, rays with field angles of greater than about 30° produce rather unusual results. This was found to be due to marginal rays at one edge of the pupil missing the surface. For the maximum p value of 3.21 the points representing the peripheral astigmatism found for field angles of 30° and greater have been excluded from the plot. The fitted curve will, therefore, only accurately

predict the peripheral astigmatism values up to the limits set by the remaining points and the PAF, calculated between the limits of -40° and 40°, is hypothetical.

Such a posterior lenticular surface would be impractical in a real eye. It is likely that any surface with such high asphericity values would have a relatively large apical radius of curvature to compensate.

The small effect that further flattening of the anterior lenticular surface, beyond the mean value, has on peripheral astigmatism can be explained by its position relative to the pupil. Smith (1990 - chapter ten) demonstrated that when the aperture is coincident with an aspheric surface the only third-order aberration affected by changing the asphericity is spherical aberration. This may equally apply to the posterior lenticular surface. Smith (1990 - chapter 3) also showed that, for a thin lens coincident with the limiting aperture, variation in lens curvature would not cause any variation in third-order peripheral astigmatism and coma. Figs. 7.21 and 7.24 clearly illustrate how the peripheral astigmatism varies with radii for both lenticular surfaces. This may be attributed, in part, to the finite thickness of the lens and variation in higher-order aberrations. However, it must also be remembered that in this study the calculated aberration is not pure peripheral astigmatism (see section 1.3.2). Further variations may be due to other aberrations, i.e. coma. The large increases in PAF which occur when the lens surfaces are steepened beyond the mean value could also be explained by this.

Dunne and Barnes (1987) attempted to model the peripheral astigmatism found in real eyes (see section 5.4). They initially studied the effects of altering the asphericity of the two lenticular surfaces on the peripheral astigmatism for a 60° field angle. Dunne and Barnes found that altering the asphericity of the posterior lenticular surface in either direction from a value of -1.5 increased the peripheral astigmatism. This study concured with these findings. However, for lower field angles the peripheral astigmatism was reduced as the posterior lenticular asphericity reduced. The overall effect was a reduction in the PAF. This suggests that PAF values provide better comparisons of peripheral astigmatism levels than comparing the value for just one field angle. In order to reduce peripheral astigmatism to levels found in type A and Type B eyes of Ferree et al. (1931), Dunne and Barnes peripherally flattened the anterior lenticular surface. When considering the results of this study it is not surprising that the surface had to be flattened considerably, giving very large negative conic constants, far beyond the limits found in human eyes. The high levels of over-corrected spherical aberration resulting from these surfaces could also be predicted from the evidence presented in chapter 6. Peripheral flattening of the anterior lens surface

beyond a certain limit has a greater affect on spherical aberration than on peripheral astigmatism.

Dunne and Barnes (1987) concluded that to model the low levels of peripheral astigmatism found in real eyes the model must include a lens with a gradient index structure. However, they restricted their attempts to manipulation of the anterior lenticular asphericity. From the evidence presented in this chapter it can be concluded that peripheral astigmatism is more effectively reduced by variation of other parameters, particularly the anterior chamber depth and the anterior corneal asphericity.

7.7 SUMMARY

A study of the variation in peripheral astigmatism with variation in parameter value has revealed that:-

i) No single parameter variation can reduce peripheral astigmatism to the minimum levels found in human eyes.

ii) Anterior chamber depth variations have the greatest effect on the level of peripheral astigmatism. It is the only parameter which can, alone, reduce the peripheral astigmatism to the mean level found in human eyes. The maximum depth reduces the PAF to about half way between the mean and minimum values. The minimum depth increases the PAF to a value much higher than the maximum value.

iii) Decreasing the anterior corneal asphericity to its minimum value produces a PAF value which is almost as low as the mean human value.

iv) The maximum PAF value can also be modelled by increasing either the anterior corneal asphericity, the anterior lenticular asphericity or the posterior lenticular asphericity.

v) Variation in surface asphericity has the same directional effect on peripheral astigmatism as on spherical aberration.

vi) variation in apical radius has the opposite directional effect on peripheral astigmatism as on spherical aberration.

vii) Peripheral flattening of the anterior and posterior lenticular surfaces to conic constants below the mean value reduces the peripheral astigmatism by very little. However,

peripheral steepening of these surfaces beyond the mean level increases peripheral astigmatism considerably.

viii) Corneal thickness, posterior corneal radius, posterior corneal asphericity and lens thickness variations have negligible effect on the peripheral astigmatism.

CHAPTER 8
THE EFFECT OF INDIVIDUAL OCULAR PARAMETER CHANGES ON COMA

8.1 INTRODUCTION

In this chapter the effect on comatic distortion of the ocular parameter variations, considered in the previous two chapters, is discussed. As coma has never been directly measured in human eyes no comparison can be made with empirical data. However, some studies have found evidence of comatic distortion in human eyes. This is discussed in the initial part of the chapter.

8.2 EVIDENCE OF COMATIC DISTORTION IN HUMAN EYES

The measurement of wavefront aberration and spread functions in human eyes was discussed in sections 1.4.1 and 1.5.1 respectively. Plots of axial wavefront aberration have shown evidence of comatic distortion on-axis and have led researches to conclude that coma, and not spherical aberration, may be the dominant axial aberration. Spread function measurements have been made both on and off-axis using an objective method called the double pass method (Westheimer and Campbell, 1962; Campbell and Gubisch, 1966; Jennings and Charman, 1978,1981; Santamaria et al., 1987; Navarro et al., 1993). None of these studies have revealed any evidence of coma type distortion in the ocular images.

Jennings and Charman attributed the lack of on and off-axis coma to the homocentricity of the eyes optical system, as suggested by Guidarelli (1972). An homocentric optical system is one in which the centres of all the optical surfaces and the image surface coincide at the same point on the optical axis. Guidarelli considered that the eyes homocentre fell approximately at the vertex of the posterior lenticular surface. Close to this position are the centres of curvature of the most powerful optical surface (the anterior cornea) and the imaging surface (the retina). Guidarelli argued that the effects of the posterior lens surface could be ignored, as this surface is coincident with the homocentre. The centre of curvature of the anterior lens surface falls about 6 mm behind the homocentre but Guidarelli felt that its effects are relatively insignificant because of its low dioptric power relative to the anterior cornea. In an homocentric system any oblique ray passing through the centre of the pupil acts as an optical axis. Therefore, all rays entering such a system will be parallel to an optical axis and the system will not suffer from off-axis aberrations.

The author has investigated the homocentricity of the human eyes in a previous publication (white et al., 1992). A commercially available ray tracing program (Beam 4) was used to trace a large number of parallel rays through Kooijman's schematic eye (Kooijman 1983). A short description of the relevant parts of this program is given.

8.2.1 THE 'BEAM 4' OPTICAL RAY TRACING PROGRAM

The mathematical foundation of this program follows the ray tracing procedures developed by Spencer and Murty (1962). This involves tracing each ray to its intercept with an optical surface and then calculating its change of direction using Snell's law. These steps are then repeated to completion, the final calculation giving the intercept with the imaging surface.

Optical parameter and ray data is entered into the program in two separate spreadsheets. A ray is fully described by its original position and the direction in which it propagates. Each ray is described by six coordinates: X, Y and Z describe the original ray position, in three dimensional space, relative to the coordinate system: U, V and W are the components of the unit-length vector indicating the direction of the ray. They are given by the cosine of the angle between the ray and the corresponding coordinate axis and are commonly known as direction cosines. Specifically, U is the cosine of the angle the ray makes with the X axis and similarly V and W are the cosines of the angles the ray makes with the Y and Z axes respectively.

In this study parallel rays are traced through the optical system and, therefore, all rays have the same initial direction. The Z axis is taken as the optical axis, the X axis as the vertical axis and the Y axis as the horizontal axis. The plane of obliquity is considered to be the horizontal or Y/Z plane. As such all rays traced into the system will be at 90° to the X axis and will thus all have a U value of 0. The direction cosines are components of a unit vector and so the sum of their squares will always equal 1. It is necessary only to enter U as 0 and one of the two other direction cosines, as the program will calculate the third direction cosine from the relationship $U^2 + V^2 + W^2 = 1$. For example, consider a ray with a 30° field angle. This is the angle the ray makes with the optical axis Z. The direction cosine W will be equal to the cosine of 30°. Given U = 0, then $V^2 + W^2 = 1$ and V = 0.5, the cosine of 60°, which is the angle the ray makes with the Y axis.

Completely random rays were traced by the program within the limits of the ray beam specified by the extreme ray positions and directions. If all the initially specified rays were parallel, the random rays were also parallel. The extreme positions were determined by tracing four rays, which, when projected through the cornea, just hit the two extreme edges of the pupil in the vertical and horizontal planes. Two further rays were also traced in each plane as the program requires a minimum of two rays passing through the system.

The optical parameters of the system were entered into an optics table. The parameters of each optical surface were entered in order. The order is specified by sequence with which rays reach the surfaces. For each surface the parameters are:-

1) The refractive index of the medium preceding the optical surface.
2) The apical curvature, which is the inverse of the apical radius.
3) The position of the vertex of the surface given by X, Y and Z coordinates. For the centred systems used in this study X and Y are zero and only the Z coordinate is specified.
4) The limiting diameter of the optical surface or pupil.
5) The surface identity, i.e. L for lens, I for iris, F for film or imaging surface.
6) For aspheric surfaces the conic constant is entered which is equal to the p value used by Kooijman (1983).

The parameters of schematic eyes can easily be translated from the format used in the program of Clement et al. (1987) to be used in the beam 4 program. Ray were traced through Kooijman's schematic eye, with the corrected lens asphericity values (see table 5.1), for field angles of 0° to 60° in steps of 5°. A minimum of 20,000 random rays were traced to give the spread function. These spread functions represent the spread of light, on the retina, in the plane of obliquity or tangential plane. The number of rays falling at each point gives a measure of the intensity of light.

8.2.2. RESULTS

The spread functions were clearly asymmetric in the plane of obliquity even at 5°. At larger field angles the asymmetry became extremely pronounced. As an example of this, the spread function for 30° rays is shown in fig. 8.1. The asymmetry, which is due to the presence of coma, shows that Guidarelli (1972) was incorrect in assuming the eye to be homocentric. If human eyes are well corrected for off-axis aberrations then there must be some other explanation. The failure of the double pass method to detect any comatic distortion, even for off-axis rays, led to some doubt in the credibility of the technique.

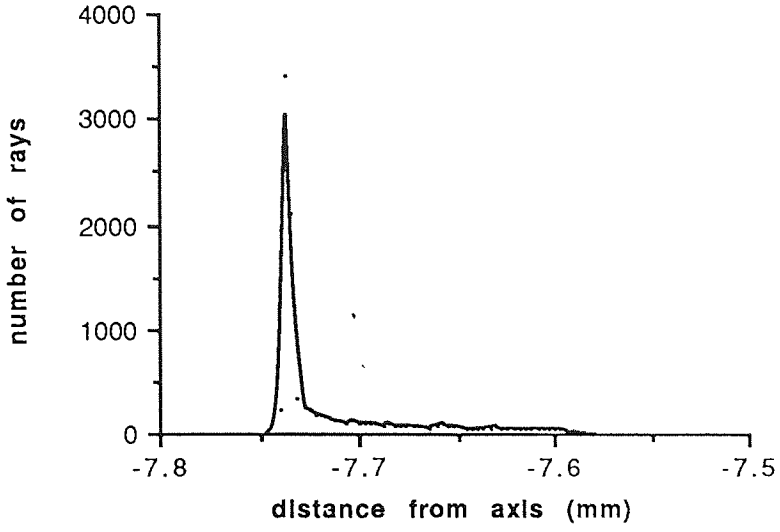

Fig. 8.1 Spread function for 30° rays of light passing through Kooijman's schematic eye.

In order to use the double pass method a number of basic assumptions have to be made. The spread of a single pass of the optics can only be calculated from the MTF of the double pass if the retina is assumed to be a diffuse reflector and causes no degradation of the image it reflects. It is also assumed that light passing out of the eye is degraded in the same way as light passing into the eye. It is the latter assumption which is questioned in this investigation. Smith (1990) demonstrated how the shape of optical elements and the position of the aperture affects the aberrations of a system. For light passing out of the eye the order of the optical elements including the pupil is the reverse of that for light passing into the eye. The sign of coma occurring during an inward passage of the eyes optics may, therefore, be opposite to that occurring during an outward passage. This would cause asymmetries in the spread functions in opposite directions and may result in symmetry of the final double pass image. Indeed, if rays are traced out of Kooijman's schematic eye the spread function is asymmetrical in the opposite direction to that shown in fig. 1.8 (see fig. 8.2).

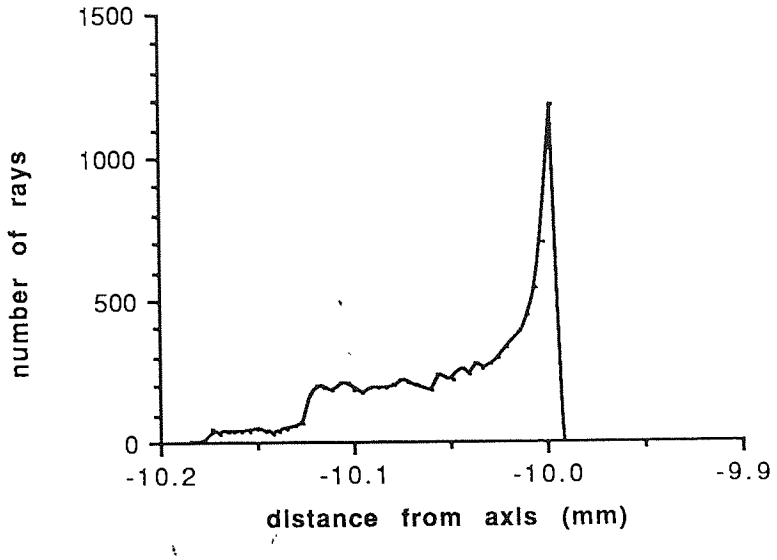

Fig. 8.2 Spread function for 30° rays of light passing out of Kooijman's schematic eye.

If the aberrations of the reverse optical system are not the same as those of the forward optical system then the MTF will also be different. Fig 8.3 shows the MTF for central, parallel rays traced into the eye and imaged on a spherical retina placed so that its vertex lies in the plane of the circle of least confusion. Fig. 8.4 shows the same for central, parallel rays traced through the reverse optical system. These examples do not attempt to illustrate the image degradation which would result during measurements using the double pass method. Rather, they present a simplified and possibly extreme case of what is happening to light as it passes in and then out of the same optical system. The optical system of the real eye would give very different results, not only because of differences in aberrations, but also because of the added degradation due to diffraction and scatter which is not accounted for in the schematic eye. In real eyes the difference may not be as pronounced as shown in figs. 8.3 and 8.4. However, what these examples do illustrate is that the assumption that the MTF of an optical system is the same for light passing through it in either direction is fundamentally incorrect. Comparing fig. 8.3 and 8.4 it can be seen the MTF for the reverse optics is lower. If this were the case in real eyes then the square root of the double pass MTF would be lower than the actual single pass MTF of the eyes optics. This throws some doubt onto the accuracy of measurements of spread functions and MTFs using the double pass method. However, the degree to which the accuracy is affected is unknown. The difference in degradation for reverse passage of the optical system may not invalidate the double pass method but may explain the lack of asymmetry found in the double pass spread function.

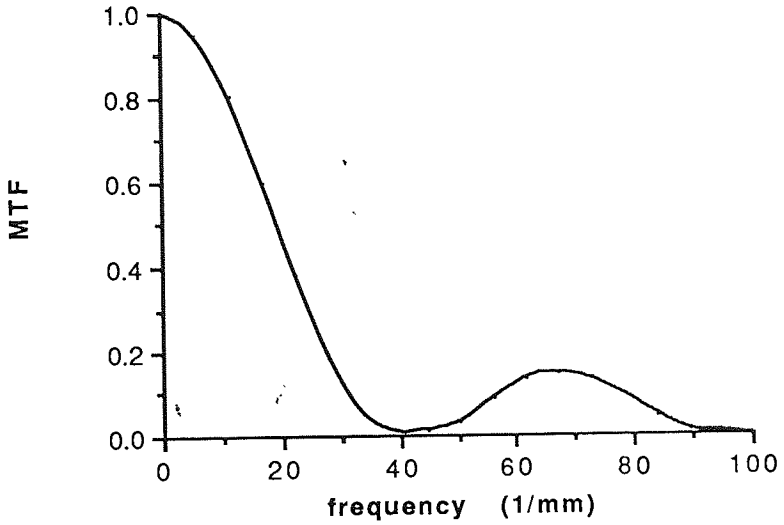

Fig. 8.3 MTF for central rays passing through Kooijman's schematic eye and focussed in the plane of the circle of least confusion.

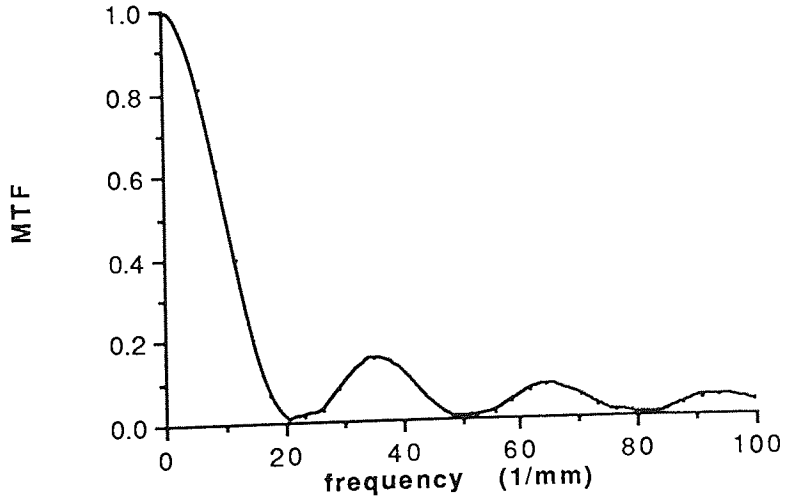

Fig. 8.4 MTF for central rays passing out of Kooijman's schematic eye and focussed in the plane of the circle of least confusion.

8.3 OCULAR PARAMETER VARIATION AND COMA

8.3.1 COMPUTERISED RAY TRACING

The amount of tangential coma (see section 1.3.3) in the schematic eyes is related to the distance, along the principal ray, between the tangential comatic image limits (TCIL). The limits are determined by the points at which the two marginal, tangential rays intercept the principal ray (fig. 8.5). Barnes et al.(1987) used the position of these two intercepts to study the effects of tilt and translation of ocular surfaces on coma (see section 5.3.3). TCIL values are easily extracted from the ray tracing computer program of Clement et al.(1987). They can be related to coma by trigonometrical calculations in terms of the angles the emerging principal ray and marginal rays make with the optical axis. As this study is only interested in the relative change in coma caused by variations in individual ocular parameters comparing TCIL values was thought to be sufficient.

The coma for the schematic eyes used in this study is generally of the type shown in the fig. 8.5, i.e the two marginal rays intercept at a position between the optical axis and principal ray. In section 1.3.3 coma which caused the marginal rays to focus further from the optical axis than the principal ray was considered to be positive. It would follow that the coma illustrated in fig. 8.5 is negative. However, in order to avoid confusion positive coma will - hence forth - be referred to as under-corrected, and negative coma as over-corrected. For under-corrected coma the comatic flare of the image spreads away from the optical axis. For over-corrected coma it flares towards the optical axis. Confusion may arise when the value for coma or TCIL is calculated for both negative and positive field angles (figs 8.2a and 8.2b respectively). Coma is calculated as the perpendicular distance from the optical axis to the intercept of the two marginal rays (o to ab) minus the perpendicular distance to the principal ray (o to p). If distances above the axis are considered to be positive and distance below negative, then for negative field angles (fig. 8.5a) the coma will be negative and for positive field angles (fig. 8.5b) it will be positive. The TCIL is calculated as the distance along the principal ray to the intercept ap minus the distance to the intercept bp. So it is also positive for positive field angles and negative for negative field angles. However, for both positive and negative field angles the coma is over-corrected.

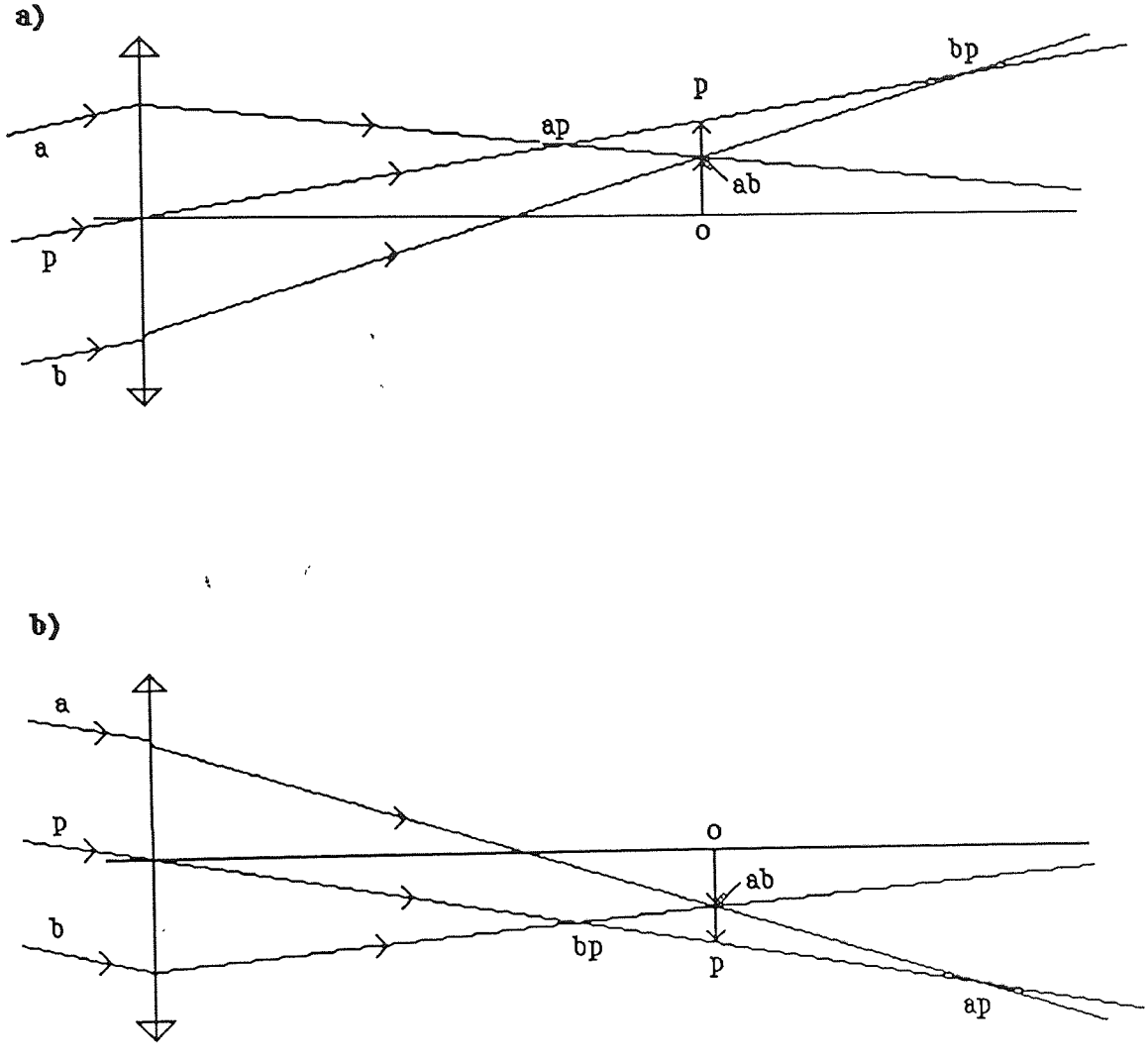

Fig. 8.5 Calculation of coma and TCIL for **a)** negative field angles and **b)** positive field angles. Coma = oab - op, TCIL = ap - bp.

TCIL values were found using the same ray-tracing procedure as that used to find the peripheral astigmatism. For each of the 45 schematic eyes the TCIL values were plotted against field angle.

8.3.2 RESULTS

The plots of TCIL versus field angle for each optical parameter are shown in figs. 8.6 to 8.16.

i) SURFACE ASPHERICITY

For all four optical surfaces, surface asphericity changes (figs. 8.7, 8.10, 8.13 and 8.16) produce more variation in TCIL than central radius changes (figs. 8.6, 8.9, 8.12 and 8.15). Variation in the posterior corneal asphericity has very little effect (fig. 8.10). The variation in TCIL with asphericity of the anterior (fig. 8.13) and posterior (fig. 8.16) lenticular surfaces follow a similar pattern to the variations in peripheral astigmatism. The TCIL increases quite rapidly when the surfaces are steepened in periphery, giving conic constants above the mean value. Very little change occurs when surfaces are peripherally flattened below the mean.

ii) SURFACE RADIUS

Only variations in the apical radius of the anterior cornea have a significant effect on TCIL (fig.8.6). Altering the radii of the other three surfaces can be seen to produce negligible change (figs 8.9, 8.12 and 8.15).

iii) SURFACE POSITION

TCIL variation due to changes in corneal thickness are negligible (fig. 8.8). Changes in the lens thickness have only a small effect. Anterior chamber depth changes (fig. 8.11) produce a fairly large variation in TCIL but not as much variation as occurs in peripheral astigmatism.

Some interesting results emerge if we compare the directional trend in TCIL variations to peripheral astigmatism variations. Variations in parameters of the corneal surfaces, which increase peripheral astigmatism, decrease TCIL. In contrast, variation in parameters of lenticular surfaces, causing increases in peripheral astigmatism, increase TCIL. Also, the directional trend of both aberrations is the same for anterior chamber depth variations and opposite for variations in the lens thickness. This may be explained if one considers the contribution of the lens and cornea to each of these two aberrations. In Kooijman's schematic eye the cornea contributes positive astigmatism and negative coma while the lens contributes positive amounts of both. In the overall schematic eye the peripheral

astigmatism is positive and the coma negative. Therefore, if changes in the corneal parameters produce increased positive amounts of both off-axis aberrations, the total peripheral astigmatism will increase but the total negative coma will decrease.

For the lens the situation seems to be different. For the same parameter variations to increase both aberrations they must induce an increase in the positive peripheral astigmatism but a decrease in the positive coma. Anterior chamber depth variations will mostly affect the aberrations of the cornea. For both aberrations to increase, the peripheral astigmatism of the cornea must become more positive and the coma more negative. Lens thickness variations will only alter the contributions of the lens to the overall aberrations. If the total amounts of both aberrations are varying in opposite directions then the positive contribution of the lens to each aberration must increase or decrease simultaneously. The difference in the effects of lens and cornea parameter variations on the simultaneous variation of peripheral astigmatism and coma may be due to their positions relative to the pupil. The sign of coma can be changed by altering the position of the pupil. It is also probable that the effects of parameter variations on coma will be reversed in this situation. This would appear to be the case if one considers, for example, the effects of peripherally steepening the three positive surfaces in the schematic eyes. Peripheral steepening of the anterior corneal surface decreases coma, while for the two lenticular surfaces it increases coma. The position of the pupil does not effect the sign of peripheral astigmatism. Parameter variations would therefore have the same directional effect on peripheral astigmatism regardless of relative pupil position. This is also shown to be the case if we consider peripheral steepening of the positive surfaces in the schematic eyes. Peripheral steepening of the anterior cornea, the anterior lenticular and the posterior lenticular surfaces all increase the peripheral astigmatism.

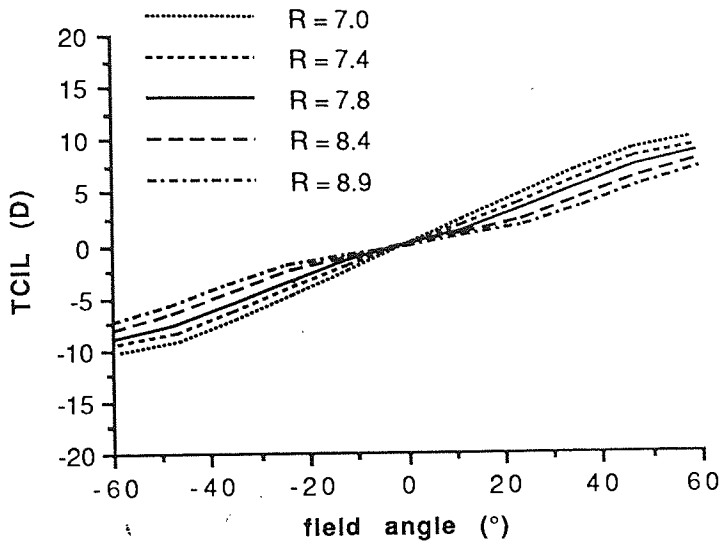

Fig. 8.6 Plot of TCIL versus field angle for the full range of anterior corneal radii, R, (mm) reported in human eyes.

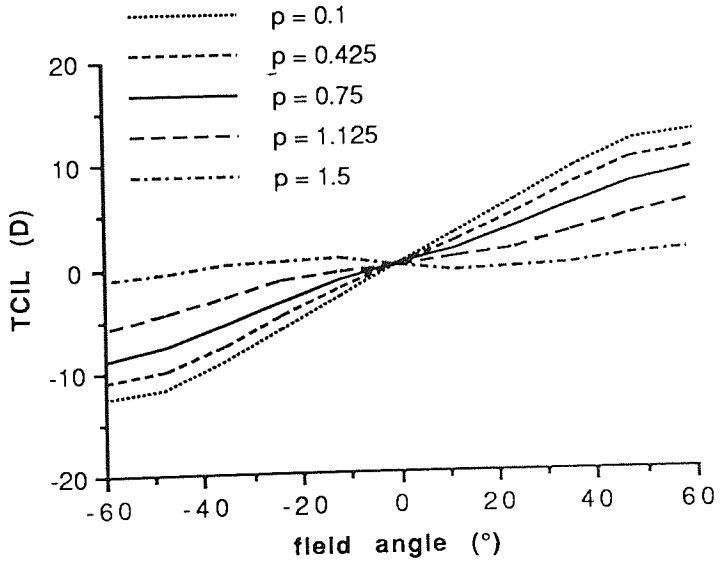

Fig. 8.7 Plot of TCIL versus field angle for the full range of anterior corneal asphericities, p, reported in human eyes.

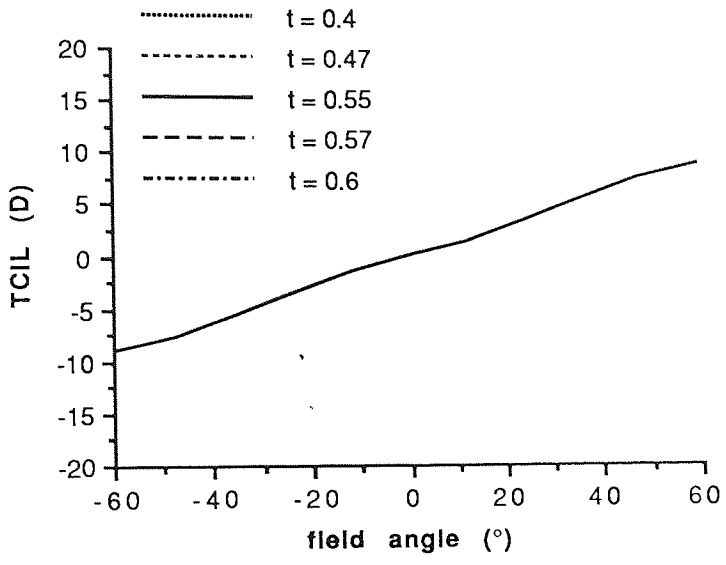

Fig. 8.8 Plot of TCIL versus field angle for the full range of corneal thicknesses, t, (mm) reported in human eyes.

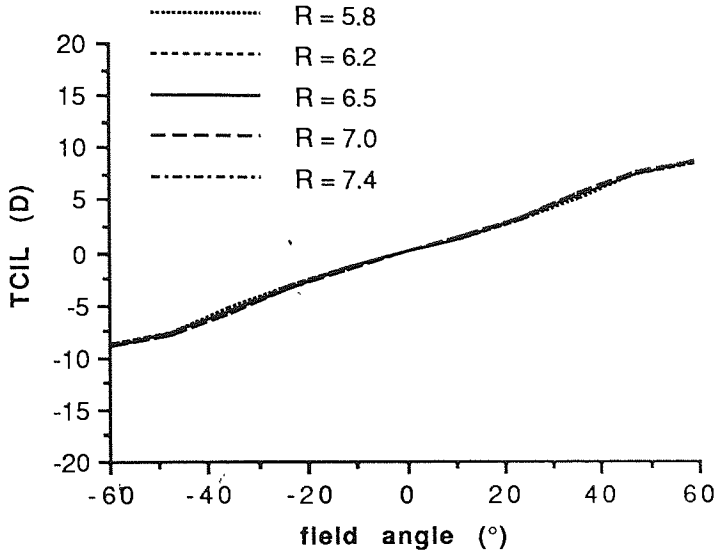

Fig. 8.9 Plot of TCIL versus field angle for the full range of the posterior corneal radii, R, (mm) reported in human eyes.

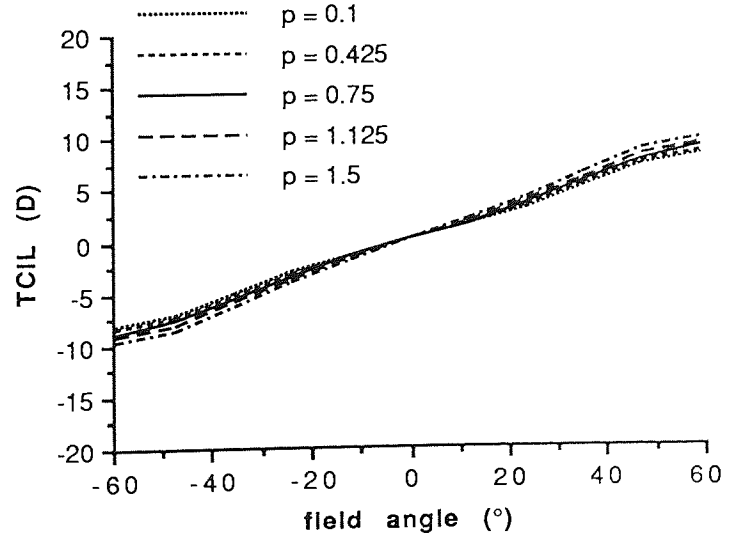

Fig. 8.10 Plot of TCIL versus field angle for the full range of posterior corneal asphericities, p, reported in human eyes.

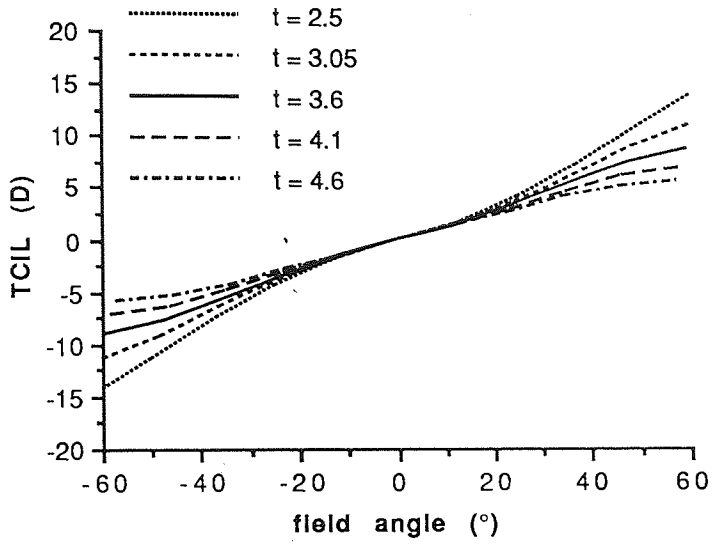

Fig. 8.11 Plot of TCIL versus field angle for the full range of anterior chamber depths, t, (mm) reported in human eyes.

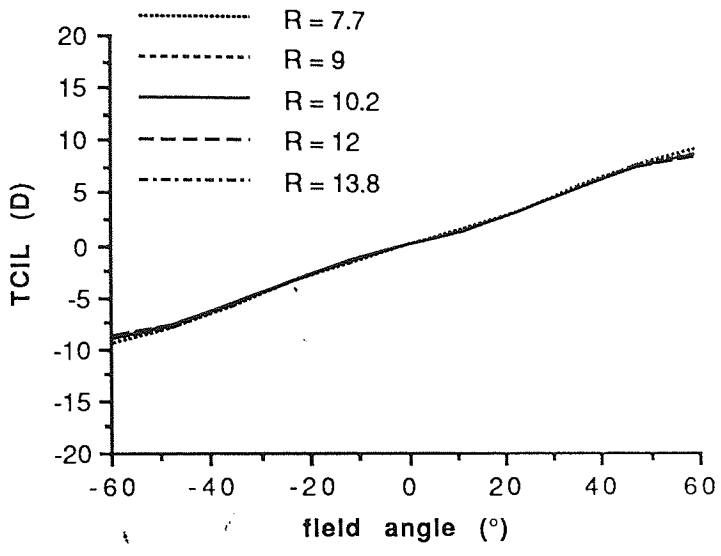

Fig. 8.12 Plot of TCIL versus field angle for the full range of anterior lenticular radii, R, (mm) reported in human eyes.

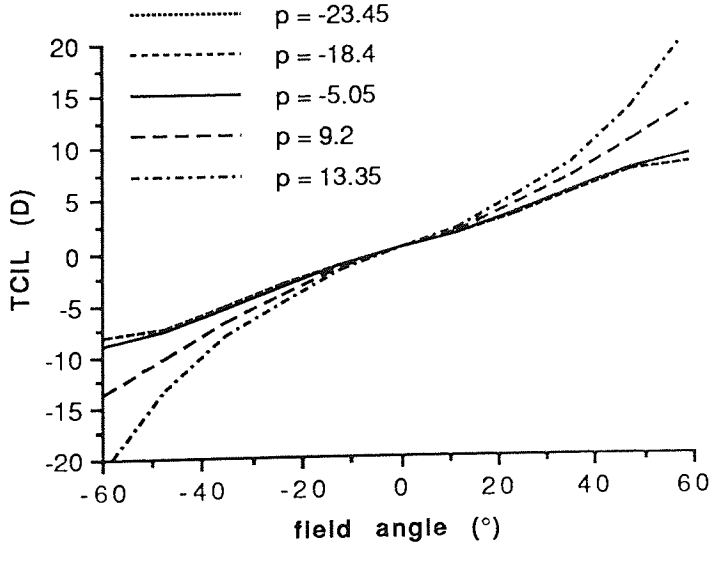

Fig. 8.13 Plot of TCIL versus field angle for the full range of anterior lenticular asphericities, p, reported in human eyes.

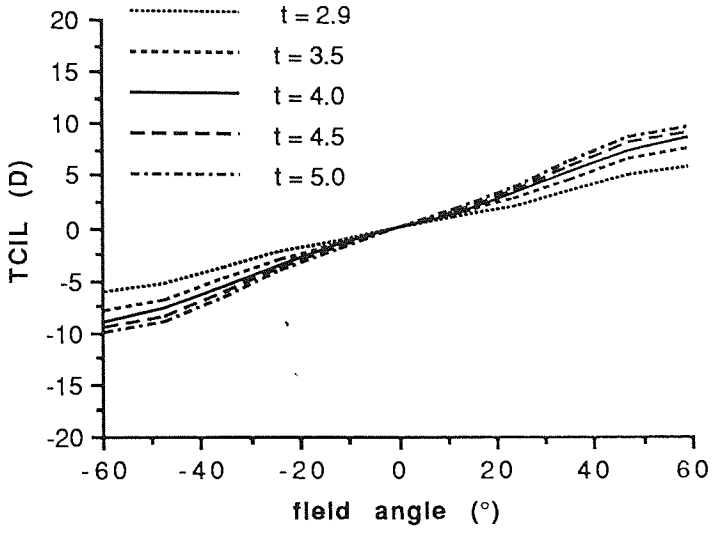

Fig. 8.14 Plot of TCIL versus field angle for the full range of lens thicknesses, t, (mm) reported in human eyes.

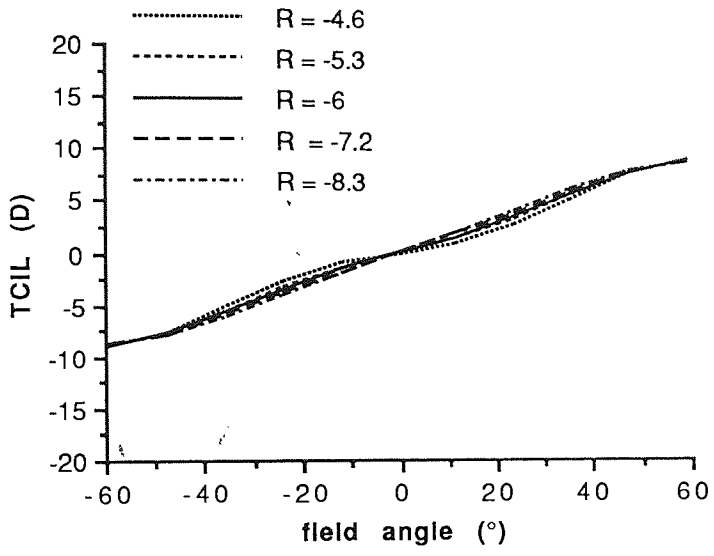

Fig. 8.15 Plot of TCIL versus field angle for the full range of posterior lenticular radii , R, (mm) reported in human eyes.

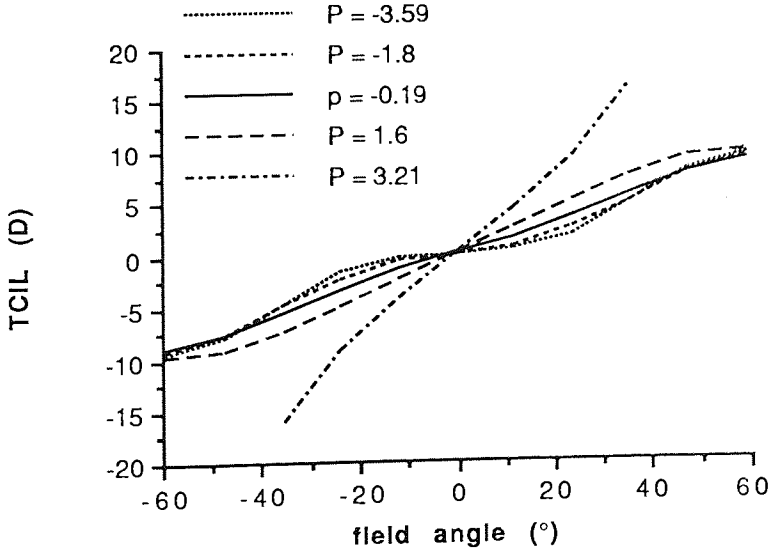

Fig. 8.16 Plot of TCIL versus field angle for the full range of posterior lenticular asphericities, p, reported in human eyes.

8.4 OCULAR PARAMETER VARIATION AND CAF

8.4.1 CALCULATION OF CAF

CAF is calculated in a similar manner to SAF and PAF. A polynomial curve is fitted to the plot of TCIL versus field angle for each of the 45 schematic eyes and its equation is noted. The area under this curve is then calculated by integration to give the CAF value.

In section 6.3.2 it was noted that the higher-orders of an aberration tend to become more significant in systems which are well corrected for that aberration. This is reflected in the results in this chapter. The datum points of all the plots of TCIL versus field angle were found to be reasonably well fitted by fifth-order polynomials. Indeed, for almost all schematic eyes fifth order polynomials gave a perfect fit. For schematic eyes where the TCIL is high (e.g. for an anterior lenticular asphericity of 13.35, giving a TCIL of 172.3, and a posterior lenticular asphericity of 3.21, giving a TCIL of 332.0), third-order polynomials were found to be sufficient to give a perfect fit to the datum points. Conversely, for the schematic eye with an anterior corneal asphericity of 1.5 and a TCIL of -14.2 a fifth-order polynomial did not fit as well as for the other schematic eyes. This suggests that a higher-order polynomial may be needed to give a perfect fit because of the higher significance of the higher-order aberrations. Unfortunately, the available program (Cricket Graph) did not allow for higher-order polynomial curve fitting. Also, a fifth-order polynomial was considered to give a sufficiently accurate fit for calculation of TCIL (correlation coefficient - $R^2 = 0.996$)

Inspection of any of the TCIL versus field angle plots reveals that the area enclosed by the curve and the horizontal axis for positive field angles is equal to the area enclosed by the curve and the horizontal axis for negative field angles. Consider, for the sake of clarity, the curve in fig. 8.8. This represents the TCIL versus field angle plot given by the mean schematic eye. Integration of this curve between field angles of -40° and 40° will give a value of 0. This results from the area under the horizontal axis being equal but of opposite sign to the area above the horizontal axis; which is true of all the TCIL versus field angle plots. Therefore, in order to be able to compare the results of the 45 schematic eyes, the CAF was calculated as the area under the curve between 0° and 40° only. The resulting CAF values are positive for under-corrected coma, which is found for almost all the schematic eyes, and negative for over-corrected coma. Five CAF values for each of the eleven parameters were calculated and plotted against parameter value.

8.4.2 RESULTS

The plots are shown in figs. 8.17 to 8.27. Second-order polynomials were fitted to the datum points. In most cases they fitted very well. They allowed a fairly accurate calculation of CAF values for any value of the individual parameter, provided all other parameters were unchanged. However, the plots of CAF versus anterior and posterior lenticular asphericity were not very accurately fitted by second-order polynomials. The datum points were considered to follow a third-order relationship. This was confirmed by executing two more ray traces for extra values of asphericity for each surface. The resulting CAF values were then added to the plots of CAF versus asphericity. Third-order polynomials were found to fit well to these two plots.

In fig. 8.27 the point for a posterior lenticular asphericity value of 3.21 is not shown. This gave a value of 332.0 for the CAF and the third-order curve fit does take this point into consideration. In this schematic eye ray traces for field angles beyond 30° could not be carried out due to marginal rays missing the posterior lenticular surface. The CAF, calculated for field angles of up to 40°, is, therefore, somewhat hypothetical as TCIL values do not exist beyond the 30° limit.

Inspection of the plots of CAF versus parameter values reveals that the results are generally similar to those found for PAF variation with parameter value. However there are some notable differences. As for PAFs and SAFs corneal thickness variations have negligible effects on the CAF (fig.8.19). Posterior corneal radius and asphericity variations also have little effect on CAF (figs 8.19 and 8.20).

As noted in section 8.3.2, variation in the parameters of the corneal surfaces produce the opposite directional effect on the CAF as they do on the PAF. For example, an increase in the apical radius or peripheral steepening of the anterior corneal surface both cause an increase in the PAF (figs 7.15 and 7.16) while decreasing the CAF (figs. 8.17 and 8.18). Variation in optical surface parameters for the lens surfaces produces similar effects on the CAF and PAF, both quantitatively and directionally. Increasing the radii of both surfaces decreases both PAF (7.21 and 7.24) and CAF (figs.8.23 and 8.26). Peripheral steepening of both surfaces increases the PAF (7.22 and 7.25) and the CAF (figs. 8.24 and 8.27).

The anterior chamber depth does not have as great an effect on the CAF (fig. 8.22) as on the PAF (fig 7.20); but as for the PAF an increase in the depth causes a decrease in its value. Lens thickness variations cause changes in the CAF (fig.8.25). These are

comparable to those in PAF (fig 8.23) but in the opposite direction. Increasing lens thickness decreases the PAF, but increases the CAF.

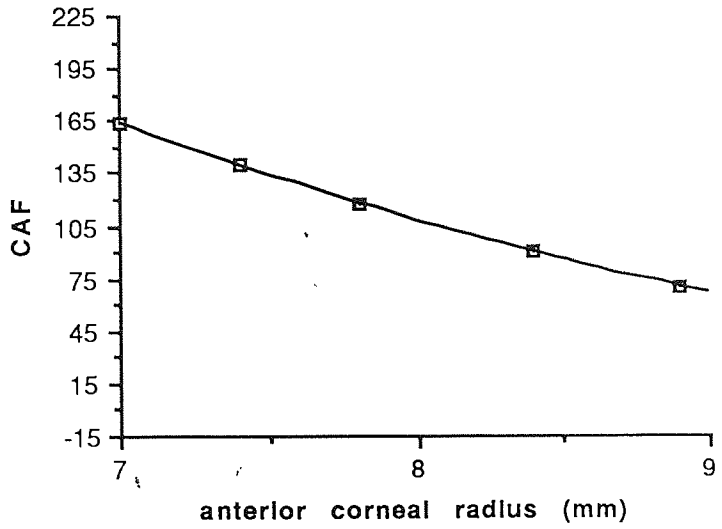

Fig. 8.17 Plot of CAF versus anterior corneal radius. The equation of the curve is: $CAF = 925.560 - 156.330R + 6.785R^2$ - where R is the anterior corneal radius.

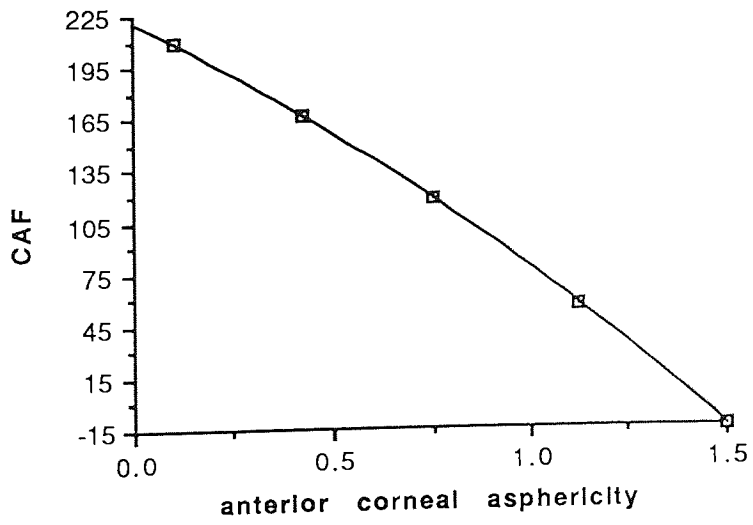

Fig 8.18 Plot of CAF versus anterior corneal asphericity. The equation of the curve is: $CAF = 220.500 - 114.900p - 27.722p^2$ - where p is the anterior corneal asphericity.

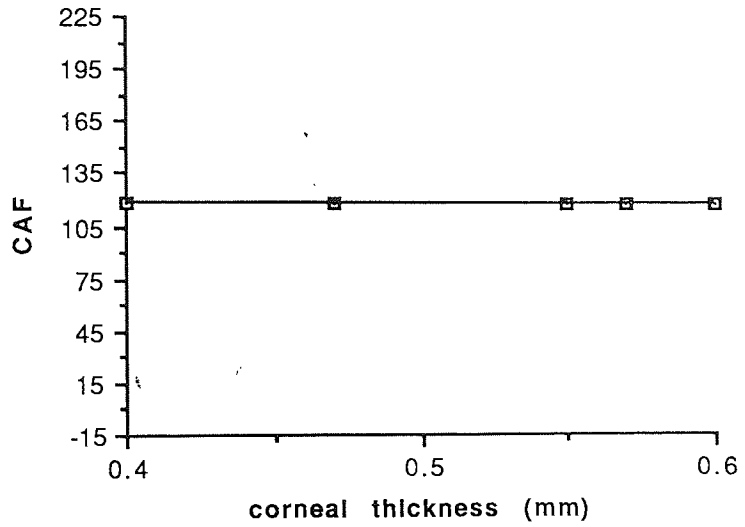

Fig. 8.19 Plot of CAF versus corneal thickness. The equation of the curve is: $CAF = 119.200 - 3.632t + 5.447t^2$ - where t is the corneal thickness.

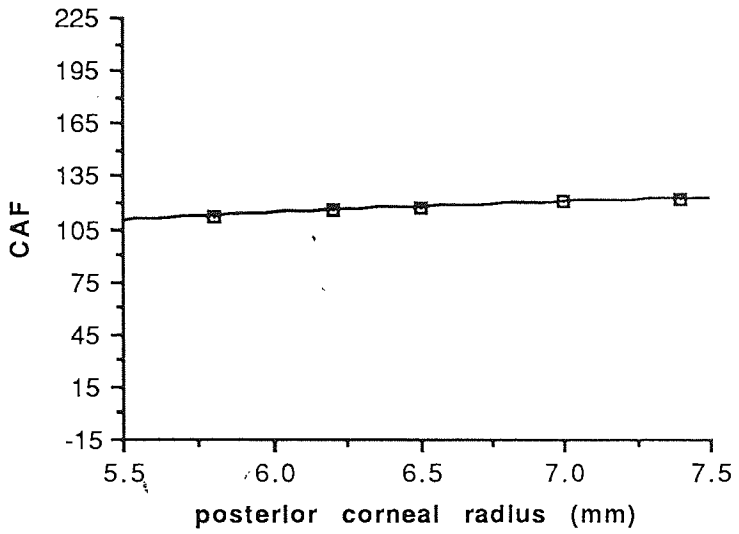

Fig. 8.20 Plot of CAF versus posterior corneal radius. The equation of the curve is: $CAF = 4.298 + 27.503R - 1.520R^2$ - where R is the posterior corneal radius.

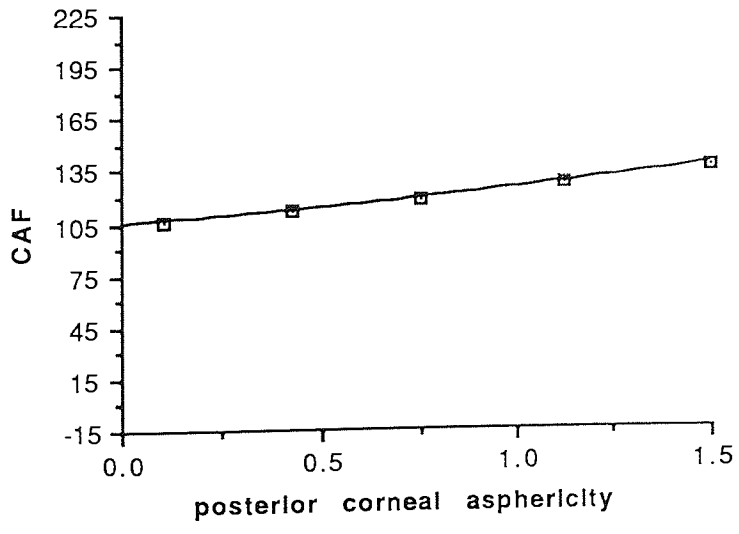

Fig. 8.21 Plot of CAF versus posterior corneal asphericity. The equation of the curve is: $CAF = 104.850 + 15.269p + 4.479p^2$ - where p is the posterior corneal asphericity.

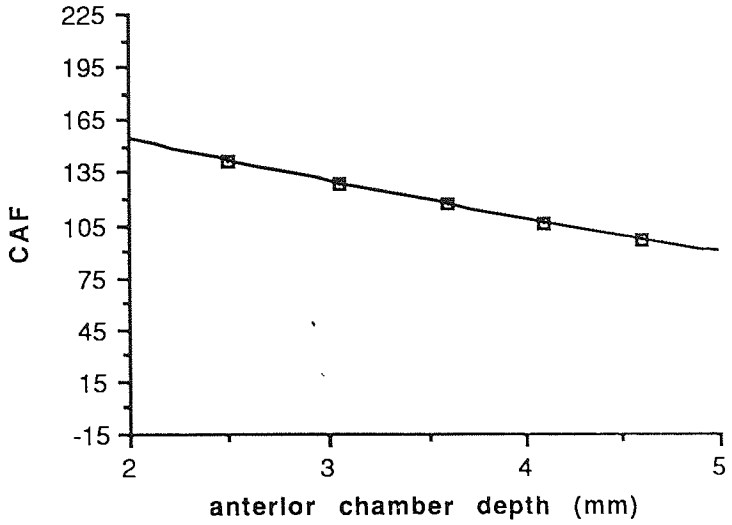

Fig. 8.22 Plot of CAF versus anterior chamber depth. The equation of the curve is: $CAF = 206.500 - 28.306t + 1.029t^2$ - where t is the anterior chamber depth.

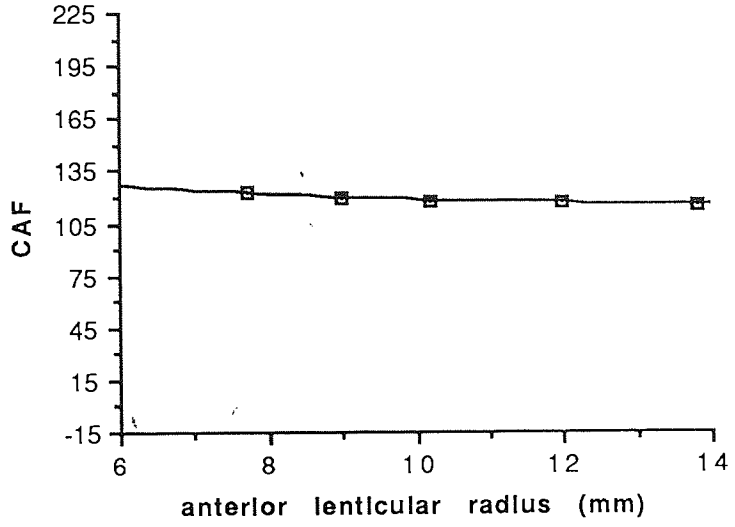

Fig. 8.23 Plot of CAF versus anterior lenticular radius. The equation of the curve is: $CAF = 146.130 - 4.334R + 0.163R^2$ - where R is the anterior lenticular radius.

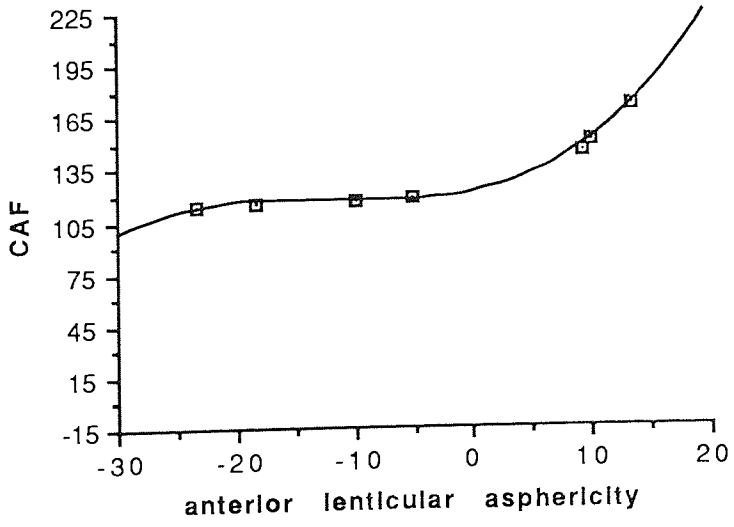

Fig. 8.24 Plot of CAF versus anterior lenticular asphericity. The equation of the curve is: $CAF = 120.660 + 1.341p + 0.131p^2 + 0.004\ p^3$ - where p is the anterior lenticular asphericity.

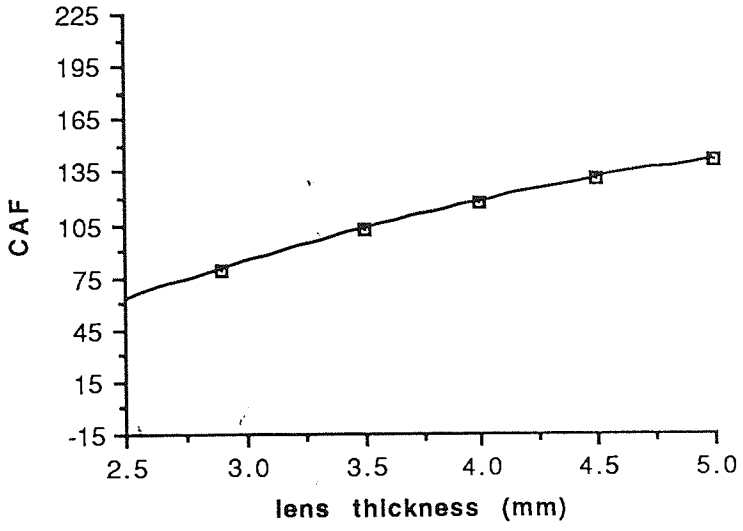

Fig. 8.25 Plot of CAF versus lens thickness. The equation of the curve is: CAF = -83.822 + 71.632t -5.238t ^{2} - where t is the lens thickness.

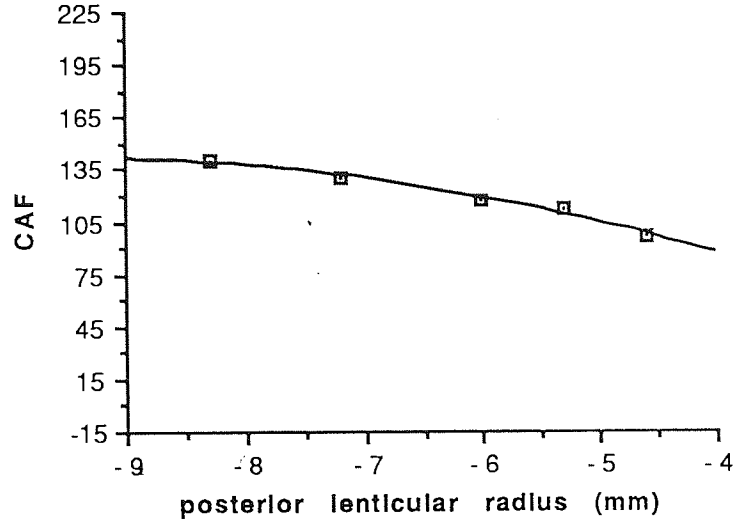

Fig. 8.26 Plot of CAF versus posterior lenticular radius. The equation of the curve is: $CAF = -17.455 - 33.473R - 1.760R^2$ - where R is the posterior lenticular radius.

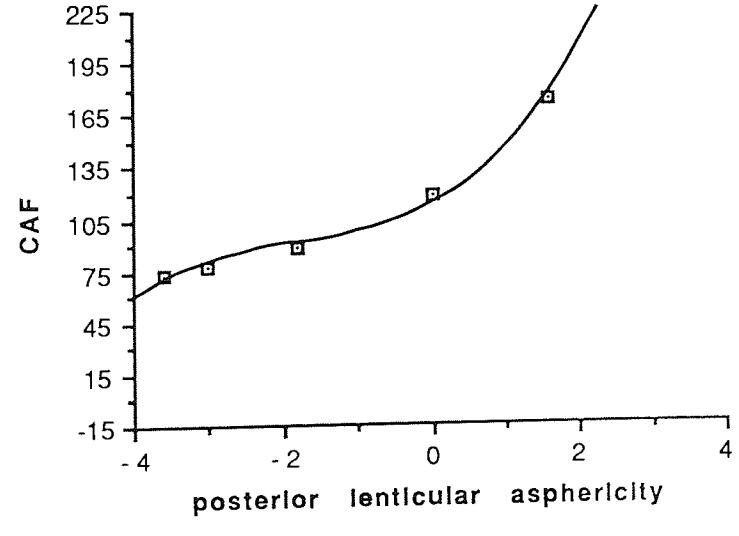

Fig. 8.27 Plot of CAF versus posterior lenticular asphericity. The equation of the curve is: $CAF = 112.630 + 21.635p + 8.994p^2 + 1.695p^3$ - where p is the posterior lenticular asphericity.

Table 8.1 summarises the effects of individual ocular parameter changes on the coma of the schematic eye. It is clear that anterior corneal asphericity has the greatest influence on the CAF and, hence, the coma of the system. For an asphericity value of 1.5 the CAF value is -14.2, the coma becoming over-corrected or positive. Other parameters producing significant decrease in the CAF are anterior cornea radius, the posterior lenticular asphericity and the lens thickness . However, compared to the decrease in CAF caused by anterior corneal asphericity the changes are only small. All other parameters are merely capable of reducing the CAF by very small amounts. The greatest increase in CAF appears to be due to an increase in the posterior lens asphericity but, as previously noted, the maximum CAF value is only hypothetical.

8.5 DISCUSSION

Variation in CAF with radii of curvature of the lenticular surfaces is very small, particularly for the anterior lenticular surface. This is due to the pupil being coincident with the anterior surface as was discussed in section 7.6.

increasing parameter	effect on CAF	maximum CAF	minimum CAF
anterior corneal radius	decrease	168.8	71.6
anterior corneal asphericity	decrease	208.8	-14.2
corneal thickness	-	118.9	118.9
posterior corneal radius	increase	124.6	112.7
posterior corneal asphericity	increase	137.9	106.4
anterior chamber depth	decrease	142.4	98.1
anterior lenticular radius	decrease	122.5	117.4
anterior lenticular asphericity	increase	172.3	114.1
lens thickness	increase	143.5	79.8
posterior lenticular radius	increase	139.7	97.7
posterior lenticular asphericity	increase	332.0	73.3

Table 8.1 Summary of the results of the variation in CAF for variation in parameter value. The table shows the effect on the CAF of increasing each parameter. An increase in the asphericity value causes peripheral steepening of the ocular surface. The final two columns show the maximum and minimum CAF achieved by altering the ocular surfaces within human limits. The CAF value for the mean schematic eye was 118.9.

Generally the variation in coma with parameter variation was similar to that of peripheral astigmatism. The most noticeable differences were the opposite directional variations for corneal surface parameter variations and variation in lens thickness.

To demonstrate the effect of coma on the symmetry of the retinal image the commercially available 'Beam 4' raytracing program was used to produce spread functions for two of the schematic eyes; one with high and one with low CAF values. The method used was the same as that described in section 8.2.1. A minimum of 20,000 parallel rays at a 40° field angle were randomly traced through each schematic eye, filling the whole of the pupil. The two schematic eyes used were Kooijman's schematic eye (Kooijman, 1983) and the schematic eye with an anterior corneal asphericity of 1.5.

Fig 8.28 shows the spread function in the tangential plane for Kooijman's schematic eye, which has a CAF of 118.9. The spread is clearly asymmetric. The ragged nature of the spread function is due to the limited number of rays traced through the system.

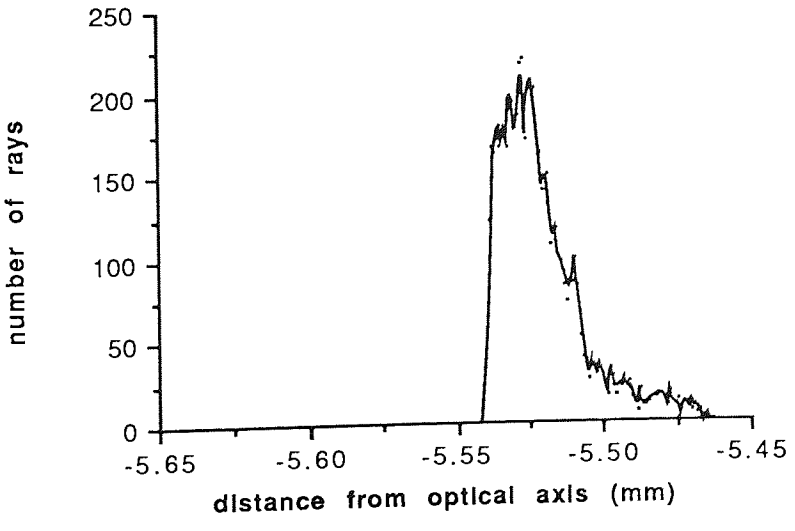

Fig. 8.28 The spread function in the tangential plane for 40° parallel rays traced through Kooijman's schematic eye.

Fig. 8.29 shows the spread function for the schematic eye with an anterior corneal asphericity of 1.5. The CAF is reduced dramatically to -14.2. The negative value indicates

that the coma has been slightly over-corrected. The small amount of coma suggested by the small CAF value is also apparent in the highly symmetrical spread function.

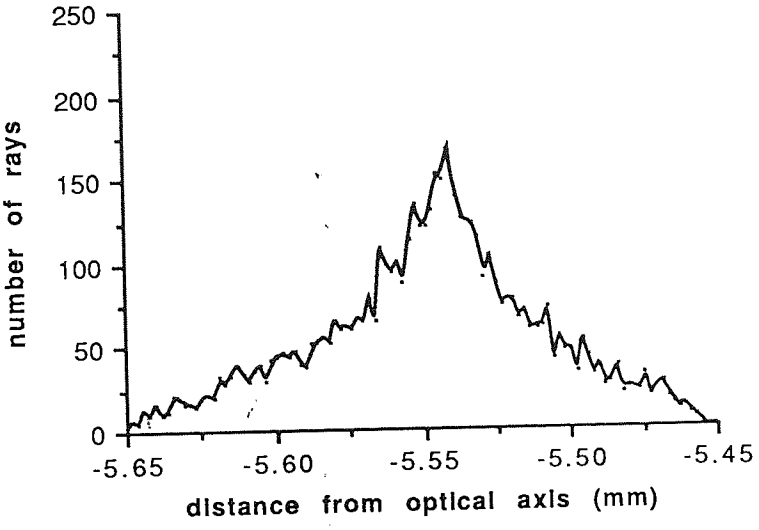

Fig. 8.29 The spread function in the tangential plane for 40° rays traced through the schematic eye with an anterior corneal asphericity of 1.5.

Comparison of the extent of the spread for the two images reveals that with an anterior corneal asphericity of 1.5 the spread is over twice as much as it is for Kooijman's schematic eye. This is due to the increase in peripheral astigmatism, which occurs with increasing anterior corneal asphericity. As peripheral astigmatism increases, the tangential focus will fall further in front of the retina, so increasing the spread of the rays as they fall on the retina.

8.6 SUMMARY

The apparent absence of coma-like distortion in the spread functions measured using the double pass method were questioned. It was suggested in the literature that this absence may be due to the optical system of the eye being nearly homocentric. However, it has been shown that a schematic eye with optical parameters based on the average values found in real eyes exhibits large amounts of coma. Examination of the theoretical basis behind the double pass method shows that it may be wrong in one of its fundamental assumptions. Ray tracing through schematic eyes show that the spread functions and MTFs for light passing into the eye are not the same as for light passing out of the eye. Also, the asymmetry of the two spread functions is in opposite directions. This may explain the apparent lack of asymmetry in the spread function for light which has passed into and then

back out of the optical system of the eye. Though to what extent this invalidates the double pass method is still uncertain.

Investigation of the variation in coma with parameter variation revealed that:-

i) Anterior corneal asphericity adjustment results in the largest variations in coma as well as producing large variations in spherical aberration and peripheral astigmatism. Coma can only be fully corrected by manipulation of this parameter. Unfortunately, peripheral flattening of the surface causes an increase in coma whilst decreasing spherical aberration and peripheral astigmatism.

ii) Other parameter changes producing relatively large reductions in CAF are increasing anterior corneal radius, decreasing lens thickness and decreasing posterior lenticular asphericity.

iii) Variations in posterior corneal surface parameters, and corneal thickness have little affect on CAF, just as they do on the SAF and PAF. Variation in the radii of curvature of the two lenticular surfaces also cause very little variation in CAF due to the close proximity of the lens to the limiting aperture.

iv) The CAF is decreased with increasing anterior chamber depth, but not by as large amounts as the simultaneous decrease in PAF. Increasing the lens thickness increases CAF, whereas it decreased both PAF and SAF.

v) For the anterior cornea, an increase in its apical radius and peripheral steepening decrease the CAF while increasing the PAF. The opposite is true for the posterior surface parameters. For the lens an increase in the anterior surface radius decreases both CAF and PAF, while peripheral steepening increases both. For the posterior surface an increased apical radius and peripheral steepening increases both CAF and PAF. Finally, reducing the asphericity of the anterior lens surface below the mean value has very little affect on the CAF as was also found for PAF values.

CHAPTER 9
SCHEMATIC MODELLING OF SPHERICAL ABERRATION AND PERIPHERAL ASTIGMATISM IN HUMAN SCHEMATIC EYE VARIANTS

9.1 INTRODUCTION

In this chapter the information from the previous three chapters is collated to give an overall picture of the effects of parameter variations on the three aberrations. This information is then used to design schematic eyes with specific levels of spherical aberration and peripheral astigmatism. The aim is to determine if schematic eyes with aspheric surfaces and no gradient index structure have the flexibility to reproduce the potential range of aberrations found in human eyes.

9.2 SIMULTANEOUS EFFECTS OF PARAMETER VARIATIONS ON SPHERICAL ABERRATION, PERIPHERAL ASTIGMATISM AND COMA.

The initial part of this chapter will examine the simultaneous effects, on the three aberrations, of single parameter variations. The levels of spherical aberration and peripheral astigmatism resulting from the parameter variations will be compared to the empirical values established in chapters two and three respectively. The SAF and PAF values for the maximum, minimum and mean empirical values were calculated in sections 2.4.1 and 3.4.1 and are shown in table 9.1. As no empirical data exists with which to compare the values of coma of the schematic eyes, the CAF is noted simply to indicate whether it has increased or decreased from its original value. It also gives some idea of the levels of coma present. A note is also made of the central refractive error for a 4 mm pupil. Any change in the refractive error could be compensated for by altering the position of the retina and hence the axial length. Zadnik et al. (1992) considered that, on average, a 1 mm change in axial length resulted in in 2.5 D change in the refractive error for human eyes. Although this will alter for each schematic eye Zadnik's approximation was considered adequate for the purpose of this study. In section 4.6 it was established that for emmetropic eyes the axial length ranged from 21 mm to 28 mm. The mean schematic eye has an axial length of 24 mm. The retina, therefore, can be moved anteriorly by a maximum of 3 mm, which will compensate for a refractive error of up to -7.5 D. Also it can be moved posteriorly by 4 mm which will compensate for a refractive error of up to +10 D. Consequently, any of the schematic eyes having a refractive error of between -7.5 D and +10 D can be made emmetropic simply by altering the axial length of the eye.

	MAXIMUM	MEAN	MINIMUM
SAF	5.2	2.9	0.8
PAF	128.8	66.0	24.7

Table 9.1 The maximum, mean and minimum SAFs and PAFs found in human eyes.

9.2.1 KOOIJMAN'S SCHEMATIC EYE (THE MEAN SCHEMATIC EYE)

From fig. 9.1 it can be seen that the spherical aberration of the mean eye is much lower than mean empirical values for all pupil sizes. The SAF is 1.6, almost half the mean empirical value. The peripheral astigmatism (fig. 9.2) is close to maximum empirical values, especially for field angles below 40°. The PAF was found to be 100.0, about half way between mean and maximum values. The CAF for the mean schematic eye was 118.9 and the refractive error for a 4 mm pupil is -0.5 D making it slightly myopic. For paraxial rays the refractive error is 0.02 D, thus Kooijman's schematic eye is very nearly emmetropic paraxially.

Previous attempts to model mean aberration values have generally used schematic eye parameters close to human mean values (see section 5.4). However, there is no evidence to suggest that an optical system constructed from mean ocular parameters will exhibit the mean aberration values found in human eyes. A number of optical systems combining very different optical parameters may give the same aberration levels. Further, as both aberrations have not been measured in the same human eyes, it has not yet been established that any human eye combines mean values of both spherical aberration and peripheral astigmatism. To produce a model which has mean values of both these aberrations clearly the spherical aberration of Kooijman's schematic eye must be increased while simultaneously decreasing the peripheral astigmatism.

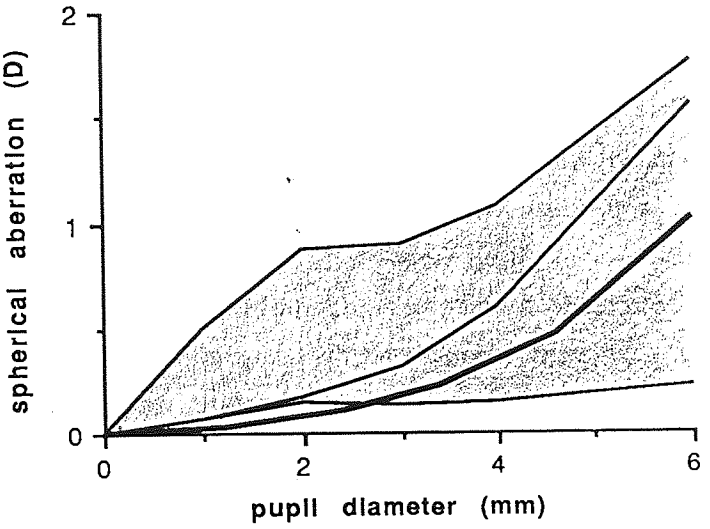

Fig. 9.1 Spherical aberration of the mean schematic eye (bold line) compared to the minimum, mean and maximum empirical values. The shaded area represents the full range of values found in human eyes.

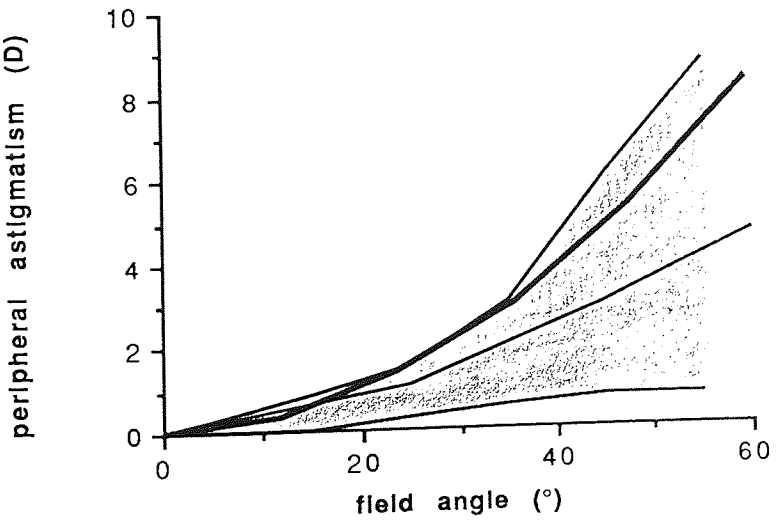

Fig. 9.2 Peripheral astigmatism of the mean schematic eye (bold line) compared to the minimum, mean and maximum empirical values. The shaded area represents the full range of values found in human eyes.

9.2.2 ANTERIOR CORNEAL RADIUS (ACR)

From Fig. 9.3 it can be seen that for the minimum radius of 7.0 mm the spherical aberration (SAF = 2.5) is increased giving values close to the mean (SAF = 2.9) found in real eyes. The peripheral astigmatism (fig. 9.4), on the other hand, is decreased (PAF = 80.4) to values approaching the human mean value (PAF = 66.0). The CAF is increased to 168.8. The central refractive error for a 4 mm pupil is -5.5 D. This can be compensated for by moving the retina approximately 2.2 mm towards the anterior of the eye. The axial length then becomes 21.8 mm which is within the range found in emmetropic human eyes.

The maximum radius of 8.9 mm reduces spherical aberration below minimum values for small pupil sizes and gives values between the minimum and mean for pupils of approximately 4 mm diameter or more (fig. 9.3). This results in an SAF of 0.8, equal to the empirical minimum. The peripheral astigmatism (fig. 9.4) is increased, the levels falling very close to maximum empirical levels for all field angles. The PAF is increased to 115, a little below the empirical maximum. The CAF falls to 71.6 and the central refractive error is 4.8 D for a 4 mm pupil. Again, the schematic eye can be made emmetropic by increasing the axial length within the range found in emmetropic human eyes.

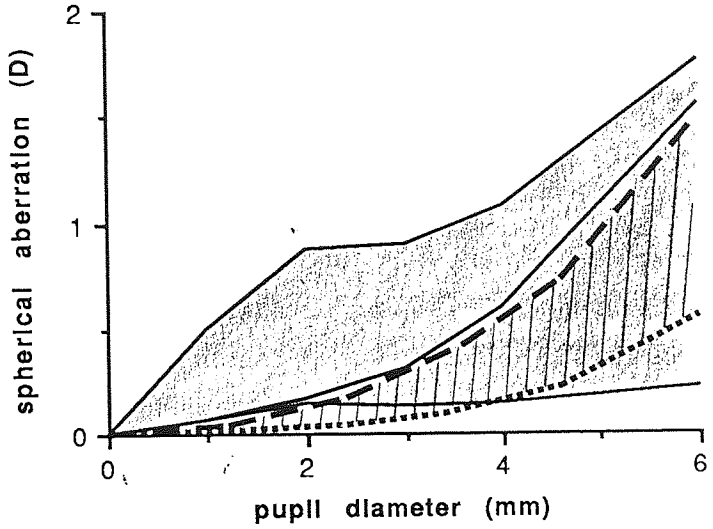

Fig. 9.3 Spherical aberration for the minimum ACR. of 7.0 mm (dashed line) and maximum ACR. of 8.9 mm (dotted line) compared to the minimum, mean and maximum empirical values (solid lines). The shaded area represents the full range of values found in human eyes. The hashed area represents the range of values obtained by varying the ACR., in the schematic eye, over the full human range.

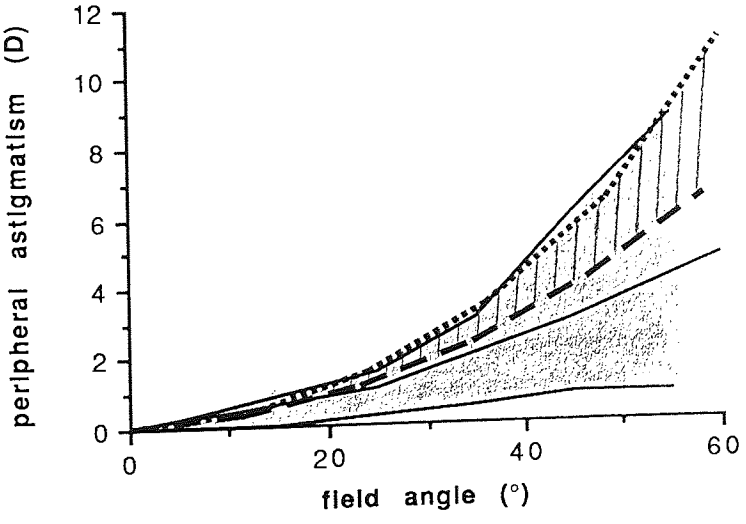

Fig. 9.4 Peripheral astigmatism for the minimum A.C.R. of 7.0 mm (dashed line) and Maximum A.C.R. of 8.9 (dotted line) compared to the minimum, mean and maximum empirical values (solid lines). The shaded area represents the full range of values found in human eyes. The hashed area represents the range of values obtained by varying the ACR., in the schematic eye, over the full human range.

9.2.3 ANTERIOR CORNEAL ASPHERICITY (ACA)

From fig. 9.5 reveals that peripherally flattening the surface to give an asphericity of 0.1 greatly over-corrects the spherical aberration and gives a SAF of -2.4. The peripheral astigmatism (fig. 9.6) is also decreased to values close to the empirical mean. The PAF is 72.0, fairly close to the mean value of 66. Coma, however, is greatly increased to give a CAF value of 208.8. The central refractive error for a 4 mm pupil is 0.7 D.

Steepening the anterior corneal surface to give an asphericity of 1.5 increases both the spherical aberration (fig. 9.5) and the peripheral astigmatism (fig. 9.6) to values which are beyond those found in human eyes. The SAF is 6.7 and the PAF is 151.4. The CAF is reduced by such an amount that it becomes negative (-14.2). This means that the coma has become slightly positive or under-corrected. The central refractive error for a 4 mm pupil is -2.0 D.

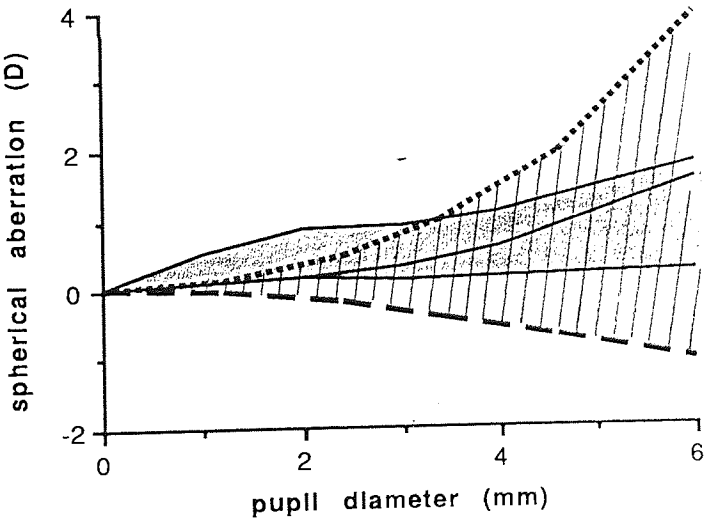

Fig. 9.5 Spherical aberration for the flattest ACA. of 0.1 (dashed line) and the steepest ACA. of 1.5 (dotted line) compared to the minimum, mean and maximum empirical values (solid lines). The shaded area represents the full range of values found in human eyes. The hashed area represents the range of values obtained by varying the ACA., in the schematic eye, over the full human range.

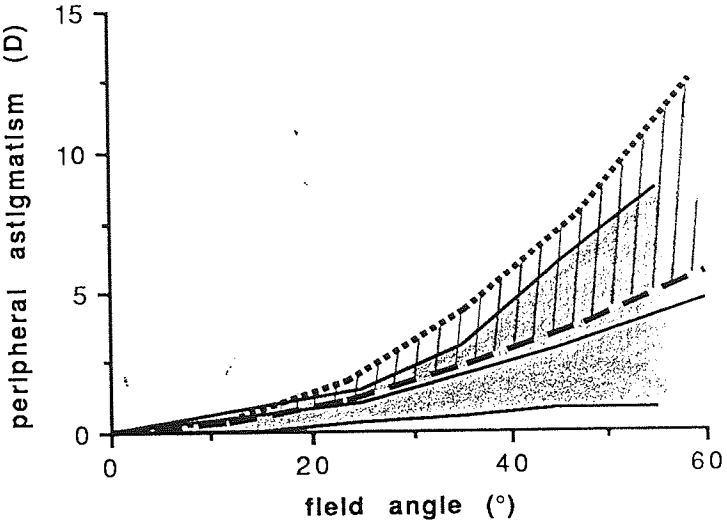

Fig. 9.6 Peripheral astigmatism for the flattest ACA. of 0.1 (dashed line) and the steepest ACA. of 1.5 (dotted line) compared to the minimum, mean and maximum empirical values (solid lines). The shaded area represents the full range of values found in human eyes. The hashed area represents the range of values obtained by varying the ACA., in the schematic eye, over the full human range.

2.2.4 CORNEAL THICKNESS (CT)

Variations in corneal thickness have negligible affect on all three aberrations. Central refractive error for a 4 mm pupil varies by only 0.1 D for the full range of corneal thicknesses. This is well below clinical significance which is considered to be ± 0.5 D.

2.2.5 POSTERIOR CORNEAL RADIUS (PCR)

Variations in this parameter also have little affect on spherical aberration and peripheral astigmatism. Consequently they remain close to the values of Kooijman's schematic eye. The minimum radius of 5.8 mm reduces the SAF to 1.5, increases PAF to 101.5 and reduces CAF to 112.7. The central refractive error becomes 0.2 D. The maximum radius of 7.4 mm increases SAF to 1.7 decreases PAF very slightly to 99.1 and increases CAF to 125.6. The central refractive error is decreased to -1.1 D.

2.2.6 POSTERIOR CORNEAL ASPHERICITY (PCA)

An asphericity of 0.1 increases the spherical aberration to slightly below mean empirical values, giving a SAF of 2.2. The PAF is only slightly increased to 102.3 and the CAF is decreased to 106.4. Central refractive error becomes -0.6 D.

Increasing asphericity to 1.5 decreases the the spherical aberration so that for pupil diameters of up to 4 mm its value is lower than the minimum, reducing the SAF to 0.7, slightly below the minimum value. The PAF is also decreased, but only slightly to a value of 95.8. The CAF is increased to 137.9 and central refractive error becomes -0.2 D.

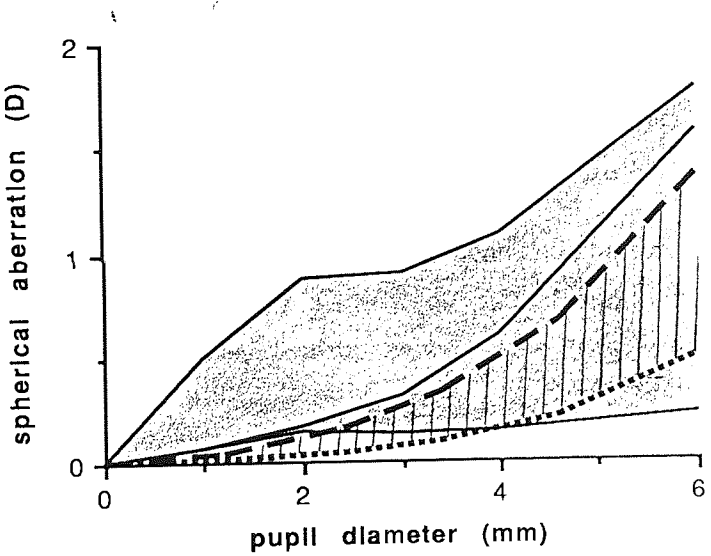

Fig. 9.7 Spherical aberration for the flattest PCA. of 0.1 (dashed line) and the steepest PCA. of 1.5 (dotted line) compared to the minimum, mean and maximum empirical values (solid lines). The shaded area represents the full range of values found in human eyes. The hashed area represents the range of values obtained by varying the PCA., in the schematic eye, over the full human range.

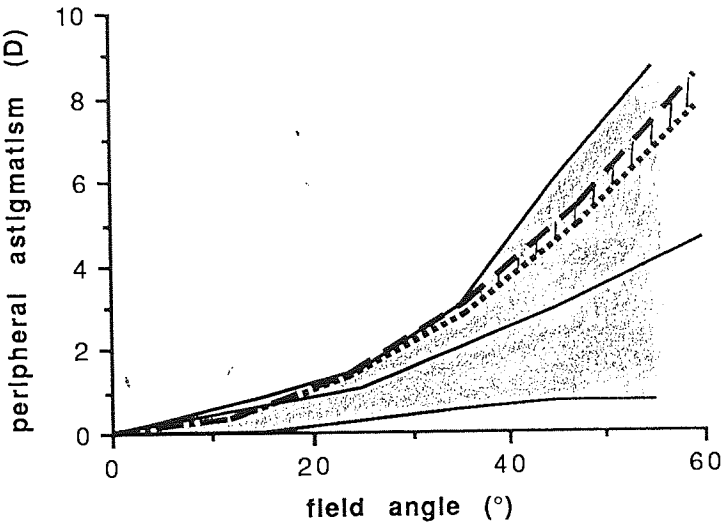

Fig. 9.8 Peripheral astigmatism for the flattest PCA. of 0.1 (dashed line) and the steepest PCA. of 1.5 (dotted line) compared to the minimum, mean and maximum empirical values (solid lines). The shaded area represents the full range of values found in human eyes. The hashed area represents the range of values obtained by varying the PCA., in the schematic eye, over the full human range.

2.2.7 ANTERIOR CHAMBER DEPTH (ACD)

From fig. 9.9 it is evident that variation in anterior chamber depth has little influence on the spherical aberration. The change in SAF given by altering the depth over the whole human range is less than 0.1. The peripheral astigmatism, however, is greatly influenced by anterior chamber depth variations (fig. 9.10). For the minimum value of 2.5 mm it is increased to values far above maximum empirical values, increasing the PAF to 178.0. The CAF is also increased to 142.4 and the refractive error becomes 0.9 D. Increasing the anterior chamber depth to its maximum decreases the peripheral astigmatism to values below mean empirical values decreasing the PAF to 46.8. This is approximately half way between the mean and minimum values. The CAF is also decreased to 98.1 and the refractive error becomes -1.6 D.

The reduction in peripheral astigmatism with increasing anterior chamber depth may explain the finding that aphakic eyes have less peripheral astigmatism than phakic eyes (Millodot, 1984). Millodot measured peripheral astigmatism in 10 phakic eyes (age range 62 to 67)

and 16 aphakic eyes (age range 63 to 85). He found that, at eccentricities beyond 20°, the peripheral astigmatism in aphakic eyes was from half to a third that of the phakic eyes. Millodot concluded that the crystalline lens had higher peripheral astigmatism than the cornea. He also measured the peripheral astigmatism in two young aphakic eyes (ages 31 and 34) and compared the results to those found in 62 young phakic eyes. On average the peripheral astigmatism of young aphakic eyes was discovered to be approximately half that of young phakic eyes. This suggests that the peripheral astigmatism of the crystalline lens and cornea is approximately equal in young eyes.

Dunne et al. (1991) considered that the posterior iris displacement, observed following removal of cataractous crystalline lenses, could be responsible for the reduction in peripheral astigmatism. They demonstrated that, when the lens was removed from a schematic eye, the level of reduction in peripheral astigmatism was small. Contrary to the conclusions of Millodot (1984), this suggests that the crystalline lens has less peripheral astigmatism than the cornea. Posterior displacement of the iris, however, gave much larger reductions. From this it may be concluded that the major reason for the reduction of peripheral astigmatism in aphakic eyes is the decrease in corneal peripheral astigmatism caused by the increased anterior chamber depth. Dunne et al. also measured the displacement of the iris in 8 patients following cataractous crystalline lens removal. They found that the average posterior displacement of 1.19 mm was capable of producing, in schematic eyes, the experimentally observed reduction in peripheral astigmatism given by Millodot (1984). The large decrease in peripheral astigmatism with increased anterior chamber depth, found in the present study, further substantiates the findings of Dunne et al. (1991).

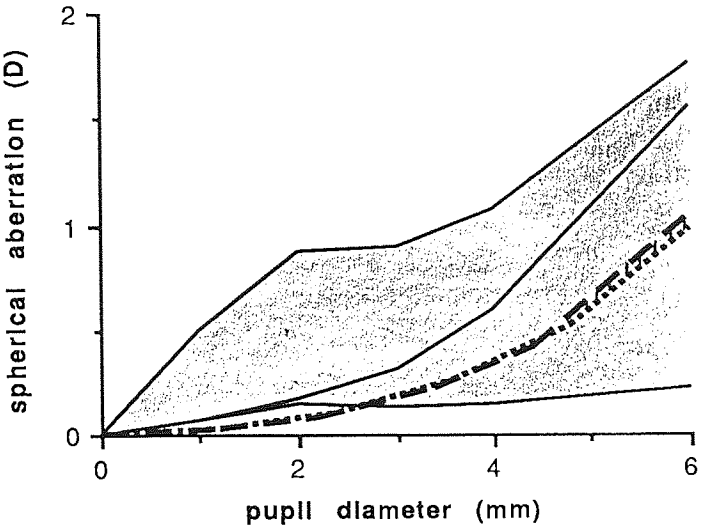

Fig. 9.9 Spherical aberration for the minimum ACD of 2.5 mm (dashed line) and the maximum ACD of 4.6 mm (dotted line) compared to the minimum, mean and maximum empirical values (solid lines). The shaded area represents the full range of values found in human eyes. The hashed area represents the range of values obtained by varying the ACD., in the schematic eye, over the full human range.

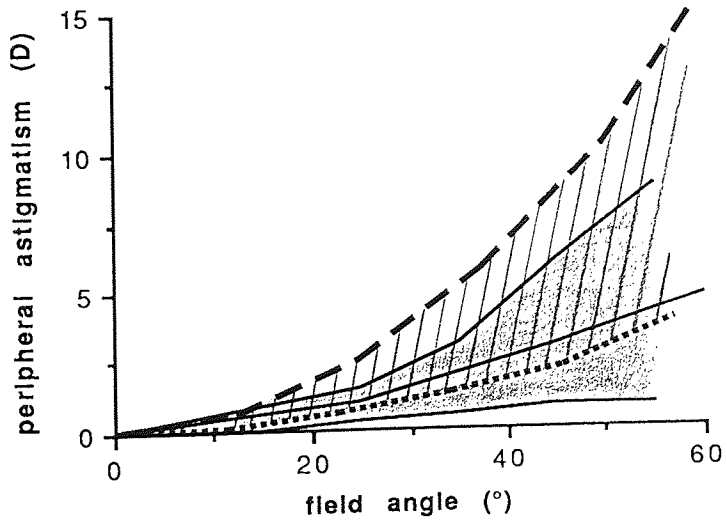

Fig. 9.10 Peripheral astigmatism for the minimum ACD of 2.5 mm (dashed line) and the maximum ACD of 4.6 mm (dotted line) compared to the minimum, mean and maximum empirical values (solid lines). The shaded area represents the full range of values found in human eyes. The hashed area represents the range of values obtained by varying the ACD., in the schematic eye, over the full human range.

9.2.8 ANTERIOR LENTICULAR RADIUS (ALR)

A radius of 7.7 mm over-corrects spherical aberration (fig. 9.11) giving an SAF of -0.3. The peripheral astigmatism is increased to give values close to the maximum (fig.9.12); the PAF is 112.4. The CAF increased only slightly to 122.5 and the central refractive error becomes -1.6 D.

When the radius equals 13.8 mm the SAF increases to 2.6, the spherical aberration being close to the mean empirical values (fig. 9.11). The peripheral astigmatism (fig 9.12) is decreased slightly (PAF = 87.9) and the CAF is very slightly decreased to 117.4. The central refractive error becomes 0.7 D.

How these changes relate to the changes in aberrations during accommodation and with age will be discussed later, when the effect of all lens parameter variations have been noted.

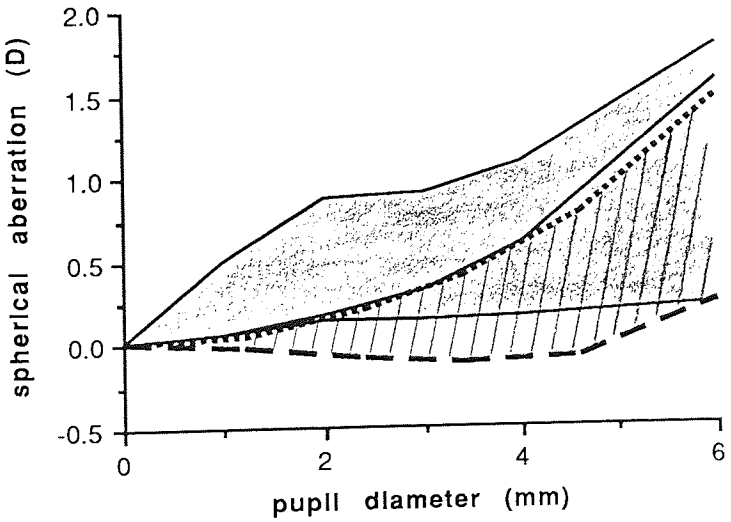

Fig. 9.11 Spherical aberration for the minimum ALR. of 7.7 mm (dashed line) and the maximum ALR. of 13.8 mm (dotted line) compared to the minimum, mean and maximum empirical values (solid lines). The shaded area represents the full range of values found in human eyes. The hashed area represents the range of values obtained by varying the ALR., in the schematic eye, over the full human range.

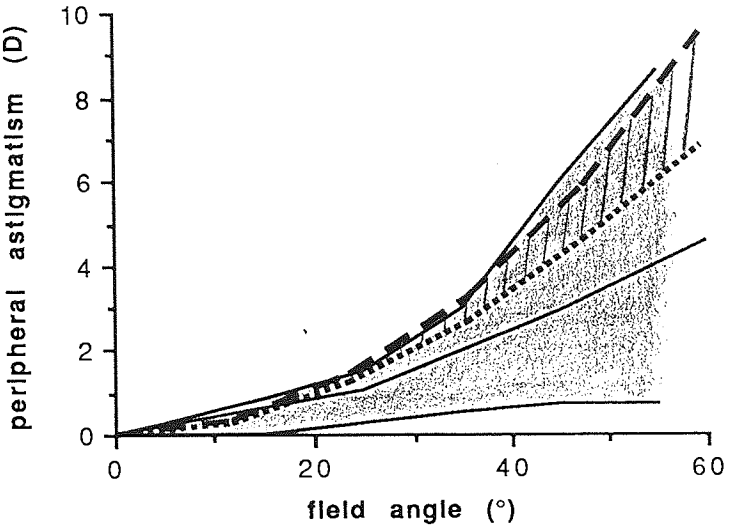

Fig. 9.12 Peripheral astigmatism for the minimum ALR. of 7.7 mm (dashed line) and the maximum ALR. of 13.8 mm (dotted line) compared to the minimum, mean and maximum empirical values (solid lines). The shaded area represents the full range of values found in human eyes. The hashed area represents the range of values obtained by varying the ALR., in the schematic eye, over the full human range.

9.2.9 ANTERIOR LENTICULAR ASPHERICITY (ALA)

Flattening the surface to an asphericity value of -23.45 (fig. 9.13) gives high levels of over-corrected spherical aberration (SAF = -1.9). The peripheral astigmatism is reduced by a comparatively small amount (fig. 9.14) giving a PAF of 87.9. These findings are in agreement with those of Dunne and Barnes (1990). The CAF is reduced very slightly to 114.1 and the refractive central error becomes 0.6 D.

Steepening the surface to an asphericity value of 13.35 increases the spherical aberration (fig.9.13) to levels much higher than the maximum empirical values. The SAF becomes 12.3, more than double the maximum value found in real eyes. The peripheral astigmatism (fig. 9.14) is also increased beyond human limits (PAF = 175.3). The CAF increases to 172.3 and the central refractive error becomes
-3.2 D.

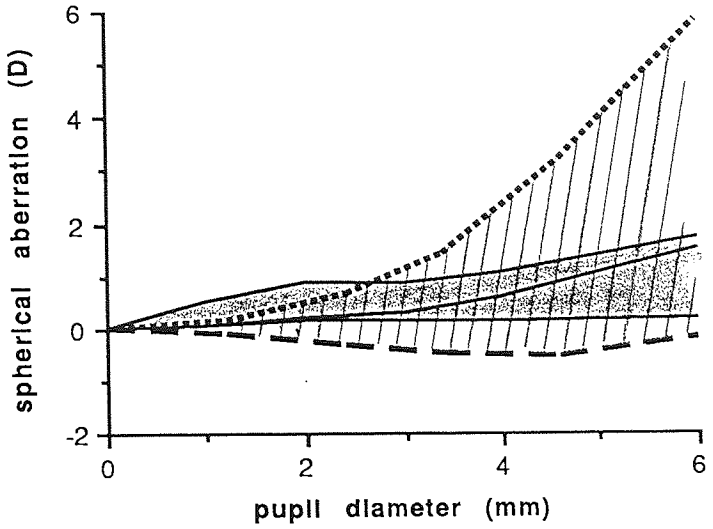

Fig. 9.13 Spherical aberration for the flattest ALA. of -23.45 (dashed line) and the steepest ALA. of 13.35 (dotted line) compared to the minimum, mean and maximum empirical values (solid lines). The shaded area represents the full range of values found in human eyes. The hashed area represents the range of values obtained by varying the ALA., in the schematic eye, over the full human range.

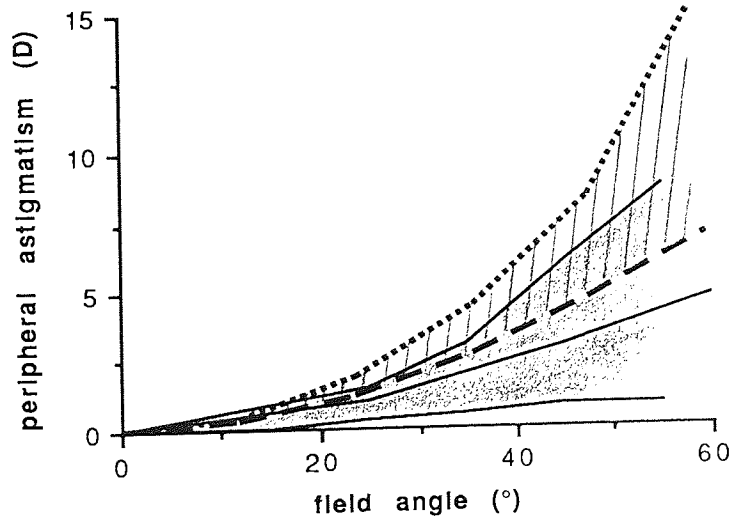

Fig. 9.14 Peripheral astigmatism for the flattest ALA. of -23.45 (dashed line) and the steepest ALA. of 13.35 (dotted line) compared to the minimum, mean and maximum empirical values (solid lines). The shaded area represents the full range of values found in human eyes. The hashed area represents the range of values obtained by varying the ALA., in the schematic eye, over the full human range.

9.2.10 LENS THICKNESS (LT)

A thin lens of 2.9 mm increases spherical aberration slightly (fig. 9.15) giving a SAF of 1.9. The peripheral astigmatism is also increased (fig. 9.16) to levels close to the human maximum (PAF = 121.0). The CAF, however, is decreased to 79.7 and the central refractive error becomes -1.5 D.

Increasing the thickness to 5.0 mm decreases both spherical aberration (fig.9.15) and peripheral astigmatism (fig. 9.16) slightly. The SAF and PAF values become 1.4 and 91.1 respectively. The CAF is increased to 143.5 and the central refractive error is 0.4 D.

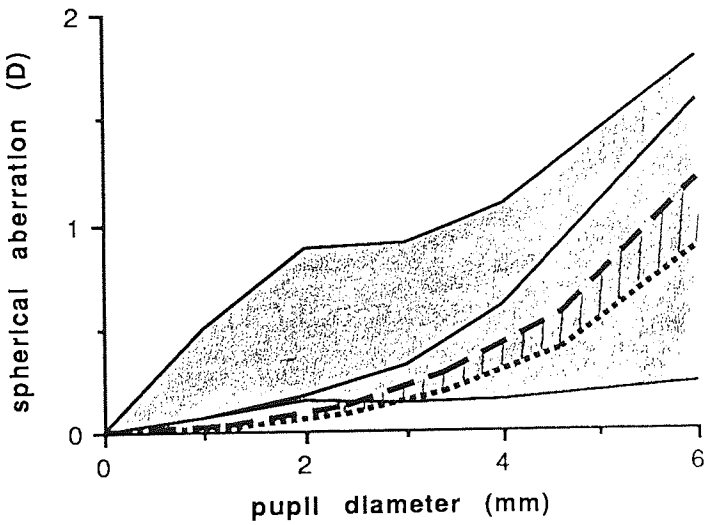

Fig. 9.15 Spherical aberration for the minimum LT. of 2.9 mm (dashed line) and the maximum LT. of 5.0 mm (dotted line) compared to the minimum, mean and maximum empirical values (solid lines). The shaded area represents the full range of values found in human eyes. The hashed area represents the range of values obtained by varying the LT., in the schematic eye, over the full human range.

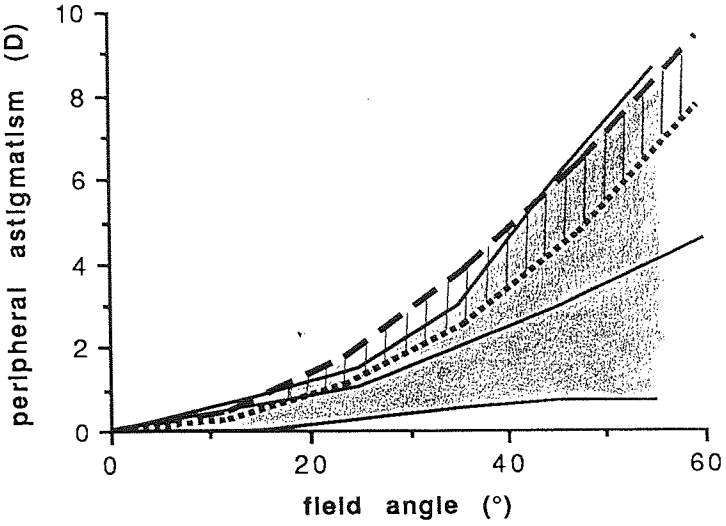

Fig. 9.16 Peripheral astigmatism for the minimum LT. of 2.9 mm (dashed line) and the maximum LT. of 5.0 mm (dotted line) compared to the minimum, mean and maximum empirical values (solid lines). The shaded area represents the full range of values found in human eyes. The hashed area represents the range of values obtained by varying the LT., in the schematic eye, over the full human range.

9.2.11 POSTERIOR LENTICULAR RADIUS (PLR)

Reducing the radius to -4.6 mm increases the spherical aberration (fig. 9.17) to levels very close to the empirical mean (SAF = 2.7). The peripheral astigmatism (fig. 9.18) is decreased to give values which are close to the mean empirical values for field angles of up to approximately 40°. The PAF decreases to 78.3. The CAF decreases to 97.7 and the refractive error becomes -2.7 D.

Increasing the radius to -8.3 mm reduces the spherical aberration (fig. 9.17). The values fall slightly below empirical minimum values for pupil diameters of less than 3.5 mm and slightly above for larger pupils (SAF = 0.8). The peripheral astigmatism (fig. 9.18) is increased to values close to the empirical maximum (PAF = 119.3). The CAF is also increased to a value of 139.7, and the refractive error becomes 1.6 D.

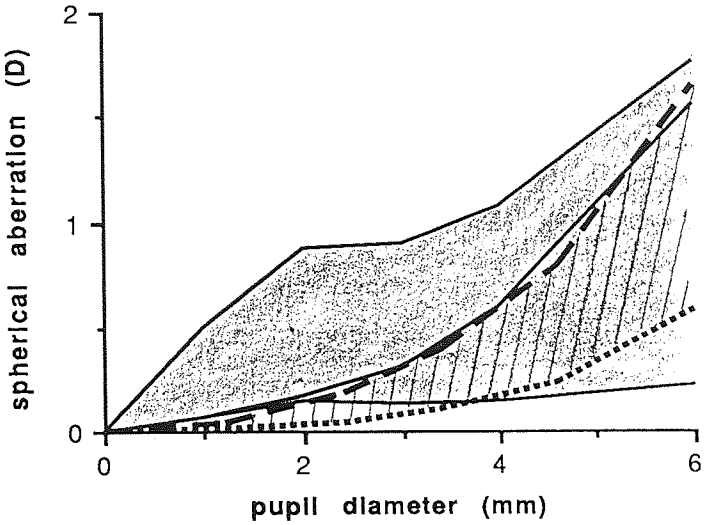

Fig. 9.17 Spherical aberration for the minimum PLR of -4.6 mm (dashed line) and the maximum PLR. of -8.3 mm (dotted line) compared to the minimum, mean and maximum empirical values (solid lines). The shaded area represents the full range of values found in human eyes. The hashed area represents the range of values obtained by varying the PLR., in the schematic eye, over the full human range.

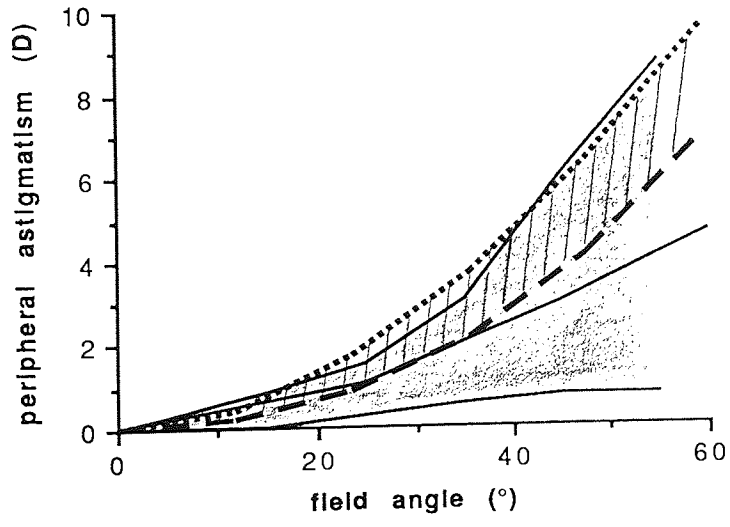

Fig. 9.18 Peripheral astigmatism for the minimum PLR of -4.6 mm (dashed line) and the maximum PLR. of -8.3 mm (dotted line) compared to the minimum, mean and maximum empirical values (solid lines). The shaded area represents the full range of values found in human eyes. The hashed area represents the range of values obtained by varying the PLR., in the schematic eye, over the full human range.

9.2.12 POSTERIOR LENTICULAR ASPHERICITY (PLA)

Flattening the surface to an asphericity value of -3.59 over-corrects the spherical aberration, giving a SAF value of -1.5 (fig. 9.19). The peripheral astigmatism (fig. 9.20) is reduced only slightly, giving a PAF of 97.1. The CAF is reduced to 73.3 and the central refractive error is 0.5 D.

Steepening the surface to an asphericity value of 3.21 increases the spherical aberration beyond the maximum values for pupil sizes greater than 3.5 mm diameter (fig. 9.19). The SAF increases to 6.3. The peripheral astigmatism is increased to levels which are vastly above the human maximum (fig. 9.20), resulting in a PAF of 255.9. The CAF is increased to 331.9. However, for field angles greater than approximately 30° marginal rays miss the surface. As discussed in sections 7.3.2 and 8.4.2, this makes the PAF and CAF somewhat hypothetical. The central refractive error for this schematic eye was found to be -1.7 D.

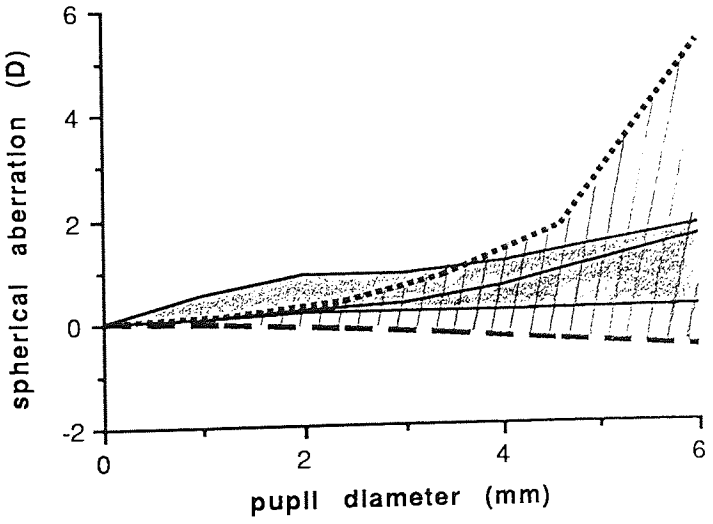

Fig. 9.19 Spherical aberration for the flattest PLA of -3.59 (dashed line) and the steepest PLA. of 3.21 (dotted line) compared to the minimum, mean and maximum empirical values (solid lines). The shaded area represents the full range of values found in human eyes. The hashed area represents the range of values obtained by varying the PLA., in the schematic eye, over the full human range.

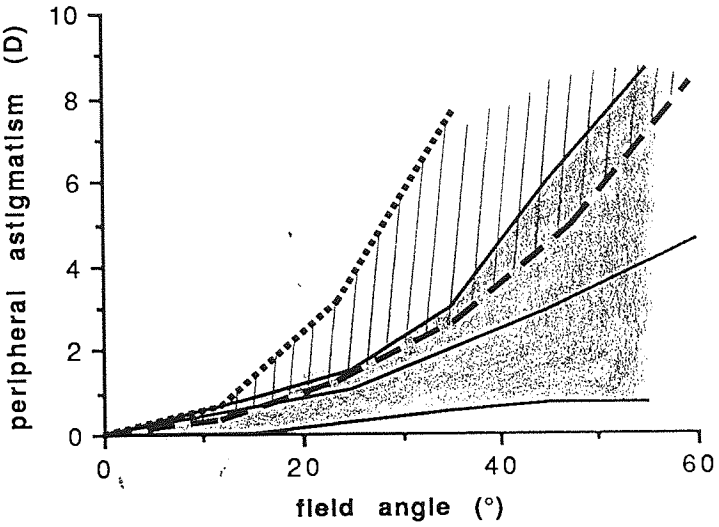

Fig. 9.20 Peripheral astigmatism for the flattest PLA of -3.59 (dashed line) and the steepest PLA. of 3.21 (dotted line) compared to the minimum, mean and maximum empirical values (solid lines). The shaded area represents the full range of values found in human eyes. The hashed area represents the range of values obtained by varying the PLA., in the schematic eye, over the full human range.

9.2.13 EXPLANATION OF ACCOMMODATION AND AGE RELATED CHANGES IN ABERRATIONS IN TERMS OF LENS PARAMETER VARIATIONS.

The lens parameter changes which take place during accommodation and aging were discussed in section 4.5. Briefly, during accommodation the central radii of both surfaces are reduced but the posterior radius to a lesser extent than the anterior. Both surfaces also become relatively flatter in the periphery; again the change is less marked for the posterior surface. The thickness of the lens is increased and the anterior chamber depth will decrease due to the increased curvature of the anterior surface.

There is some disagreement as to the changes in the crystalline lens parameters with increasing age. The anterior lens was originally thought to get flatter with age. However, recent research shows that the central and peripheral radii of the anterior lens decrease giving a more steeply curved surface. The same is true for the posterior surface. The change occurs, however, at a slower rate. The thickness of the lens increases with age and is thought to move forward in the eye, reducing the anterior chamber.

The changes in spherical aberration with accommodation and age were discussed in sections 2.3.3 and 2.3.4 respectively. It is generally found to be under-corrected or positive for relaxed eyes and reduces with accommodation, sometimes becoming over-corrected at high levels. Young eyes were found to have small amounts of over-corrected spherical aberration which change to small under-corrected values in the next few years. After the age of about 35 years a large increase in under-corrected spherical aberration was evident. Jenkins (1963) attributed this to the central zone of the eye becoming hypermetropic while the periphery remained constant.

The changes in peripheral astigmatism with accommodation and age are discussed in sections 3.3.4 and 3.3.5 respectively. No significant change in peripheral astigmatism was found with accommodation, although it increases with age. Millodot (1984) felt this was due to the lens becoming flatter at the centre and more steeply curved in the periphery.

The results presented in this section demonstrate how each lens parameter variation effects spherical aberration and peripheral astigmatism. From this it should be possible to predict how the two aberrations will be altered by during accommodation and aging. During accommodation spherical aberration will decrease due to the reduction in anterior lenticular radius and asphericity and posterior lenticular asphericity. It will also be decreased by the increase in lens thickness. Any increase in spherical aberration, caused by Posterior lenticular radius reduction, is likely to be relatively small. The finding that spherical aberration decreases with accommodation is, therefore, corroborated by the evidence of this study.

For peripheral astigmatism all the parameter changes which occur during accommodation decrease its level; except for the decrease in anterior lens radius and anterior chamber depth which increase it. Changes due to lenticular asphericity reduction below the mean value are small, as are changes due to lens thickness variations. The decrease due to the relatively small variations in the posterior radius can also be expected to be minimal. It is probable, therefore, that the relatively small decreases in peripheral astigmatism due to four of the parameters is cancelled out by the larger increases due to the other two. This would explain why no significant change in peripheral astigmatism was found.

The changes which take place in the aging lens will now be examined. The belief that the radii of curvature of the lens surfaces reduce both centrally and peripherally will be considered first. If the peripheral radii reduce by a relatively large amount, making the surface steeper in the periphery, then spherical aberration and peripheral astigmatism will

be increased for both lens surfaces. Reduction in the central radius of the anterior surface reduces spherical aberration but increases peripheral astigmatism. The reverse is true for a reduction in the posterior surface central radius. An increase in the lens thickness reduces both aberrations and a decrease in anterior chamber depth increases spherical aberration slightly while greatly increasing peripheral astigmatism.

Three of the parameter variations reduce spherical aberration while three increase it. The overall effect will, therefore, depend on their relative influence. Lens thickness and anterior chamber depth changes have a minimal effect on spherical aberration. Increases due to the posterior lenticular surface variations are likely to have less influence due to the slower rate of change of its shape compared to the anterior surface. The changes due to the anterior surface will partially cancel each other out. This would suggest that if the final result is an increase in spherical aberration it would not be a very large increase.

If, as earlier research suggested, the central radii of the lens surfaces increase with age the increase in spherical aberration would be more easily explained. This would also account for the tendency for the aging eye to become hypermetropic. The anterior lens changes will clearly increase the spherical aberration as not only does the central radius increase but the peripheral steepening is likely to be more pronounced if, either the peripheral radii remains constant, as believed by Jenkins (1963), or decreases, as found by Brown (1974). Although the posterior lenticular central radius increase will decrease spherical aberration its effect is likely to be relatively small compared to its relative peripheral steepening which increases it.

For peripheral astigmatism the increase due to the decrease in the anterior chamber depth may be the over-riding factor. Between the ages of 20 and 65 years the depth may reduced by as much as 0.6 mm (Bennett and Rabbetts, 1984). Reduction in peripheral astigmatism due to increases in lens thickness will be small. Decreasing the central radius and peripherally steepening the anterior lenticular surface will increase peripheral astigmatism. Similar changes to the posterior lenticular surface will probably be small. This is due, not only to the slower rate of change of its shape with age, but also to the opposing effects the two parameter changes have on peripheral astigmatism. The overall effect would, therefore, be an increase in peripheral astigmatism. Considering the alternative theory that the central radii increase then the anterior surface parameter changes will have opposing effects. However, the increase due to relative peripheral steepening will probably outweigh the decrease due to central radius increase. The posterior lens changes will increase peripheral astigmatism and, again, the overall effect is an increase in peripheral astigmatism. It appears, therefore, that parameter changes consistent with both theories of how the crystalline lens aters with age, lead to an increase in peripheral astigmatism.

In conclusion, lens parameter changes which occur during accommodation are clearly defined and explain the changes in the two aberrations. There is some disagreement about the lens surface changes in the aging eye. The belief that the central radii increase with age more readily explains the large increases in spherical aberration. However, no conclusion can be drawn from consideration of the peripheral astigmatism changes as both theories are likely to lead to an increase in its level.

It is important to remember that the gradient index structure of the lens will also change during accommodation and aging. This element has not been considered, as its variation is unknown. It is evident that any changes will affect the aberrations of the lens. Knowledge of the nature of the changes taking place would provide a better understanding of the reasons for the aberration variations.

9.3 MODELLING SAFS AND PAFS USING SINGLE PARAMETER VARIATIONS

Peripheral astigmatism and spherical aberration levels found in human eyes were initially modelled using single parameter changes. This was achieved simply by solving the second-order quadratic equations. These describe the curves fitted to the plots of SAF and PAF versus parameter value.

9.3.1 METHODS

Second-order (quadratic) equations ($y = ax^2 + bx + c$) can be solved using the quadratic formula:-

$$x = \frac{- b \pm \sqrt{(b^2 - 4ad)}}{2a}$$

where $d = c - y$

The polynomials fitted to the plots of SAF or PAF versus parameter value are almost all quadratic equations. The y term is the SAF or PAF and the x term the parameter value. The quadratic formula can, therefore, be used to determine the parameter value which will give a particular SAF or PAF; provided all other parameter values keep their mean values. For example: what anterior corneal radius value would give the Minimum empirical SAF of 0.8? The polynomial fitted to the plot of SAF versus anterior corneal radius is:-

$$SAF = 0.18243\ R^2 - 3.8067R + 20.201$$

Substituting 0.8 for SAF then solving using the quadratic formula gives two solutions:

$$R = 8.9 \text{ mm} \quad \text{or} \quad R = 12.0 \text{ mm}$$

The polynomials can only be assumed to be accurate within the range of the plotted values. However, as no values will be used outside this range this poses no problem. As the maximum value for the anterior corneal radius is 8.9 mm the first solution is the only viable one. The result of the calculation is substantiated by the result of the ray trace through the schematic eye with an anterior corneal radius of 8.9 mm. This did give a SAF of 0.8.

All parameter values, within the human range, which gave SAFs and PAFs equal to maximum, mean and minimum empirical values were calculated by solving the quadratic equations . This was initiated by firstly reviewing the range of SAF and PAF values given by each parameter range, established in chapters 6 and 7. In the case of PAFs no single ocular parameter variation was capable of reducing the modelled PAF to the minimum empirical value. Further, only an increase in the anterior chamber depth was capable of decreasing the modelled PAF to the mean empirical value.

Some plots were fitted with polynomials higher than second-order. The plot of SAF versus anterior lenticular asphericity needed a third-order polynomial. However, in order to calculate parameter values for specific SAF values a second-order polynomial was considered to be accurate enough. The plots of PAF versus anterior and posterior lenticular asphericity were fitted by third- and forth-order polynomials respectively. As these higher-order polynomials are not easily solved, alternative methods were found to estimate the parameter which gave the maximum empirical PAF. The anterior lenticular asphericity value was estimated from the graph. The accuracy of this estimate was then checked by substitution into the third-order polynomial. For the posterior lens an asphericity value of 1.6, chosen as the value for one of the original 45 schematic eyes (see table 6.1), gave a PAF of 128.5 very close to the maximum of 128.8.

Having found the ocular parameter values giving the maximum, minimum and mean SAF values, the corresponding PAF and CAF values were calculated by substitution into their polynomial equations. Similarly, the SAF and CAF values corresponding to parameter values giving mean and maximum empirical PAF values were calculated.

9.3.2 RESULTS

parameter	value	SAF	PAF	CAF	Rx
A.C.R (mm)	8.871	0.8 (min)	114.5	72.7	4.7 D
A.C.A	1.292	5.2 (max)	135.1	25.8	-1.5 D
	0.951	2.9 (mean)	111.8	86.2	-0.9 D
	0.627	0.8 (min)	93.5	137.6	-0.2 D
	1.205	4.6	128.8 (max)	41.8	-1.4 D
P.C.A	1.441	0.8 (min)	96.0	136.1	-0.2 D
A.C.D (mm)	4.197	1.6	66.0 (mean)	105.8	-1.1 D
	3.146	1.6	128.8 (max)	127.6	+0.1 D
A.L.R (mm)	8.979	0.8 (min)	105.8	120.4	-1.0 D
A.L.A	3.182	5.2 (max)	107.5	158.5	-1.3 D
	-1.531	2.9 (mean)	101.4	118.9	-0.8 D
	-7.000	0.8 (min)	98.4	116.4	-0.3 D
	12	10.8	128.8 (max)	162.1	-2.9 D
P.L.A	2.554	5.2 (max)	164.9	254.8	-1.4 D
	1.007	2.9 (mean)	111.3	145.3	-0.8 D
	-0.726	0.8 (min)	98.8	101.0	-0.2 D
	1.6	3.6	128.8 (max)	172.7	-1.0 D

Table 9.2 Showing the parameter values within the Kooijman's schematic eye which give maximum, minimum and Mean SAFs and PAFs. The parameter values are deduced from the SAF and PAF polynomials. The corresponding PAFs or SAFs and CAFs were calculated by substitution of these parameter values into the appropriate polynomial equation. The central refractive error (Rx) was found by ray tracing through a 4 mm pupil.

The results are given in table 9.2. The 'value' column gives the calculated parameter value. Whether this parameter value is the solution for a SAF or PAF value is indicated by maximum, minimum or mean in the 'SAF' or 'PAF' column.

9.3.3 DISCUSSION

The results presented in table 9.2 show how the full range of empirical SAF values can be modelled by varying either the anterior corneal, the anterior lenticular or the posterior lenticular asphericity. Only the minimum empirical SAF can be modelled by varying the anterior corneal radius, the posterior corneal asphericity or the anterior lenticular radius. It is possible to model the maximum empirical PAF with four single parameter changes.

These are changes in the asphericity values of the anterior cornea and the anterior and posterior lens and the anterior chamber depth. The mean empirical PAF can only be reached by increasing the anterior chamber depth and the minimum empirical PAF cannot be modelled by any single parameter variation.

9.4 INVESTIGATION INTO THE EFFECTS OF COMBINED SURFACE RADIUS AND ASPHERICITY VARIATION ON SPHERICAL ABERRATION, PERIPHERAL ASTIGMATISM AND COMA.

From the previous section it is clear that single parameter changes are not capable of reproducing the full range of aberrations found in human eyes. In particular, the minimum empirical PAF cannot be reproduced by any single parameter variation. Only increases in the anterior chamber depth are capable of reproducing the mean empirical PAF. Therefore, in this section the effects of combining extreme values of surface radius and asphericity are investigated to ascertain the range of aberration values they produce.

Posterior corneal surface variations are not included in this investigation as variation in its parameters had negligible effect on peripheral astigmatism. For the other three surfaces the effects of combining the maximum apical radius with the flattest asphericity value and the minimum apical radius with the steepest asphericity are investigated. There is no evidence to suggest whether or not such extreme surface shapes would be found in real eyes. It is possible that steep asphericity values are only found for optical surfaces with large central radii and vica versa.

9.4.1 RESULTS

The results are shown in table 9.3. The values for the extreme radii and mean asphericity values were given in section 6.2.2.

parameter	SAF	PAF	CAF	Rx
ACR = 7.0 mm				
ACA = 0.1	-3.0	56.7	287.0	-3.8 D
ACA = 0.75	2.5	80.4	163.8	-5.5 D
ACA = 1.5	9.7	141.2	-28.6	-7.5 D
ACR = 8.9 mm				
ACA = 0.1	-1.9	91.5	135.4	+5.6 D
ACA = 0.75	0.8	115.0	71.6	+4.8 D
ACA = 1.5	4.1	142.2	-17.8	+3.9 D
ALR = 7.7 mm				
ALA = -23.45	-6.5	93.3	112.1	+0.1 D
ALA = -5.05	-0.3	112.4	122.5	-1.6 D
ALA = 13.35	error	error	error	-17.5 D
ALR = 13.8 mm				
ALA = -23.45	0.8	87.0	116.0	+1.2 D
ALA = -5.05	2.6	87.9	117.4	+0.7 D
ALA = 13.35	5.9	99.3	124.3	-0.3 D
PLR = -4.6 mm				
PLA = -3.59	-3.562	63.6	26.3	-0.9 D
PLA = 0	2.721	78.3	97.7	-2.7 D
PLA = 3.21	error	error	error	-6.4 D
PLR = -8.3 mm				
PLA = -3.59	-0.5	115.2	115.5	+2.0 D
PLA = 0	0.8	119.3	139.7	+1.6 D
PLA = 3.21	2.3	154.0	191.9	+1.2 D

Table 9.3 Showing aberration variation for extreme surface shapes. Each set of results shows the SAF, PAF and CAF values for an extreme value of the central radius with minimum, mean and maximum asphericity values. The central refractive error (Rx) for each radius is also given. Error occurs when marginal rays miss the surface producing erroneous values for the aberrations.

9.4.2 DISCUSSION

i) Anterior corneal surface

The range of SAF values for the extreme shapes of the anterior cornea easily encompass the range found in human eyes. It has been revealed by previous results (chapter six), that increasing the central radius decreases spherical aberration. However, for an asphericity value of 0.1, increasing the central radius increases the SAF, or rather makes it less negative. Confirmation of this trend is given by the SAF for ACR = 7.8 and ACA = 0.1. This has a value of -2.4. Clearly the effect of central radius variations on spherical aberration depend on the surface asphericity value.

The range of PAF values for extreme anterior corneal surface shape encompasses the maximum and mean empirical values but not the minimum. The general trend of variations was discovered to be the same as found in chapter seven in all cases.

The CAF ranges from -28.6 to as high as 287.0. The results also show a contradiction to a general trend found in chapter eight. For an asphericity value of 1.5 increasing the radius from 7.0 mm to 8.9 mm increases the CAF, making it less negative. For other asphericity values the CAF decreases as the radius is increased. The CAF for ACA = 1.5 and ACR = 7.8 mm was found to be -14.2. Comparing this with the values given by ACRs of 7.0 and 8.9 suggests that, for an asphericity of 1.5, increasing the central radius of the the anterior corneal surface initially increases and then decreases coma.

ii) Anterior lenticular surface

Again, the full range of empirical SAF values are encompassed by the extreme surface shapes. In all cases increasing the central radius and asphericity values increases the spherical aberration, as found in chapter six.

The ranges of PAF and CAF values are small. The PAF is neither increased to the maximum value nor decreased to the mean value.

For an anterior lens radius of 7.7 mm and an asphericity of 13.35 the computer program gave error messages for some of the ray traces due to internal reflection. This is not surprising, as the small central radius and high asphericity will result in a surface which is very steep in the periphery. Such a surface would clearly be impractical in real eyes.

Therefore, where such high levels of peripheral steepening do occur it would most likely be compensated for by a relatively large central radius.

The central refractive error for a radius of 7.7 mm and an asphericity of 13.35 (-17.5 D) is too great to be compensated for by altering the axial length within the human range for emmetropic eyes (see section 9.2). To make the eye emmetropic would require the retina to be moved 7 mm inwards resulting in an axial length of 17 mm. This is beyond the range of axial lengths found in any human eye (see section 4.8).

iii) Posterior lenticular surface

The extreme surface shapes are capable of reducing the SAF to the minimum empirical value and almost increasing it to the mean value. The range of PAF values includes the maximum and mean empirical values and the CAF ranges from 26.3 to 191.9. All variations for these aberrations follow the general trends previously established in chapters six, seven and eight.

As for the anterior lenticular surface, a combination of minimum central radius with maximum asphericity results in rays missing the surface.

9.5 MODELLING SAF AND PAF VALUES FOUND IN REAL EYES BY VARIATION OF COMBINATIONS OF OCULAR PARAMETERS.

In section 5.4 previous attempts to model spherical aberration and peripheral astigmatism levels found in real eyes were reviewed. No one has yet managed to model the empirical mean peripheral astigmatism and spherical aberration values simultaneously. Dunne and Barnes (1987) attempted to model the low levels of peripheral astigmatism found in some eyes as well as the mean values. They increasingly flattened the anterior lenticular surface until the peripheral astigmatism for a 40° field angle reached the required value. The resulting anterior lenticular surfaces were flattened far beyond levels found in real eyes and the corresponding spherical aberration became vastly over-corrected. Their failure to model both aberrations simultaneously led Dunne and Barnes to conclude that this could only be achieved if a gradient index structure for the crystalline lens was included in the model. However, it is possible that by varying a number of ocular parameters simultaneously the levels of aberrations found in human eyes may be modelled successfully without inclusion of gradient index.

A brief summary of the information gathered in chapters six, seven and eight is provided by table 9.4. The table shows the effects of increasing each of the eleven parameters on the three aberrations.

increasing parameter	spherical aberration	peripheral astigmatism	coma
ACR.	decrease	increase	decrease
ACA.	increase	increase	decrease
CT.	-	-	-
PCR.	increase	decrease	increase
PCA.	decrease	decrease	increase
AGD.	decrease	decrease	decrease
ALR.	increase	decrease	decrease
ALA.	increase	increase	increase
LT.	decrease	decrease	increase
PLR.	decrease	increase	increase
PLA.	increase	increase	increase

Table 9.4 Showing the effect of increasing each of the eleven parameters within the schematic eye on the levels of each of the three aberrations.

The degree by which variation of each parameter altered spherical aberration and peripheral astigmatism was established in chapters six and seven respectively. The empirical ranges for these two aberrations were established in chapters two and three and are given in table 9.1. Both aberrations will be considered to have three levels, low, mean and high. The intention is to design schematic eyes to represent the nine categories which occur if the three levels of the two aberrations are combined in all possible ways.

A number of useful points were gleaned from the information given in chapters six and seven. In order to increase one of the aberrations while simultaneously decreasing the other the central radii of the optical surfaces should be manipulated. Variation in surface asphericity will increase or decrease both aberrations at the same time. It is also useful to note that variations in the anterior chamber depth produces large changes in peripheral astigmatism but have little affect on spherical aberration. In addition, decreasing the anterior and posterior lenticular asphericities reduces peripheral astigmatism by very little but has a slightly greater affect on spherical aberration.

Kooijman's schematic eye (Kooijman, 1983), used as the mean eye in this study, has quite high peripheral astigmatism but low spherical aberration. It is, therefore, easier to model high levels of peripheral astigmatism than low levels, and easier to model low levels of spherical aberration than high levels with just single parameter changes. For spherical aberration, all levels can be modelled by single parameter variations. For peripheral astigmatism, however, the range of values for most parameters will only produce high peripheral astigmatism. The mean level can be reached by increasing the anterior chamber depth but no single parameter changes will reduce the peripheral astigmatism to the minimum level found in real eyes. In order to achieve this level a combination of parameter variations must be used.

Each of the nine categories were considered separately. In some cases single parameter variations or combined apical radius and asphericity variations give SAF and PAF values which fall into one of the nine categories. For the remaining categories a combination of parameters were varied to give the required SAF and PAF values. A ray trace was carried out for each model, the SAF, PAF and CAF were calculated and the central refractive error for a 4 mm pupil was noted. Plots of spherical aberration versus pupil size and peripheral astigmatism versus field angle were then compared to the plots for the maximum, mean or minimum empirical values. Further adjustment was made to parameter values if this was necessary to achieve an adequate match.

9.5.1 RESULTS

Table 9.5 shows nine schematic eyes which fulfil the requirements of the nine categories detailed above. These models were arrived at by manipulating the ocular parameters through a number of stages, until the required SAF and PAF values were obtained. Only one example is shown for each category but a great many different schematic eyes may give similar SAF and PAF values. For example, another model producing mean SAF and mean PAF values is given by:-

ACA = 0.5
ACD = 4.1 mm
ALA = 4

This gives SAF = 2.9, PAF = 62.8, CAF = 160.3, Rx = -1.4 D.
Although this model provides SAF and PAF values very close to those given by the model detailed in the table, the CAF value is much larger. This demonstrates that even if the levels of peripheral astigmatism and spherical aberration in an individual eye are exactly modelled

in a schematic eye the image quality of the two systems may still be very different as a result of the difference in other aberrations.

SPHERICAL ABERRATION \ PERIPHERAL ASTIGMATISM	LOW	MEAN	HIGH
LOW	ACD = 4.6 mm PLR = 5.3 mm ACA = 0.55 SAF = 0.7 PAF = 19.1 CAF = 128.7 Rx = -2.1 D	ACD = 3.8 mm ACA = 0.6 PLR = -5.5 mm SAF = 1.0 PAF = 73.3 CAF = 131.5 Rx = -1.1 D	Kooijman's schematic eye SAF = 1.6 PAF = 100 CAF = 118.9 Rx = -0.5 D
MEAN	ACD = 4.6 mm PLR = -4.6 mm SAF = 2.5 PAF = 20.1 CAF = 78.8 Rx = -3.7 D	ACR = 7.7 mm ACA = 0.85 PCA = 0.85 ACD = 4.0 mm ALR = 11 mm PLR = -5.4 mm SAF = 2.9 PAF = 64.8 CAF = 91.2 Rx = -1.1 D	ACA = 0.951 SAF = 2.9 PAF = 111.8 CAF = 86.2 Rx = -0.9 D
HIGH	ACD = 4.6 mm PLR = -4.6 mm ALA = 6 SAF = 5.9 PAF = 27.0 CAF = 93.7 Rx = -4.8 D	PLR = -4.6 mm ALR = 13.8 mm ALA = 2 SAF = 4.6 PAF = 68.0 CAF = 97.4 Rx = -2.0 D	Spherical surfaces SAF = 6.0 PAF = 127.7 CAF = 117.7 Rx = -1.8 D

Table 9.5 Detailing nine schematic eyes which produce aberration levels covering the whole range found in human eyes. Only the parameter values which differ from the values in the Kooijman eye are given. The table also shows the SAF, PAF, CAF and Rx values for each model.

Even though the SAF and PAF values are close to the human minimum, maximum or mean, it does not follow that the individual spherical aberration and peripheral astigmatism values will also be close. The plots of spherical aberration versus pupil diameter and peripheral astigmatism versus field angle for the schematic eyes were compared to those for real eyes. Examples are shown below.

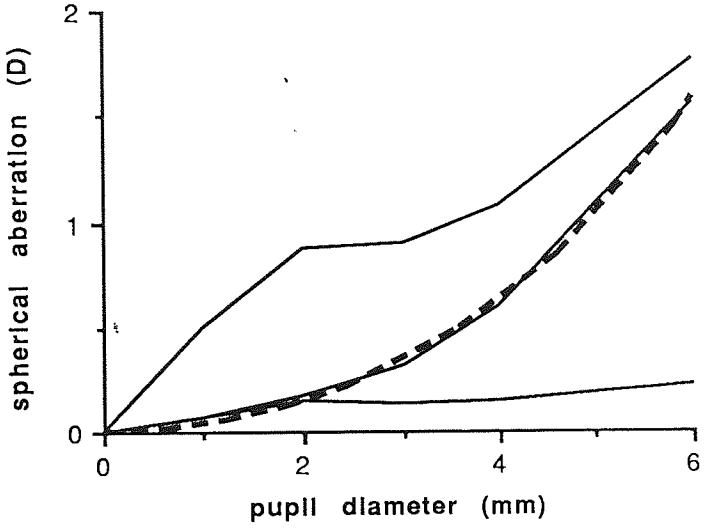

Fig. 9.21 Plot of spherical aberration against pupil diameter for the range of human values (solid line) and a schematic eye giving mean SAF and PAF values.

Fig. 9.21 shows the spherical aberration plot for the schematic eye which gives mean SAF and PAF values. The parameter values for this schematic eye are detailed in table 9.5. It is clear that the plot closely follows the spherical aberration plot considered to represent mean human values.

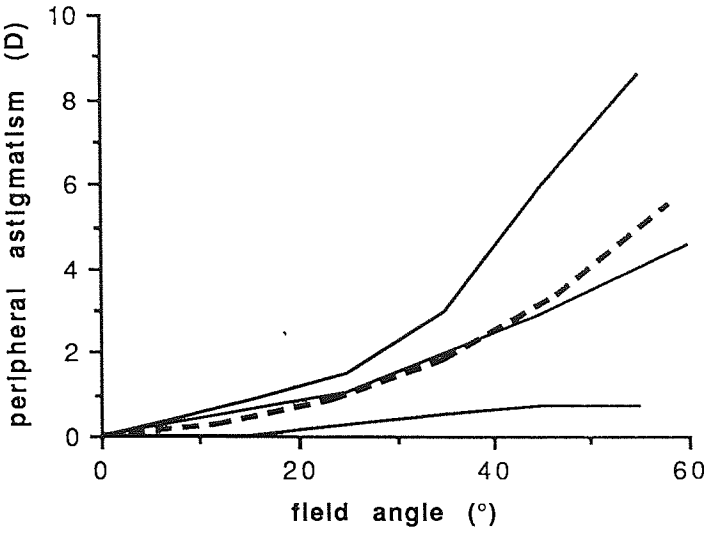

Fig. 9.22 Plot of peripheral astigmatism against field angle for the human range (solid line) and a schematic eye giving mean SAF and PAF values (dashed line).

Fig 9.22 shows the peripheral astigmatism plot for the eye giving mean SAF and PAF values. The plot is very close to human mean values up to a field angle of 40°. For higher field angles the peripheral astigmatism is higher than human mean values, becoming approximately 1 D higher at 60°. As the PAF is calculated for field angles of up to 40° it is clear why the two plots gave similar PAF values. However, if the PAF was, instead, calculated for 0° to 60° the schematic eye would give a much higher PAF than the human mean value. It was felt that it may be more appropriate to compare PAFs calculated for up to 60° field angles. However, it was found that, while reducing the peripheral astigmatism in the far periphery to values closer to the human mean, the peripheral astigmatism at lower field angles fell below the human mean. The conclusion reached was that schematic eyes with second-order surfaces can only model mean peripheral astigmatism successfully up to 40°. Therefore, it is appropriate to calculated the PAF only up to 40° field angles. It may be possible to model peripheral astigmatism for field angles greater than 40° using higher-order polynomials. All schematic eyes with a PAF value close to the mean human PAF were found to have correspondingly close individual peripheral astigmatism values for field angles of up to 40°. Above this field angle the values were always found to be higher than the mean.

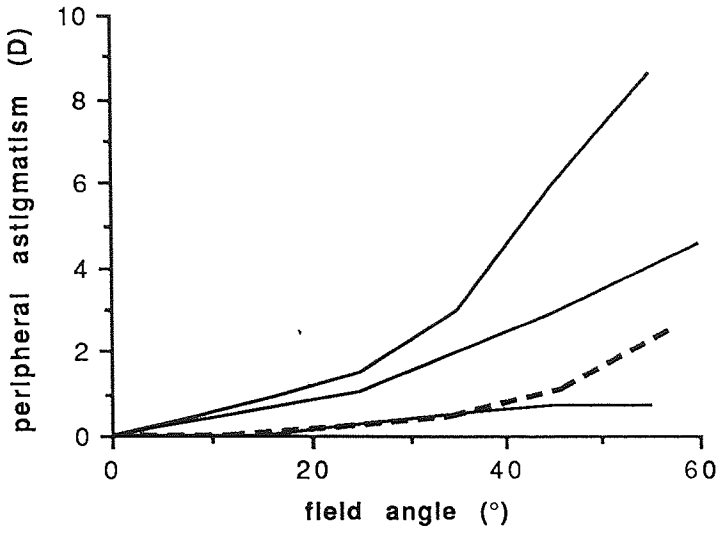

Fig. 9.23 Plot of peripheral astigmatism against field angle for the human range (solid line) and a schematic eye giving the minimum PAF value.

Fig 9.23 shows the plot of peripheral astigmatism versus field angle for the schematic eye, giving the mean SAF and Minimum PAF values. The parameter values for this model are shown in table 9.5. As for the schematic eye giving the mean PAF value, the peripheral astigmatism values are close to human values for field angles of up to 40°. This again led to the conclusion that, to model peripheral astigmatism for higher field angles, higher-order polynomial optical surfaces are needed.

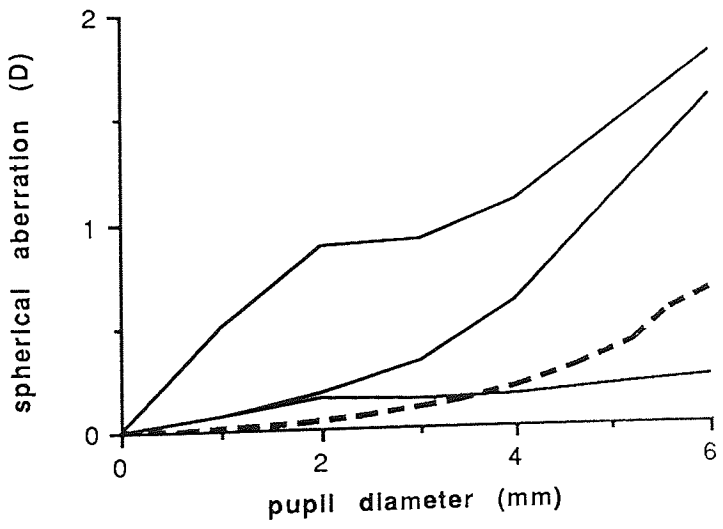

Fig. 9.24 Plot of spherical aberration against pupil diameter for the human range (solid lines) and for a schematic eye giving the minimum SAF.

The final example is shown in fig 9.24. This shows the spherical aberration plot for the schematic eye giving the minimum SAF values and mean PAF value, as detailed in table 9.5. For small pupils the spherical aberration of the schematic eye falls below human value. For large pupils it falls above human values. This again illustrates the need for higher-order polynomial optical surfaces.

9.5.2 DISCUSSION

This investigation illustrates that it is possible to model all levels of peripheral astigmatism and spherical aberration found in human eyes using schematic eyes with second-order polynomial surfaces and no gradient index. Contrary to the belief of Dunne and Barnes (1987) it was shown to be possible to model mean and low levels of ocular peripheral astigmatism in schematic eyes with realistic ocular surface parameters and spherical aberration levels.

Comparison of the spherical aberration and peripheral astigmatism plots of the schematic eyes with the plots given by real eyes revealed some discrepancies. It was considered that closer fits to the human data could be achieved by the the inclusion of one or more higher-order polynomial surfaces.

It was also revealed that different schematic eyes giving the same SAF and PAF values can have very different CAF values. In order, therefore, to give a true representative of image quality in an human eye all the aberrations must be considered.

9.6 SUMMARY

In section 9.2 the three aberrations discussed in chapters six, seven and eight were examined in combination. The ranges of spherical aberration and peripheral astigmatism values obtained by altering each parameter across its full range were compared to the empirical ranges established in chapters 2 and 3. The main points of interest were:

i) The mean schematic eye used in this study (Kooijman, 1983) has spherical aberration levels lower than the mean values for human eyes proposed by Van Meeteren (1974). The peripheral astigmatism is much higher than the mean values found by Lotmar and Lotmar (1974), from the data of Rempt et al. (1971).

ii) The full range of empirical spherical aberration values could be modelled using single parameter variations.

iii) Only anterior chamber depth variations were capable of reducing the peripheral astigmatism to the mean empirical level. No single parameter variation could reduce peripheral astigmatism to the minimum empirical level.

iv) The relatively large decrease in peripheral astigmatism with increasing anterior chamber depth was related to the findings of Millodot (1984). He discovered that on average peripheral astigmatism was less in aphakic than in phakic eyes. Dunne et al.(1991) attributed the large reduction in peripheral astigmatism to the posterior displacement of the pupil which accompanies removal of the cataractous crystalline lens. The findings of this study concur with those of Dunne et al. (1991). They considered that, although some reduction may be due to removal of the lens, particularly in older eyes, the major contribution is due to the increase in anterior chamber depth.

v) Variation in spherical aberration and peripheral astigmatism due to lenticular parameter changes were compared to the variations which occur with accommodation and aging. The Variation in the two aberrations during accommodation was easily explained by the predicted changes caused by the altered lenticular parameters. There is some dispute as to how the shape of the lens varies with age. Considering the large increase in spherical aberration with age, this is more easily explained by the belief that central lenticular radii increase with age. No clear conclusion could be drawn from peripheral astigmatism changes. No evidence exists as to gradient index changes in the crystalline lens with accommodation or age. Knowledge of these changes, and how they effect the aberrations, would give an even clearer idea of what occurs.

In section 9.3 The SAF and PAF polynomials, derived in chapters 6 and 7 respectively, were used to calculated the parameter values giving maximum, mean and minimum empirical SAF and PAF values.

Section 9.4 looked at the effects of combined extreme apical radius and asphericity values. The main points of interest were:

i) Lens surfaces with the smallest radii and highest asphericity values were found to be impractical as marginal rays missed these surfaces.

ii) In some cases the general directional trend of aberration variations with parameter changes were different to those established in chapters 6,7 and 8. For example, with an anterior corneal asphericity of 1.5 the CAF was found to initially increase and then decrease

with increasing apical radius. Decreasing CAF was revealed to occur for increasing apical radii with the two other asphericity values.

iii) Mean PAF values can be achieved by small anterior corneal radii and asphericity values and by small posterior lenticular radii and asphericity values.

iv) Anterior lenticular changes were found to have relatively little effect on peripheral astigmatism and coma. This is as expected due to the surface being coincident with the pupil.

Finally, in section 9.5 the information accumulated from chapters 6 and 7 was used to model all levels of peripheral astigmatism and spherical aberration found in human eyes. The aim was to demonstrate the flexibility of schematic eyes with second-order polynomials and no gradient index. This was illustrated by designing schematic eyes which combined spherical aberration and peripheral astigmatism levels covering the whole range found in human eyes. Combining three levels, Maximum, minimum and mean, of the two aberrations in all possible ways led to nine categories of schematic eye. Schematic eyes were designed to fill these categories. The findings were:

i) It was possible to design schematic eyes to represent all nine categories by manipulating a combination of parameters within the measured human ranges. The three categories where high peripheral astigmatism is combined with low, mean and high spherical aberration were represented by schematic eyes with only single parameter variations.

ii) When the modelled SAF was equal to the mean empirical SAF the plot of spherical aberration versus pupil diameter was almost indistinguishable from the plot for mean empirical values. When the modelled PAF was equal to the mean empirical value the plot of peripheral astigmatism against field angle was extremely close to the mean empirical plot for field angles up to 40°. Above 40° the modelled values were higher. This led to the conclusion that conic (second-order) optical surfaces were sufficient to model mean peripheral astigmatism only up to 40° field angles. To model the peripheral astigmatism further into the periphery, higher-order polynomial surfaces must be employed or a gradient index lens structure must be introduced.

iii) The plots of spherical aberration versus pupil diameter given by schematic eyes with maximum and minimum SAFs do not resemble the actual empirical plots. The modelled values are generally smaller for small pupils and larger for large pupils. The plots of peripheral astigmatism versus field angle for schematic eyes giving the minimum PAF are

only close to the minimum human values for field angles of up to 40°. Clearly neither individual spherical aberration or peripheral astigmatism can be closely modelled by second-order polynomial optical surfaces in all cases. They could, however, probably be modelled by higher-order polynomials or introduction of gradient index.

iv) For some schematic eyes with the same or similar SAF and PAF values the CAFs were seen to vary over a wide range. This demonstrates the possible flexibility of these schematic eyes in modelling all three aberrations. It also indicates that, when attempting to model spherical aberration and peripheral astigmatism simultaneously by manipulating parameters, no solution will be unique and cannot be guaranteed to give the correct level of coma. Therefore, in order to produce realistic models of human eyes as many ocular parameters and aberrations as possible must be measured and reproduced in the schematic eye.

CHAPTER 10

SUMMARY

10.1 REVIEW OF PREVIOUS CHAPTERS
10.2 SUGGESTIONS FOR FUTURE STUDY

10.1 REVIEW OF PREVIOUS CHAPTERS

The principal aim of this study was to investigate the flexibility of schematic eyes with second-order aspheric surfaces but no gradient index crystalline lens structure. Specifically the intent was to determine whether such schematic eyes could successfully model monochromatic aberration levels found in human eyes.

Chapter one introduced the concepts of image quality and optical aberrations. Particular attention was paid to the three main aberrations considered in this study; namely spherical aberration, peripheral astigmatism and coma.

Ocular spherical aberration and peripheral astigmatism were of particular interest as they have been extensively measured in previous investigations. This work was reviewed in chapters two and three, and a mean and range of values was established for each aberration. Spherical aberration and peripheral astigmatism functions (SAFs and PAFs) were introduced. These were single values intended to allow easy comparison of the levels of the two aberrations in different optical systems.

Chapter four provided a brief description of the structure of the human eye. The methods used to measure each of the optical parameters were assessed. The literature concerning ocular parameter measurement was reviewed in order to establish the range of values found in human eyes.

Chapter five gave a resume of previous work on schematic eyes. It was noted that no schematic eye had been successful in modelling human levels of peripheral astigmatism and spherical aberration simultaneously. Further, an attempt to model mean peripheral astigmatism and the low levels found in some eyes resulted in unrealistic ocular surfaces. This failure to model human aberrations led some investigators to conclude that this cannot be achieved without inclusion of the gradient index structure of the crystalline lens.

Chapters six, seven and eight investigated the effects of single parameter variations on spherical aberration, peripheral astigmatism and coma respectively. The range of variation for each parameter was limited to by ocular values established in chapter four. The main points of interest were:

i) All levels of spherical aberration found in human eyes could be modelled by a number of single parameter variations.

ii) No single parameter variation reduced peripheral astigmatism to the minimum ocular levels. Only an increase in the anterior chamber depth could reduce it to below the mean ocular level. The maximum ocular level could be modelled by some single parameter variations.

iii) Anterior chamber depth variations produced the greatest effect on peripheral astigmatism but had very little effect on spherical aberration. This was related to the reduction in peripheral astigmatism, observed following removal of cataractous crystalline lenses. The effect was considered to be due, largely, to posterior movement of the pupil which increases the anterior chamber depth.

iv) The majority of parameter variations had little effect on coma. The only parameter variation capable of fully correcting coma was anterior corneal asphericity. Peripherally steepening this surface to its maximum gave slightly over-corrected coma. At the same time spherical aberration and peripheral astigmatism are increased.

In chapter nine the information gathered in chapters 6, 7 and 8 was used to model ocular spherical aberration and peripheral astigmatism. It was found that schematic eyes with second-order optical surfaces and homogenous optical media were flexible enough to model the full range of empirical SAF and PAF values. It was not always possible, however, to match the spherical aberration against pupil diameter and peripheral astigmatism against field angle plots to those given by real eyes. Consequently it was concluded that to model accurately the aberrations of individual eyes polynomial surfaces of a higher-order than two would be required.

The results of chapter nine also revealed that the schematic eyes designed to model specific levels of spherical aberration and peripheral astigmatism were not unique solutions. A number of different optical systems produced the same levels of these two aberrations. Additionally, it was demonstrated that schematic eyes having the same amounts of peripheral astigmatism and spherical aberration could have differing amounts of coma.

10.2 SUGGESTIONS FOR FURTHER STUDY

An obvious development of this work would be the inclusion of higher-order polynomial surfaces in schematic eyes. The ability of these surfaces to model ocular aberrations could then be investigated.

The effects of gradient index variations have not been investigated in this study. The available empirical data relating to this parameter is scarce and unreliable. With improved methods of measurement more data may soon become available. It would then be interesting to investigate the effect of variations of gradient index on aberrations. Specifically, to determine if gradient index generally decreases aberrations as believed by some investigators (Lotmar, 1971; Dunne and Barnes, 1987) or if its effect is random as suggested by Dunne et al. (1993a).

Dunne et al. (1993a) measured peripheral astigmatism in 34 eyes. In the same eyes they also measured all optical parameters except lens surface asphericity and gradient index. Schematic eyes were constructed from these measured parameter values. The difference between modelled and measured peripheral astigmatism was assumed to be due to the neglected parameters. It may be possible to extend this study to include measured values of lens surface asphericities in the schematic eyes. Any difference between modelled and measured peripheral astigmatism could then be attributed to gradient index. This difference may possibly be eliminated by manipulation of one or more of the polynomial optical surfaces. Greater accuracy in modelling would be achieved if spherical aberration was also measured and then modelled.

This study could be further developed to include the effects of accommodation. Comparison of modelled and measured aberration values for different states of accommodation has the potential to reveal how the gradient index varies.

The principal problem anticipated in such extensive studies is the demands it would place on the subjects. Measuring both aberrations and all the biometric data would prove very time consuming and require a large number of visits. If measurements were also to be made for a number of states of accommodation participants with a high degree of commitment would be needed.

For a large number of subjects it may be feasible to establish a relationship between peripheral astigmatism and anterior chamber depth. This would reveal if eyes with low levels of peripheral astigmatism generally have large anterior chamber depths.

To achieve unique solutions to the problem of modelling image quality in human eyes it is necessary to consider other aberrations in addition to spherical aberration and peripheral astigmatism. The wavefront aberration found in human eyes has led some researchers to suggest that coma and not spherical aberration is the major aberration on-axis (see section 1.3.3). As there has been no direct measurement of coma, axial coma was neglected in this study. However it is possible that comparison of modelled and measured wavefront aberration may provide some insight into the asymmetries of the human optical system.

REFERENCES

Alsbirk, P.H. (1974). Optical pachymetry of the anterior chamber. A methodological study of errors of measurement using Haag Streit 900 instruments. Acta Ophthalmologica, 52, 747-758.

Ames, J.R. and Proctor, C.A. (1921). Dioptrics of the eye. Journal of the Optical Society of America, 5, 22-84.

Arnulf, A. and Dupuy, O. (1960). La transmission des contraste par la systeme optique de l'oeil et les seuils de contrastes retiniens. C.R. Hebd. Seanc. Acad. Sci., Paris, 250, 2757-2759.

Azen, S.P., Burg, K.A., Smith, R.E. and Maguen, E. (1979). A comparison of three methods for the measurement of corneal thickness. Investigative Ophthalmology and Vision Science, 18, 535-538.

Barnes, D.A., Dunne, M.C.M. and Clement, R.A. (1987). A schematic eye model for the effects of translation and rotation of ocular components on peripheral astigmatism. Ophthalmic and Physiological Optics, 7, 153-158.

Beam Four - Optical Ray Tracer Manual. Stellar Software, P.O. box 10183, Berkeley, CA 94709, USA.

Bennett, A.G. and Rabbetts, R.B. (1984). Clinical Visual Optics. Butterworths:London.

Blaker, J.W. (1980). Toward an adaptive model of the human eye. Journal of the Optical Society of America, 70, 220-223.

Blix, M (1880) Ofthalmometriska studier. Acta. Soc. Med. Upsal., 15, 349-421. Cited by Von Bahr (1948)

Bonnet, R. and Cochet, P. (1964). La Topographie Corneanne. Descroches, Paris. (cited by Lotmar, 1971)

Bonnet, R. and Cochet, P. (1962). New method of topographic ophthalmometry - its theoretical and clinical applications. American Journal of Optometry, 39, 227-251.

Bonnet, R. and Cochet, P. (1960). Bull. Soc. Franç. Ophthalmol., 73, 688 (cited by Lotmar, 1971)

Borish, I.M. (1970) Clinical Refraction, 3rd edition. The Professional Press Inc.: Chicago.

Bour, L.J. (1980). MTF of the defocussed optical system of the human eye for incoherent monochromatic light. Journal of the Optical Society of America, 70, 321-328.

Brown, N. (1974). The change in lens curvature with age. Experimental Eye Research, 19, 175 - 183.

Brown, N. (1973). The change in shape and internal form of the eye on accommodation. Experimental eye research, 15, 441-459.

Calmettes, Deodati, Huron and Bechac (1966). Study of the depth of the anterior chamber - physiological variations with particular emphasis on ametropia. Translated by D.A. Pitts and M.Millodot. American Journal of Optometry and Archives of American Academy of Optometry, 43, 765-794.

Campbell, F.W. and Green D.G. (1965). Optical and retinal factor affecting visual resolution. Journal of Physiology (London), 152, 67-74.

Campbell, F.W. and Gubisch R.W. (1966). Optical image quality of the human eye. Journal of Physiology (London), 186, 558-578.

Campbell, M.C.W. (1984). Measurement of refractive index in an intact crystalline lens. Vision Research, 24, 409-415.

Charman, W.N. (1991a). Optics of the human eye. In Vision and Visual Dysfunction. General Editor: Cronly-Dillon, J.R. vol. 1. Visual Optics and Instrumentation. pp.1-26. London: Macmillan

Charman, W.N. (1991b). Non-optical techniques for visualising the eye. In Vision and Visual Disfunction. General Editor: J.R. Cronly-Dillon. vol. 1. Visual Optics and Instrumentation. pp.359-370. London: Macmillan

Charman, W.N.(1991c). Limits on visual performance set by the eyes optics and the retinal cone mosaic. In vision and visual disfunction. General Editor: J.R. Cronly-Dillon. vol. 7. Limits of vision, pp81-96. London: Macmillan.

Charman, W.N. (1983).The retinal image in the human eye. In Progress in Retinal Research. eds. Osborne, N. and Chader, G. Vol.2. pp. 1-50. Oxford: Pergamon.

Charman, W.N. (1972). Diffraction and the precision of measurement of cornea and other small radii. American Journal of Optometry and Physiological Optics, 49, 672 - 680.

Charman, W.N. and Jennings, J.A.M. (1982). Ametropia and peripheral refraction. American Journal of Optometry and Physiological Optics. 59, 922-923.

Charman, W.N. and Jennings, J.A.M. and Whitefoot, H (1978). The refraction of the eye in relation to spherical aberration and pupil size. British Journal of Physiological Optics, 32, 78-93.

Clark, B.A.J. (1974). Mean Topography of Normal Corneas. Australian Journal of Optometry, 57, 107-114.

Clark, B.A.J. (1973). Time Variations in observed corneal topography. Australian Journal of Optometry, 56, 443-447.

Clement, R.A., Dunne, M.C.M. and Barnes D.A. (1987). A method for raytracing through schematic eyes with off-axis components. Ophthalmic and physiological optics,7. 149-152.

Dingeldein, S.A. And Klyce, S.D. (1989). The topography of normal corneas. Archives of ophthalmology, 107, 512-518.

Donaldson, D.D. (1966). Measurement of the corneal thickness. Archives of Ophthalmology, 76, 25-31.

Drasdo, N. and Fowler, C.W. (1974) Non-linear projecton of the retinal image in a wide angle schematic eye. British Journal of Ophthalmology, 58, 709-714.

Dunne, M.C.M. (1992). Scheme for the calculation of ocular components in a four-surfaced eye without need for measurement of the anterior crystalline lens surface Purkinje images. Ophthalmic and Physiological Optics, 12, 370 - 375.

Dunne, M.C.M. (1987). An optical Study of Human Ocular Dimensions. Unpublished thesis. Aston University.

Dunne, M.C.M. and Barnes, D.A. (1993). A comparison of the errors arising from three methods of phakometric computation. Ophthalmic and Visual optics - Noninvasive Assessment of the Visual System. Technical Digest Series Vol.3, 62-65

Dunne, M.C.M. and Barnes, D.A. (1990). Modelling oblique astigmatism in eyes with known peripheral refraction and optical dimensions. Ophthalmic and Physiological Optics, 10, 46-48.

Dunne, M.C.M. and Barnes, D.A. (1989). Modelling angle alpha. Ophthalmic and Physiological Optics, 9, 338-339.

Dunne, M.C.M. and Barnes, D.A. (1987). Schematic modelling of peripheral astigmatism in real eyes. Ophthalmic and Physiological Optics, 7, 235-239.

Dunne, M.C.M., Barnes, D.A. and Clement, R.A. (1987). A model for retinal shape changes in ametropia. Ophthalmic and Physiological optics, 7, 159-160.

Dunne, M.C.M., Misson, G.P. and Barnes, D.A. (1991). The effect of iris displacement on oblique astigmatism in aphakic eyes. Optometry and vision science, 68, 957-959.

Dunne, M.C.M., Misson, G.P., White, E.K.and Barnes, D.A. (1993a). Ocular component variations and peripheral astigmatism. Investigative Ophthalmology and Visual Science, 34/4, p775. (supplement - ARVO 1993).

Dunne, M.C.M., Misson, G.P., White, E.K.and Barnes, D.A. (1993b). Peripheral astigmatic asymmetry and angle alpha. Opthalmic and physiological optics, 13, 303-305.

Dunne, M.C.M., Royston, J.M. and Barnes, D.A. (1992). Normal Variations of the posterior corneal surface. Acta Ophthalmologica, 70, 255-261.

Edmund,C. and La Cour, M. (1986). Some components effecting precision of corneal thickness measurement performed by optical pachometry. Acta Ophthalmologica, 64, 499-503.

Edmund, C and Sjontoft, E. (1985). The central - peripheral radius of the normal corneal curvature. Acta Ophthalmologica, 63, 670-677.

Ehlers, N. (1965). The precorneal film. Acta Ophthalmologica (supplement), 81, 21-34.

El Hage, S.G. and Berny, F (1973). Contribution of the crystalline lens to the spherical aberration of the eye. Journal of the Optical Society of America, 63, 205-211.

Ferree, C.E. and Rand,G. (1933). Interpretation of refractive conditions in the peripheral field of vision. Archives of Ophthalmology, New York, 9, 925-938.

Ferree, C.E., Rand, G. and Hardy, C. (1932). Refractive asymmetry in the temporal and nasal halves of the visual field. American Journal of Ophthalmology, 15, 513-522.

Ferree, C. E., Rand G. and Hardy, C. (1931). Refraction for the peripheral field of vision. Archives of Ophthalmology, Chicago, 5, 717-731.

Fincham, W.H.A. and Freeman, M.H. (1980). Optics. 9th edition. Butterworths: London.

Fitzke, F.W. (1981). Optical properties of the eye (abstract). Investigative Ophthalmology and Vision Science, 20 (supplement), 144.

Francois, J. and Goes, F. (1977). Ultrasonographic study of 100 emmetropic eyes. Ophthalmologica, Basel, 175, 321-327.

Francon,M. (1951). Aberration spherique, chromatisme et pouvoir separateur de l'oeil. Rev. Opt. Theor. Instrum., 30, 71-80. (cited by Van Meeteren, 1974).

Fujii, T., Maruyama, S. And Ikeda, M. (1972). Determination of corneal configuration by measurement of its derivative. Optica Acta, 19, 425-430.

Gernet, H and Franceschetti, A. (1967). Ultrasound biometry of the eye (review). Ultrasonics in ophthalmology, Symposium, Munster, August 1966, pp175-206, Karger, Basel / New York 1967.

Giglio, E.J., Ludlam, W.M. and Wittenberg, S. (1968). Improvement in the measurement of intraocular distances using ultrasound. The Journal of the Acoustical Society of America, 44, 1359-1364.

Gorrand, J.M. (1979). Diffusion of the human retina and quality of the optics of the eye on the fovea and the peripheral retina. Vision Research, 19, 909-912.
Guidarelli, S. (1972). Off-axis imaging in the human eye. Atti Fondation de Giorgio Ronchi, 27, 449-460.

Guillon, M., Lyndon, D.P.M. and Wilson, C. (1986). Corneal Topography: a clinical model. Ophthalmic and physiological Optics, 6, 47-56.

Gullstrand, A. (1924) Appendices to Physiological Optics Vol.1 by H Von Helmholtz, translated by J.P.C. Southall. Optical Society of America. Rochester.

Hannush, S.B., Crawford, S.L., Waring G.A., Gennmill, M.C., Lynn M.J. and Nizam, A. (1990). Reproducibility of normal corneal power measurements with a keratometer, photokeratoscope and video imaging system. Archives of Ophthalmology, 108, 539-544

Henson, D.B. (1991). Optical methods for measurement of ocular parameters. in Vision and Visual Disfunction. General editor J.R. Cronley-Dillon. vol.1. Visual Optics and Instrumentation. pp 371 - 398.

Hirji, N.K. and Larke, J.R. (1978). Thickness of the human cornea measured by topographic pachometry. American Journal of Optometry and Physiological optics, 55, 97-100.

Hosaka, A. (1988). The growth of the eye and its components. Acta Ophthalmologica, Supplement 185, 65-68.

Howcroft, M.J. and Parker, J.A. (1977). Aspheric curvatures for the human lens. Vision Research, 17,1217-1223.

Howland, H.C. and Howland, B. (1977). A subjective method for the measurement of the monochromatic aberrations of the eye. Journal of the Optical Society of America, 67, 1508-1518.

Howland, B and Howland, H.C. (1976). Subjective measurement of High-order aberrations of the eye. Science, 193, 580-582.

Ivanoff, A.(1956). About the spherical aberration of the eye. Journal of the Optical Society of America, 46, 901-903.

Ivanoff, A. (1947). On the influence of accommodation on spherical aberration of the eye. Journal of the Optical Society of America, 37, 730-731.

Jenkins, T.C.A. (1963a). Aberrations of the eye and their effects on vision; part I. British Journal of Physiological Optics, 20, 59-91.

Jenkins, T.C.A. (1963b). Aberrations of the eye and their effects on vision: Part II. British Journal of Physiological Optics, 20, 161-201.

Jennings, J.A.M. and Charman, W.N. (1981). Off-axis image quality in the human eye. Vision Research, 21, 445-455.

Jennings, J.A.M. and Charman, W.N. (1978). Optical image quality in the peripheral retina. American Journal of Optometry and Physiological Optics, 55, 582-590.

Kiely, P.M., Smith, G. and Carney, L.G. (1982). The shape of the human cornea. Optica Acta, 29, 1027-1040.

Knoll, H.A. (1961). Corneal contours in the general population as revealed by the photokeratoscope. American Journal of Optometry, 38, 389-397.

Kooijman, A.C. (1983). Light distribution on the retina of a wide-angle theoretical eye. Journal of the Optical Society of America, 73, 1544-1550.

Kooijman, A.C. and Witmer,K.(1986). Ganzfield light distribution on the retina of human and rabbit eyes: calculations and in vitro measurements. Journal of the Optical Society of America A, 3, 2116-2120.

Koomen, M.J., Scolnik, R. and Tousey, R. (1956). Spherical aberration of the eye and the choice of axis. Journal of the Optical Society of America, 46, 903-904.

Koomen, M.J., Tousey, R. and Skolnik, R. (1949). The spherical aberration of the eye. Journal of the Optical Society of America, 39, 370-376.

Kruse-Hansen, F. (1971). A clinical study of the normal human corneal thickness. Acta Ophthalmologica, 49, 82-88.

Le Grand, Y. (1967). Form and Space Vision. Bloomington, Indiana, USA.
Le Grand, Y and El Hage S.G. (1980). Physiological Optics. Springer-Verlag: Berlin.

Leighton, D.A. and Tomlinson, A.(1972). Changes in axial length and other dimensions of the eyeball with increasing age. Acta Ophthamologica, 50, 815-826.

Lotmar, W. (1971) Theoretical eye model with aspherics. Journal of the Optical Society of America, 61, 1522-1529.

Lotmar, W. and Lotmar, T. (1974). Peripheral astigmatism in the human eye: experimental data and theoretical model predictions. Journal of the Optical Society of America. 64, 510-513.

Lowe, R.F. (1969a). Corneal radius and ocular correlations. American Journal of Ophthalmology, 67, 864-868.

Lowe R.F. (1969b). Central corneal thickness. British Journal of Ophthalmology, 53, 824-826.

Lowe, R.F.(1966) New instruments for measuring anterior chamber depth and corneal thickness. American Journal of Ophthalmology, 62, 7-11.

Lowe, R.F. and Clark, B.A.J. (1973). Posterior corneal curvature: Correlations in normal eyes and in eyes involved with primary angle-closure glaucoma. British Journal of Ophthalmology, 59, 464-470.

Ludlam, W.M., Wittenberg,S and Rosenthal, J (1965). Measurement of the ocular dioptric elements utilizing photographic methods. Part 1 Errors analysis of Sorsby's photographic ophthalmophakometry. American Journal of Optometry and Archives of the American Academy of optometry, 42, 394 - 416.

Mandell, R.B. (1979). Reply to comments by Ludlam (1969) on Mandell and St Helen (1969). American Journal of Optometry and A.A.A.O., 46, 768 - 772.

Mandell, R.B. and Polse, K.A. (1969). Keratonus: spatial variation of corneal thickness as a diagnostic test. Archives of Ophthalmology, 82, 182 - 187.

Mandell, R.B. and St Helen, R. (1971). Mathematical model of the corneal contour. British Journal of Physiological optics, 26, 183-197.
Martola, E.L. and Baum, J.L. (1968). Central and peripheral corneal thickness. A clinical study. Archives of Ophthalmology, 79, 28-30.

Maurice, D.M. (1967) The structure and transparency of the cornea, Journal of Physiology (London), 136, 263-286.

Maurice, D.M. and Giardini, A.A. (1951). A simple optical apparatus for measuring the corneal thickness and the average thickness of the human cornea. British Journal of Ophthalmology, 35, 169-177.

Michaels, D.D. (1980). Visual Optics and Refraction: A Clinical Approach, 2nd edition, Chapter 16 - Ametropia, pp499-530. Mosby : St Louis.

Millodot, M. (1984). Peripheral refraction in aphakic eyes. American Journal of Optometry & Physiological Optics, 61, 586-589.

Millodot, M. (1981). Effect of Ametropia on peripheral refraction. American Journal of Optometry and Physiological Optics, 58, 691-695.

Millodot, M. and Lamont, A. (1974). Refraction of the periphery of the eye. Journal of the Optical Society of America, 64, 110-111.

Millodot, M. and Sivak, J. (1979). Contribution of the cornea and lens to the spherical aberration of the eye. Vision Research, 19, 685-687.

Millodot, M. and Thibault, C. (1985). Variation of astigmatism with accommodation and its relationship with dark focus. Ophthalmic & Physiological optics, 5, 297-301.

Munger, R., Campbell, M.C.W., Kroger, R.H.H. and Burns, C.M. (1992). Refractive index profiles of crystalline lenses with a visible region of opacity. Investigative Ophthalmology and Visual Science, Vol. 33/4, p1169. (Supplement - ARVO 1992).

Nakao,S., Mine, K.,Nishioka,K. and Kamiya,S. (1969). The distribution of refractive indices in the human crystalline lens. Japanese Journal of Clinical Ophthalmology, 23, 41-44.

Navarro, R., Artal, P. and Williams, D.R. (1993). Modulation transfer of the human eye as a function of retinal eccentricity. Journal of the Optical Society of America, 10, 201-212.

Navarro, R. Santamaria, J. and Bescos, J. (1985). Accommodation dependent model of the human eye with aspherics. Journal of the Optical Society of America A, 2, 1273-1281.

Ogle, K.N. (1950). Binocular Vision. Saunders: Philadelphia. (cited by Charman, 1991a).

Olsen, T. and Ehlers, N. (1984). The thickness of the human cornea as determined by a specular method. Acta Ophthalmologica, 62, 859-871.

Otero, J.M. and Duran, A. (1942). Anales de Fisica y Quimica. (cited by Koomen et al. 1949)

Pierscionek, B.K. and Chan, D.Y.C. (1989). Refractive index gradient of human lenses. Optometry and Vision Science, 66, 822 - 829.

Pomerantzeff, O. Fish, H. Govignon, J. and Schepens, C.L. (1971). Wide angle optical model of the human eye. Annals of Ophthalmology, August 1971, 815-819.

Pomerantzeff, O., Pankratov, M., Wang, G. and Dufault, P. (1984). Wide-angle optical model of the eye. American Journal of Optometry and Physiological Optics, 61, 166-176.

Pretchtel, L.A. And Wesley, N.K. (1970). Corneal topography and its application to contact lenses. British Journal of Physiological Optics, 25, 117-126.

Raasch, T. and Lakshminarayanan, V. (1989). Optical matrices of lenticular polyindicial schematic eyes. Ophthalmic and Physiological optics, 9, 61-65.

Raeder, J.C. (1922). Unter suchungen uber die lage und dicke der linse im menschlichen auge bei physiologischen und pathologischen zustander, nach einer neuen methode gemessen. 1. Die lage und dicke der linse bei emmetropen, hypermetropen und myopen. Albrecht V. Graefe Arch. Klin. Exp. Opthal., 110, 73-108.

Rempt, F., Hoogerheide, J. and Hoogenboom, W.P.H. (1971). Peripheral retinoscopy and the skiagram. Ophthalmologica, 162, 1-10.

Rosenblum, W.M. and Christensen, J.L. (1976). Objective and subjective aberration measurement of the human eye. In Progress in Optics Vol. 13. pp. 69-91. Ed: Wolf, E. Amsterdam.

Royston, J.M. (1990). The influence of posterior corneal surface astigmatism on residual astigmatism. Unpublished thesis. Aston University.

Santamaria, J., Artal, P. and Bescos, J. (1987). Determination of the point-spread function of human eyes using a hybrid optical-digital method. Journal of the Optical Society of America A, 4, 1109-1114.

Scammon, R.E. and Wilmer, H.A. (1950). Growth of the components of the human eyeball. Archives of Ophthalmology, 43, 620-637.

Schober, H., Munker, H. and Zolleis, F. (1968). Die aberration des menschlichen auges und ihre messung. Optica Acta, 15, 47-57. (cited by Van Meeteren, 1974).

Sivak, J.R. and Kreuzer, R.O. (1983). Spherical aberration of the crystalline lens. Vision Research, 23, 59 - 70.

Smirnov, M.S. (1962). Measurement of the wave aberration of the human eye. Biophysics, 6, 766-795.

Smith, G., Pierscionek, B.K. and Atchison, D.A. (1991). The optical modelling of the human lens. Ophthalmic and Physiological Optics, 11, 359-396.

Smith, W.J. (1990). Modern Optical Engineering - The Design of Optical Systems. 2nd edition. McGraw-Hill Inc: New York.

Sorsby, A. Benjamin, B. Davey, J.B., Sheridan, M. and Tanner, J.M. (1957). Emmetropia and its aberrations. A study in the correlation of the optical components of the eye. Medical Research Council, special report series No. 293. HMSO: London.

Sorsby, A. Benjamin, B and Sheriden, M. (1961). Refraction and its components during the growth of the eye from the age of three. Medical Research Council Spec. Report. Service no. 301. H.M. Stationary Office:London.

Sorsby, A., Leary, G.A. and Richards, M.J. (1962). Correlation ametropia and component ametropia. Vision Research, 2, 309-313.

Sorsby, A., Leary, G.A. Richards, M.J. and Cheston J. (1963). Ultrasonic measurements of the components of ocular refraction in life. 2. Clinical procedures: Ultrasonic measurements compared with phakometric measurements in a series of 140 eyes. Vision Research, 3, 499-505

Spencer, G.H. and Murty, M.V.R.K (1962). General ray-tracing procedure. Journal of the Optical Society of America, 52, 672-678.

Stenstrom, S. (1948a). Investigation of the variation and the correlation of the optical elements of human eyes. Translated by D. Woolf. Part III. American Journal of Optometry, 25, 340-350.

Stenstrom, S. (1946). Investigation of the variation and the correlation of the optical elements of human eyes. American Journal of Optometry, 25, 218-232.

Stimson, R. L. (1957). Lenses for aphakics. British Journal of Physiological Optics, 14, 78-89.

Tomlinson, A. (1972) A clinical study of the central and peripheral thickness and curvature of the human cornea. Acta Ophthalmologica, 49, 73-82.

Tomlinson, A. Hemenger, R.P. and Garriott, R. (1993). Method for estimating the spherical aberration of the human crystalline lens in vivo. Investigative Opthalmology and Visual science, 34, 621-629.

Tscherning, M. (1924). Physiological Optics. Keystone publishing Co, Philadelphia.

Tscherning, M. (1898). Optique Physiologique. Carre et Naud: Paris.

Tscherning, M. (1890). Etude sur le position du crystallin de l'oeil humain. in Javal, L.E., Memoires d'Ophthalmometrie. Paris:Masson. (cited by Bennett and Rabbetts, 1984)

Van Meeteren, A., (1974). Calculations on the optical modulation transfer function of the human eye for white light. Optica Acta, 21(5), 395-412.

Von Bahr, G. (1948). Measurements of the thickness of the cornea. Acta Ophthalmologica, 26, 247-265.

Von Bahr, G. (1945). Investigations into the spherical and chromatic aberrations of the eye and their influence on its refraction. Acta Ophthalmologica, 23, 1-47.

Walsh, G. and Charman, W.N. (1985). Measurement of the axial wavefront aberration of the human eye. Ophthalmic and Physiological Optics, 4, 23-31.

Wang, G., Pomerantzeff, O. and Pankrotov, M. M. (1983). Astigmatism of oblique incidence in the human model eye. Vision Research, 23, 1079-1085.

Watkins, R.D. (1972). A finite aperture model of the optical system of the human eye. Flinders University, Australia. PhD Thesis.

Weale, R.A. (1963). The Aging Eye. London: H.K.Lewis.

Welford, W.T. (1986). Aberrations of optical systems. Adam Hilger, Bristol.

Westheimer, G (1960). Modulation thresholds for sinusoidal light distributions on the retina. Journal of Physiology (London), 152, 67-74.

Westheimer, G. and Campbell, F.W. (1962). Light distributions in the image formed by the living human eye. Journal of the Optical Society of America, 52, 1040-1045.

White, E.K., Dunne, M.C.M. and Barnes, D.A. (1991). Investigation into axis changes of oblique astigmatism. Ophthalmic and physiological optics, 11, 397. (Abstract).

White E.K., Dunne, M.C.M., Misson, G.P. and Barnes, D.A. (1992). The eyes optics - An approximate homocentric system? Investigative Ophthalmology and Visual Science, 33/4. 712. (Supplement - ARVO 1992).

Zadnik, K. Mutti, D.O. and Adams, A.J. (1992). The repeatability of measurements of the ocular components. Investigative Ophthalmology and Visual Science, 33, 2325 - 2333.

Zinn, K.M. (1972). The pupil. Springfield, Illonois: Thomas

APPENDICES

Research Note

Peripheral astigmatic asymmetry and angle alpha

M. C. M. Dunne, G. P. Misson, E. K. White and D. A. Barnes

Ophthalmic and Physiological Optics Research Group, Department of Vision Sciences, Aston University, Aston Triangle, Birmingham B4 7ET, UK

(Received 7 December 1992, in revised form 8 February 1993)